Volume 16, Issue 1, March 2026
pISSN 2158-0510 eISSN - 2158-0529

IJBM

International Journal of BIOMEDICINE

www.ijbm.org

IJBM

INTERNATIONAL JOURNAL OF BIOMEDICINE

Aims and Scope: *International Journal of Biomedicine (IJBM)* publishes peer-reviewed articles on the topics of basic, applied, and translational research on biology and medicine. Original research studies, reviews, hypotheses, editorial commentary, and special reports spanning the spectrum of human and experimental and tissue research will be considered. All research studies involving animals must have been conducted following animal welfare guidelines such as the National Institutes of Health (NIH) Guide for the Care and Use of Laboratory Animals, or equivalent documents. Studies involving human subjects or tissues must adhere to the Declaration of Helsinki and Title 45, US Code of Federal Regulations, Part 46, Protection of Human Subjects, and must have received approval of the appropriate institutional committee charged with oversight of human studies. Informed consent must be obtained.

International Journal of Biomedicine endorses and behaves in accordance with the codes of conduct and international standards established by the Committee on Publication Ethics (COPE).

International Journal of Biomedicine (ISSN 2158-0510) is published four times a year by International Medical Research and Development Corp. (IMRDC), 767 Broadway #1549, Manhattan, NY 10003, USA

Customer Service: International Journal of Biomedicine, 767 Broadway #1549, Manhattan, NY 10003, USA; Tel: 1-917-740-3053; E-mail: editor@ijbm.org

Manuscript Submission: Original works will be accepted with the understanding that they are contributed solely to the Journal, are not under review by another publication, and have not previously been published except in abstract form. Accepted manuscripts become the sole property of the Journal and may not be published elsewhere without the consent of the Journal. A form stating that the authors transfer all copyright ownership to the Journal will be sent from the Publisher when the manuscript is accepted; this form must be signed by all authors of the article. All manuscripts must be submitted through the International Journal of Biomedicine`s online submission and review website. Authors who are unable to provide an electronic version or have other circumstances that prevent online submission must contact the Editorial Office prior to submission to discuss alternate options (editor@ijbm.org).

IJBM

INTERNATIONAL JOURNAL OF BIOMEDICINE

IJBM
INTERNATIONAL JOURNAL OF BIOMEDICINE
www.ijbm.org
Volume 16 Issue 1 March 2026

CONTENTS

CONTENTS

International Journal of Biomedicine 16(1) (2026) 6-13
http://dx.doi.org/10.21103/Article16(1)_RA1

REVIEW ARTICLE

INTERNATIONAL JOURNAL OF BIOMEDICINE

The Impact of Diabetes Mellitus on Apical Periodontitis: Insights from Animal and Human Studies

Artana Kajtazi [1,2], Leutrim Etemi[3*]

[1] *"Dani" Specialist Dental Clinic, Ferizaj, Kosovo*
[2] *Danube Private University, Krems an der Donau, Austria*
[3] *Dini Dent Private Dental Clinic, Prishtina, Kosovo*

Abstract

Objective: This review examines the interrelation between diabetes mellitus (DM) and apical periodontitis (AP), explaining key biological mechanisms and summarizing the main findings from animal and human studies.
Methods and Results: A comprehensive literature search was conducted across PubMed, Scopus, and Web of Science, focusing on peer-reviewed studies published over the last two decades. Several studies have shown that hyperglycemia impairs VEGF-regulated angiogenesis, reduces osteoblast activity, and maintains elevated levels of inflammatory cytokines such as TNF-α and IL-6, thereby increasing periradicular lesion size and delaying tissue healing. Diabetic animal models showed reduced bone density, increased vascular calcification, and accelerated progression from caries to pulp necrosis. Clinically, T2DM (type 2 diabetes mellitus) was associated with higher AP prevalence, greater bacterial endotoxin load, and lower root-canal success rates. These effects were magnified by poor glycemic control.
Conclusion: Diabetes mellitus exacerbates AP through impaired angiogenesis, dysregulated immune response, and impaired bone metabolism. To reduce these risks, strategies such as strict blood glucose control, enhanced antimicrobial disinfection, minimally invasive interventions, and the use of bioactive materials are recommended. Future research should explore how controlling oral infections impacts systemic metabolic health. Investigating the role of bioactive materials and anti-inflammatory treatments in improving AP outcomes is also essential.(**International Journal of Biomedicine. 2026;16(1):6-13.**)

Keywords: diabetes mellitus • periapical periodontitis • animal experimentation • root canal therapy

For citation: Kajtazi A, Etemi L. The Impact of Diabetes Mellitus on Apical Periodontitis: Insights from Animal and Human Studies. Efficacy and Safety of PD-1 Inhibitor-Based Treatment in Advanced Cervical Cancer. International Journal of Biomedicine. 2026;16(1):6-13. doi:10.21103/Article16(1)_RA1

Abbreviations

AP, apical periodontitis; **BMD**, bone mineral density; **BMP-2**, bone morphogenetic protein-2; **CT**, computed tomography; **DM**, diabetes mellitus; **DXA**, dual-energy X-ray absorptiometry; **ET**, endodontically treated; **MTA**, mineral trioxide aggregate; **T1DM**, type 1 diabetes mellitus; **T2DM**, type 2 diabetes mellitus; **VEGF**, vascular endothelial growth factor; **VEGFA**, vascular endothelial growth factor A; **VEGFR2**, vascular endothelial growth factor receptor 2.

Introduction

Diabetes mellitus (DM) is a long-term metabolic condition characterized by elevated blood glucose levels due to abnormalities in insulin function and/or production.[1] This disease has multiple consequences, including retinopathy, nephropathy, neuropathy, angiopathy, and impaired wound healing.[2,3] Studies also highlight the association between DM and periodontitis.[4,5] Among the many oral complications associated with DM, apical periodontitis (AP), an inflammatory disorder of the periapical tissues typically resulting from untreated dental pulp infections,[6,7] stands out due to its prevalence and impact on endodontic outcomes. [8,9] In Europe, AP affects about 61% of the population, with prevalence increasing with age, while endodontic treatment rates are estimated at around 41%.[10]

The relationship between DM and AP is of particular concern because of the altered immune responses associated with diabetes, which may exacerbate the severity of AP and complicate its treatment.[11] Clinical observations and epidemiological surveys increasingly suggest that patients with

DM experience a higher frequency of AP, larger osteolytic lesions, and slower periapical healing than subjects with normal blood glucose levels.[12] Proposed biological links include dysregulated innate immunity, chronic hyperglycemia, and the accumulation of AGEs (advanced glycation end-products), each of which may disrupt vascular integrity, bone remodeling, and cytokine profiles in periapical tissues.[12-15]

To better understand the biological interplay between DM and AP, researchers have increasingly relied on both animal models and clinical studies. Rodent models, particularly diabetic rats, have proven invaluable due to their anatomical and physiological similarities to human dentition and their controlled experimental conditions.[16] Experimental work by Uysal et al.[17] and Takashima et al.[18] in these models has suggested that hyperglycemia may impair angiogenesis, delay tissue repair, and alter inflammatory signaling in oral tissues. In addition, studies indicate that diabetes may influence mandibular and alveolar bone development, with reduced bone density that could, in turn, affect endodontic treatment outcomes.[19-21] Some studies also suggest that DM may worsen AP by increasing inflammation around the root tip, enlarging lesion size, and slowing the healing process.[22]

Based on the available evidence, this narrative review comprehensively explores the interrelationship between DM and AP, synthesizing key findings from both animal and human studies. Despite growing interest in this field, the underlying mechanisms remain incompletely understood, and published data often vary in methodological quality.[12] This review examines the impact of diabetes on angiogenesis, bone remodeling, inflammatory responses, and endodontic treatment outcomes in the context of apical periodontitis. A better understanding of these relationships is crucial for developing more effective treatment strategies and improving endodontic care for patients with diabetes.

Materials and Methods

A structured narrative literature review was conducted to explore the relationship between DM and AP. The literature search was performed across three major databases: PubMed, Web of Science, and Scopus. A combination of Medical Subject Headings (MeSH) and free-text terms was used to build the search queries. Boolean operators structured the search logic. A representative PubMed query was: ("Diabetes Mellitus" [MeSH Terms]) AND ("Periapical Periodontitis" [MeSH Terms] OR "Apical Periodontitis" [All Fields]) AND ("Root Canal Therapy" [MeSH Terms]) AND ("Animal Experimentation" [MeSH Terms] OR "Humans" [MeSH Terms]) AND (English [Filter]). Additional keywords included "angiogenesis," "bone remodeling," "VEGF," and "pulpal healing," and filters were applied to prioritize peer-reviewed articles with full-text access.

Studies were included if they were experimental or clinical investigations published in English between 2005 and 2025, assessed the effects of type 1 diabetes mellitus (T1DM) or type 2 diabetes mellitus (T2DM) on pulpal or periapical tissues, evaluated angiogenesis, inflammatory markers, or bone turnover in the context of AP, and employed validated methodologies such as histological, immunohistochemical, radiographic, or molecular techniques. Both animal and human studies were eligible, provided they included appropriate control groups.

Exclusion criteria comprised studies lacking diabetic comparison groups or clinical diabetic parameters (e.g., HbA1c), research limited to periodontal disease without apical or pulpal analysis, non-mammalian models, and non-original publications such as reviews, abstracts, or editorials. Studies with small sample sizes (fewer than 10 animals or 20 human participants) and studies lacking control groups were also excluded.

The initial search identified 70 records (33 from PubMed, 19 from Web of Science, and 18 from Scopus). After title and abstract screening, 41 full-text articles were assessed. After applying inclusion and exclusion criteria, 23 studies were selected for final synthesis, comprising 11 animal and 12 human studies. Thematic analysis was used to categorize the included studies into three domains: (1) vascular effects focusing on angiogenic markers and microvascular changes; (2) bone remodeling covering osteoblast and osteoclast activity and alveolar bone integrity; and (3) apical periodontitis progression addressing lesion development, inflammatory cytokine profiles, and healing outcomes following endodontic treatment.

Results

Vascular Changes and Angiogenic Dysregulation in Diabetic Dental Pulp

Animal Studies

Multiple studies have investigated how DM affects dental pulp regeneration, focusing on changes in angiogenesis and growth factor expression. In a study using Goto-Kakizaki (GK) rats as a model for T2DM, Martinho et al.[23] observed significantly elevated fasting glycemia and triglyceride levels ($P<0.001$; $P<0.05$), along with larger apical periodontitis lesions compared to healthy controls ($P<0.05$). VEGF levels were also significantly lower in diabetic rats than in Wistar rats ($P<0.05$), and unlike the control group, the diabetic animals did not exhibit an increase in VEGF expression following the induction of apical periodontitis.

In contrast, Uysal et al.[17] observed elevated VEGF and CD68 expression in the pulp of streptozotocin-induced diabetic rats, alongside dilated blood vessels and increased hemorrhage. Ilić et al.[24] demonstrated that direct pulp capping in diabetic rats produced a peak VEGF level of 19.3±0.9 pg/mg on Day 1 ($P<0.001$), with a delayed increase in BMP-2 by Day 7. Additionally, sustained hyperglycemia in SDT-fatty rats (Spontaneously Diabetic Torii) led to progressive pulpal calcification starting at week 6, as observed by Takashima et al.,[18] with the authors attributing these changes to AGEs and vascular fragility.

Human and In Vitro Evidence

Human histological data mirror findings in animal models. In a comparative human study, VEGF and BMP-2 levels were measured in dental pulp samples from 28 healthy

and 28 T2DM patients using ELISA. Diabetic patients exhibited significantly higher concentrations of both growth factors in intact pulp tissue compared to healthy controls. Following indirect pulp capping, VEGF and BMP-2 levels decreased markedly in both groups. The Kruskal–Wallis test confirmed statistically significant differences in VEGF and BMP-2 levels among the study groups (P<0.001).[25] Another study found that although VEGFA, a key proangiogenic factor, was actively transcribed and translated under hyperglycemic conditions, its primary receptor, VEGFR2, was absent in all diabetic samples. Additionally, dental pulp cell viability was significantly reduced at high glucose concentrations (25 mM) compared to controls (P=0.005).[26]

In a pilot study comparing clinically normal teeth from T2DM and non-diabetic patients, diabetic pulps showed reduced vascularity, increased calcification, and thickened vessel walls. Immunohistochemical markers of inflammation were significantly elevated in the diabetic group (e.g., CD68, P<0.001; IL-6, P<0.0001; TNF-α, P=0.01), while regulatory FOXP3 expression was significantly lower (P=0.01).[27]

Alveolar Bone Remodeling and Bone Loss

Animal Models

In a study by Yilmaz et al.,[19] streptozotocin-induced diabetic rats exhibited significantly elevated blood glucose levels compared to controls (P<0.05). Histological analysis revealed vascular dilation and hemorrhage in the periodontal membrane, along with increased inflammatory cell infiltration. Osteonectin expression was positive in the periodontal ligament but absent in alveolar bone osteocytes. At the same time, osteopontin showed strong positivity in fibroblasts, collagen fibrils of the periodontal membrane, and the alveolar bone matrix.

Abbassy et al.[20] reported significantly reduced mineral apposition and bone formation rates in Wistar rats with T1DM. Additionally, micro-CT analysis revealed a significant deterioration in bone quality, characterized by reduced trabecular bone volume and increased trabecular separation in the T1DM group. Statistical analysis showed a significantly higher number of osteoclasts in the control group than in the T1DM group (P<0.05).

Hendrijantini et al.[21] investigated the effects of DM and osteoporosis on mandibular bone remodeling in Wistar rats over a 12-week period. The study included control, diabetic, and osteoporotic groups. Results showed that the diabetic group exhibited the lowest levels of Osterix expression, a key transcription factor in osteoblast differentiation. In addition, both the diabetic and osteoporotic groups demonstrated a significant reduction in the osteoblast/osteoclast ratio compared to controls.

Human Clinical and Radiographic Studies

In a retrospective study of 124 patients, Tabassum et al.[28] reported significantly greater mean alveolar bone loss in patients with T2DM than in non-diabetic individuals (3.07±1.14 mm vs. 2.59±1.08 mm, P=0.018), and a higher prevalence of moderate-to-severe periodontitis in the diabetic group. Exceptionally few case-control studies have examined the relationship between diabetes mellitus and the severity of mean alveolar bone loss. Kayal et al.[29] observed greater alveolar bone loss in diabetic patients (3.59±1.37 mm) than in controls (2.66±1.05 mm, P=0.001). This pattern was consistent across both genders and age groups. Tooth loss was significantly more prevalent among individuals with diabetes, particularly those aged over 55 or with more than 10 missing teeth.

In contrast, Ay et al.[30] found no statistically significant differences in mandibular BMD (bone mineral density) between patients with T2DM and healthy individuals. The study included 19 diabetic participants and 17 control subjects matched by age and sex. Panoramic radiographs calibrated with a DXA phantom were used for quantitative analysis, and BMD measurements were performed using Scion Image software on digitized images. The mean mandibular BMD values in diabetic women and men were 1.53±0.27 g/cm² and 1.52±0.29 g/cm², respectively, compared to 1.56±0.28 g/cm² and 1.46±0.23 g/cm² in controls.

Development and Severity of Apical Periodontitis

Animal Studies

In streptozotocin-induced diabetic rats, significantly larger periradicular lesions were observed at both 21 and 40 days following pulp exposure (P<0.05), accompanied by greater tissue destruction and inflammatory exudate compared to non-diabetic controls.[22] Similarly, GK rats with T2DM developed more extensive bone resorption and larger periapical lesions, especially when maintained on a high-sucrose diet.[31]

Prasetyo et al.[32] showed that LPS (lipopolysaccharide)-induced AP in diabetic rats led to elevated inflammatory markers. IL-6 expression increased significantly only by Day 42 (P<0.05), whereas TNF-α was elevated as early as Day 14 and remained sustained through Day 42. There were significant differences between the control and experimental groups (P<0.05).

Another model using WBN/KobSlc diabetic rats showed faster progression of caries to pulp necrosis and periapical inflammation than controls. Lesion severity strongly correlated with caries extent, and the inflammatory process extended into periapical tissues, resulting in pronounced alveolar bone resorption.[33]

Human Studies

Clinical research aligns with animal models, showing increased AP prevalence and severity in individuals with diabetes. In a retrospective study, Segura-Egea et al.[34] reported that 81.3% of T2DM patients had at least one tooth with AP, compared with 58% in non-diabetic controls (P=0.040; OR=3.2). Additionally, 6.9% of all teeth examined in diabetic patients had AP, compared with 4% in controls (P=0.007), and the average number of teeth with AP was higher in diabetics (1.5±1.1) than in controls (0.9±1.1).

Subsequent cross-sectional studies reinforced this association. One study found that T2DM was significantly associated with AP (OR=2.05; 95% CI: 1.73–2.43), particularly

in patients with poor glycemic control (HbA1c>8.0; OR=2.46). Conversely, metformin and statin therapy were each independently associated with a lower AP prevalence.[35]

Using cone-beam CT, Barros et al. reported that 64.8% of diabetic participants had periapical index scores ≥4, compared with 17.7% of controls (P<0.05). Diabetic canals had higher bacterial and endotoxin levels, which correlated with larger lesion size (P<0.05).[36]

Radiographic surveillance in a separate study revealed that AP was significantly more prevalent in T2DM patients (74%) than in non-diabetic controls (42%) (P=0.002), and root-filled teeth were also more common among diabetics (70% vs. 50%, P=0.043). Multivariate logistic regression, adjusted for the number of teeth, confirmed that both periapical status (P=0.0071) and the number of root-filled teeth (P=0.0035) were significantly associated with diabetic status. Additionally, persistent AP in root-filled teeth was observed more frequently in diabetic patients (46%) than in controls (24%), although this difference was not statistically significant (P>0.05).[37] In addition to prevalence data, outcome-based studies further support this association. Martinho et al.[23] reported a significantly lower success rate following root canal treatment in diabetic patients compared to healthy control patients (P<0.001).

The influence of glycemic control on apical periodontitis outcomes was clearly demonstrated in this analysis. Patients with poorly controlled diabetes showed a significantly higher prevalence of AP lesions (18.29%) compared to well-controlled diabetics (9.21%). Diabetic patients had more endodontically treated teeth (ET) than nondiabetic patients, with averages of 4.18% versus 1.82%, respectively. Furthermore, the AP/ET ratio was higher in diabetics (27.7%) than in nondiabetics (19.3%).[38]

Discussion

Diabetes Mellitus and Pulpal Angiogenesis

Ethical and practical limitations limit the ability to conduct in vivo studies of dental pulp repair processes in humans, necessitating the use of animal models that may not fully mimic human biological responses to diabetes and dental pulp injury. The animal studies consistently demonstrate that DM impairs angiogenic signaling and compromises dental pulp healing. In diabetic rat models, VEGF expression remains suppressed even after AP induction, suggesting a deficient angiogenic response that may contribute to delayed tissue repair.[23] Conversely, other animal studies have reported increased expression of VEGF and CD68 in diabetic pulp tissue, accompanied by dilated blood vessels and hemorrhage, which may reflect dysregulated inflammatory angiogenesis rather than effective neovascularization.[17] Temporal disruptions in key regenerative markers have also been observed. In particular, VEGF levels have been shown to peak prematurely, whereas BMP-2 exhibits a delayed increase following pulp-capping procedures, indicating altered timing and dynamics of repair.[24]

This experimental evidence finds support in clinical observations. Human studies have revealed that, despite elevated VEGF and BMP-2 levels in intact diabetic pulp tissue, their reduction following indirect pulp capping may reflect a diminished reparative capacity in hyperglycemic conditions. The consistent pattern of change between the two growth factors across both diabetic and healthy samples suggests that they may act in a coordinated manner during pulp tissue response, regardless of baseline concentration differences.[25] The absence of VEGFR2 expression in hyperglycemic conditions, despite VEGFA upregulation, further highlights a disrupted downstream angiogenic response, which could compromise vascular regeneration. This dissociation implies that even when angiogenic mediators are present, the downstream signaling or cellular responsiveness is compromised, likely due to hyperglycemia-induced receptor downregulation.[26]

Additionally, diabetic pulp tissues consistently exhibit heightened inflammation, vascular calcification, and reduced cellularity, all of which suggest compromised tissue homeostasis and impaired immune regulation. However, the supporting in vitro study included only 20 extracted molars, 10 from well-controlled T2DM patients and 10 from non-diabetics, limiting statistical power and generalizability.[27] Supporting these findings, another study reported that DM appears to increase inflammation, degeneration, and mineralization in the pulp tissue while reducing cell proliferation, emphasizing the complex pathological alterations driven by hyperglycemia.[39]

These cumulative findings underscore the complex interplay among hyperglycemia, vascular dysfunction, and inflammation in undermining pulp vitality and regeneration in individuals with diabetes. Clinically, this disrupted healing response helps explain the increased risk of endodontic failure and slower recovery observed in diabetic patients.

Alveolar Bone Remodeling and Bone Loss in Diabetes Mellitus

The collective evidence indicates that DM disrupts bone remodeling through impaired vascular integrity, altered inflammatory responses, and suppression of osteogenic signaling pathways. Findings suggest that chronic inflammation under hyperglycemic conditions delays osteoblast differentiation and inhibits normal bone formation.[19] A rat model of diabetes showed a marked reduction in the osteoblast-to-osteoclast ratio and the lowest Osterix expression among all experimental groups, indicating impaired osteoblast maturation. Although the study's interpretation is limited by the differing observation periods between the diabetes and osteoporosis models, the findings still reinforce the notion that diabetes compromises mandibular bone remodeling by downregulating osteogenic signaling pathways.[21]

Another study similarly reported that DM significantly impairs mandibular bone formation and alters bone microarchitecture, as evidenced by decreased mineral apposition and bone formation rates in diabetic rats compared to the control group. Additionally, the findings indicated fewer osteoclasts in the diabetic group, suggesting diminished bone resorption activity. This imbalance between bone formation and resorption may contribute to a state of osteopenia in the diabetic rats, highlighting the adverse effects of diabetes on craniofacial bone health.[20] The research focused on a specific age range of rats (3 to 8 weeks old) to observe dynamic changes

in bone formation, which may limit the generalizability of the findings to other age groups or species, as bone formation and turnover rates can vary significantly with age and developmental stage.

Clinical evidence suggests that T2DM is associated with more severe alveolar bone loss and a higher risk of periodontitis progression.[40] Studies reinforce that diabetic individuals are more susceptible to periodontal destruction and tooth loss, likely due to chronic inflammatory and metabolic disturbances.[28,29] Diabetes has an essential effect on enhancing osteoclastogenesis and on increasing osteoblast apoptosis. Interestingly, the impact of diabetes on bone loss and coupled bone formation is likely to involve its effects on both innate and adaptive immune responses.[41,42]

In contrast, Ay et al.[30] found no statistically significant difference in BMD between diabetic and non-diabetic subjects. However, this finding may reflect the limited sensitivity of panoramic radiographs to detect early diabetes-induced changes, rather than a genuine absence of bone alterations. The small sample size and lack of microstructural analysis further limit the generalizability of these results. Advanced imaging, such as CBCT or DXA, may better capture early diabetic bone alterations.

These vascular and bone-related alterations driven by chronic hyperglycemia likely contribute to the progression of periodontal disease and compromise the regenerative capacity of alveolar bone in individuals with diabetes.

Experimental and Clinical Evidence Linking Diabetes Mellitus to Apical Periodontitis

Animal studies provide compelling evidence that DM exacerbates both the development and severity of AP through multiple pathological mechanisms. Investigations using streptozotocin-induced diabetic rats demonstrated significantly larger periradicular lesions and a reduced defensive capacity against microbial pathogens.[22] In Goto-Kakizaki rats, systemic hyperglycemia combined with a high-sucrose diet further amplified bone resorption and lesion size, indicating a synergistic effect between metabolic imbalance and dietary factors.[31] LPS-induced models show a delayed yet sustained rise in TNF-α and IL-6 under diabetic conditions, reflecting a defective inflammatory resolution.[32] Experimental DM also accelerates progression from caries to pulp necrosis and AP, with lesion severity closely paralleling caries extent.[33]

Clinical studies support these experimental findings. A retrospective cohort study reported AP in 81.3% of individuals with T2DM, compared with 58% of normoglycemic controls, establishing DM as an epidemiological risk factor. The study's exclusion of patients with seven or fewer remaining teeth aimed to reduce confounding by periodontal disease, but it may limit generalizability to the broader diabetic population.[34]

A large cross-sectional analysis showed that T2DM is independently associated with increased AP prevalence. Notably, poor glycemic control, as reflected by elevated HbA1c levels, was associated with an even greater risk, suggesting that metabolic instability exacerbates periapical disease. In contrast, the use of metformin and statins appeared to have a protective effect: both treatments were associated with a lower prevalence of AP, possibly due to their anti-inflammatory or glycemic-modulating effects. Because the study was cross-sectional, it cannot establish a causal relationship between T2DM and AP and may be influenced by unspecified factors such as diet or genetics. Additionally, reliance on medical records and a single hospital network limits data accuracy and generalizability.[35]

Cone-beam CT and microbiological assessments have linked T2DM to higher bacterial and endotoxin loads, contributing to more severe periapical bone destruction and potentially affecting endodontic treatment outcomes.[36] Long-term radiographic surveillance has demonstrated that diabetic patients harbor more root-filled teeth and experience a greater likelihood of persistent periapical inflammation.[37]

The role of glycemic regulation was further underscored by evidence that poorly controlled diabetics show a higher prevalence of AP and a higher AP/ET ratio compared to well-controlled patients, highlighting the negative impact of uncontrolled diabetes on dental health. However, the cross-sectional design, small sample size, and reliance on radiographic diagnosis limit the ability to draw causal inferences and generalisability.[38] Finally, outcome-based research has demonstrated significantly lower root canal success rates in diabetic patients compared to normoglycemic individuals, reinforcing diabetes as a negative prognostic factor.[23]

Additionally, a cross-sectional study analyzing full-mouth radiographs from a Brazilian population found that AP was significantly more prevalent in untreated teeth of T2DM patients (10%) than in those of nondiabetics (7%), supporting the hypothesis that diabetes may act as a disease modifier in the development of primary endodontic disease. However, no significant difference in AP prevalence was found between the two groups in root canal–treated teeth, suggesting that diabetes may not adversely affect post-treatment healing. These findings align with previous clinical research showing increased AP prevalence in diabetics but mixed evidence regarding endodontic treatment outcomes.[43]

Taken together, evidence from both experimental and clinical studies indicates that DM increases the prevalence, severity, and progression of AP. Prolonged inflammation (e.g., sustained TNF-α and IL-6), greater microbial burden, impaired immune responses, and reduced post-treatment healing capacity all contribute to this elevated risk. These findings underscore the need for strict glycemic control and individualized treatment planning in the endodontic management of diabetic patients.

Management Strategies for Diabetic Patients Undergoing Endodontic Therapy

Endodontic management in diabetic patients requires a comprehensive approach that addresses both systemic and local factors. Given their heightened risk of delayed healing and infection, maintaining optimal glycemic control is essential to improve treatment outcomes.[44] Research has shown that patients with well-controlled DM exhibit better healing responses and lower complication rates than those with poor control.[45] Therefore, close collaboration with the

patient's primary care physician or endocrinologist to stabilize glycemic status before and after endodontic treatment is critical.

Another key management strategy involves enhanced antimicrobial protocols to mitigate the increased risk of infection in diabetic patients. Because of their compromised immune response, higher concentrations of sodium hypochlorite and adjunctive agents such as chlorhexidine or calcium hydroxide may be recommended to improve canal disinfection.[46] Additionally, due to the delayed healing observed in diabetic tissues, minimally invasive approaches such as smaller access cavities and conservative root canal instrumentation can help preserve tooth structure and reduce post-operative complications.[44]

To improve endodontic outcomes in diabetic patients, adjunctive use of NSAIDs (nonsteroidal anti-inflammatory drugs) can help manage post-operative inflammation. Ibuprofen 600 mg, alone or combined with acetaminophen 1000 mg, is effective for short-term pain relief, though optimal dosing strategies for prolonged pain control remain unclear.[47] Given the impaired healing dynamics in diabetes, using biomaterials with proven bioactivity and immunotolerance, such as MTA (mineral trioxide aggregate), may help mitigate the risks of delayed tissue repair and chronic inflammation. Thus, the selection of bioactive materials should be considered a key component of endodontic management in this patient population. MTA is suitable for diabetic patients, as preclinical studies show that it maintains biocompatibility and promotes mineralization regardless of diabetic status. In rats, Angelus MTA® induced similar mineralized tissue formation and mild inflammation in both diabetic and non-diabetic groups, supporting its use in regenerative endodontic procedures.[48]

Patient education is also essential. Informing diabetic patients about the importance of blood glucose control, adherence to medications, and compliance with post-treatment care can significantly enhance treatment outcomes.[49]

Limitations

While this review offers a comprehensive synthesis of current evidence, certain limitations should be acknowledged. First, as a narrative review, it does not follow the rigorous methodology of a systematic review or meta-analysis, which may introduce some selection bias despite predefined inclusion and exclusion criteria. Second, the body of evidence is highly heterogeneous: studies vary in animal models, diabetic subtypes, diagnostic protocols, and outcome measures, making direct comparisons difficult and weakening the generalizability of overarching conclusions. Translational challenges further complicate interpretation. Most animal studies employ streptozotocin-induced or genetic models (e.g., GK, SDT rats) that mimic T1DM or exaggerated metabolic states, whereas most clinical cases involve T2DM with variable glycemic control, obesity, and systemic inflammation. Additionally, key clinical variables, such as medication regimens and diabetes duration, are seldom reported or controlled in human studies, limiting causal inference. Finally, many animal and in-vitro investigations rely on small sample sizes, which reduces statistical power and makes it harder to apply the findings to human clinical scenarios.

Conclusion

This review highlights the complex interplay between diabetes mellitus and apical periodontitis, demonstrating that hyperglycemia impairs angiogenesis, suppresses bone remodeling, elevates pro-inflammatory cytokines, and delays periapical healing. Both animal and human studies confirm that diabetic patients are more prone to larger lesions, poorer healing outcomes, and lower root canal treatment success rates.

To reduce these risks, endodontic care for diabetic patients should prioritize strict glycemic control, enhanced antimicrobial disinfection, minimally invasive techniques, and the use of bioactive materials such as MTA. Adjunctive anti-inflammatory therapies (e.g., NSAIDs) may help reduce post-operative complications, especially in patients with pre-existing inflammation. Diabetic individuals should be treated as a high-risk group, with individualized protocols and close coordination between dental and medical providers.

Future research should explore how controlling oral infections impacts systemic metabolic health. Research into the role of bioactive materials and anti-inflammatory drugs in improving treatment outcomes for apical periodontitis is also essential. Strengthening our understanding of this oral-systemic connection will help optimize care for individuals with diabetes.

Conflicts of Interest

The authors declare that they have no competing interests.

References

1. American Diabetes Association. Diagnosis and classification of diabetes mellitus. Diabetes Care. 2010 Jan;33 Suppl 1(Suppl 1):S62-9. doi: 10.2337/dc10-S062. Erratum in: Diabetes Care. 2010 Apr;33(4):e57. PMID: 20042775; PMCID: PMC2797383.

2. Mealey BL, Ocampo GL. Diabetes mellitus and periodontal disease. Periodontol 2000. 2007;44:127-53. doi: 10.1111/j.1600-0757.2006.00193.x. PMID: 17474930.

3. Shlossman M, Knowler WC, Pettitt DJ, Genco RJ. Type 2 diabetes mellitus and periodontal disease. J Am Dent Assoc. 1990 Oct;121(4):532-6. doi: 10.14219/jada.archive.1990.0211. PMID: 2212346.

4. Mealey BL. Periodontal implications: medically compromised patients. Ann Periodontol. 1996 Nov;1(1):256-321. doi: 10.1902/annals.1996.1.1.256. PMID: 9118261.

5. Papapanou PN. Periodontal diseases: epidemiology. Ann Periodontol. 1996 Nov;1(1):1-36. doi: 10.1902/annals.1996.1.1.1. PMID: 9118256.

6. Yamasaki M, Kumazawa M, Kohsaka T, Nakamura H, Kameyama Y. Pulpal and periapical tissue reactions after experimental pulpal exposure in rats. J Endod. 1994 Jan;20(1):13-7. doi: 10.1016/s0099-2399(06)80020-8. PMID: 8182380.

7. KAKEHASHI S, STANLEY HR, FITZGERALD RJ. THE EFFECTS OF SURGICAL EXPOSURES OF DENTAL PULPS IN GERM-FREE AND CONVENTIONAL LABORATORY RATS. Oral Surg Oral Med Oral Pathol. 1965 Sep;20:340-9. doi: 10.1016/0030-4220(65)90166-0. PMID: 14342926.
8. BENDER IB, SELTZER S, FREEDLAND J. THE RELATIONSHIP OF SYSTEMIC DISEASES TO ENDODONTIC FAILURES AND TREATMENT PROCEDURES. Oral Surg Oral Med Oral Pathol. 1963 Sep;16:1102-15. doi: 10.1016/0030-4220(63)90226-3. PMID: 14061146.
9. Britto LR, Katz J, Guelmann M, Heft M. Periradicular radiographic assessment in diabetic and control individuals. Oral Surg Oral Med Oral Pathol Oral Radiol Endod. 2003 Oct;96(4):449-52. doi: 10.1016/s1079-2104(03)00034-9. PMID: 14561970.
10. Jiménez-Pinzón A, Segura-Egea JJ, Poyato-Ferrera M, Velasco-Ortega E, Ríos-Santos JV. Prevalence of apical periodontitis and frequency of root-filled teeth in an adult Spanish population. Int Endod J. 2004 Mar;37(3):167-73. doi: 10.1111/j.0143-2885.2004.00759.x. PMID: 15009405.
11. Iwama A, Morimoto T, Tsuji M, Nakamura K, Higuchi N, Imaizumi I, Shibata N, Yamasaki M, Nakamura H. Increased number of anaerobic bacteria in the infected root canal in type 2 diabetic rats. Oral Surg Oral Med Oral Pathol Oral Radiol Endod. 2006 May;101(5):681-6. doi: 10.1016/j.tripleo.2005.06.007. Epub 2005 Oct 12. PMID: 16632284.
12. Segura-Egea JJ, Martín-González J, Castellanos-Cosano L. Endodontic medicine: connections between apical periodontitis and systemic diseases. Int Endod J. 2015 Oct;48(10):933-51. doi: 10.1111/iej.12507. Epub 2015 Aug 3. PMID: 26174809.
13. Lima SM, Grisi DC, Kogawa EM, Franco OL, Peixoto VC, Gonçalves-Júnior JF, Arruda MP, Rezende TM. Diabetes mellitus and inflammatory pulpal and periapical disease: a review. Int Endod J. 2013 Aug;46(8):700-9. doi: 10.1111/iej.12072. Epub 2013 Feb 26. PMID: 23442003.
14. Bender IB, Bender AB. Diabetes mellitus and the dental pulp. J Endod. 2003 Jun;29(6):383-9. doi: 10.1097/00004770-200306000-00001. PMID: 12814220.
15. Dienelt A, zur Nieden NI. Hyperglycemia impairs skeletogenesis from embryonic stem cells by affecting osteoblast and osteoclast differentiation. Stem Cells Dev. 2011 Mar;20(3):465-74. doi: 10.1089/scd.2010.0205. Epub 2010 Nov 30. PMID: 20939707.
16. Dammaschke T, Stratmann U, Wolff P, Sagheri D, Schäfer E. Direct pulp capping with mineral trioxide aggregate: an immunohistologic comparison with calcium hydroxide in rodents. J Endod. 2010 May;36(5):814-9. doi: 10.1016/j.joen.2010.02.001. Epub 2010 Mar 15. PMID: 20416425.
17. Uysal I, Gokalp-Ozkorkmaz E, Deveci E. Experimentally induced diabetes mellitus influences expression of VEFGand CD68 in rat teeth pulp. Int J Morphol. Published online 2019:606-611.
18. Takashima A, Miura J, Sugiyama K, Shimizu M, Okada M, Otani T, Nagashima T, Tsuda T, Araki T. Glycation promotes pulp calcification in Type 2 diabetes rat model. Oral Dis. 2024 Mar;30(2):593-603. doi: 10.1111/odi.14529. Epub 2023 Mar 13. PMID: 36843542.
19. Yılmaz UN, Uysal I, Eratilla V, et al. Effects on Alveolar Bone of Diabetes Mellitus Induced by Streptozotocin in Rats. Histopathologic and Immunohistochemical Study. Int J Morphol. 2018;36:206-211. doi:10.4067/S0717-95022018000100206
20. Abbassy MA, Watari I, Soma K. The effect of diabetes mellitus on rat mandibular bone formation and microarchitecture. Eur J Oral Sci. 2010 Aug;118(4):364-9. doi: 10.1111/j.1600-0722.2010.00739.x. PMID: 20662909.
21. Hendrijantini N, Suisan YC, Megantara RWA, Tumali BAS, Kuntjoro M, Ari MDA, Sitalaksmi RM, Hong G. Bone Remodeling in Mandible of Wistar Rats with Diabetes Mellitus and Osteoporosis. Eur J Dent. 2023 May;17(2):319-329. doi: 10.1055/s-0042-1745768. Epub 2022 Jul 4. PMID: 35785822; PMCID: PMC10329528.
22. Armada-Dias L, Breda J, Provenzano JC, Breitenbach M, Rôças Id, Gahyva SM, Siqueira JF Jr. Development of periradicular lesions in normal and diabetic rats. J Appl Oral Sci. 2006 Oct;14(5):371-5. doi: 10.1590/s1678-77572006000500013. PMID: 19089060; PMCID: PMC4327230.
23. Martinho JP, Coelho A, Oliveiros B, Pires S, Abrantes AM, Paulo S, Carvalho AC, Carrilho E, Paula A, Carvalho L, Seiça R, Botelho MF, Marto CM, Spagnuolo G, Matafome P, Ferreira MM. Impairment of the angiogenic process may contribute to lower success rate of root canal treatments in diabetes mellitus. Int Endod J. 2021 Oct;54(10):1687-1698. doi: 10.1111/iej.13572. Epub 2021 Jul 10. PMID: 33999433.
24. Ilic J, Radovic K, Brkovic B, Vasic J, Roganovic J. The diabetic dental pulp repair: involvement of vascular endothelial growth factor and bone morphogenetic protein 2. Srp Arh Celok Lek. 2020;148(11-12):673-678. doi:10.2298/SARH200228057I
25. Ilić J, Radović K, Roganović J, Brković B, Stojić D. The levels of vascular endothelial growth factor and bone morphogenetic protein 2 in dental pulp tissue of healthy and diabetic patients. J Endod. 2012 Jun;38(6):764-8. doi: 10.1016/j.joen.2012.03.016. Epub 2012 Apr 24. PMID: 22595109.
26. Patel S, Yang E, Milne TJ, Hussaini H, Cooper PR, Friedlander LT. Angiogenic effects of Type 2 diabetes on the dental pulp. Int Endod J. 2025 Mar;58(3):434-448. doi: 10.1111/iej.14181. Epub 2024 Dec 9. PMID: 39652136.
27. Alsamahi S, Milne TM, Hussaini H, Rich AM, Friedlander LT. Type 2 diabetes and the clinically normal pulp: An in vitro study. Int Endod J. 2022 Jun;55(6):660-671. doi: 10.1111/iej.13732. Epub 2022 Apr 1. PMID: 35322881; PMCID: PMC9324782.
28. Tabassum A. Alveolar Bone Loss in Diabetic Patients: A Case-Control Study. Eur J Dent. 2024 Feb;18(1):168-173. doi: 10.1055/s-0042-1758071. Epub 2022 Dec 15. PMID: 36522180; PMCID: PMC10959629.
29. Kayal RA, Almutadares M, Algarni A, Alfaifi K, Bahammam MA, Alhazzazi TY. The Effect of Self-Reported Diabetes on Alveolar Bone Loss and Number of Missing Teeth. The Open Dentistry Journal. doi:10.2174/1874210602115010526
30. Ay S, Gursoy UK, Erselcan T, Marakoglu I. Assessment of mandibular bone mineral density in patients with type 2 diabetes mellitus. Dentomaxillofac Radiol. 2005 Nov;34(6):327-31. doi: 10.1259/dmfr/52540810. PMID: 16227473.
31. Iwama A, Nishigaki N, Nakamura K, Imaizumi I, Shibata N, Yamasaki M, Nakamura H, Kameyama Y, Kapila Y. The

effect of high sugar intake on the development of periradicular lesions in rats with type 2 diabetes. J Dent Res. 2003 Apr;82(4):322-5. doi: 10.1177/154405910308200416. PMID: 12651940.
32. Prasetyo EP, Sampoerno G, Juniarti DE, Cahyani F, Saraswati W, Kuntjoro M, Tjendronegoro E. Effect of Lipopolysaccharide-Induced Apical Periodontitis in Diabetes Mellitus Rats on Periapical Inflammation. Eur J Dent. 2023 Oct;17(4):1146-1152. doi: 10.1055/s-0042-1758790. Epub 2023 Jan 4. PMID: 36599453; PMCID: PMC10756800.
33. Kodama Y, Matsuura M, Sano T, Nakahara Y, Ozaki K, Narama I, Matsuura T. Diabetes enhances dental caries and apical periodontitis in caries-susceptible WBN/KobSlc rats. Comp Med. 2011 Feb;61(1):53-9. PMID: 21819682
34. Segura-Egea JJ, Jiménez-Pinzón A, Ríos-Santos JV, Velasco-Ortega E, Cisneros-Cabello R, Poyato-Ferrera M. High prevalence of apical periodontitis amongst type 2 diabetic patients. Int Endod J. 2005 Aug;38(8):564-9. doi: 10.1111/j.1365-2591.2005.00996.x. PMID: 16011776.
35. Yip N, Liu C, Wu D, Fouad AF. The association of apical periodontitis and type 2 diabetes mellitus: A large hospital network cross-sectional case-controlled study. J Am Dent Assoc. 2021 Jun;152(6):434-443. doi: 10.1016/j.adaj.2021.01.005. Epub 2021 Mar 29. PMID: 33795142.
36. Barros MC, Velasquez-Espedilla EG, Oliveira LD, Gomes BPFA, Duarte MAH, Negrato CA, Andrade FB. Impact of Type 2 Diabetes Mellitus on Apical Periodontitis Size, Endotoxin Levels, and Bacterial Load in Root Canals with Necrotic Pulp. J Endod. 2025 Aug;51(8):1036-1043. doi: 10.1016/j.joen.2025.05.003. Epub 2025 May 9. PMID: 40350031.
37. López-López J, Jané-Salas E, Estrugo-Devesa A, Velasco-Ortega E, Martín-González J, Segura-Egea JJ. Periapical and endodontic status of type 2 diabetic patients in Catalonia, Spain: a cross-sectional study. J Endod. 2011 May;37(5):598-601. doi: 10.1016/j.joen.2011.01.002. Epub 2011 Mar 2. PMID: 21496655.
38. Smadi L. Apical Periodontitis and Endodontic Treatment in Patients with Type II Diabetes Mellitus: Comparative Cross-sectional Survey. J Contemp Dent Pract. 2017 May 1;18(5):358-362. doi: 10.5005/jp-journals-10024-2046. PMID: 28512272.
39. Pimenta RMN, Dos Reis-Prado AH, de Castro Oliveira S, Goto J, Cosme-Silva L, Cintra LTA, Benetti F. Effects of diabetes mellitus on dental pulp: A systematic review of in vivo and in vitro studies. Oral Dis. 2024 Mar;30(2):100-115. doi: 10.1111/odi.14267. Epub 2022 Jun 20. PMID: 35657117.
40. Wu YY, Xiao E, Graves DT. Diabetes mellitus related bone metabolism and periodontal disease. Int J Oral Sci. 2015 Jun 26;7(2):63-72. doi: 10.1038/ijos.2015.2. PMID: 25857702; PMCID: PMC4817554.
41. Nikolajczyk BS, Jagannathan-Bogdan M, Shin H, Gyurko R. State of the union between metabolism and the immune system in type 2 diabetes. Genes Immun. 2011 Jun;12(4):239-50. doi: 10.1038/gene.2011.14. Epub 2011 Mar 10. PMID: 21390053; PMCID: PMC6826342.
42. Graves DT, Oates T, Garlet GP. Review of osteoimmunology and the host response in endodontic and periodontal lesions. J Oral Microbiol. 2011 Jan 17;3. doi: 10.3402/jom.v3i0.5304. PMID: 21547019; PMCID: PMC3087239.
43. Marotta PS, Fontes TV, Armada L, Lima KC, Rôças IN, Siqueira JF Jr. Type 2 diabetes mellitus and the prevalence of apical periodontitis and endodontic treatment in an adult Brazilian population. J Endod. 2012 Mar;38(3):297-300. doi: 10.1016/j.joen.2011.11.001. Epub 2011 Dec 22. PMID: 22341063.
44. Alshargawi WK, Alghamdi FM, Alziyad SA, et al. Impact of diabetes mellitus on endodontic treatment outcomes. Int J Community Med Public Health. 2024;11(10):4123-4126. doi:10.18203/2394-6040.ijcmph20242687
45. Segura-Egea JJ, Castellanos-Cosano L, Machuca G, López-López J, Martín-González J, Velasco-Ortega E, Sánchez-Domínguez B, López-Frías FJ. Diabetes mellitus, periapical inflammation and endodontic treatment outcome. Med Oral Patol Oral Cir Bucal. 2012 Mar 1;17(2):e356-61. doi: 10.4317/medoral.17452. PMID: 22143698; PMCID: PMC3448330.
46. Zehnder M, Schmidlin P, Sener B, Waltimo T. Chelation in root canal therapy reconsidered. J Endod. 2005 Nov;31(11):817-20. doi: 10.1097/01.don.0000158233.59316.fe. PMID: 16249726.
47. Smith EA, Marshall JG, Selph SS, Barker DR, Sedgley CM. Nonsteroidal Anti-inflammatory Drugs for Managing Postoperative Endodontic Pain in Patients Who Present with Preoperative Pain: A Systematic Review and Meta-analysis. J Endod. 2017 Jan;43(1):7-15. doi: 10.1016/j.joen.2016.09.010. Epub 2016 Dec 6. PMID: 27939729.
48. Gomes-Filho JE, de Azevedo Queiroz ÍO, Watanabe S, da Silva Santos LM, Lodi CS, Okamoto R, Ervolino E, Dezan E Jr, Cintra LT. Influence of diabetes mellitus on tissue response to MTA and its ability to stimulate mineralization. Dent Traumatol. 2015 Feb;31(1):67-72. doi: 10.1111/edt.12130. Epub 2014 Sep 27. PMID: 25264083.
49. Ryan ME. Diagnostic & therapeutic strategies for the management of the diabetic patient. Compend Contin Educ Dent. 2008 Jan-Feb;29(1):32-8, 40-4. PMID: 18361339.

***Corresponding author:** Dr. Leutrim Etemi. E-mail: leutrim.etemi1999@gmail.com*

International Journal of Biomedicine 16(1) (2026) 14-16
http://dx.doi.org/10.21103/Article16(1)_RA2

BRIEF REVIEW

INTERNATIONAL JOURNAL OF BIOMEDICINE

Evolution of the Classification Criteria for Antiphospholipid Syndrome: From Hughes Syndrome to ACR/EULAR Criteria

Ina Toska[1*], Ervin Rapushi[2], Rexhep Shkurti[1], Anila Mitre[3]

[1]*University of Tirana, Faculty of Natural Sciences, Department of Biotechnology, Tirana, Albania*
[2]*University of Medicine, Tirana, Albania*
[3]*University of Tirana, Faculty of Natural Sciences, Department of Biology, Tirana, Albania*

Abstract

Antiphospholipid syndrome (APS) is an autoimmune disorder defined by thrombotic events or obstetrical morbidity in the presence of persistent antiphospholipid antibodies, such as lupus anticoagulant (LAC), anticardiolipin (aCL), and ß2-glycoprotein I (ß2-GPI). The need for standardized classification criteria has been recognized as essential for diagnosis, patient stratification, research consistency, and comparison of clinical studies since their initial description. The classification criteria for APS have evolved over the years in response to advances in clinical practice and laboratory standardization. First, based on clinical observations, the preliminary Sapporo criteria highlighted an association among thrombosis, pregnancy morbidity, and antiphospholipid antibodies. The Sydney criteria, an international consensus statement, introduced structured clinical and laboratory criteria and incorporated persistence of antiphospholipid antibodies to improve specificity. The recent classification criteria of the American College of Rheumatology (ACR) and the European Alliance of Associations for Rheumatology (EULAR), published in 2023, introduced a weighted point system across clinical and laboratory domains, with the aim of achieving high specificity for research. (**International Journal of Biomedicine. 2026;16(1):14-16.**)

Keywords: antiphospholipid syndrome • Sapporo criteria • Sydney criteria • ACR/EULAR criteria

For citation: Toska I, Rapushi E, Shkurti R, Mitre A. Evolution of the Classification Criteria for Antiphospholipid Syndrome: From Hughes Syndrome to ACR/EULAR Criteria. International Journal of Biomedicine. 2026;16(1):14-16. doi:10.21103/Article16(1)_RA2

Abbreviations

APS, antiphospholipid syndrome; **aCL**, anticardiolipin; **LAC**, lupus anticoagulant; **ß2-GPI**, ß2-glycoprotein I; **SLE**, systemic lupus erythematosus.

Introduction

Antiphospholipid syndrome (APS) is an autoimmune disorder defined by thrombotic events or obstetrical morbidity in the presence of persistent antiphospholipid antibodies.[1] Antiphospholipid syndrome was initially described in the early 1980s, based on recurrent associations between thrombosis, pregnancy losses, and the presence of lupus anticoagulant (LAC), especially in patients with systemic lupus erythematosus (SLE).[2] This early conceptualization, even without formalized criteria, provided the fundamental recognition of APS as a clinical entity. Given the clinical and immunological heterogeneity of the syndrome, standardized classification criteria were necessary to ensure homogeneity within the research population and to facilitate comparisons across studies. Classification criteria for APS have undergone multiple revisions in response to clinical evidence and advances in laboratory diagnostics (Table 1).

Hughes Syndrome: Early Clinical Description

The earliest descriptions of APS, known as Hughes syndrome, were based on clinical observations linking thrombotic events and recurrent pregnancy loss with the presence of lupus anticoagulant. These were largely

***Corresponding author**: Ina Toska. E-mail: ina.toska@yahoo.com*

descriptive, and APS was not defined by formal classification criteria.[3]

Table 1.

Evolution of APS classification criteria

1983	1999	2006	2023
Hughes Syndrome	Sapporo Criteria	Syndey Criteria	ACR/EULAR
Clinical observation	First Consensus	Revised Criteria	Score-point system
Thrombosis, Pregnancy loss	Clinical + Laboratory Criteria	Added Anti-ß2GPI	Research purposes
LAC	LAC, aCL IgG/IgM	Persistent positivity within 12 weeks	High specificity
	Persistent positivity within 6 weeks		

Sapporo Criteria

The need for standardized classification criteria for APS became more evident in 1990, with the increase in heterogeneous clinical studies reported, characterized by variable clinical manifestations and laboratory findings. The first international consensus classification criteria were established at the Eighth International Symposium on Antiphospholipid Antibodies in 1999 in Sapporo (Japan).

The Sapporo criteria required the coexistence of clinical manifestations and laboratory evidence of antiphospholipid antibodies to classify as APS. Clinical criteria included vascular thrombosis and pregnancy morbidity. Vascular thrombosis is represented by one or more confirmed episodes of arterial, venous, or small vessel thrombosis in any organ or tissue. Pregnancy morbidity included: one or more unexplained deaths of a morphologically normal fetus at or beyond the 10th week of gestation, one or more premature births of a morphologically normal neonate before the 34th week of gestation due to severe preeclampsia, eclampsia or placental insufficiency, three or more unexplained consecutive spontaneous abortions before the 10th week of gestation, excluding maternal anatomical or hormonal abnormalities and chromosomal causes.

Laboratory criteria comprise the detection of LAC and/or anticardiolipin antibodies IgM/IgG in medium or high titer, on two or more occasions within six weeks.[4]

Sydney Criteria

Although the Sapporo criteria represented an important step in standardizing the definition of APS, their application in clinical studies revealed some limitations regarding laboratory characterization, heterogeneity of clinical manifestations, and antibody persistence. The Sapporo criteria did not include anti-β2GPI antibodies, lacked strict rules for repeat testing, and exhibited limited standardization of laboratory assays.[5]

The international consensus meeting, held in Sydney in 2006, revised the previously established criteria for the APS classification. For the first time, the Sydney criteria included anti-ß2GPI antibodies (IgG or IgM) as a laboratory criterion, based on evidence of their pathogenic and diagnostic relevance. Additionally, revised criteria expanded the interval for persistence of antiphospholipid antibody positivity from 6 to 12 weeks.[5] In this way, the cases with transient antibody positivity related to other conditions can be excluded. Regarding clinical criteria, the obstetric domain is more precisely defined with clearer distinctions for fetal loss, preterm birth, and recurrent pregnancy loss. Revised criteria improved the APS classification and homogeneity in research studies. This way, the revised Sapporo criteria became the gold standard for APS classification, widely used for years in clinical and practical research.[6]

ACR/EULAR 2023 Classification Criteria

The Sydney classification criteria also demonstrated limitations, particularly for research in heterogeneous populations. According to clinical experience, thrombotic events don't carry the same diagnostic weight, and in the laboratory setting, LAC positivity carries a higher risk than other antiphospholipid antibodies. The ACR/EULAR initiated an effort to develop APS classification criteria with high specificity for use in observational studies and trials.[7] For the first time, "entry criteria" were introduced, which had to be met for the patient to be classified as having APS.

The maximum interval between the occurrence of one clinical symptom and the detection of antiphospholipid antibodies was reduced to three years. Clinical manifestations are organized in domains including venous thromboembolism, arterial thrombosis, microvascular thrombosis, obstetric morbidity, cardiac valve disease, and hematology. Each has a specific score reflecting its association with APS. Laboratory criteria were also structured as a weighted scoring system and included LAC, anti-cardiolipin IgM/IgG titers (medium or high), and anti-ß2GPI IgG/IgM titers (medium or high). To be classified as APS, it is required to accumulate at least three points from the clinical domain and at least three points from the laboratory domain.[8,9] The new ACR/EULAR 2023 classification can improve specificity and provide a robust framework for APS research and clinical trials; however, new criteria may exclude patients with non-criteria manifestations. As understanding of APS evolves, the validity of the latest criteria and their revisions are likely to follow.

Discussion and Recommendations

For more than four decades, all knowledge of APS has been reflected in the evolution of classification criteria. From the earliest to the latest criteria, each iteration has sought to address the limitations of its predecessors as scientific evidence has evolved. Early descriptive observations prioritized sensitivity, enabling recognition of a broad clinical phenotype, whereas subsequent criteria increased specificity and reproducibility, particularly for research.

The Sapporo criteria defined APS by combining clinical and laboratory evidence. They improved standardization and facilitated epidemiological research. Nevertheless, they had limitations, including the absence of anti-β2GPI antibodies, insufficient specificity, and insufficient emphasis on antibody persistence, which led to the Sapporo-revised criteria (Sydney). They improved standardization and were the gold standard for clinical and research applications. Even the Sydney criteria showed limitations: their binary structure, inability to account for antibody profiles, and differential risk contributed to heterogeneity in study populations and limited interpretation of clinical outcomes. The new ACR/EULAR 2023 classification introduced a weighted, point-based system that emphasized specificity, antibody profiling, and pathogenic relevance. New criteria, by prioritizing specificity and homogeneity, are optimized for research. As noted above, they may exclude patients with non-criteria clinical manifestations, underscoring the importance of ongoing clinical judgment in practice. From a research perspective, a weighted point-based classification system improves homogeneity across studies, whereas stratification by antibody profiles enables precise risk assessment. Elimination of non-criteria patients highlights the limitations of current classification, underscoring the need for research to integrate non-criteria manifestations into clinical frameworks to bridge the gap between classification and clinical complexity.

Competing Interests

The authors declare that they have no conflicts of interest.

References

1. Alijotas-Reig J, Esteve-Valverde E, Anunciación-Llunell A, Marques-Soares J, Pardos-Gea J, Miró-Mur F. Pathogenesis, Diagnosis and Management of Obstetric Antiphospholipid Syndrome: A Comprehensive Review. J Clin Med. 2022 Jan 28;11(3):675. doi: 10.3390/jcm11030675. PMID: 35160128; PMCID: PMC8836886.

2. Hughes GR. The antiphospholipid syndrome: ten years on. Lancet. 1993 Aug 7;342(8867):341-4. doi: 10.1016/0140-6736(93)91477-4. PMID: 8101587.

3. Hughes GR. Thrombosis, abortion, cerebral disease, and the lupus anticoagulant. Br Med J (Clin Res Ed). 1983 Oct 15;287(6399):1088-9. doi: 10.1136/bmj.287.6399.1088. PMID: 6414579; PMCID: PMC1549319.

4. Wilson WA, Gharavi AE, Koike T, Lockshin MD, Branch DW, Piette JC, et al. International consensus statement on preliminary classification criteria for definite antiphospholipid syndrome: report of an international workshop. Arthritis Rheum. 1999 Jul;42(7):1309-11. doi: 10.1002/1529-0131(199907)42:7<1309::AID-ANR1>3.0.CO;2-F. PMID: 10403256.

5. Miyakis S, Lockshin MD, Atsumi T, Branch DW, Brey RL, Cervera R, Derksen RH, DE Groot PG, Koike T, Meroni PL, Reber G, Shoenfeld Y, Tincani A, Vlachoyiannopoulos PG, Krilis SA. International consensus statement on an update of the classification criteria for definite antiphospholipid syndrome (APS). J Thromb Haemost. 2006 Feb;4(2):295-306. doi: 10.1111/j.1538-7836.2006.01753.x. PMID: 16420554.

6. Schreiber K, Sciascia S, de Groot PG, Devreese K, Jacobsen S, Ruiz-Irastorza G, Salmon JE, Shoenfeld Y, Shovman O, Hunt BJ. Antiphospholipid syndrome. Nat Rev Dis Primers. 2018 Jan 11;4:17103. doi: 10.1038/nrdp.2017.103. Erratum in: Nat Rev Dis Primers. 2018 Jan 25;4:18005. doi: 10.1038/nrdp.2018.5. PMID: 29321641.

7. Cervera R. Antiphospholipid syndrome. Thromb Res. 2017 Mar;151 Suppl 1:S43-S47. doi: 10.1016/S0049-3848(17)30066-X. PMID: 28262233.

8. Barbhaiya M, Zuily S, Naden R, Hendry A, Manneville F, Amigo MC, et al.; ACR/EULAR APS Classification Criteria Collaborators. 2023 ACR/EULAR antiphospholipid syndrome classification criteria. Ann Rheum Dis. 2023 Oct;82(10):1258-1270. doi: 10.1136/ard-2023-224609. Epub 2023 Aug 28. PMID: 37640450.

9. Musiał J. New classification criteria for antiphospholipid syndrome — 2023. Journal of Transfusion Medicine [Internet]. Journal of Transfusion Medicine 2023;16(3):103-109. doi: 10.5603/jtm.97795

International Journal of Biomedicine 16(1) (2026) 17-25
http://dx.doi.org/10.21103/Article16(1)_OA1

ORIGINAL ARTICLE

Mental Health

INTERNATIONAL JOURNAL OF BIOMEDICINE

Gamma-Glutamyl Transferase to High-Density Lipoprotein Cholesterol Ratio as a Marker of Cognitive Dysfunction in Older Adults: A Cross-Sectional Study from NHANES 2011–2014

Meng Du[1,2#], Yanan Zhao[1,2#], Panpan Zheng[1,2], Xian Xiu[1,2], Yang Li[1,2], Haiyan Gu[1,2], Jinghua Sun[1,2], Lili Zhang[1,2], Zanchao Liu[1,2*]

[1]*Hebei Key Laboratory of Basic Medicine for Diabetes, Shijiazhuang Second Hospital, Shijiazhuang, China*
[2]*Shijiazhuang Technology Innovation Center of Precision Medicine for Diabetes, Shijiazhuang Second Hospital, Shijiazhuang, China*

Abstract

Background: The gamma-glutamyl transferase to high-density lipoprotein cholesterol (GGT/HDL-C) ratio has been reported to be associated with various metabolic diseases, but its relationship with cognitive dysfunction remains limited. This study aimed to investigate the relationship between the GGT/HDL-C ratio and cognitive dysfunction in older adults.

Methods and Results: This cross-sectional study included 2,769 participants and used data from the National Health and Nutrition Examination Survey (NHANES) database (2011~2014). Natural logarithmic (ln) transformation was performed on GGT/HDL-C before analysis. After adjusting for various covariates, logistic regression models showed that the association between ln(GGT/HDL-C) and cognitive dysfunction assessed by total-CF and AFT remained significant [OR (95% CI): 1.374 (1.126~1.676), 1.220 (1.030~1.444)], whereas no significant correlation was found with CERAD W-L or DSST (P>0.05). Then, restricted cubic spline (RCS) regression and threshold effect analyses were conducted, and we observed nonlinear associations between ln(GGT/HDL-C) and cognitive dysfunction measured by total-CF, CERAD W-L and DSST (all $P_{nonlinear}$<0.05). Subgroup analyses were performed based on multiple variables, including age, gender, BMI, race, education level, DM, sleep problems, hypertension, drinking, and smoking status. The results suggested that the association between ln(GGT/HDL-C) and cognitive dysfunction was comparable across most subgroups.

Conclusion: Our study suggested that higher levels of ln(GGT/HDL-C) might be associated with an increased risk of cognitive dysfunction in older adults.**(International Journal of Biomedicine. 2026;16(1):17-25.)**

Keywords: cognitive dysfunction • gamma-glutamyl transferase • high-density lipoprotein cholesterol • cross-sectional study

For citation: Du M, Zhao Y, Zheng P, Xiu X, Li Y, Gu H, Sun J, Zhang L, Liu Z. Gamma-Glutamyl Transferase to High-Density Lipoprotein Cholesterol Ratio as a Marker of Cognitive Dysfunction in Older Adults: A Cross-Sectional Study from NHANES 2011–2014. International Journal of Biomedicine. 2026;16(1):17-25. doi:10.21103/Article16(1)_OA1

Abbreviations

AD, Alzheimer's disease; **AFT**, Animal Fluency Test; **ALT**, alanine aminotransferase; **AST**, aspartate aminotransferase; **BMI**, body mass index; **CERAD W-L**, Consortium to Establish a Registry for Alzheimer's Disease Word Learning subtest; **DSST**, Digit Symbol Substitution Test; **DM**, diabetes mellitus; **DRT**, delayed recall test; **GGT**, gamma-glutamyl transferase; **HDL-C**, high-density lipoprotein cholesterol; **IRT**, immediate recall test; **LDH**, lactate dehydrogenase; **NHANES**, National Health and Nutrition Examination Survey; **RCS**, restricted cubic spline; **total-CF**, total cognitive function; **TG**, triglyceride; **TC**, total cholesterol.

# These authors contributed equally to this work
*Corresponding author

Introduction

Cognitive dysfunction, particularly dementia, has become a major global public health concern due to increased life expectancy and population aging. Worldwide, nearly 57.4 million people are living with dementia. Alzheimer's Disease International (ADI) predicts that this number will increase to 152.8 million in 2050.[1] This increase may occur unless interventions are taken to prevent the occurrence and progression of Alzheimer's disease (AD) or other dementia-related disorders.[2] Despite extensive research efforts over recent decades, effective clinical treatments for dementia remain scarce. Hence, identifying modifiable factors that may lead to cognitive dysfunction is crucial for developing effective preventive strategies.

The pathogenesis of cognitive dysfunction is not fully understood. However, multiple investigations have demonstrated that oxidative stress and inflammation are crucial factors leading to cognitive dysfunction.[3,4] Glutathione is an important antioxidant in cells, and gamma-glutamyl transferase (GGT) is essential for glutathione metabolism. Serum GGT mainly originates from the liver and has been used clinically as an indicator of potential liver or biliary tract diseases.[5,6] Numerous studies have investigated the relationship between GGT levels and dementia. GGT levels, along with GGT variability, have been shown to be positively correlated with cognitive impairment.[7-9] Furthermore, elevated serum GGT levels are significantly linked to reduced total brain and gray matter volumes, as well as diminished cerebral blood flow and perfusion.[10] High-density lipoprotein cholesterol (HDL-C) is considered a beneficial lipoprotein due to its various protective roles, such as promoting atheroprotection, supporting endothelial health, regulating the immune system, inhibiting oxidative stress, reducing inflammation, and providing antithrombotic effects.[11] These functions are essential for preventing cognitive decline. Although the relationship between HDL-C and cognitive dysfunction is inconsistent, various studies have suggested that increased HDL-C levels are correlated with a decreased risk of dementia.[12-14]

Recent studies have highlighted the GGT/HDL-C ratio as a promising new biomarker. Evidence has indicated its utility in predicting nonalcoholic fatty liver disease (NAFLD), liver fibrosis, cardiovascular disease and diabetes mellitus.[15-17] Nonetheless, exploration of its correlation with cognitive function remains limited. Consequently, we employed the NHANES database to retrospectively examine the relationship between the GGT/HDL-C ratio and the risk of cognitive dysfunction.

Materials and Methods

Study Design and Participants

This cross-sectional study uses data from the NHANES database (https://www.cdc.gov/nchs/nhanes). It consists of five main parts: demographic data, dietary data, examination data, laboratory data, and questionnaire data, all updated every two years. Our analysis focused on the 2011-2012 and 2013-2014 surveys, as both cycles evaluated GGT, HDL-C and cognitive function. Approval of the NHANES procedures and protocols was granted by the NCHS Research Ethics Review Committee, and informed consent was secured from all participants.

In this study, we investigated 3,472 subjects from the NHANES 2011-2014 dataset. After excluding individuals with incomplete cognitive function data, missing GGT or HDL-C data, 2,769 participants were ultimately included. The screening process is illustrated in Figure 1.

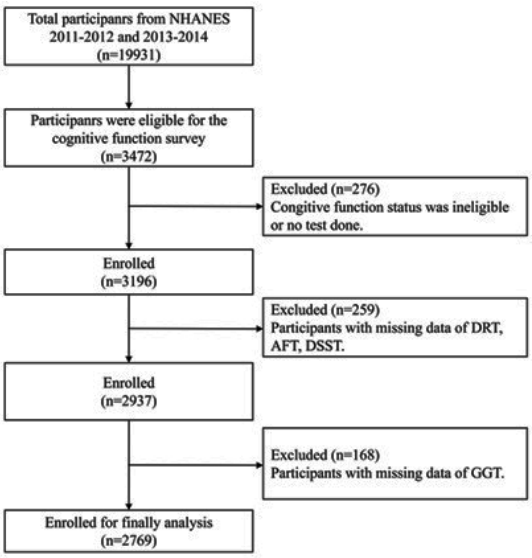

Figure 1. *Flow chart of the participants' selection from the National Health and Nutrition Examination Survey (NHANES) 2011-2014.*

GGT and HDL-C Measurement

The activity of GGT was measured via an enzymatic rate method with a Beckman Coulter UniCel DxC800 instrument. HDL-C levels were determined via polyethylene glycol-coupled cholesteryl esterase with a Roche modular P or Roche Cobas 6000 chemistry analyzer. Additional methodological details of the measurement can be found in the NHANES database.

Identification of Cognitive Dysfunction

This study assessed cognitive dysfunction through three tests: the Consortium to Establish a Registry for Alzheimer's Disease Word Learning subtest (CERAD W-L), the Animal Fluency Test (AFT), and the Digit Symbol Substitution Test (DSST). The CERAD W-L specifically measures both immediate and delayed learning capabilities concerning new verbal information. This assessment comprises three immediate recall tests (IRTs) and a delayed recall test (DRT). The IRT scores were processed as follows: for participants who completed two or three trials, the IRT score was determined by averaging the two highest scores, and for those who took only one test, that score was the IRT score. The sum of the IRT and DRT score was CERAD W-L score. The AFT evaluates verbal fluency, an aspect of executive function, while also assessing semantic memory and processing speed. The DSST, a subset of the Wechsler Adult Intelligence Scale III, assesses

processing speed, sustained attention, and working memory. The total cognitive function (total-CF) score is the aggregate of the CERAD W-L, AFT and DSST scores. As previously reported, the participants were divided into three age groups (60~69, 70~79, and ≥80 years). For each group, the lowest quartile of the cognitive function score (Supplementary Table 1) was set as the threshold for defining cognitive dysfunction.[18] Participants who scored below the cutoff values were classified as having cognitive dysfunction, whereas those who scored above the cutoff values were categorized as having normal cognitive performance.

Covariates

This analysis included a series of covariates. The demographic data included age, gender, BMI, race (divided into Mexican American, other Hispanic, non-Hispanic White, non-Hispanic Black, and other races), education level (below high school, high school and higher than high school), smoking status and drinking status. Medical conditions included hypertension, diabetes mellitus (DM) and sleep problems. The examination results included alanine aminotransferase (ALT), aspartate aminotransferase (AST), lactate dehydrogenase (LDH), triglyceride (TG) and total cholesterol (TC) levels. Smoking status was divided into two groups (yes or not) on the basis of self-reports to the question "Smoked at least 100 cigarettes in life." Participants were defined as alcohol drinkers if they had ever had at least 12 alcohol drinks lifetime. A history of hypertension and sleep problems was defined as self-reported or physician diagnosis. Diabetes mellitus was defined by any of the following criteria: a medical diagnosis of diabetes, HbA1c(%) ≥6.5, fasting glucose level ≥7.0 mmol/L, or 2h OGTT blood glucose ≥11.1 mmol/L.

Statistical analysis

Data processing and analysis were performed using SPSS software (version 21.0), R (version 4.3.3), and Zstats 1.0 (www.zstats.net). Normally distributed data were reported as mean ± standard deviation (SD), and the differences between groups were evaluated by One-Way ANOVA. Nonnormally distributed variables were presented as median (M) and interquartile range (IQR), and the Kruskal-Wallis test was used to detect the differences among groups. Categorical variables were expressed as case numbers (n) and frequencies (percentages), and χ^2-test was used for inter-group comparison. Because the GGT/HDL-C ratio was significantly skewed, a natural logarithm transformation (ln) was performed before analysis. $P<0.05$ was considered statistically significant.

Logistic regression models were used to calculate the odds ratios (ORs) and 95% confidence intervals (95% CIs) for the association between ln(GGT/HDL-C) and cognitive dysfunction. Model 1 was unadjusted. Model 2 was adjusted for age, gender, BMI, race, education level, DM, hypertension, sleep problems, ALT, AST, LDH, TG, TC, smoking and drinking status. Subsequently, ln(GGT/HDL-C) was processed from a continuous variable to a four-categorical variable to test for trends.

Furthermore, we employed restricted cubic spline (RCS) regression models to investigate the potential nonlinear relationship between ln(GGT/HDL-C) and cognitive dysfunction. P for nonlinearity <0.05 indicates a nonlinear relationship. Threshold effect analyses were performed to calculate the turning points within Model 2. Subgroup analyses and interaction tests were conducted to identify other relevant risk factors that may influence the association between ln(GGT/HDL-C) and cognitive dysfunction.

Results

ln(GGT/HDL-C) was divided into quartiles: Q1 (≤2.29), Q2 (2.29~2.69), Q3 (2.69~3.15), and Q4 (≥3.15) (Table 1). The analysis revealed that participants with higher ln(GGT/HDL-C) levels had lower scores in CERAD W-L, AFT, DSST, and total-CF. They also displayed higher body mass index (BMI), fasting glucose, HbA1c, ALT, AST, TG levels, history of DM, hypertension, sleep problems and smoking status. The four groups also differed in race, education level, gender and TC, and showed no significant difference in drinking status.

Table 2 illustrates the associations between ln(GGT/HDL-C) and cognitive dysfunction. Model 1 revealed significant correlations between ln(GGT/HDL-C) and cognitive dysfunction assessed by the CERAD W-L, AFT, DSST and total-CF ($P<0.05$). Specifically, the data indicated that for each unit increment in ln(GGT/HDL-C), the risk of cognitive dysfunction evaluated by the CERAD W-L, AFT, DSST or total-CF was increased 28.6%, 21.4%, 36.5% or 39.7% respectively [OR (95% CI): 1.286 (1.139~1.451), 1.214 (1.078~1.366), 1.365 (1.210~1.541) and 1.397 (1.236~1.578)]. After adjusting for various covariates, the associations between ln(GGT/HDL-C) and total-CF, as well as AFT, remained significant [OR (95% CI): 1.374 (1.126~1.676), 1.220 (1.030~1.444)], while no significant associations were found with CERAD W-L or DSST ($P>0.05$).

Furthermore, the ORs for cognitive dysfunction were computed for each ln(GGT/HDL-C) quartile using Q1 as the reference category. After multivariate adjustments, the OR for cognitive dysfunction assessed by total-CF was 1.540 (95% CI: 1.075~2.207, $P=0.019$, $P_{trend}= 0.012$). For AFT, the OR was 1.394 (95% CI: 1.024~1.897, $P=0.035$, $P_{trend}= 0.072$) for the highest quartile.

In Model 2, further exploration of the relationship between ln(GGT/HDL-C) and cognitive dysfunction evaluated by total-CF revealed a nonlinear relationship (Figure 2A). A two-piecewise logistic regression model was used to calculate the threshold effect. If the P value for the likelihood test is <0.05, it means the two-piecewise logistic regression model is superior to the single-line logistic regression model.[19] We observed that the inflection point was 3.055 (Table 3). Before reaching the inflection point, no correlation was identified [OR (95% CI): 1.044 (0.702~1.555), $P=0.830$], and above the inflection point, a significant association was identified with an OR of 2.091 (95% CI: 1.360~3.216). Similarly, a nonlinear relationship was observed between ln(GGT/HDL-C) and cognitive dysfunction assessed by CERAD W-L or DSST (Figure 2B, 2D), which was further supported by the threshold effect analysis (Table 3). However, there was no correlation observed between ln(GGT/HDL-C) and cognitive dysfunction evaluated by AFT in the RCS curve (Figure 2C).

Table 1.

Baseline characteristics of participants grouped according to ln(GGT/HDL-C) quartiles.

	Total	Q1	Q2	Q3	Q4	*P*-value
ln(GGT/HDL-C)	2.69 (2.29, 3.15)	2.05 (1.84, 2.17)	2.50 (2.39, 2.61)	2.90 (2.79, 3.02)	3.55 (3.33, 3.90)	-
Age (years)	69.46±6.79	70.54±6.97	70.03±6.78	69.03±6.61	68.20±6.54	<0.001
BMI (kg/m^2)	29.06±6.32	26.99±6.05	29.09±6.59	29.95±6.08	30.26±6.03	<0.001
Gender						
Male	1357 (49.01)	205 (29.40)	307 (43.60)	426 (62.10)	419 (61.50)	<0.001
Female	1412 (50.99)	493 (70.60)	397 (56.40)	260 (37.90)	262 (38.50)	
CERAD W-L	13.5 (10.5, 16.0)	14.0 (10.5, 16.5)	13.5 (11.0, 16.0)	13.0 (10.5, 15.5)	13.0 (10.5, 15.5)	0.001
AFT	16.0 (13.0, 20.0)	17.0 (13.0, 20.0)	16.0 (13.0, 20.0)	16.0 (13.0, 20.0)	16.0 (12.0, 20.0)	0.027
DSST	46.0 (33.0, 59.0)	49.0 (36.0, 62.0)	46.0 (34.0, 59.0)	45.0 (33.0, 56.0)	43.0 (31.5, 56.0)	<0.001
total-CF	76.0 (59.0, 92.5)	80.0 (62.5, 97.5)	76.5 (60.5, 92.9)	75.0 (58.5, 89.5)	72.0 (56.5, 89.0)	<0.001
FG (mmol/L)	6.41±1.97	5.82±1.32	6.29±1.80	6.71±2.29	6.89±2.19	<0.001
HbA1c (%)	6.07±1.09	5.79±0.82	5.95±0.82	6.23±1.29	6.31±1.26	<0.001
ALT (U/L)	20 (16, 25)	17 (14, 21)	18 (15, 22)	20 (16, 26)	25 (19, 32)	<0.001
AST (U/L)	23 (20, 27)	22 (19, 26)	23 (20, 26)	23 (20, 27)	26 (22, 33)	<0.001
LDH (U/L)	131 (117, 148)	134 (119, 150)	131 (115, 147)	130 (116, 146)	131 (117, 152)	0.022
TG (mmol/L)	1.41 (0.95, 2.13)	1.04 (0.77, 1.46)	1.36 (0.98, 1.89)	1.61 (1.13, 2.38)	1.87 (1.24, 2.90)	<0.001
TC (mmol/L)	4.89 (4.16, 5.64)	5.12 (4.34, 5.87)	4.89 (4.19, 5.61)	4.80 (4.09, 5.59)	4.76 (3.98, 5.51)	<0.001
Race						
MA	244 (8.81)	46 (6.60)	63 (8.90)	56 (8.20)	79 (11.60)	<0.001
OH	278 (10.04)	52 (7.40)	74 (10.50)	77 (11.20)	75 (11.00)	
NHW	1352 (48.83)	403 (57.70)	355 (50.40)	309 (45.00)	285 (41.90)	
NHB	630 (22.75)	123 (17.60)	147 (20.90)	184 (26.80)	176 (25.80)	
OR	265 (9.57)	74 (10.60)	65 (9.20)	60 (8.70)	66 (9.70)	
Education level						
BHS	690 (24.94)	134 (19.20)	171 (24.30)	189 (27.60)	196 (28.80)	<0.001
HS	657 (23.74)	157 (22.50)	157 (22.30)	171 (24.90)	172 (25.30)	
AHS	1420 (51.32)	407 (58.30)	376 (53.40)	325 (47.40)	312 (45.90)	
DM						
No	1865 (69.75)	562 (82.80)	503 (74.00)	417 (63.50)	383 (58.20)	<0.001
Yes	809 (30.25)	117 (17.20)	177 (26.00)	240 (36.50)	275 (41.80)	
Hypertension						
No	1044 (37.77)	320 (45.90)	269 (38.40)	250 (36.40)	205 (30.10)	<0.001
Yes	1720 (62.23)	377 (54.10)	432 (61.60)	436 (63.60)	475 (69.90)	
High cholesterol						
No	1198 (43.56)	353 (50.90)	297 (42.30)	266 (39.00)	282 (42.00)	<0.001
Yes	1552 (56.44)	341 (49.10)	405 (57.70)	416 (61.00)	390 (58.00)	
Sleep problems						
No	1860 (67.17)	482 (69.10)	485 (68.90)	465 (67.80)	428 (62.80)	0.047
Yes	909 (32.83)	216 (30.90)	219 (31.10)	221 (32.20)	253 (37.20)	
Drinking status						
No	425 (15.61)	121 (17.60)	118 (17.10)	100 (14.80)	86 (12.90)	0.064
Yes	2298 (84.39)	567 (82.40)	574 (82.90)	575 (85.20)	582 (87.10)	
Smoking status						
No	1366 (49.37)	413 59.30)	368 (52.30)	314 (45.80)	271 (39.90)	<0.001
Yes	1401 (50.63)	284 (40.70)	336 (47.70)	372 (54.20)	409 (60.10)	

Abbreviations: *FG, fasting glucose; ALT, alanine aminotransferase; AST, aspartate aminotransferase; LDH, lactate dehydrogenase; TG, triglycerides; TC, total cholesterol; DM, diabetes mellitus; MA, Mexican American; OH, other Hispanic; NHW, non-Hispanic White; NHB, non-Hispanic Black; NHA, non-Hispanic Asian; OR, other races; BHS, below high school; HS, high school; AHS, above high school.*

Table 2.

Association between ln(GGT/HDL-C) and cognitive dysfunction.

	total-CF			
	Model 1	*P*-value	Model 2	*P*-value
ln(GGT/HDL-C)	1.397 (1.236~1.578)	<0.001	1.374 (1.126~1.676)	0.002
ln(GGT/HDL-C) quartile				
Q1 2.05 (≤2.29)	1(reference)		1(reference)	
Q2 2.50 (2.29-2.69)	1.180 (0.915~1.521)	0.203	1.033 (0.747~1.429)	0.846
Q3 2.90 (2.69-3.15)	1.435 (1.118~1.843)	0.005	1.067 (0.763~1.492)	0.706
Q4 3.55 (≥3.15)	1.782 (1.394~2.278)	<0.001	1.540 (1.075~2.207)	0.019
P_{trend}		<0.001		0.012
	CERAD W-L			
	Model 1	*P*-value	Model 2	*P*-value
ln(GGT/HDL-C)	1.286 (1.139~1.451)	<0.001	1.187 (0.998~1.411)	0.053
ln(GGT/HDL-C) quartile				
Q1 2.05 (≤2.29)	1(reference)		1(reference)	
Q2 2.50 (2.29-2.69)	1.021 (0.797~1.308)	0.869	0.896 (0.679~1.183)	0.440
Q3 2.90 (2.69-3.15)	1.160 (0.907~1.483)	0.236	0.868 (0.648~1.163)	0.343
Q4 3.55 (≥3.15)	1.570 (1.237~1.994)	<0.001	1.258 (0.921~1.717)	0.149
P_{trend}		<0.001		0.095
	AFT			
	Model 1	*P*-value	Model 2	*P*-value
ln(GGT/HDL-C)	1.214 (1.078~1.366)	0.001	1.220 (1.030~1.444)	0.021
ln(GGT/HDL-C) quartile				
Q1 2.05 (≤2.29)	1(reference)		1(reference)	
Q2 2.50 (2.29-2.69)	1.335 (1.052~1.693)	0.017	1.323 (1.010~1.734)	0.042
Q3 2.90 (2.69-3.15)	1.338 (1.053~1.699)	0.017	1.236 (0.927~1.649)	0.148
Q4 3.55 (≥3.15)	1.479 (1.165~1.875)	0.001	1.394 (1.024~1.897)	0.035
P_{trend}		0.003		0.072
	DSST			
	Model 1	*P*-value	Model 2	*P*-value
ln(GGT/HDL-C)	1.365 (1.210~1.541)	<0.001	1.174 (0.965~1.428)	0.109
ln(GGT/HDL-C) quartile				
Q1 2.05 (≤2.29)	1(reference)		1(reference)	
Q2 2.50 (2.29-2.69)	1.164 (0.906~1.495)	0.235	0.899 (0.652~1.241)	0.519
Q3 2.90 (2.69-3.15)	1.432 (1.120~1.832)	0.004	0.955 (0.685~1.330)	0.785
Q4 3.55 (≥3.15)	1.735 (1.362~2.210)	<0.001	1.239 (0.868~1.767)	0.238
P_{trend}		<0.001		0.149

Notes: *Model 1: unadjusted; Model 2: adjusted for age, gender, BMI, race, education level, DM, hypertension, sleep problems, drinking status, smoking status, ALT, AST, LDH, TG and TC.*

Table 3.

Threshold effect analysis of ln(GGT/HDL-C) on cognitive dysfunction.

	total-CF		CERAD W-L		AFT		DSST	
	OR (95% CI)	*P*	OR (95% CI)	*P*	OR (95% CI)	*P*	OR (95% CI)	*P*
Model A	1.374 (1.126~1.677)	0.002	1.187 (0.999~1.412)	0.052	1.219 (1.030~1.444)	0.021	1.174 (0.965~1.428)	0.108
Model B Inflection point	3.055		3.019		2.361		2.848	
< Inflection point	1.044 (0.702~1.555)	0.830	1.008 (0.710~1.432)	0.962	1.297 (0.586~2.874)	0.521	0.806 (0.507~1.281)	0.361
≥ Inflection point	2.091 (1.360~3.216)	<0.001	1.697 (1.178~2.444)	0.004	1.173 (0.940~1.464)	0.159	1.625 (1.134~2.329)	0.008
P for likelihood test		0.013		0.020		0.371		0.021

Notes: *Model A: Fitting model by single line regression; Model B: Fitting model by two piecewise linear regression. P for likelihood test <0.05, it means model B is superior to model A.*

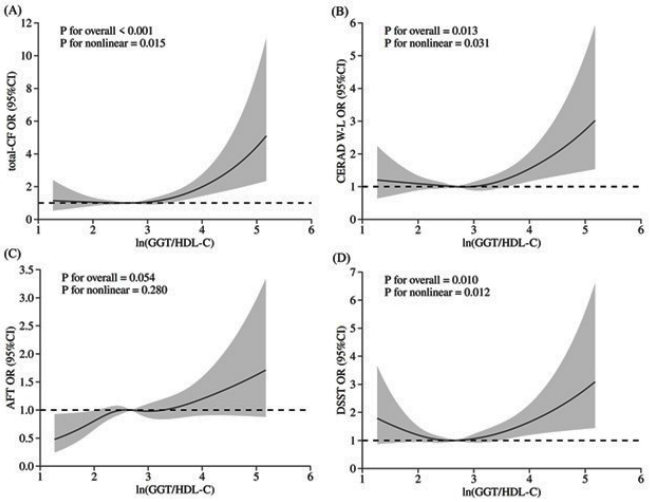

Figure 2. *Restricted cubic spline (RCS) analysis between ln(GGT/HDL-C) and cognitive dysfunction assessed by total-CF (A), CERAD W-L (B), AFT (C), or DSST (D).*

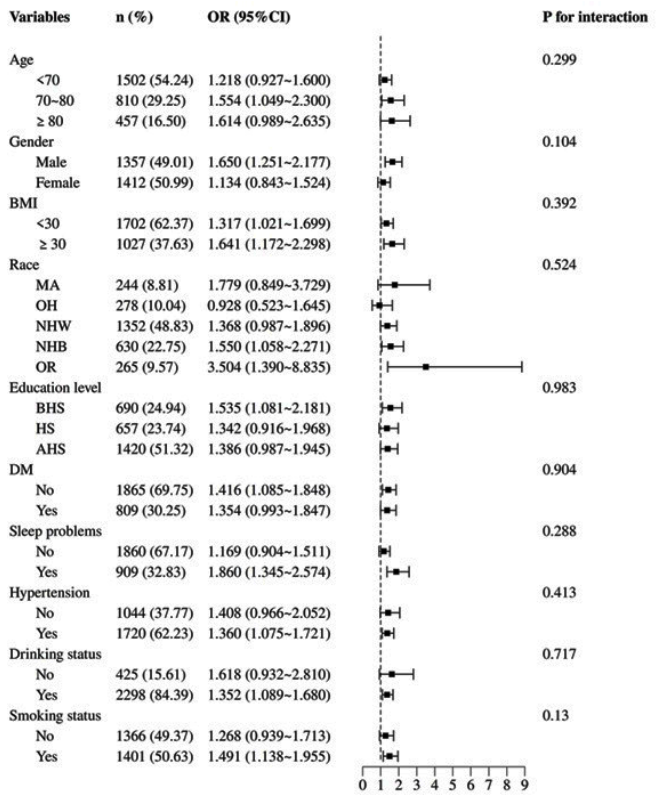

Figure 3. *Forest map of ORs for the relationship between ln(GGT/HDL-C) and cognitive dysfunction stratified by different subgroups.*

Subgroup analyses were performed based on multiple variables including age, gender, BMI, race, education level, DM, sleep problems, hypertension, drinking and smoking status. These analyses accounted for all confounding variables except the grouping variable itself. There were no significant interactions between subgroup variables and ln(GGT/HDL-C), with all $P_{interaction}$>0.05 (Figure 3). The results suggested that the associations of ln(GGT/HDL-C) with cognitive dysfunction were comparable in most subpopulations.

Discussion

In this study, we evaluated the relationship between ln(GGT/HDL-C) and cognitive dysfunction in 2,769 participants aged 60 years and older from the NHANES 2011-2014 cycles. After adjusting for covariates, we discovered that ln(GGT/HDL-C) was positively associated with the risk of cognitive dysfunction assessed by total-CF.

Previous studies have established associations between GGT or HDL-C and cognitive function. In a large-scale population of middle-aged to older Finnish men, GGT was positively associated with the future risk of dementia.[8] Research conducted among Chinese female patients with mild cognitive impairment has shown similar results.[7] Additionally, Lee et al.[9] indicated that both baseline GGT and GGT variability are independent predictors of dementia. Zhang et al.[20] identified a nonlinear relationship wherein the risk of cognitive impairment escalated with increasing GGT levels in 25~94 U/L. Consistent with the above results, our study demonstrated that elevated GGT levels were associated with an increased risk of cognitive dysfunction and for every one unit increase in GGT, the risk increased by 0.7% (Supplementary Table 2). Although Kunutsor et al.[21] did not find a strong causal relationship between GGT and AD via the mendelian randomization method, the potential pro-inflammatory and pro-oxidative roles of GGT may significantly contribute to cognitive dysfunction. Moreover, GGT levels are directly implicated in atheromatous plaque formation, which is also considered as a fundamental pathological mechanism underlying cognitive impairment.[7]

The correlation between HDL-C and cognitive dysfunction is still controversial. Previous studies have suggested that higher levels of HDL-C are linked to improved cognitive function, while lower HDL-C levels are related to adverse outcomes.[14,22-25] These findings underscore the potential benefits of high HDL-C for preserving cognitive function during aging. However, our study did not identify a correlation between HDL-C and overall cognitive function (Supplementary Table 3), and similar results have been reported.[26,27] In addition, compared with that in women, the HDL-C level in men was negatively correlated with the risk of AFT injury (Supplementary Table 3), which is like the results reported by Boccardi et al.[28] The differences in the correlation between HDL-C and cognitive function may be influenced by multiple factors, including age, gender, stage of cognitive impairment, assessment criteria and the nonlinear relationship between them, and even by other lipid levels.[28-31]

Notably, a recent study conducted by Wang et al.[32] provided initial evidence of a negative correlation between the GGT/HDL-C ratio and cognitive performance (assessed by DSST score) in older adults, with diabetes mellitus serving as a mediator. In our study, we incorporated multiple indicators and constructed a composite cognitive score (total-CF), which could reduce measurement bias from single-indicator assessment and provide a more holistic representation of global cognitive capacity. Furthermore, unlike the data-analytical approach adopted by Wang et al., we focused on the relationship between ln(GGT/HDL-C) and the risk of cognitive

dysfunction and thus employed logistic regression analysis. Although no significant association was observed between ln(GGT/HDL-C) and cognitive dysfunction (assessed by DSST) in the adjusted model (Table 2), subsequent restricted cubic spline (RCS) and threshold effect analyses revealed a nonlinear association: for each 1-unit increase in ln(GGT/HDL-C) above the threshold of 2.848, the risk of cognitive dysfunction increased by 62.5%. In summary, the two studies are fundamentally consistent in confirming the association between the GGT/HDL-C ratio and cognitive function, albeit with differences in assessment methods and analytical depth.

The GGT/HDL-C ratio provides a comprehensive measure that reflects the interplay between liver enzyme and serum lipid concentrations in relation to cognitive dysfunction. The potential mechanisms underlying the association between an elevated GGT/HDL-C ratio, positively associated with the risk of cognitive dysfunction, may include the following: 1) The elevation of GGT levels potentially exacerbates oxidative damage within the brain by disrupting glutathione metabolism, while the anti-inflammatory and antioxidant functions of HDL-C are inhibited, which may weaken the protection of neurons and blood vessels; 2) abnormalities of GGT and HDL-C may reflect endothelial dysfunction or arteriosclerosis, resulting in reduced cerebral blood flow and microvascular lesions; 3) an increased GGT/HDL-C ratio acts as an indicator of metabolic disturbances that may indirectly impair cognitive function through mechanisms such as insulin resistance, obesity, or diabetes; and 4) impaired liver function (indicated by elevated GGT) potentially affects neurological health by crossing the blood-brain barrier via inflammatory mediators or toxins such as ammonia. However, the exact mechanism requires further investigation.

The main advantage of our study is that it used the NHANES database, allowing us to obtain a large sample size. Additionally, three standard tests were employed, and a comprehensive score was generated to assess cognitive performance. We used a different method from previous studies to calculate the IRT score. This approach reduces the impact of deviations among the three trials. Furthermore, as a new indicator, GGT/HDL-C may explain the impact of the interaction between oxidative stress and lipid metabolism on cognition.

However, it is imperative to recognize the potential limitations of our research. First, the study design precludes the establishment of causality. Second, the possibility of residual confounding variables remains elusive. Finally, it is important to note that our research did not include a clinical assessment that could diagnose and further stratify cognitive dysfunction. Therefore, further prospective studies or fundamental research are necessary to elucidate the causal relationships and mechanisms between GGT/HDL-C and cognitive dysfunction.

In conclusion, our study suggested that higher levels of ln(GGT/HDL-C) might be associated with an increased risk of cognitive dysfunction in older adults.

Data Availability

Publicly available datasets were analyzed in this study. The data can be found at: https://www.cdc.gov/nchs/nhanes.

Sources of Funding

This study was supported by the Shijiazhuang Science and Technology Planning Project (2414606003) and the Medical Science Research Project of Hebei (20231625).

Ethical Statement

Approval for the NHANES procedures and protocols was granted by the NCHS Research Ethics Review Committee, and informed consent was obtained from all participants. Under the premise of complying with data usage specifications, this study is exempt from obtaining secondary informed consent.

Competing Interests

The authors declare that they have no conflicts of interest.

References

1. Gauthier S, Rosa-Neto P, Morais JA, Webster C. World Alzheimer Report 2021: Journey through the Diagnosis of Dementia. Alzheimer's Disease International; London, UK: 2021.
2. Kivipelto M, Mangialasche F, Snyder HM, Allegri R, Andrieu S, Arai H, et al. World-Wide FINGERS Network: A global approach to risk reduction and prevention of dementia. Alzheimers Dement. 2020 Jul;16(7):1078-1094. doi: 10.1002/alz.12123. Epub 2020 Jul 5. PMID: 32627328.
3. Zafrilla P, Mulero J, Xandri JM, Santo E, Caravaca G, Morillas JM. Oxidative stress in Alzheimer patients in different stages of the disease. Curr Med Chem. 2006;13(9):1075-83. doi: 10.2174/092986706776360978. PMID: 16611085.
4. Gackowski D, Rozalski R, Siomek A, Dziaman T, Nicpon K, Klimarczyk M, et al. Oxidative stress and oxidative DNA damage is characteristic for mixed Alzheimer disease/vascular dementia. J Neurol Sci. 2008 Mar 15;266(1-2):57-62. doi: 10.1016/j.jns.2007.08.041.
5. Gasecka A, Siwik D, Gajewska M, Jaguszewski MJ, Mazurek T, Filipiak KJ, et al. Early Biomarkers of Neurodegenerative and Neurovascular Disorders in Diabetes. J Clin Med. 2020 Aug 30;9(9):2807. doi: 10.3390/jcm9092807.
6. Kunutsor SK. Gamma-glutamyltransferase-friend or foe within? Liver Int. 2016 Dec;36(12):1723-1734. doi: 10.1111/liv.13221.
7. Tang Z, Chen X, Zhang W, Sun X, Hou Q, Li Y, et al. Association Between Gamma-Glutamyl Transferase and Mild Cognitive Impairment in Chinese Women. Front Aging Neurosci. 2021 Feb 10;13:630409. doi: 10.3389/fnagi.2021.630409.
8. Kunutsor SK, Laukkanen JA. Gamma glutamyltransferase and risk of future dementia in middle-aged to older Finnish men: A new prospective cohort study. Alzheimers Dement. 2016 Sep;12(9):931-941. doi: 10.1016/j.jalz.2016.03.003.
9. Lee YB, Han K, Park S, Kim SM, Kim NH, Choi KM, et al. Gamma-glutamyl transferase variability and risk of dementia: A nationwide study. Int J Geriatr Psychiatry. 2020 Oct;35(10):1105-1114. doi: 10.1002/gps.5332.

10. Yilmaz P, Alferink LJM, Cremers LGM, Murad SD, Niessen WJ, Ikram MA, Vernooij MW. Subclinical liver traits are associated with structural and hemodynamic brain imaging markers. Liver Int. 2023 Jun;43(6):1256-1268. doi: 10.1111/liv.15549.
11. Navab M, Reddy ST, Van Lenten BJ, Fogelman AM. HDL and cardiovascular disease: atherogenic and atheroprotective mechanisms. Nat Rev Cardiol. 2011 Apr;8(4):222-32. doi: 10.1038/nrcardio.2010.222.
12. Reitz C, Tang MX, Schupf N, Manly JJ, Mayeux R, Luchsinger JA. Association of higher levels of high-density lipoprotein cholesterol in elderly individuals and lower risk of late-onset Alzheimer disease. Arch Neurol. 2010 Dec;67(12):1491-7. doi: 10.1001/archneurol.2010.297.
13. van den Kommer TN, Dik MG, Comijs HC, Jonker C, Deeg DJ. Role of lipoproteins and inflammation in cognitive decline: do they interact? Neurobiol Aging. 2012 Jan;33(1):196.e1-12. doi: 10.1016/j.neurobiolaging.2010.05.024.
14. Crichton GE, Elias MF, Davey A, Sullivan KJ, Robbins MA. Higher HDL cholesterol is associated with better cognitive function: the Maine-Syracuse study. J Int Neuropsychol Soc. 2014 Nov;20(10):961-70. doi: 10.1017/S1355617714000885.
15. Jung DH, Park B, Ryu HE, Lee YJ. Sex-specific associations of γ-glutamyltransferase to HDL-cholesterol ratio and the incident risk of cardiovascular disease: three Korean longitudinal cohorts from different regions. Front Endocrinol (Lausanne). 2023 Aug 15;14:1231502. doi: 10.3389/fendo.2023.1231502.
16. Liang S, Yang T. Analysis of the Association Between Changes in the GGT/HDL-C Ratio and the Risk of Diabetes Mellitus Based on a Latent Class Growth Mixed Modeling: A Longitudinal Cohort Study of Adults in China. Diabetes Metab Syndr Obes. 2024 Aug 24;17:3139-3150. doi: 10.2147/DMSO.S475067.
17. Xuan Y, He F, Liu Q, Dai D, Wu D, Shi Y, et al. Elevated GGT to HDL ratio as a marker for the risk of NAFLD and liver fibrosis. Sci Rep. 2025 Jan 2;15(1):10. doi: 10.1038/s41598-024-84649-w.
18. Li S, Sun W, Zhang D. Association of Zinc, Iron, Copper, and Selenium Intakes with Low Cognitive Performance in Older Adults: A Cross-Sectional Study from National Health and Nutrition Examination Survey (NHANES). J Alzheimers Dis. 2019;72(4):1145-1157. doi: 10.3233/JAD-190263.
19. Shi Y, Yu C. U shape association between triglyceride glucose index and congestive heart failure in patients with diabetes and prediabetes. Nutr Metab (Lond). 2024 Jul 2;21(1):42. doi: 10.1186/s12986-024-00819-7.
20. Zhang YL, Jia SY, Yang B, Miao J, Su C, Cui ZG, et al. Non-linear association of liver enzymes with cognitive performance in the elderly: A cross-sectional study. PLoS One. 2024 Jul 23;19(7):e0306839. doi: 10.1371/journal.pone.0306839.
21. Kunutsor SK, Laukkanen JA, Burgess S. Genetically elevated gamma-glutamyltransferase and Alzheimer's disease. Exp Gerontol. 2018 Jun;106:61-66. doi: 10.1016/j.exger.2018.03.001.
22. Formiga F, Ferrer A, Chivite D, Pinto X, Badia T, Padrós G, Pujol R. Serum high-density lipoprotein cholesterol levels correlate well with functional but not with cognitive status in 85-year-old subjects. J Nutr Health Aging. 2012 May;16(5):449-53. doi: 10.1007/s12603-012-0018-z.
23. Bates KA, Sohrabi HR, Rainey-Smith SR, Weinborn M, Bucks RS, Rodrigues M, et al. Serum high-density lipoprotein is associated with better cognitive function in a cross-sectional study of aging women. Int J Neurosci. 2017 Mar;127(3):243-252. doi: 10.1080/00207454.2016.1182527.
24. Svensson T, Sawada N, Mimura M, Nozaki S, Shikimoto R, Tsugane S. The association between midlife serum high-density lipoprotein and mild cognitive impairment and dementia after 19 years of follow-up. Transl Psychiatry. 2019 Jan 18;9(1):26. doi: 10.1038/s41398-018-0336-y.
25. Arafa A, Kawachi H, Kato Y, Nosaka S, Teramoto M, Khairan P, et al. The association between serum cholesterol levels and mild-to-moderate cognitive impairment in the Suita Study and evidence from other epidemiological studies. J Neurol Sci. 2024 Nov 15;466:123244. doi: 10.1016/j.jns.2024.123244.
26. Power MC, Rawlings A, Sharrett AR, Bandeen-Roche K, Coresh J, Ballantyne CM, et al. Association of midlife lipids with 20-year cognitive change: A cohort study. Alzheimers Dement. 2018 Feb;14(2):167-177. doi: 10.1016/j.jalz.2017.07.757.
27. Yu Y, Yan P, Cheng G, Liu D, Xu L, Yang M, et al. Correlation between serum lipid profiles and cognitive impairment in old age: a cross-sectional study. Gen Psychiatr. 2023 Apr 28;36(2):e101009. doi: 10.1136/gpsych-2023-101009.
28. Boccardi V, Mancinetti F, Guazzarini AG, Murasecco I, Melis F, Bastiani P, Scamosci M, Cecchetti R, Mecocci P. Sex-specific associations between serum lipid levels and cognitive performance in older adults: results from a cross-sectional real-world study. Aging Clin Exp Res. 2025 Mar 1;37(1):62. doi: 10.1007/s40520-025-02976-y.
29. Hussain SM, Robb C, Tonkin AM, Lacaze P, Chong TT, Beilin LJ, Yu C, Watts GF, Ryan J, Ernst ME, Zhou Z, Neumann JT, McNeil JJ. Association of plasma high-density lipoprotein cholesterol level with risk of incident dementia: a cohort study of healthy older adults. Lancet Reg Health West Pac. 2023 Nov 29;43:100963. doi: 10.1016/j.lanwpc.2023.100963.
30. Huang H, Yang B, Yu R, Ouyang W, Tong J, Le Y. Very high high-density lipoprotein cholesterol may be associated with higher risk of cognitive impairment in older adults. Nutr J. 2024 Jul 17;23(1):79. doi: 10.1186/s12937-024-00983-9.
31. Ferguson EL, Zimmerman SC, Jiang C, Choi M, Meyers TJ, Hoffmann TJ, Gilsanz P, Oni-Orisan A, Wang J, Whitmer RA, Risch N, Krauss RM, Schaefer CA, Glymour MM. Independent associations of high-density lipoprotein cholesterol and triglyceride levels with Alzheimer's disease and related dementias. Alzheimers Dement. 2025 Feb;21(2):e14575. doi: 10.1002/alz.14575.
32. Wang Y, Mao Y, Xu T, Han L, Zhang W, Sun W, Xu J, Yu E. A cross sectional study of the diabetes mediated GGT to HDL ratio and cognitive function in older adults. Sci Rep. 2025 Jul 1;15(1):20928. doi: 10.1038/s41598-025-06439-2.

***Corresponding author**: Zanchao Liu; Email: liuzanchao2007@163.com; Shijiazhuang Second Hospital, Shijiazhuang, China*

Supplementary Material

Supplementary Table 1.

Cutoff values for cognitive dysfunction across age groups.

Age (years)	total-CF	CERAD W-L	AFT	DSST
60-69	64.5	11.5	14.0	37.0
70-79	57.0	10.5	12.0	32.0
≥80	50.0	8.5	11.0	28.0

Supplementary Table 2.

Association between GGT and cognitive dysfunction.

	total-CF			
	Model 1	*P*-value	Model 2	*P*-value
ln(GGT)	1.360(1.185~1.562)	<0.001	1.361(1.103~1.679)	0.004
GGT	1.006(1.003~1.008)	<0.001	1.007(1.003~1.012)	0.001
Male	1.007(1.003~1.010)	<0.001	1.008(1.002~1.013)	0.008
Female	1.003(0.998~1.007)	0.224	1.010(1.002~1.017)	0.017
	CERAD W-L			
	Model 1	*P*-value	Model 2	*P*-value
ln(GGT)	1.182(1.029~1.357)	0.018	1.183(0.984~1.422)	0.074
GGT	1.004(1.001~1.006)	0.007	1.005(1.001~1.009)	0.006
Male	1.002(0.999~1.006)	0.168	1.003(0.998~1.007)	0.210
Female	1.004(0.999~1.008)	0.093	1.014(1.007~1.021)	<0.001
	AFT			
	Model 1	*P*-value	Model 2	*P*-value
ln(GGT)	1.152(1.007~1.319)	0.040	1.154(0.964~1.380)	0.119
GGT	1.002(0.999~1.004)	0.185	1.003(0.999~1.006)	0.129
Male	1.000(0.996~1.004)	0.991	1.002(0.998~1.007)	0.299
Female	1.005(1.000~1.009)	0.031	1.005(0.999~1.012)	0.103
	DSST			
	Model 1	*P*-value	Model 2	*P*-value
ln(GGT)	1.280(1.116~1.468)	<0.001	1.113(0.904~1.370)	0.314
GGT	1.005(1.002~1.007)	0.001	1.004(1.000~1.008)	0.079
Male	1.006(1.002~1.009)	0.001	1.005(1.000~1.010)	0.070
Female	1.001(0.997~1.006)	0.586	1.003(0.996~1.011)	0.388

Model 1: unadjusted; Model 2: adjusted for age, gender, BMI, race, education level, DM, hypertension, sleep problems, drinking status, smoking status, ALT, AST, LDH, TG, and TC. Male: association of GGT and cognitive dysfunction in male participants. Female: association of GGT and cognitive dysfunction in female participants.

Supplementary Table 3.

Association between HDL-C and cognitive dysfunction.

	total-CF			
	Model 1	*P*-value	Model 2	*P*-value
ln(HDL-C)	0.565(0.419~0.761)	<0.001	0.732(0.439~1.220)	0.231
HDL-C	0.720(0.583~0.890)	0.002	0.896(0.633~1.267)	0.534
Male	0.820(0.594~1.133)	0.229	0.686(0.420~1.120)	0.132
Female	0.781(0.577~1.056)	0.109	1.275(0.764~2.128)	0.352
	CERAD W-L			
	Model 1	*P*-value	Model 2	*P*-value
ln(HDL-C)	0.483(0.358~0.650)	<0.001	0.850(0.547~1.322)	0.471
HDL-C	0.637(0.514~0.788)	<0.001	0.941(0.697~1.270)	0.690
Male	0.832(0.611~1.133)	0.244	0.860(0.573~1.292)	0.468
Female	0.805(0.586~1.106)	0.181	1.109(0.702~1.754)	0.658
	AFT			
	Model 1	*P*-value	Model 2	*P*-value
ln(HDL-C)	0.610 (0.458~0.814	0.001	0.565(0.363~0.879)	0.011
HDL-C	0.715(0.583~0.876)	0.001	0.684(0.506~0.926)	0.014
Male	0.621(0.443~0.872)	0.006	0.589(0.374~0.930)	0.023
Female	0.708(0.535~0.936)	0.015	0.826(0.545~1.252)	0.367
	DSST			
	Model 1	*P*-value	Model 2	*P*-value
ln(HDL-C)	0.486(0.361~0.654)	<0.001	0.606(0.363~1.011	0.055
HDL-C	0.646(0.523~0.799)	<0.001	0.805(0.569~1.139)	0.220
Male	0.750(0.544~1.034)	0.079	0.672(0.412~1.096)	0.111
Female	0.701(0.517~0.951)	0.022	0.980(0.586~1.637)	0.938

Model 1: unadjusted; Model 2: adjusted for age, gender, BMI, race, education level, DM, hypertension, sleep problems, drinking status, smoking status, ALT, AST, LDH, TG, and TC. Male: association of HDL-C and cognitive dysfunction in male participants. Female: association of HDL-C and cognitive dysfunction in female participants.

International Journal of Biomedicine 16(1) (2026) 26-32
http://dx.doi.org/10.21103/Article16(1)_OA2

ORIGINAL ARTICLE

Rheumatology

INTERNATIONAL JOURNAL OF BIOMEDICINE

Interplay of Serum IL-6 and Vitamin D in Overweight, Non-Anemic Women of Reproductive Age with Systemic Lupus Erythematosus

Abdulsalam A. Noorwali[1], Zahir Hussain[2*]

[1]*Department of Internal Medicine, Faculty of Medicine, Umm Al-Qura University, Makkah 21955, Saudi Arabia*
[2]*Department of Physiology, Faculty of Medicine, Umm Al-Qura University, Makkah 21955, Saudi Arabia*

Abstract

Background: Systemic lupus erythematosus (SLE) is a chronic, potentially life-threatening autoimmune disorder that damages various tissues and organs. It is more prevalent in women than in men. Real-world medical practice provides comprehensive clinical and laboratory information. A variety of factors complicate processes in patients with SLE. Two important risk factors, serum interleukin-6 (IL-6) and vitamin D, are to be investigated to determine their precise role in SLE.
Methods and Results: We analyzed variation in serum IL-6 and vitamin D, their association, and other characteristics in normal-weight SLE (NW-SLE) and overweight SLE (OW-SLE), compared with NW controls (NW-C) and OW controls (OW-C). The enzyme-linked immunosorbent assay (ELISA) kit methods were used for diagnostic purposes and to determine vitamin D and IL-6 levels. Conventional methods were used to record the other variables, including hemoglobin (Hb), hepcidin (Hp), body mass index (BMI), menstrual cycle length (MCL), and menstrual phase duration (MPD). Serum levels of IL-6 presented significant variations for NW-SLE compared to NW-C (P<0.02), and OW-SLE compared to OW-C, and OW-SLE compared to NW-SLE (P<0.01). The serum levels of vitamin D indicated a significant difference between OW-SLE compared to NW-SLE (P<0.03) and NW-SLE compared to NW-C, OW-SLE compared to OW-C, and OW-C compared to NW-C (P<0.01). Furthermore, vitamin D and IL-6 showed a significant negative correlation in OW-SLE and NW-SLE patients (P<0.01).
Conclusion: The results of this study highlight the importance of measuring serum IL-6 and vitamin D levels in conjunction with BMI assessment in patients with SLE. This study revealed an inverse relationship between vitamin D and IL-6 in patients with SLE. Since vitamin D is an important modifiable factor in SLE, and its deficiency is associated with disease activity and the risk of complications, correction of vitamin D deficiency can complement standard therapy and improve the prognosis of SLE. (**International Journal of Biomedicine. 2026;16(1):26-32.**)

Keywords: reproductive age women • overweight • non-anemic • systemic lupus erythematosus • interleukin-6 • vitamin D

For citation: Noorwali AA, Hussain Z. Interplay of Serum IL-6 and Vitamin D in Overweight, Non-Anemic Women of Reproductive Age with Systemic Lupus Erythematosus. International Journal of Biomedicine. 2026;16(1):26-32. doi:10.21103/Article16(1)_OA2

Abbreviations

25(OH)D, 25-hydroxyvitamin D; **ADA,** American Diabetes Association; **BMI,** body mass index; **BW,** body weight; **CRP,** C-reactive protein; **dsDNA,** double-stranded DNA; **ELISA,** enzyme linked immunosorbent assay; **Hb,** hemoglobin; **Hp,** hepcidin; **IL-6**, interleukin-6; **KSA,** Kingdom of Saudi Arabia; **MCL,** menstrual cycle length; **MPD,** menstrual phase duration; **NW,** normal weight; **NW-C,** normal weight control; **NW-SLE,** normal weight systemic lupus erythematosus; **OW,** overweight; **OW-SLE,** overweight systemic lupus erythematosus; **SLE,** systemic lupus erythematosus.

Introduction

Systemic lupus erythematosus (SLE) is a chronic, potentially life-threatening autoimmune disorder that can damage multiple tissues and organs.[1] It is more prevalent in women than men.[2] A medical practice specializing in rheumatology provides comprehensive clinical and laboratory information in SLE diagnostics..[3] Interleukin-6

(IL-6) functions as a proinflammatory cytokine in SLE[4,5] by binding to its membrane receptor, IL-6R, on leukocytes and hepatocytes, and contributes significantly to pathogenesis and disease activity. Some of the recent case-control and meta-analyses present elevated levels of IL-6 in patients with SLE.[6-8] Genetic polymorphism studies, however, did not establish a significant association of IL-6 with SLE.[9,10] Furthermore, the therapeutic approaches for blocking IL-6 in SLE did not present the efficacy as appears in other autoimmune diseases, and despite that, IL-6 remains an important factor, especially against certain risks associated with the pathogenesis of SLE and comorbidities.[11]

Another important factor in the pathogenesis of SLE is vitamin D. Vitamin D, a steroid hormone, regulates cell growth and modulates the immune system, and its insufficiency and deficiency complicate these processes in patients with SLE.[12] Pathogenesis of SLE and several other autoimmune diseases emphasize the potential immunomodulatory role of vitamin D.[13] Decreased levels and deficiency of vitamin D obtained in SLE patients indicate the involvement of vitamin D in the increased disease activity in SLE patients[14] though non-significant association of vitamin D has also been reported [15] possibly due to methodological/ study design, different indices employed for assessing the disease activity, little sun exposure, diverse lifestyles, cultural and ethnic background, deficient dietary intake, and geographical and seasonal variations of vitamin D levels.[15,16]The levels of Hb and Hp were investigated in patients with anemia and other hematological abnormalities in patients with SLE.[8,17,18] The influence of overweight status/ obesity on serum vitamin D and immune responses, including IL-6, was investigated in patients with SLE.[19] However, various studies show controversy about the association of BMI and vitamin D, and IL-6 and vitamin D.[16,20,21] The association of serum vitamin D and IL-6 was investigated,[22,23] and that was linked to its therapeutic potential via IL-6 and other pro-inflammatory biomarkers.[24,25]

The important roles of IL-6 and vitamin D in inflammation, immune processes, injury, and related aspects are established. Understanding their impact on SLE pathogenesis is essential. However, further research is needed to clarify the interaction between IL-6 and vitamin D in patients with SLE. We analyzed changes in serum IL-6 and vitamin D levels and their relationship, along with other characteristic features, in normal-weight and overweight patients with SLE.

Materials and Methods

A current case-control observational study was conducted at Umm Al-Qura University (UQU) and associated hospitals/clinical institutions in Makkah, Kingdom of Saudi Arabia (KSA). The study was conducted from January 1, 2023, to April 10, 2025. The number of reproductive-age women subjects in the current study (n = 409) exceeded the calculated sample size (385). Age (years) and body mass index (BMI, kg/m^2) matched subjects were consulted. Age range was 20-29 in the normal-weight controls (NW-C, n=105, BMI range: 18.5-24.9 kg/m^2), overweight controls (OW-C, n=105, BMI range: 25-29.9 kg/m^2), NW-SLE (n=100, BMI range: 18.5-24.9 kg/m^2), and OW-SLE (n=99, BMI range: 25-29.9 kg/m^2) women subjects.

The women of reproductive age included in the present work were not pregnant or breastfeeding. Obtaining subjects' consent was considered necessary. Samples/history were obtained only from ovulatory menstrual cycles. Only women with BMI levels not less than 18.5 kg/m^2 and not more than 24.9 kg/m^2 for NW-C and NW-SLE, and not less than 25 kg/m^2 and not more than 29.9 kg/m^2 for OW-C and OW-SLE, were included in the present study. Furthermore, they were not anemic, smokers, or had serious medical complications.

BMI, menstrual cycle length (MCL), menstrual phase duration (MPD), and other subject characteristics were recorded using a questionnaire.

For the identification and proper diagnosis of SLE, the key biomarker, anti-double-stranded DNA (anti-dsDNA) antibodies, was determined using an enzyme-linked immunosorbent assay (ELISA). Vitamin D was determined using ELISA kits. A hematology analyzer, Sysmex XN 100i (Sysmex Europe SE, Norderstedt, Germany), was used to measure Hb. To estimate serum IL-6 and hepcidin (Hp), ELISA kits for IL-6 and Hp, respectively, were used.

The data analysis was carried out employing the basic principles published elsewhere.[26] Statistical analysis was performed using the statistical software package SPSS version 24.0 (IBM Corp., Armonk, NY). For the descriptive analysis, results are presented as mean (M) ± standard deviation (SD). Multiple comparisons were performed with one-way ANOVA and a post-hoc Tukey HSD test. The coefficient of determination (R^2) was estimated to assess the strength of the linear relationship. A probability value of $P \leq 0.05$ was considered statistically significant.

Results

The total women subjects studied in the present study was 409. The number of subjects in the NW-C, NW-SLE, OW-C, and OW-SLE groups was 105, 105, 100, and 99 women, respectively. The data of their age (years), MCL (days), MPD (days), BMI (kg/m^2), IL-6 (pg/mL), Hp (ng/mL), HB (g/dL), and 25(OH)D (ng/mL) were collected and analyzed (Table 1).

Among groups, variation showed significant results for serum IL-6 and vitamin D ($P<0.01$). BMI varied significantly among groups ($P<0.01$) as two of our groups had NW-related BMI and two other groups had OW-related BMI. All other variables did not show significant differences among groups (Table 1).

Table 1 shows that the age values (range: 20-29 years) were 25.08±3.04, 24.87±3.14, 25.13±3.14, and 25.11±3.07 years for the NW-C, NW-SLE, OW-C, and OW-SLE groups, respectively.

The MCL presented 28.35±1.34, 28.40±1.38, 28.38±1.29, and 28.41±1.36 days, respectively, for NW-C, NW-SLE, OW-C, and OW-SLE groups. A P-value of 0.05 was obtained for group comparisons.

The MPD indicated 5.30±1.29, 5.34±1.22, 5.23±1.29, and 5.20±1.28 days, respectively, for NW-C, NW-SLE, OW-C, and OW-SLE groups.

BMI was 21.67±2.08, 21.68±2.06, 27.56±1.50, and 27.53±1.50 kg/m^2 for NW-C, NW-SLE, OW-C, and OW-SLE groups. NW-C vs. OW-C and NW-SLE vs. OW-SLE showed significant differences in BMI (P<0.01).

Serum levels of IL-6 showed 4.71±4.07, 6.13±4.32, 5.53±4.26, and 8.01±5.70 pg/mL, respectively, for NW-C, NW-SLE, OW-C, and OW-SLE women groups (Table 1). Serum levels of IL-6 presented significant variations for NW-SLE compared to NW-C (P<0.02), and OW-SLE compared to OW-C, and OW-SLE compared to NW-SLE (P<0.01) (Fig.1).

Table 1.

Characteristic variables in normal-weight and overweight reproductive-age women with SLE

Variables	Study groups				*P-value*
	NW-C	NW-SLE	OW-C	OW-SLE	
Subjects (n)	105	105	100	99	-
Age (years)	25.08±3.04	24.87±3.14	25.13±3.14	25.11±3.07	0.92
MCL (days)	28.35±1.34	28.40±1.38	28.38±1.29	28.41±1.36	0.99
MPD (days)	5.30±1.29	5.34±1.22	5.23±1.29	5.20±1.28	0.86
BMI (kg/m^2)	21.67±2.08	21.68±2.06	27.56±1.50	27.53±1.50	<0.01
IL-6 (pg/mL)	4.71±4.07	6.13±4.32	5.53±4.26	8.01±5.70	<0.01
Hp (ng/mL)	8.49±4.01	8.49±4.07	8.51±4.29	8.83±4.66	0.92
Hb (g/dL)	13.74±1.22	13.68±1.18	13.56±1.03	13.55±1.02	0.21
25(OH)D (ng/mL)	34.16±5.26	30.08±6.38	30.68±6.20	28.11±6.45	<0.01

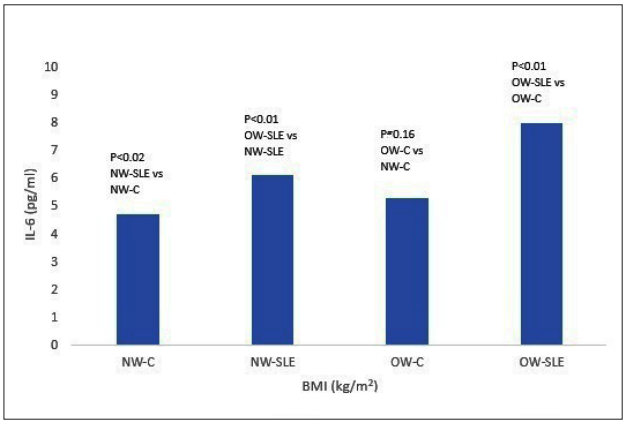

Fig.1*. Serum levels of IL-6 in the study groups*

The Hp serum levels were 8.49±4.01, 8.49±4.07, 13.56±1.03, and 8.83±4.66 ng/mL, respectively, for NW-C, NW-SLE, OW-C, and OW-SLE groups (Table 1). No significant variation of serum Hp was obtained.

The Hb values were 13.74±1.22, 13.68±1.18, 13.56±1.03, and 13.55±1.02 g/dL, respectively, for NW-C, NW-SLE, OW-C, and OW-SLE women groups (Table 1) that also showed non-significant alterations of Hb (P>0.05).

The vitamin D serum levels obtained for the NW-C, NW-SLE, OW-C, and OW-SLE women groups were 34.16±5.26, 30.08±6.38, 30.68±6.20, and 28.11±6.45 ng/mL, respectively (Table 1).

The vitamin D serum levels indicated a significant difference between OW-SLE compared to NW-SLE (P<0.03) and NW-SLE compared to NW-C, OW-SLE compared to OW-C, and OW-C compared to NW-C (P<0.01) (Fig.2).

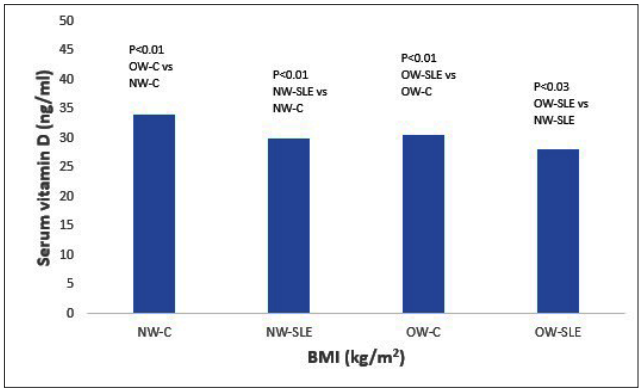

Fig.2. *Serum levels of vitamin D in the study groups.*

Table 2 shows a significant positive association between IL-6 and BMI in the OW-C (P=0.03) and OW-SLE (P<0.01) groups of women. Vitamin D correlated significantly and negatively with IL-6 in NW-SLE and OW-SLE (P<0.01).

Table 2.

Correlation of serum IL-6 with other characteristics/variables in normal-weight and overweight reproductive age women with SLE.

Variables		NW-C	NW-SLE	OW-C	OW-SLE
Age (years)	R^2	0.00	0.00	0.01	0.00
	P	0.48	0.74	0.30	0.90
MCL (days)	R^2	0.02	0.00	0.00	0.01
	P	0.16	0.50	0.61	0.31
MPD (days)	R^2	0.00	0.02	0.00	0.00
	P	0.86	0.18	0.56	0.56
BMI (kg/m^2)	R^2	0.00	0.00	0.05	0.34
	P	0.54	0.76	0.03	<0.01
Hp (ng/mL)	R^2	0.00	0.00	0.00	0.01
	P	0.89	0.80	0.82	0.46
HB (g/dL)	R^2	0.01	0.00	0.01	0.01
	P	0.23	0.66	0.48	0.31
25(OH)D (ng/mL)	R^2	0.01	0.23	0.00	0.33
	P	0.23	<0.01	0.90	<0.01

Vitamin D presented a significantly negative correlation with BMI in NW-SLE (P=0.02), and in OW-C and OW-SLE (P<0.01) (Table 3). All other characteristics/variables were not significantly associated with vitamin D.

Table 3.

Correlation of serum vitamin D with other characteristics/variables in normal-weight and overweight reproductive age women with SLE.

Variables		NW-C	NW-SLE	OW-C	OW-SLE
Age (years)	R^2	0.01	0.02	0.00	0.00
	P	0.30	0.14	0.67	0.59
MCL (days)	R^2	0.00	0.02	0.03	0.00
	P	0.71	0.17	0.06	0.61
MPD (days)	R^2	0.00	0.01	0.02	0.00
	P	0.93	0.40	0.18	0.61
BMI (kg/m^2)	R^2	0.03	0.05	0.33	0.48
	P	0.06	0.02	<0.01	<0.01
IL-6 ((pg/mL)	R^2	0.01	0.23	0.00	0.33
	P	0.23	<0.01	0.90	<0.01
Hp (ng/mL)	R^2	0.00	0.00	0.01	0.00
	P	0.79	0.95	0.32	0.62
HB (g/dL)	R^2	0.00	0.02	0.02	0.00
	P	0.93	0.17	0.14	0.64

Discussion

Various studies found elevated levels of IL-6 in patients with SLE compared with controls,[6-8,27-29] whereas other studies reported a non-significant increase in IL-6 concentration in SLE patients compared with healthy control women.[30-32] The present study finds a significant increase in IL-6 in NW-SLE women compared to NW-C, in OW-SLE women compared to OW-C, and in OW-SLE women compared to NW-SLE women.

The present investigation showed no significant association between IL-6 and age across all subject groups. Age-associated changes in IL-6 in SLE have rarely been studied. A positive association between IL-6 and age in SLE patients was reported,[11] consistent with the observation that aging is associated with enhanced production of inflammatory cytokines, including IL-6, leading to low-grade inflammation.[33] The absence of a significant association of age with any of the SLE or control groups in the present study seems due to the fact that our subjects had quite a limited age range of 20-29 years. Further studies, including a broader age range, may clarify the association between age and serum IL-6.

The elevated IL-6 levels in SLE patients across studies may be due to methodological variability, treatment effects, increased disease activity, age, sex, BMI, and other factors. It is possible that reduced or increased IL-6 levels measured at specific times reflect decreased or increased disease activity, respectively. These findings indicate that IL-6 might serve as an indicator of disease activity, inflammatory status, or post-treatment effects, rather than as a diagnostic marker. SLE patients present with various clinical manifestations driven by immunological, genetic, and environmental factors, and vitamin D is considered an immunomodulatory factor that influences patients with SLE in active disease more than in inactive disease.[1,3]

A variety of clinical features studied in SLE patients[15] reveal that the maximum incidence of SLE occurs in reproductive-age women of 20-29 years.[34] Since we collected the data for the present study in reproductive age women of 20-29 years, it can appropriately be compared with such study,[34] where vitamin D deficiency (mean 16.82±11.24 ng/mL) was suggested to occur in view of multiple interacting factors, including sun avoidance due to photosensitivity, nutritional deficiency of vitamin D, and using full length/ full body clothes that limit the skin exposure to sun.[16,35] Similar conditions were present in SLE patients in the present study.

Vitamin D plays an immunoregulatory role by decreasing autoimmune responses and disease activity in SLE. However, it is not necessary that vitamin D is a causal factor. It could possibly be a consequence of photosensitivity that inclines the patients to limit the exposure to the sun, which leads to less synthesis of vitamin D. Furthermore, certain types of medication for SLE patients may increase the catabolism of vitamin D and decrease the intestinal absorption of vitamin D, thereby enhancing the vitamin D deficiency.[34] Further studies may confirm the medication influences.

Routine and annual comprehensive screening are required to maintain serum vitamin D (25(OH)D) levels above 30 ng/mL, especially in SLE patients with active disease, glucocorticoid use, and photosensitivity. This helps manage SLE patients.[34] Control of the dietary intake of vitamin D and the effect of medication on vitamin D levels were not recorded in the present study. Furthermore, genetic polymorphisms influencing vitamin D metabolism were not studied. A larger sample size, interventional, and longitudinal investigations may confirm the precise association of vitamin D with SLE.

The levels of Hb and Hp did not vary significantly in NW and OW patients with SLE and control subjects in the present study, since the anemic patients were not included in the current study, though anemia and other hematological abnormalities are found prevalent in patients with SLE.[8,17]

The role of BMI in patients with SLE is not well understood [36] because patients with varying BMI levels have not been studied in depth. Obesity playing a pathogenetic role was investigated at a much higher level in patients with SLE than in healthy people. It was found that the overweight status/ obesity has a profound influence on serum vitamin D and inflammatory responses in patients with SLE.[19] Low serum levels of vitamin D were found to have an association with high body weight/BMI in patients with SLE,[21] though this study [21] did not provide findings by comparing the normal weight, overweight, and obese subjects. We did not study the obese subjects with SLE. However, the data from our

overweight subjects were properly compared with those from normal-weight subjects.

Obesity was found to be associated with vitamin D insufficiency in patients with SLE.[16] The lowered levels of vitamin D with increased levels of IL-6 but without the influence of BMI were found in patients with SLE.[20] This report is not in accordance with our present study. We noticed that a study by Guimarães et al.[20] did not report vitamin D and IL-6 levels across BMI levels. This could be a major reason why vitamin D concentrations did not vary among SLE patients in the quoted study.[20] To clarify this, we carried out the present study for SLE patients with NW BMI and OW BMI compared to healthy NW BMI and OW BMI controls.

Vitamin D is considered an immunomodulator that regulates adaptive and innate immune responses.[22,23] Vitamin D helps decrease pro-inflammatory adipokines, such as IL-6.[25] Decreased vitamin D levels in SLE patients are associated with elevated IL-6 and other inflammation mediators.[24,25] For example, a study by Partan et al.[12] showed the effectiveness of seluang fish oil in reducing the inflammatory response in patients with SLE by increasing serum vitamin D levels. The precise association between vitamin D and IL-6 in SLE patients requires further investigation.[25]

It would be worthwhile to conduct studies with a larger dataset of patients with SLE, both women and men, with follow-up. Since we collected data on IL-6, vitamin D, and other variables only once, this is likely insufficient to assess variation. Furthermore, changes in these variables during follow-up are necessary to assess disease activity and appropriate medication dosages. It would be necessary to evaluate age, gender, and BMI in conjunction with serum CRP levels and other cytokines, including TNF-α, as well as anti-inflammatory cytokines/biomarkers, to better understand the relationship of vitamin D with inflammatory and anti-inflammatory responses in patients with SLE.

Conclusion

The results of this study highlight the importance of measuring serum IL-6 and vitamin D levels in conjunction with BMI assessment in SLE patients. The study found an inverse relationship between vitamin D and IL-6 and demonstrated that vitamin D deficiency is the most common factor in patients with systemic lupus erythematosus. Since vitamin D is an important modifiable factor in systemic lupus erythematosus, and its deficiency is associated with disease activity and the risk of complications, correction of vitamin D deficiency can complement standard therapy and improve the prognosis of systemic lupus erythematosus.

Ethical Considerations

The study was conducted in accordance with ethical principles of the WMA Declaration of Helsinki (1964, ed. 2013) and approved by the Ethical Committee of the Faculty of Medicine, Umm Al-Qura University (UQU); Approval Number:"HAPO-02-K-012-2022-01-1069." Written informed consent was obtained from all participants.

Sources of Funding

This research received no external funding.

Competing Interests

The authors declare that they have no conflicts of interest.

Acknowledgments

The authors thank the medical consultants and laboratory experts for their invaluable support.

References

1. Amital H, Szekanecz Z, Szücs G, Dankó K, Nagy E, Csépány T, Kiss E, Rovensky J, Tuchynova A, Kozakova D, Doria A, Corocher N, Agmon-Levin N, Barak V, Orbach H, Zandman-Goddard G, Shoenfeld Y. Serum concentrations of 25-OH vitamin D in patients with systemic lupus erythematosus (SLE) are inversely related to disease activity: is it time to routinely supplement patients with SLE with vitamin D? Ann Rheum Dis. 2010 Jun;69(6):1155-7. doi: 10.1136/ard.2009.120329. Epub 2010 May 3. PMID: 20439290.
2. Izmirly PM, Parton H, Wang L, McCune WJ, Lim SS, Drenkard C, Ferucci ED, Dall'Era M, Gordon C, Helmick CG, Somers EC. Prevalence of Systemic Lupus Erythematosus in the United States: Estimates From a Meta-Analysis of the Centers for Disease Control and Prevention National Lupus Registries. Arthritis Rheumatol. 2021 Jun;73(6):991-996. doi: 10.1002/art.41632. Epub 2021 Apr 23. PMID: 33474834; PMCID: PMC8169527.
3. Borba VZ, Vieira JG, Kasamatsu T, Radominski SC, Sato EI, Lazaretti-Castro M. Vitamin D deficiency in patients with active systemic lupus erythematosus. Osteoporos Int. 2009 Mar;20(3):427-33. doi: 10.1007/s00198-008-0676-1. Epub 2008 Jul 4. PMID: 18600287.
4. Xu YD, Cheng M, Shang PP, Yang YQ. Role of IL-6 in dendritic cell functions. J Leukoc Biol. 2022 Mar;111(3):695-709. doi: 10.1002/JLB.3MR0621-616RR. Epub 2021 Aug 18. PMID: 34405445.
5. Zhang Z, Zhu S, Li Q, Wei S, Yin L, Zhu J, Yang S, Zhang W, Lai K. Investigating the role of IL-6 in the pathogenesis of systemic lupus erythematosus: Insights from bone marrow mesenchymal stem cells. Lupus. 2025 Mar;34(3):225-233. doi: 10.1177/09612033251317783. Epub 2025 Jan 30. PMID: 39882783.
6. Ding J, Su S, You T, Xia T, Lin X, Chen Z, Zhang L. Serum interleukin-6 level is correlated with the disease activity of systemic lupus erythematosus: a meta-analysis. Clinics (Sao Paulo). 2020 Oct 19;75:e1801. doi: 10.6061/clinics/2020/e1801. PMID: 33084768; PMCID: PMC7536892.
7. Pattanaik SS, Panda AK, Pati A, Padhi S, Tripathy R, Tripathy SR, Parida MK, Das BK. Role of interleukin-6 and interferon-α in systemic lupus erythematosus: A case-control

study and meta-analysis. Lupus. 2022 Aug;31(9):1094-1103. doi: 10.1177/09612033221102575. Epub 2022 May 17. PMID: 35581679.
8. Winikajtis-Burzyńska A, Brzosko M, Przepiera-Będzak H. Increased Serum Interleukin 10 Levels Are Associated with Increased Disease Activity and Increased Risk of Anti-SS-A/Ro Antibody Positivity in Patients with Systemic Lupus Erythematosus. Biomolecules. 2023 Jun 11;13(6):974. doi: 10.3390/biom13060974. PMID: 37371554; PMCID: PMC10296207.
9. Behzadi P, Sameer AS, Nissar S, Banday MZ, Gajdács M, García-Perdomo HA, Akhtar K, Pinheiro M, Magnusson P, Sarshar M, Ambrosi C. The Interleukin-1 (IL-1) Superfamily Cytokines and Their Single Nucleotide Polymorphisms (SNPs). J Immunol Res. 2022 Mar 26;2022:2054431. doi: 10.1155/2022/2054431. PMID: 35378905; PMCID: PMC8976653.
10. Metwally YF, Elsaid AM, Elsadda RR, Refaat S, Zahran RF. Impact of IL-6 and IL-1β Gene Variants on Non-small-cell Lung Cancer Risk in Egyptian Patients. Biochem Genet. 2024 Oct;62(5):3367-3388. doi: 10.1007/s10528-023-10596-2. Epub 2023 Dec 16. PMID: 38103126; PMCID: PMC11427554.
11. Mercader-Salvans J, García-González M, Gómez-Bernal F, Quevedo-Abeledo JC, de Vera-González A, González-Delgado A, López-Mejías R, Martín-González C, González-Gay MÁ, Ferraz-Amaro I. Relationship between Disease Characteristics and Circulating Interleukin 6 in a Well-Characterized Cohort of Patients with Systemic Lupus Erythematosus. Int J Mol Sci. 2023 Sep 12;24(18):14006. doi: 10.3390/ijms241814006. PMID: 37762312; PMCID: PMC10531425.
12. Partan RU, Hidayat R, Saputra N, Rahmayani F, Prapto H, Yudha TW. Seluang Fish (*Rasbora Spp*.) Oil Decreases Inflammatory Cytokines Via Increasing Vitamin D Level in Systemic Lupus Erythematosus. Open Access Maced J Med Sci. 2019 May 5;7(9):1418-1421. doi: 10.3889/oamjms.2019.308. PMID: 31198446; PMCID: PMC6542399.
13. Fragoso TS, Dantas AT, Marques CD, Rocha Junior LF, Melo JH, Costa AJ, Duarte AL. 25-Hydroxyivitamin D3 levels in patients with systemic lupus erythematosus and its association with clinical parameters and laboratory tests. Rev Bras Reumatol. 2012 Jan-Feb;52(1):60-5. English, Portuguese. PMID: 22286646.
14. Hamza RT, Awwad KS, Ali MK, Hamed AI. Reduced serum concentrations of 25-hydroxy vitamin D in Egyptian patients with systemic lupus erythematosus: relation to disease activity. Med Sci Monit. 2011 Dec;17(12):CR711-8. doi: 10.12659/msm.882131. PMID: 22129903; PMCID: PMC3628141.
15. Isenberg DA. BILAG, SLEDAI, SIS, ECLAM, WAM, SLAM .... thank you MAM. Lupus. 2007;16(11):849-51. doi: 10.1177/0961203307085124. PMID: 17971356.
16. Muñoz-Ortego J, Torrente-Segarra V, Prieto-Alhambra D, Salman-Monte TC, Carbonell-Abello J. Prevalence and predictors of vitamin D deficiency in non-supplemented women with systemic lupus erythematosus in the Mediterranean region: a cohort study. Scand J Rheumatol. 2012;41(6):472-5. doi: 10.3109/03009742.2012.697189.
17. Aldakheel FM, Alshanqiti MA, Alduraywish SA, Alshammary AF, Dabwan KH, Syed R. Clinical Assessment of Cytokine Profiles and Haematological Parameters in Patients with Systemic Lupus Erythematosus: A Cross-Sectional Study from Saudi Arabia. Front Biosci (Landmark Ed). 2023 Dec 28;28(12):358. doi: 10.31083/j.fbl2812358. PMID: 38179775.
18. Markina MV, Milovanova LY, Lysenko LV, Milovanova SY, Volkov AV, Beketov VD, Lebedeva MV, Nezhdanov KS, Moiseev SV. [Anemia of chronic diseases in the early stages of chronic kidney disease as a risk factor for cardiovascular complications in patients with glomerulonephritis]. Ter Arkh. 2024 Jul 7;96(6):606-613. Russian. doi: 10.26442/00403660.2024.06.202729. PMID: 39106502.
19. Kono M, Nagafuchi Y, Shoda H, Fujio K. The Impact of Obesity and a High-Fat Diet on Clinical and Immunological Features in Systemic Lupus Erythematosus. Nutrients. 2021 Feb 4;13(2):504. doi: 10.3390/nu13020504. PMID: 33557015; PMCID: PMC7913625.
20. Guimarães PM, Scavuzzi BM, Stadtlober NP, Franchi Santos LFDR, Lozovoy MAB, Iriyoda TMV, Costa NT, Reiche EMV, Maes M, Dichi I, Simão ANC. Cytokines in systemic lupus erythematosus: far beyond Th1/Th2 dualism lupus: cytokine profiles. Immunol Cell Biol. 2017 Oct;95(9):824-831. doi: 10.1038/icb.2017.53. Epub 2017 Jun 26. PMID: 28649995.
21. Meza-Meza MR, Vizmanos-Lamotte B, Muñoz-Valle JF, Parra-Rojas I, Garaulet M, Campos-López B, Montoya-Buelna M, Cerpa-Cruz S, Martínez-López E, Oregon-Romero E, De la Cruz-Mosso U. Relationship of Excess Weight with Clinical Activity and Dietary Intake Deficiencies in Systemic Lupus Erythematosus Patients. Nutrients. 2019 Nov 6;11(11):2683. doi: 10.3390/nu11112683. PMID: 31698711; PMCID: PMC6893805.
22. Adams JS, Hewison M. Unexpected actions of vitamin D: new perspectives on the regulation of innate and adaptive immunity. Nat Clin Pract Endocrinol Metab. 2008 Feb;4(2):80-90. doi: 10.1038/ncpendmet0716. PMID: 18212810; PMCID: PMC2678245.
23. Szymczak I, Pawliczak R. The Active Metabolite of Vitamin D3 as a Potential Immunomodulator. Scand J Immunol. 2016 Feb;83(2):83-91. doi: 10.1111/sji.12403. PMID: 26678915.
24. Gröndal G, Gunnarsson I, Rönnelid J, Rogberg S, Klareskog L, Lundberg I. Cytokine production, serum levels and disease activity in systemic lupus erythematosus. Clin Exp Rheumatol. 2000 Sep-Oct;18(5):565-70. PMID: 11072595.
25. Shevchuk S, Marynych L, Malovana T, Denyshchych L. Vitamin D level in patients with systemic lupus erythematosus: its relationship to disease course and bone mineral density. Lupus Sci Med. 2023 Aug;10(2):e000968. doi: 10.1136/lupus-2023-000968. PMID: 37558268; PMCID: PMC10414063.
26. Zahir H, Javaid A, Rehman R, Hussain Z. Statistical concepts in biology and health sciences. J Ayub Med Coll Abbottabad. 2014 Jan-Mar;26(1):95-7. PMID: 25358229.
27. Jin S, Yu C, Yu B. Changes of serum IL-6, IL-10 and TNF-α levels in patients with systemic lupus erythematosus and their clinical value. Am J Transl Res. 2021 Apr 15;13(4):2867-2874. PMID: 34017450; PMCID: PMC8129414.

28. Singh RP, Hahn BH, Bischoff DS. Interferon Genes Are Influenced by 17β-Estradiol in SLE. Front Immunol. 2021 Oct 18;12:725325. doi: 10.3389/fimmu.2021.725325. PMID: 34733276; PMCID: PMC8558410.
29. Peliçari KO, Postal M, Sinicato NA, Londe AC, Fernandes PT, Marini R, Costallat LTL, Appenzeller S. Longitudinal comparison of IL-6, IL-10, and IL-12 cytokine profiles in adult and childhood-onset systemic lupus erythematosus. J Transl Autoimmun. 2022 May 26;5:100158. doi: 10.1016/j.jtauto.2022.100158. PMID: 36683864; PMCID: PMC9846463.
30. Mak A, Tang CS, Ho RC. Serum tumour necrosis factor-alpha is associated with poor health-related quality of life and depressive symptoms in patients with systemic lupus erythematosus. Lupus. 2013 Mar;22(3):254-61. doi: 10.1177/0961203312471872. Epub 2013 Jan 18. PMID: 23334278.
31. Raymond WD, Eilertsen GØ, Nossent J. Principal component analysis reveals disconnect between regulatory cytokines and disease activity in Systemic Lupus Erythematosus. Cytokine. 2019 Feb;114:67-73. doi: 10.1016/j.cyto.2018.10.013. Epub 2018 Dec 12. PMID: 30551949.
32. Tanaka A, Ito T, Kibata K, Inagaki-Katashiba N, Amuro H, Nishizawa T, Son Y, Ozaki Y, Nomura S. Serum high-mobility group box 1 is correlated with interferon-α and may predict disease activity in patients with systemic lupus erythematosus. Lupus. 2019 Aug;28(9):1120-1127. doi: 10.1177/0961203319862865. Epub 2019 Jul 12. PMID: 31299881.
33. Giunta S, Wei Y, Xu K, Xia S. Cold-inflammaging: When a state of homeostatic-imbalance associated with aging precedes the low-grade pro-inflammatory-state (inflammaging): Meaning, evolution, inflammaging phenotypes. Clin Exp Pharmacol Physiol. 2022 Sep;49(9):925-934. doi: 10.1111/1440-1681.13686. Epub 2022 Jul 4. PMID: 35684970.
34. Oo ATZ, Oo WT, Tun KL, Myint AK, Thu Zar Aye M, Khin NE, Sone KP, Sonn P. Serum Vitamin D Level and Disease Activity in Patients With Systemic Lupus Erythematosus. Cureus. 2025 Oct 5;17(10):e93853. doi: 10.7759/cureus.93853. PMID: 41054434; PMCID: PMC12496543.
35. Kamen DL, Aranow C. The link between vitamin D deficiency and systemic lupus erythematosus. Curr Rheumatol Rep. 2008 Aug;10(4):273-80. doi: 10.1007/s11926-008-0044-3. PMID: 18662506.
36. Li H, Du X, Lv X, Hao Z, He L. Correlation between body mass index and disease activity in patients with systemic lupus erythematosus from China. Adv Rheumatol. 2025 Nov 29;66(1):3. doi: 10.1186/s42358-025-00502-2. PMID: 41318544.

***Corresponding author**: Prof. Dr. Zahir Hussain, PhD. Department of Physiology, Faculty of Medicine, Umm Al-Qura University, Makkah 21955, Saudi Arabia. E-mail: zahirhussa@gmail.com*

International Journal of Biomedicine 16(1) (2026) 33-40
http://dx.doi.org/10.21103/Article16(1)_OA3

ORIGINAL ARTICLE

Experimental Surgery

INTERNATIONAL JOURNAL OF BIOMEDICINE

Negative Pressure Regulates BMP-9 Expression Through the MAPK/ERK5 Signaling Pathway and Thereby Promotes Fracture Healing

Hai Long Wang[1], Yuan Yuan Dou[1], Mu Hai Mai Ti A Bu Du Re Zha Ke[1], Yi Li Ya Yi Li Ha Mu[1], Kun Wang[1], Cheng Li[1], Qiu Cheng Chen[1], Yi Fei Huang[1], Zhan Jun Ma[2*]

[1]*Xinjiang Medical University Fourth Clinical Medical College: Traditional Chinese Medicine Hospital of Xinjiang Uyghur Autonomous Region, Urumqi City, China*
[2]*Xinjiang Uygur Autonomous Region Institute of Traditional Chinese Medicine, Urumqi City, Xinjiang Uygur Autonomous Region, China*

Abstract

Negative pressure wound therapy (NPWT) has been widely used in wound repair and tissue regeneration, and its mechanistic role in fracture healing is gaining increasing attention. Bone morphogenetic protein-9 (BMP-9), a recognized and highly effective osteoinductive factor, plays a crucial role in bone repair. However, the regulatory mechanism of its expression under negative pressure remains unclear. This study aimed to investigate whether negative pressure wound therapy (NPWT) accelerates fracture healing by upregulating BMP-9 and osteocalcin (OCN) expression through activation of the MAPK/ERK5 signaling pathway. A tibial fracture model was established in Sprague-Dawley (SD) rats. The rats were randomly divided into the control group, the Model+Gauze group, the Model+Gauze+BIX group, the Model+NPWT group, and the Model+NPWT+BIX group. Fracture tissue was obtained 14 days after surgery for molecular and histological analysis. Real-time fluorescence quantitative PCR results showed that mRNA expression of BMP-9, OCN, MEK5, and ERK5 in the Model+NPWT group was significantly higher than that in the other groups (P<0.05). Western blot analysis was consistent with this finding, demonstrating a significant increase in protein expression. Further immunohistochemistry revealed that OCN expression in the fracture area of the Model+NPWT group was significantly increased, suggesting a stimulatory effect on osteoblastic activity. This study demonstrates that NPWT may upregulate BMP-9 and OCN expression by activating the MAPK/ERK5 signaling pathway, thereby enhancing the osteogenic response at the fracture site and ultimately promoting fracture repair. This study provides a new perspective on the molecular mechanisms by which NPWT promotes fracture healing and provides a theoretical basis for its clinical application in fracture treatment.(**International Journal of Biomedicine. 2026;16(1):33-40.**)

Keywords: negative pressure • wound therapy • bone morphogenetic protein-9 • osteocalcin

For citation: Wang H, Dou Y, Ke M, Mu Y, Wang K, Li C, Chen Q, Huang Y, Ma Z. Negative Pressure Regulates BMP-9 Expression Through the MAPK/ERK5 Signaling Pathway and Thereby Promotes Fracture Healing. International Journal of Biomedicine. 2026;16(1):33-40. doi:10.21103/Article16(1)_OA3

Abbreviations

ALP, alkaline phosphatase; **BMP-9**, bone morphogenetic protein-9; **ERK5**, extracellular-signal-regulated kinase 5; **MSCs**, mesenchymal stem cells; **MAPK**, mitogen-activated protein kinase; **NPWT**, negative pressure wound therapy; **OCN**, osteocalcin; **SD**, Sprague-Dawley.

Introduction

Fracture is one of the most common orthopedic diseases in clinical practice, and its repair process is regulated by multiple factors, including inflammatory response, cell migration, angiogenesis, and osteoblast differentiation.[1] Although most fractures heal with traditional treatment methods, in complex situations such as open fractures, concomitant infections, large bone defects, and osteoporosis in the elderly, there is a risk of delayed healing or even complete failure to heal.[2] Therefore, exploring methods that can effectively promote fracture repair and enhance the capacity for bone regeneration has always been a hot topic in bone tissue engineering and translational medicine research. In recent years, negative pressure wound therapy (NPWT) has been widely used in managing chronic wounds, diabetic foot, and postoperative wounds due to its

advantages of accelerating wound healing, promoting tissue perfusion, reducing edema, and inducing cell remodeling.[3,4] The therapeutic mechanism of NPWT is not limited to physical drainage but also includes the regulation of the local cell mechanical environment, thereby activating related signaling pathways and inducing tissue regeneration. In the field of orthopedics, researchers have begun to pay attention to whether NPWT can further promote bone tissue repair by regulating related signaling pathways. Zhu et al.[5] found that NPWT can enhance blood supply and osteoblast activity in the fracture area, shorten fracture-healing time, and promote bone-bridge formation. Li et al.[6] also observed that NPWT can promote angiogenesis in a diabetic trauma model, indirectly improving the physiological environment for fracture repair.

During fracture repair, bone morphogenetic protein-9 (BMP-9), a member of the TGF-β family, has been increasingly recognized in recent years as one of the cytokines with the greatest osteogenic induction potential. Compared with the traditionally used BMP-2 and BMP-7, BMP-9 has a stronger ability to induce mesenchymal stem cells (MSC) differentiation into osteoblasts and to sustainably upregulate osteogenic markers, such as ALP, OCN, and Runx2.[7-9] Mostafa et al.[10] showed that the regulatory transduction mechanism of BMP-9 involves not only the Smad-dependent pathway but also further enhances the expression of transcription factors and the synthesis of osteogenic proteins by activating non-classical signaling axes, such as the MAPK family. In particular, the MAPK/ERK5 (mitogen-activated protein kinase/ extracellular-signal-regulated kinase 5) signaling pathway plays a crucial role in osteogenic protein synthesis.[11-13] Although BMP-9 is widely recognized for its role in promoting fracture healing, little research has examined whether it is preferentially activated by negative pressure. Furthermore, little has been reported on whether its differentiation and proliferation are regulated by the MAPK/ERK5 signaling pathway under negative pressure, and whether negative pressure preferentially activates this pathway to regulate BMP-9. To this end, we established an SD rat tibial fracture model and used an NPWT intervention strategy. Combining immunohistochemistry, qPCR, and Western blot, we investigated the expression of key factors, including BMP-9, OCN, MEK5, ALP, and ERK5, and analyzed the effects of negative pressure on fracture repair. To examine whether negative pressure regulates BMP-9 and OCN via the MAPK/ERK5 signaling pathway and thereby promotes fracture healing, we included the ERK5 pathway inhibitor BIX02189 as a functional intervention.

This study is expected to reveal the function and role of BMP-9 and the MAPK/ERK5-BMP-9 axis under negative pressure, providing a theoretical basis and potential targets for interventions to repair clinical bone tissue.

Materials and Methods

Experimental Animals and Groups

Sixty healthy 8-week-old SD rats (weighing 220–250 g), half male and half female, were purchased from Hubei Provincial Laboratory Animal Center (License number: SCXK-2022-0011). All animals were housed in a SPF environment at 22–25°C, 50%–60% humidity, and a 12-h day/night cycle, with free access to food and water. To ensure animal welfare, humane endpoints were established, including weight loss exceeding 20%; severe infection or injury that could not be healed; noticeable pain or discomfort that could not be alleviated by medication; or the animal exhibiting excessive mental or behavioral stress during the experiment. All animals were sacrificed under deep anesthesia with sodium pentobarbital (50 mg/kg, intraperitoneal) before cervical dislocation.

If any of these conditions were observed, the experiment would be terminated immediately, and the animals would be euthanized in accordance with procedures approved by the ethics committee. After 7 days of acclimation, the animals were randomly assigned to 5 groups (n=12): Control group: no treatment; Model+Gauze group: fracture model established and covered with saline gauze; Model+Gauze+BIX group: ERK5 pathway inhibitor BIX02189 was added to the model group; Model+NPWT group: negative pressure treatment; Model+NPWT+BIX group: negative pressure treatment plus ERK5 inhibitor intervention. The experiment was carried out from March to July 2024.

Tibial Fracture Model Construction and Negative Pressure Treatment

After the animals were anesthetized (sodium pentobarbital, 40 mg/kg, i.p.), a longitudinal incision was made in the proximal tibia of the right hind limb to expose the bone surface. A surgical drill (Elbo EL-21) was used to create a bone defect approximately 3mm in the mid-tibial region (Figure 1A). Subsequently, a 0.8mm diameter Kirschner wire (Jiangsu Kangda) was inserted into the medullary canal for internal fixation. The fracture ends were reduced, and X-rays confirmed the successful model (Figure 1B). NPWT treatment was performed using a disposable, medical, negative-pressure sealing and drainage dressing (Jiangsu Yaguang Medical Technology Co., Ltd., model YX9800-01) connected to a continuous negative-pressure aspirator (set to –125 mmHg) (Figure 1C). The dressing was changed every 3 days for 14 days. The control group was covered with moist sterile gauze. BIX02189 (MCE, HY-12056) was dissolved in DMSO and diluted with 25% DMSO. The Model+Gauze+BIX group and the Model+NPWT+BIX group were intraperitoneally injected daily at a dose of 5 mg/kg for 7 days.

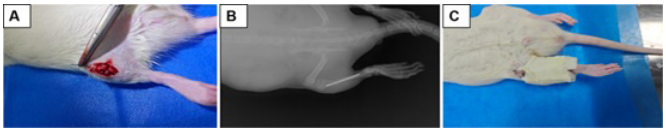

Figure. 1. *Rat tibial fracture model establishment and negative pressure treatment. (A) A 3 mm bone defect was created by drilling in the mid-tibial region of the rat. (B) X-ray imaging demonstrates the successful establishment of a tibial fracture model. (C) The wound in the negative pressure wound treatment group was covered with a vacuum-sealed drainage dressing. Negative pressure was applied continuously at -125 mmHg.*

Tissue Sample Collection

On Day 14 after the intervention, the animals were killed by cervical dislocation. All animals were deeply anesthetized with an intraperitoneal injection of 50 mg/kg sodium

pentobarbital before cervical dislocation. The callus tissue at the fracture site was collected and divided into 2 parts: one part was fixed with 4% paraformaldehyde for 48 hours and embedded in paraffin for immunohistochemistry; the other part was quickly frozen in liquid nitrogen and stored at -80°C for qPCR and Western blotting.

Real-Time Fluorescence Quantitative PCR Detection

Total RNA was extracted using a RNeasy Mini kit (Qiagen AB, Sollentuna, Sweden) and a thermocycler (Bio-Rad Laboratories, Inc., Hercules, CA, USA). RNA was reverse transcribed into cDNA using the First Strand cDNA Synthesis kit (Fermentas; Thermo Fisher Scientific, Inc., Waltham, MA, USA) according to the manufacturer's protocols. Primer sequences were:

BMP-9 forward primer, 5′- AGACCGTGCTTGTGAAGACAT -3`′ and reverse primer, 5′- CACGATGGCGTGTTTGGTG -3′

ALP forward primer, 5′- TGGACGGTGAACGGGAGAACG -3′ and reverse primer, 5′- TGAAGCAGGTGAGCCATAGGG -3′

OCN forward primer, 5′-GCCCTGACTGCATTCTGCCTC-3′and reverse primer, 5- TCACCACCTTACTGCCCTCCT -3′

GAPDH forward primer, 5′-ACAGCAACAGGGTGGTGGAC-3′ and reverse primer, 5′- TTTGAGGGTGCAGCGAACTT -3′

RT-PCR was performed using a SYBR qPCR mix (2×; Toyobo Co., Ltd., Osaka, Japan) and an RT-PCR detection system (Bio-Rad Laboratories Inc.). Thermocycling parameters were an initial denaturation for 1min at 95°C, followed by 40 denaturation cycles at 95°C for 15 s, annealing at 60°C for 15 s, and elongation at 72°C for 60 s. Samples were run in triplicate. Relative gene expression was analyzed with reference to GAPDH expression and the $2^{-\triangle\triangle Ct}$ method.

Western Blot Assay

Protein was extracted using RIPA lysis buffer (Meilunbio, MA0151) supplemented with PMSF (1 mM) and phosphatase inhibitors (Beyotime, P1260). Tissue homogenization was followed by centrifugation at 12,000 rpm for 15 min at 4°C, and the supernatant was collected. Protein concentration was determined using the BCA assay (Beyotime, P0012). Forty micrograms of protein were separated by 10% SDS-PAGE and electrophoresed at 100 V for 90 min. The membrane was then transferred to a PVDF membrane (Millipore, IPVH00010) at a constant voltage of 300 mA for 90 min. After blocking with 5% skim milk powder (diluted in TBST) for 1 hour, the membranes were incubated overnight at 4°C with the following primary antibodies: BMP-9 (Affinity, DF7758, 1:1000); ALP (Affinity, DF6225, 1:1000); OCN (Affinity, DF12303, 1:1000); MEK5/p-MEK5, ERK5/p-ERK5, and Nur77/p-Nur77 (all Affinity products); and internal control: GAPDH (Hangzhou Xianzhi, AB-P-R001, 1:10,000).. Secondary antibodies were used: HRP-conjugated goat anti-rabbit IgG (Boster, BA1051, 1:10,000). Incubation was performed at room temperature for 1 hour. Color was developed with an ECL solution (Affinity, KF8003) and exposed on an SH-523 imaging system. Grayscale values were analyzed in ImageJ, and GAPDH was used as an internal control for normalization.

Immunohistochemistry (IHC) Staining

For immunohistochemistry staining, paraffin sections were routinely deparaffinized and rehydrated with graded alcohols. Antigens were retrieved with 0.25% trypsin at 37°C for 20 minutes. Endogenous enzymes were blocked with 3% H_2O_2 for 10 minutes, followed by blocking with 10% goat serum for 30 minutes. The primary antibody against osteocalcin (LSBio, LS-C83497, 1:100) was incubated overnight at 4°C. The next day, a secondary antibody conjugated with HRP (Tongling Biotechnology) was added, and DAB (Servicebio, G1212) was used for color development. The sections were counterstained with hematoxylin, dehydrated, and mounted. The stained areas appeared brownish-yellow. Positive intensity was measured using a Nikon Fi3 microscope, and the percentage of positive area was analyzed using Image-Pro Plus 6.0.

Statistical analysis

All data are presented as the means ± SD, and statistical significance was assessed by one-way analysis of variance (ANOVA). SPSS 18.0 software (SPSS, Chicago, IL, USA) was used for statistical analysis. Differences between groups were considered statistically significant at $P<0.05$.

Results

Changes in BMP-9, ALP, and OCN mRNA Expression

In this study, the qPCR was used to measure gene mRNA levels. The results showed that BMP-9 mRNA expression was significantly higher in the Model+NPWT group than in the Model+Gauze group ($P<0.01$), suggesting that NPWT activated BMP-9 transcription (Figure 2E). In contrast, BMP-9 expression was significantly decreased in the Model+Gauze+BIX group, which was treated with the ERK5 pathway inhibitor BIX02189, indicating that the MAPK/ERK5 pathway positively regulates its expression. ALP and OCN mRNA expression levels were also significantly higher in the Model+NPWT group than in the Model+Gauze group ($P<0.05$ or $P<0.001$), indicating that NPWT not only affects the expression of inducible factors but also broadly promotes mid- and late-stage osteogenic differentiation (Figures 2F and 2G). BIX02189 intervention significantly inhibited the MAPK/ERK5 signaling pathway, leading to decreased ALP and OCN expression.

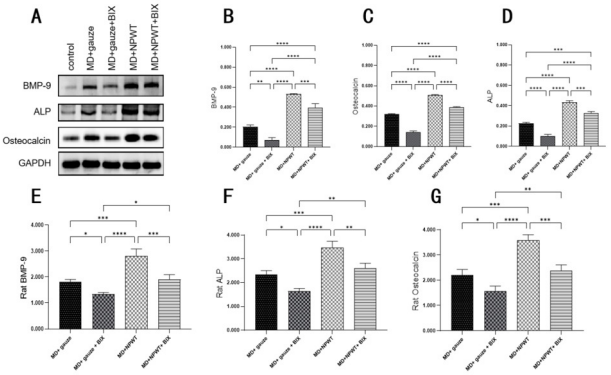

Figure. 2. *Expression changes of BMP-9, ALP, and OCN in fracture healing. (A) Representative protein blots showing the BMP-9, OCN, and ALP levels in each group. (B) Statistical analysis of BMP-9 protein levels in each group. (C) Statistical analysis of OCN protein levels in each group. (D) Statistical analysis of ALP protein levels in each group. (E) BMP-9 gene expression levels in each group were detected by qRT-PCR. (F) ALP gene expression levels in each group were detected by qRT-PCR. (G) OCN gene expression levels in the two groups were detected by qRT-PCR. The control group was normal bone tissue of rats without fractures, which was only used for normalization analysis and not presented in the statistical analysis graph. *P<0.05, **P<0.01, ***P<0.001, ****P<0.0001.*

Changes in Protein Expression of BMP-9, ALP, MEK5, ERK5, NUR77, and OCN

To further validate these transcriptional changes at the protein level, this study used a Western blot to examine the protein expression levels of BMP-9, ALP, MEK5, ERK5, and OCN in each group. The phosphorylation levels of MEK5 and ERK5 were also measured. The results showed that the protein expression trends of BMP-9, ALP, and OCN were consistent with those of their mRNA counterparts. BMP-9 protein expression was significantly higher in the NPWT group than in the Model+Gauze group (P<0.01), while that in the Model+Gauze+BIX group was significantly lower than in the NPWT group (P<0.05) (Figure 2A, 2B). Furthermore, ALP and OCN protein expressions were significantly increased in the NPWT group, with statistically significant differences, (P<0.01) suggesting that NPWT enhances the expression of proteins associated with fracture repair (Figure 2A, 2C, 2D). BIX02189 treatment significantly decreased the expression levels of these proteins. Further analysis of key proteins in the MAPK/ERK5 signaling pathway, MEK5 and ERK5, as well as their phosphorylated forms (p-MEK5 and p-ERK5), and the downstream transcription factors Nur77 and p-Nur77, revealed significant upregulation of p-MEK5, p-ERK5, and p-Nur77 expression in the Model+NPWT group (P<0.01 or P<0.001, respectively) (Figures 3A, 3C, 3E, and 3G). However, phosphorylation levels of p-MEK5 and p-ERK5 were significantly decreased in the Model+NPWT+BIX group. Significant changes in the phosphorylation levels of p-MEK5 and p-ERK5 were also observed between the Model+Gauze+BIX and Model+Gauze groups (Figures 3A, 3C, and 3E). This demonstrates that the ERK5 pathway inhibitor BIX02189 can significantly inhibit the MAPK/ERK5 signaling pathway, whereas NPWT can activate it and its downstream factors.

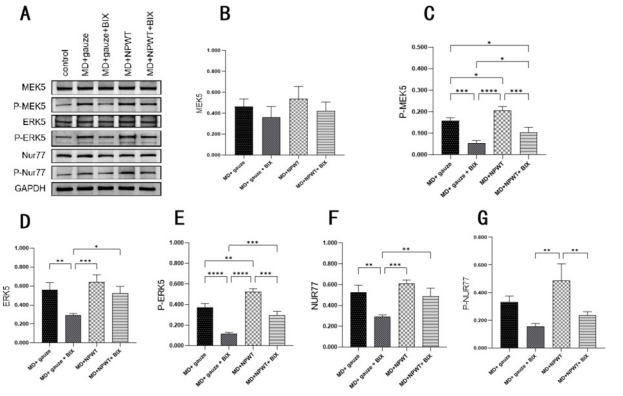

Figure. 3. *Altered expression of MEK5, P-MEK5, ERK5, P-ERK5, NUR77, and P-NUR77 during fracture healing. (A) Representative Western blots showing the protein levels of MEK5, P-MEK5, ERK5, P-ERK5, NUR77, and P-NUR77 in each group. (B) Statistical analysis of MEK5 protein levels in each group. (C) Statistical analysis of P-MEK5 protein levels in each group. (D) Statistical analysis of ERK5 protein levels in each group. (E) Statistical analysis of P-ERK5 protein levels in each group. (F) Statistical analysis of NUR77 protein levels in each group. (G) Statistical analysis of P-NUR77 protein levels in each group. The control group represents normal bone tissue from rats without fractures and is used only for normalization analysis and is not shown in the statistical analysis graphs.*P<0.05, **P<0.01, ***P<0.001, ****P<0.0001.*

Immunohistochemistry

To validate the spatial regulation of NPWT on bone formation in the fracture area, this study used immunohistochemistry to detect OCN expression at the tissue level. Immunohistochemistry results showed that under 100× and 400× magnifications, a distinct brown OCN-positive signal was visible in the fracture end tissue of the Model+NPWT group. In the Model+NPWT+BIX group, the intensity and distribution of OCN-positive signals were significantly lower than those in the NPWT group, further suggesting that activation of the ERK5 signaling pathway plays a key role in NPWT-induced osteogenesis (Figure 4). Immunohistochemical observations were consistent with the trends of qRT-PCR and Western blot assays, further confirming that NPWT enhances local bone formation by upregulating OCN expression, which is positively correlated with BMP-9 expression.

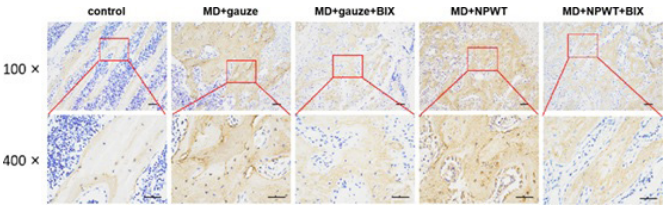

Figure. 4. *Histological changes in each group. At 100× and 400× magnification, distinct brown OCN-positive signals were observed in the fracture tissue of the Model+NPWT group, widely distributed in the newly formed trabeculae and callus areas (red frame). Scale bar, 50 μm.*

Discussion

Fracture repair is a complex biological process involving the activation and regulation of multiple signaling pathways. In recent years, with the application of vacuum sealing drainage technology in clinical fracture treatment, its role in promoting bone repair has gradually attracted attention. Although studies have demonstrated a link between vacuum sealing and fracture healing,[14,15] the related signaling pathways are rarely reported. This study aimed to establish an SD rat tibial fracture model and systematically explore whether NPWT promotes fracture healing by preferentially activating the MAPK/ERK5 signaling pathway, thereby regulating the expression of osteogenic factors BMP-9 and OCN.

BMP-9, a member of the TGF-β superfamily, is considered one of the factors with the greatest known osteogenic potential.[16,17] It can not only effectively induce MSCs to differentiate into osteoblasts but also upregulate a variety of osteoblast-related genes, including *Runx2*, *OCN*, and *ALP*.[7,18,19] Park et al.[20] reported that BMP-9 has a stronger osteogenic effect than BMP-2 and BMP-7, providing a theoretical basis for its application in bone tissue engineering and fracture repair. In this study, the results of PCR and Western blot showed that after negative pressure treatment of the fracture ends of rats, the expression of BMP-9 mRNA and protein levels in the callus tissue of the fracture ends was significantly higher than that in the gauze group and the blank group, and the difference was

statistically significant. This demonstrates that the osteogenic potential of the fracture ends was significantly enhanced after NPWT treatment, thereby improving the fracture-healing microenvironment and promoting fracture healing.

It is worth noting that BMP-9 promotes callus formation, osteoblast maturation, and trabecular reconstruction, as well as ectopic bone formation and angiogenesis.[12,23-25] In this study, a complete fracture model was used. Under the conditions of bone-end contact and periosteum retention, the function of BMP-9 is more reflected in regulating the activity and differentiation level of osteoblasts in the fracture area. This expression background under this physiological environment enables us to more accurately evaluate the role of BMP-9 in the natural process of fracture repair. NPWT, as a non-drug, exogenous factor-free, physiological stimulation method, induces BMP-9 expression, suggesting that this technology may intervene in the molecular chain of bone repair by activating endogenous factors. Our results confirmed that NPWT preferentially promotes BMP-9 overexpression and thereby enhances fracture healing. The plasma concentration of ALP is a biochemical indicator of bone formation, and its changes are the core biomarkers of bone formation and mineralization during fracture healing.[21] The study by Moss et al.[22] showed that ALP activity began to increase significantly 2 weeks after surgery, indicating enhanced osteoblast activity and the initiation of mineralization. In this study, ALP activity was consistent with that of BMP-9. At 2 weeks, RNA and protein levels in the negative-pressure group were significantly higher than those in other groups, demonstrating that negative pressure enhances osteoblast activity and accelerates bone formation. In this study, immunohistochemical results also confirmed that the callus tissue content in the negative pressure group was significantly higher than in the gauze and blank groups, indicating that negative pressure enhances osteoblast activity.

Osteogenesis is an essential stage in fracture healing. OCN, as a marker of osteogenic transformation, is widely used to reflect the degree of bone formation and mineralization activity.[26-29] Zhang et al.[30] observed in a mouse ectopic osteogenesis model that OCN expression was strong in BMP-9-induced bone-like tissue and was positively correlated with new bone density. Studies have shown that BMP-9 can not only regulate early osteogenic genes such as *Runx2* and *COL1A1*, but also significantly upregulate OCN expression, thereby promoting osteoblast maturation and bone matrix calcification.[20,31,32] In this experiment, immunohistochemical OCN-positive staining in the NPWT group was significantly enhanced, indicating accelerated local bone formation. At the same time, the mRNA and protein expression of OCN in the callus of the negative pressure group was significantly higher than that in the gauze group and the blank group. This shows that NPWT can significantly increase OCN expression, promoting osteoblast maturation and accelerating bone formation and fracture healing. On the other hand, OCN expression in the negative pressure group showed a positive correlation with BMP-9, indicating that the significantly elevated OCN expression and the promotion of osteoblast maturation and fracture healing were inseparable from BMP-9 regulation. It also showed that negative pressure preferentially activated BMP-9 to participate in fracture repair, while regulating OCN to promote the conversion of bone tissue into osteoblasts, thereby accelerating fracture healing.

Although negative pressure can preferentially mobilize BMP-9 to the fracture site, the underlying molecular mechanism remains unclear. Studies have shown that the transduction and expression of BMP-9 are regulated by multiple signaling pathways, including the canonical Smad-dependent pathway and the non-canonical MAPK pathway. [10,33-36] Among these, the MAPK/ERK5 pathway has recently been shown to play an essential role in the early stages of bone formation. Studies have shown that MEK5 activation of ERK5 can promote the expression of osteogenic transcription factors such as MEF2C and c-Fos, thereby regulating the activity of downstream osteogenic factor genes.[37-39] MEK5, as its upstream kinase, can specifically phosphorylate and activate ERK5, thereby controlling the transcriptional activity of its target transcription factors. In this study, immunohistochemistry showed that after negative-pressure treatment of the fracture ends, the protein expression levels of ERK5 and MEK5 in the NPWT group were significantly higher than those in the gauze and blank groups. At the same time, the expression of p-MEK5 and p-ERK5 was significantly upregulated in the Model+NPWT group, indicating that negative pressure preferentially activates the MAPK/ERK5 signaling pathway and promotes ERK5 phosphorylation.

In addition, ERK5 signaling plays a unique role in osteogenesis regulation. Under BMP-9 stimulation, activation of the ERK5 pathway can significantly enhance the expression of transcription factors such as Runx2 and Osterix, thereby driving MSC differentiation into mature osteoblasts.[40-43] In this study, we found that BMP-9 increased significantly after negative pressure treatment, proving that it has activated ERK5 signaling and thereby increased the overexpression of downstream factors. At the same time, MEK5, ERK5, BMP-9, and OCN in the negative pressure group + inhibitor group were significantly higher than those in the gauze+inhibitor group, demonstrating that BMP-9 stimulates ERK5 signaling and increases the overexpression of osteogenesis-related factors, thereby promoting fracture healing. It also showed that NPWT promotes the overexpression of ERK5 and MEK5, suggesting that this intervention may integrate the BMP-9 regulatory chain with ERK5 as the hub.

The therapeutic effect of NPWT in fracture healing stems not only from its fluid- drainage and decompression functions, but also from the activation of cellular mechanical signaling through micro-negative-pressure mechanical stimulation and the tension environment it creates. Multiple studies [5,44,45] have shown that NPWT can regulate local tissue stress distribution and cytosol circulation, thereby activating mechanosensitive elements (such as integrins, FAK, and YAP/TAZ) in osteoblasts and endothelial cells, and upregulating the expression of a series of osteogenesis-related signaling molecules. The MAPK/ERK family itself is a core component of the mechanical stimulation response pathway and is highly activated under stressful environments, which is consistent with the mechanical stimulation by negative pressure. This

may also be related to the preferential activation of the MAPK/ERK signaling pathway by negative pressure. Wen et al.[46] showed that cyclic tensile stress can significantly enhance ERK5 phosphorylation in MSCs and induce the expression of bone-specific markers. In this study, we observed that the expression levels of ERK5 and MEK5 in the NPWT group were significantly higher than those in the other 3 groups, suggesting that the ERK5/MEK5 signaling pathway may respond to the mechanical stimulation of negative pressure and the stress signals induced by stretching, thereby activating the signaling pathway and regulating related factors.

In summary, this study, based on an SD rat fracture model, systematically demonstrated for the first time that NPWT may enhance the osteogenic response at the fracture site by activating the MAPK/ERK5 signaling pathway and upregulating BMP-9 and OCN expression. This mechanism was validated through multiple experimental approaches, including changes in mRNA expression and protein levels, as well as enhanced OCN expression at the tissue level, establishing a complete chain of evidence from signaling to functional manifestation. If this strategy is combined with NPWT, it may open new therapeutic avenues for patients at high risk of severe fractures, nonunion, and bone infections.

Ethical Statement

All animal experiments in this study were approved by the Laboratory Animal Ethics Committee of Xinjiang Medical University (IACUC-20240227-18, approval date: February 27, 2024) and strictly adhered to the Standards for the Administration of Laboratory Animals and the Guide for the Care and Use of Laboratory Animals.

Acknowledgements

This research was supported by the Natural Science Foundation of Xinjiang Uygur Autonomous Region and the Department of Science and Technology of Xinjiang Uygur Autonomous Region (Grant No. 2023D01C144).

Sources of Funding

This research was supported by the Natural Science Foundation of Xinjiang Uygur Autonomous Region and the Department of Science and Technology of Xinjiang Uygur Autonomous Region (Grant No. 2023D01C144).

Conflicts of Interest

The authors declare that they have no competing interests.

References

1. Ye G, Li C, Xiang X, Chen C, Zhang R, Yang X, Yu X, Wang J, Wang L, Shi Q, Weng Y. Bone morphogenetic protein-9 induces PDLSCs osteogenic differentiation through the ERK and p38 signal pathways. Int J Med Sci. 2014 Aug 6;11(10):1065-72. doi: 10.7150/ijms.8473. PMID: 25136261; PMCID: PMC4135228.
2. Mende W, Götzl R, Kubo Y, Pufe T, Ruhl T, Beier JP. The Role of Adipose Stem Cells in Bone Regeneration and Bone Tissue Engineering. Cells. 2021 Apr 21;10(5):975. doi: 10.3390/cells10050975. PMID: 33919377; PMCID: PMC8143357.
3. Ma Z, Shou K, Li Z, Jian C, Qi B, Yu A. Negative pressure wound therapy promotes vessel destabilization and maturation at various stages of wound healing and thus influences wound prognosis. Exp Ther Med. 2016 Apr;11(4):1307-1317. doi: 10.3892/etm.2016.3083. Epub 2016 Feb 17. PMID: 27073441; PMCID: PMC4812564.
4. Ma Z, Li Z, Shou K, Jian C, Li P, Niu Y, Qi B, Yu A. Negative pressure wound therapy: Regulating blood flow perfusion and microvessel maturation through microvascular pericytes. Int J Mol Med. 2017 Nov;40(5):1415-1425. doi: 10.3892/ijmm.2017.3131. Epub 2017 Sep 13. PMID: 28901392; PMCID: PMC5627868.
5. Zhu J, Wang F, Yan L, Wang J, Wu M, Hu R, An Y. Negative pressure wound therapy enhances bone regeneration compared with conventional therapy in a rabbit radius gap-healing model. Exp Ther Med. 2021 May;21(5):474. doi: 10.3892/etm.2021.9905. Epub 2021 Mar 12. PMID: 33767769; PMCID: PMC7976378.
6. Li X, Liu J, Liu Y, Hu X, Dong M, Wang H, Hu D. Negative pressure wound therapy accelerates rats diabetic wound by promoting agenesis. Int J Clin Exp Med. 2015 Mar 15;8(3):3506-13. PMID: 26064242; PMCID: PMC4443076.
7. Huang M, Cheng YL, Zeng JT, Su XY, Liu H. Inhibin α-subunit inhibits BMP9-induced osteogenic differentiation through blocking BMP/Smad signal and activating NF-κB signal in mesenchymal stem cells. J Cell Biochem. 2018 Nov;119(10):8271-8281. doi: 10.1002/jcb.26843. Epub 2018 Jun 20. PMID: 29923343.
8. Park JH, Koh EB, Seo YJ, Oh HS, Byun JH. BMP-9 Improves the Osteogenic Differentiation Ability over BMP-2 through p53 Signaling In Vitro in Human Periosteum-Derived Cells. Int J Mol Sci. 2023 Oct 17;24(20):15252. doi: 10.3390/ijms242015252. PMID: 37894931; PMCID: PMC10607732.
9. Yao X, Li P, Deng Y, Yang Y, Luo H, He B. Role of p53 in promoting BMP9induced osteogenic differentiation of mesenchymal stem cells through TGFβ1. Exp Ther Med. 2023 Apr 13;25(6):248. doi: 10.3892/etm.2023.11947. PMID: 37153899; PMCID: PMC10160913.
10. Mostafa S, Pakvasa M, Coalson E, Zhu A, Alverdy A, Castillo H, Fan J, Li A, Feng Y, Wu D, Bishop E, Du S, Spezia M, Li A, Hagag O, Deng A, Liu W, Li M, Ho SS, Athiviraham A, Lee MJ, Wolf JM, Ameer GA, Luu HH, Haydon RC, Strelzow J, Hynes K, He TC, Reid RR. The wonders of BMP9: From mesenchymal stem cell differentiation, angiogenesis, neurogenesis, tumorigenesis, and metabolism to regenerative medicine. Genes Dis. 2019 Jul 24;6(3):201-223. doi: 10.1016/j.gendis.2019.07.003. PMID: 32042861; PMCID: PMC6997590.
11. Wen L, Liu Z, Zhou L, Liu Z, Li Q, Geng B, Xia Y. Bone and Extracellular Signal-Related Kinase 5 (ERK5). Biomolecules. 2024 May 4;14(5):556. doi: 10.3390/biom14050556. PMID: 38785963; PMCID: PMC11117709.
12. David L, Mallet C, Keramidas M, Lamandé N, Gasc JM, Dupuis-Girod S, Plauchu H, Feige JJ, Bailly S. Bone morphogenetic protein-9 is a circulating vascular quiescence

factor. Circ Res. 2008 Apr 25;102(8):914-22. doi: 10.1161/CIRCRESAHA.107.165530. Epub 2008 Feb 28. PMID: 18309101; PMCID: PMC2561062.
13. Greenblatt MB, Shim JH, Bok S, Kim JM. The Extracellular Signal-Regulated Kinase Mitogen-Activated Protein Kinase Pathway in Osteoblasts. J Bone Metab. 2022 Feb;29(1):1-15. doi: 10.11005/jbm.2022.29.1.1. Epub 2022 Feb 28. PMID: 35325978; PMCID: PMC8948490.
14. Wang C, Zhang Y, Qu H. Negative pressure wound therapy for closed incisions in orthopedic trauma surgery: a meta-analysis. J Orthop Surg Res. 2019 Dec 11;14(1):427. doi: 10.1186/s13018-019-1488-z. PMID: 31829217; PMCID: PMC6907184.
15. Zhu J, Yu A, Qi B, Li Z, Hu X. Effects of negative pressure wound therapy on mesenchymal stem cells proliferation and osteogenic differentiation in a fibrin matrix. PLoS One. 2014 Sep 12;9(9):e107339. doi: 10.1371/journal.pone.0107339. PMID: 25216182; PMCID: PMC4162584.
16. Su XY, Zou X, Chen QZ, Zeng YH, Shao Y, He BC, Liu H. Follicle-Stimulating Hormone β-Subunit Potentiates Bone Morphogenetic Protein 9-Induced Osteogenic Differentiation in Mouse Embryonic Fibroblasts. J Cell Biochem. 2017 Jul;118(7):1792-1802. doi: 10.1002/jcb.25849. Epub 2017 Mar 17. PMID: 27996168.
17. Wang RN, Green J, Wang Z, Deng Y, Qiao M, Peabody M, Zhang Q, Ye J, Yan Z, Denduluri S, Idowu O, Li M, Shen C, Hu A, Haydon RC, Kang R, Mok J, Lee MJ, Luu HL, Shi LL. Bone Morphogenetic Protein (BMP) signaling in development and human diseases. Genes Dis. 2014 Sep;1(1):87-105. doi: 10.1016/j.gendis.2014.07.005. PMID: 25401122; PMCID: PMC4232216.
18. Wu JQ, Mao LB, Liu LF, Li YM, Wu J, Yao J, Zhang FH, Liu TY, Yuan L. Identification of key genes and pathways of BMP-9-induced osteogenic differentiation of mesenchymal stem cells by integrated bioinformatics analysis. J Orthop Surg Res. 2021 Apr 20;16(1):273. doi: 10.1186/s13018-021-02390-w. PMID: 33879213; PMCID: PMC8059242.
19. Nakamura T, Shinohara Y, Momozaki S, Yoshimoto T, Noguchi K. Co-stimulation with bone morphogenetic protein-9 and FK506 induces remarkable osteoblastic differentiation in rat dedifferentiated fat cells. Biochem Biophys Res Commun. 2013 Oct 18;440(2):289-94. doi: 10.1016/j.bbrc.2013.09.073. Epub 2013 Sep 21. PMID: 24064349.
20. Park JH, Koh EB, Seo YJ, Oh HS, Byun JH. BMP-9 Improves the Osteogenic Differentiation Ability over BMP-2 through p53 Signaling In Vitro in Human Periosteum-Derived Cells. Int J Mol Sci. 2023 Oct 17;24(20):15252. doi: 10.3390/ijms242015252. PMID: 37894931; PMCID: PMC10607732.
21. Oni OO, Stafford H, Gregg PJ. An experimental study of the patterns of periosteal and endosteal damage in tibial shaft fractures using a rabbit trauma model. J Orthop Trauma. 1989;3(2):142-7. doi: 10.1097/00005131-198906000-00009. PMID: 2738762.
22. Moss DW. Diagnostic aspects of alkaline phosphatase and its isoenzymes. Clin Biochem. 1987 Aug;20(4):225-30. doi: 10.1016/s0009-9120(87)80002-4. PMID: 3319285.
23. Xiao H, Wang X, Wang C, Dai G, Zhu Z, Gao S, He B, Liao J, Huang W. BMP9 exhibits dual and coupled roles in inducing osteogenic and angiogenic differentiation of mesenchymal stem cells. Biosci Rep. 2020 Jun 26;40(6):BSR20201262. doi: 10.1042/BSR20201262. PMID: 32478395; PMCID: PMC7295632.
24. Wang X, Huang J, Huang F, Zong JC, Tang X, Liu Y, Zhang QF, Wang Y, Chen L, Yin LJ, He BC, Deng ZL. Bone morphogenetic protein 9 stimulates callus formation in osteoporotic rats during fracture healing. Mol Med Rep. 2017 May;15(5):2537-2545. doi: 10.3892/mmr.2017.6302. Epub 2017 Mar 9. PMID: 28447742; PMCID: PMC5428899.
25. Lee SB, Lee HJ, Park JB. Bone Morphogenetic Protein-9 Promotes Osteogenic Differentiation and Mineralization in Human Stem-Cell-Derived Spheroids. Medicina (Kaunas). 2023 Jul 16;59(7):1315. doi: 10.3390/medicina59071315. PMID: 37512125; PMCID: PMC10384578.
26. Berezovska O, Yildirim G, Budell WC, Yagerman S, Pidhaynyy B, Bastien C, van der Meulen MCH, Dowd TL. Osteocalcin affects bone mineral and mechanical properties in female mice. Bone. 2019 Nov;128:115031. doi: 10.1016/j.bone.2019.08.004. Epub 2019 Aug 8. PMID: 31401301; PMCID: PMC8243730.
27. Zhou L, Wang J, Mu W. BMP-2 promotes fracture healing by facilitating osteoblast differentiation and bone defect osteogenesis. Am J Transl Res. 2023 Dec 15;15(12):6751-6759. PMID: 38187002; PMCID: PMC10767540.
28. Zoch ML, Clemens TL, Riddle RC. New insights into the biology of osteocalcin. Bone. 2016 Jan;82:42-9. doi: 10.1016/j.bone.2015.05.046. Epub 2015 Jun 6. PMID: 26055108; PMCID: PMC4670816.
29. Wang T, Zhang X, Bikle DD. Osteogenic Differentiation of Periosteal Cells During Fracture Healing. J Cell Physiol. 2017 May;232(5):913-921. doi: 10.1002/jcp.25641. Epub 2016 Oct 26. PMID: 27731505; PMCID: PMC5247290.
30. Zhang Yan, Wen Wei, Luo Jinyong. Bone morphogenetic protein 9 induces osteogenic differentiation of pluripotent stem cells. Progress in Biochemistry and Biophysics, 2009, 36(10): 1291-1298.
31. Zhu D, Mackenzie NC, Shanahan CM, Shroff RC, Farquharson C, MacRae VE. BMP-9 regulates the osteoblastic differentiation and calcification of vascular smooth muscle cells through an ALK1 mediated pathway. J Cell Mol Med. 2015 Jan;19(1):165-74. doi: 10.1111/jcmm.12373. Epub 2014 Oct 9. PMID: 25297851; PMCID: PMC4288360.
32. Komori T. Regulation of bone development and extracellular matrix protein genes by RUNX2. Cell Tissue Res. 2010 Jan;339(1):189-95. doi: 10.1007/s00441-009-0832-8. Epub 2009 Aug 1. PMID: 19649655.
33. Zou ML, Chen ZH, Teng YY, Liu SY, Jia Y, Zhang KW, Sun ZL, Wu JJ, Yuan ZD, Feng Y, Li X, Xu RS, Yuan FL. The Smad Dependent TGF-β and BMP Signaling Pathway in Bone Remodeling and Therapies. Front Mol Biosci. 2021 May 5;8:593310. doi: 10.3389/fmolb.2021.593310. PMID: 34026818; PMCID: PMC8131681.
34. Park JE, Shao D, Upton PD, Desouza P, Adcock IM, Davies RJ, Morrell NW, Griffiths MJ, Wort SJ. BMP-9 induced endothelial cell tubule formation and inhibition of migration involves Smad1 driven endothelin-1 production. PLoS One. 2012;7(1):e30075. doi: 10.1371/journal.pone.0030075. Epub 2012 Jan 27. PMID: 22299030; PMCID: PMC3267722.
35. Wang Y, Sima X, Ying Y, Huang Y. Exogenous BMP9 promotes lung fibroblast HFL-1 cell activation via ALK1/Smad1/5 signaling *in vitro*. Exp Ther Med. 2021 Jul;22(1):728. doi: 10.3892/etm.2021.10160. Epub 2021 May 4. PMID: 34007337; PMCID: PMC8120641.

36. Zhang S, Xie Y, Yan F, Zhang Y, Yang Z, Chen Z, Zhao Y, Huang Z, Cai L, Deng Z. Negative pressure wound therapy improves bone regeneration by promoting osteogenic differentiation via the AMPK-ULK1-autophagy axis. Autophagy. 2022 Sep;18(9):2229-2245. doi: 10.1080/15548627.2021.2016231. Epub 2021 Dec 29. PMID: 34964701; PMCID: PMC9466622.
37. Paudel R, Fusi L, Schmidt M. The MEK5/ERK5 Pathway in Health and Disease. Int J Mol Sci. 2021 Jul 15;22(14):7594. doi: 10.3390/ijms22147594. PMID: 34299213; PMCID: PMC8303459.
38. Terasawa K, Okazaki K, Nishida E. Regulation of c-Fos and Fra-1 by the MEK5-ERK5 pathway. Genes Cells. 2003 Mar;8(3):263-73. doi: 10.1046/j.1365-2443.2003.00631.x. PMID: 12622723.
39. Fujii T, Murata K, Mun SH, Bae S, Lee YJ, Pannellini T, Kang K, Oliver D, Park-Min KH, Ivashkiv LB. MEF2C regulates osteoclastogenesis and pathologic bone resorption via c-FOS. Bone Res. 2021 Jan 11;9(1):4. doi: 10.1038/s41413-020-00120-2. PMID: 33424022; PMCID: PMC7797478.
40. Horie T, Hinoi E. Role of Erk5 expressed in bone marrow mesenchymal stem cells on bone homeostasis and its potential applications in cancer treatment. Oncoscience. 2024 May 20;11:45-46. doi: 10.18632/oncoscience.601. PMID: 38770443; PMCID: PMC11104408.
41. Lamplot JD, Qin J, Nan G, Wang J, Liu X, Yin L, Tomal J, Li R, Shui W, Zhang H, Kim SH, Zhang W, Zhang J, Kong Y, Denduluri S, Rogers MR, Pratt A, Haydon RC, Luu HH, Angeles J, Shi LL, He TC. BMP9 signaling in stem cell differentiation and osteogenesis. Am J Stem Cells. 2013 Mar 8;2(1):1-21. PMID: 23671813; PMCID: PMC3636726.
42. Phimphilai M, Zhao Z, Boules H, Roca H, Franceschi RT. BMP signaling is required for RUNX2-dependent induction of the osteoblast phenotype. J Bone Miner Res. 2006 Apr;21(4):637-46. doi: 10.1359/jbmr.060109. Epub 2006 Apr 5. PMID: 16598384; PMCID: PMC2435171.
43. Li L, Lian WW. [BMP9 promotes osteogenic differentiation of periodontal ligament stem cells under inflammatory environment via ERK5/KLF4 signaling pathway]. Shanghai Kou Qiang Yi Xue. 2023 Dec;32(6):583-589. Chinese. PMID: 38494965.
44. Zhang S, Xie Y, Yan F, Zhang Y, Yang Z, Chen Z, Zhao Y, Huang Z, Cai L, Deng Z. Negative pressure wound therapy improves bone regeneration by promoting osteogenic differentiation via the AMPK-ULK1-autophagy axis. Autophagy. 2022 Sep;18(9):2229-2245. doi: 10.1080/15548627.2021.2016231. Epub 2021 Dec 29. PMID: 34964701; PMCID: PMC9466622.
45. Cai X, Wang KC, Meng Z. Mechanoregulation of YAP and TAZ in Cellular Homeostasis and Disease Progression. Front Cell Dev Biol. 2021 May 24;9:673599. doi: 10.3389/fcell.2021.673599. PMID: 34109179; PMCID: PMC8182050.
46. Wen L, Liu Z, Zhou L, Liu Z, Li Q, Geng B, Xia Y. Bone and Extracellular Signal-Related Kinase 5 (ERK5). Biomolecules. 2024 May 4;14(5):556. doi: 10.3390/biom14050556. PMID: 38785963; PMCID: PMC11117709.

***Corresponding author:** Zhan Jun Ma. E-mail: 3244985524@qq.com*

International Journal of Biomedicine 16(1) (2026) 41-45
http://dx.doi.org/10.21103/Article16(1)_OA4

ORIGINAL ARTICLE

Surgery

INTERNATIONAL JOURNAL OF BIOMEDICINE

Evaluation of Long-Term Outcomes After Total Gastrectomy for Gastric Cancer: A Comparative Analysis of Hand-Sewn Versus Mechanical Esophagojejunostomy

Evgeny A. Toneev[1,2*], Nikita A. Berestov[2], Danil D. Prokhorov[1,2], Maria A. Sypalo[3], Polina A. Nevedomskaia[3], Adel F. Rysaev[3], Eleonora A. Mitina[3]

[1]*Ulyanovsk Regional Clinical Oncology Dispensary, Ulyanovsk, Russia*
[2]*Ulyanovsk State University, Ulyanovsk, Russia*
[3]*Samara State Medical University, Samara, Russia*

Abstract

Background: Total gastrectomy remains a key component of gastric cancer treatment, and the method used to construct the esophagojejunostomy may influence long-term functional outcomes and quality of life. Evidence comparing hand-sewn and mechanical anastomoses in this context remains inconsistent. This retrospective study aimed to evaluate and compare long-term functional outcomes and quality of life in patients undergoing total gastrectomy with either hand-sewn or mechanical esophagojejunostomy.

Methods and Results: The study included 153 patients who underwent total gastrectomy for histologically confirmed gastric adenocarcinoma. Patients were divided into two groups based on the anastomotic technique: mechanical circular stapler or hand-sewn anastomosis (according to a patented method). Long-term outcomes were evaluated 12 months postoperatively using EORTC QLQ-C30 and QLQ-STO22 questionnaires, along with endoscopic assessment of reflux esophagitis using the Los Angeles classification. Postoperative complications were graded according to the Clavien–Dindo classification.

Both groups demonstrated comparable short-term postoperative outcomes and similar complication rates according to the Clavien–Dindo classification. However, patients with a hand-sewn anastomosis showed significantly better long-term quality-of-life scores *(EORTC QLQ-C30, QLQ-STO22)*, including higher functional domain scores and lower scores for reflux, pain, nausea, and dietary restriction. Endoscopic assessment revealed no significant differences in esophagitis prevalence or severity between groups.

Conclusion: While mechanical anastomosis offers advantages in operative duration and blood loss, the hand-sewn technique provides superior long-term functional outcomes and quality-of-life benefits. These findings support the consideration of hand-sewn esophagojejunostomy in clinical settings where long-term recovery and patient-reported outcomes are prioritized.(**International Journal of Biomedicine. 2026;16(1):41-45.**)

Keywords: gastrectomy • quality of life • esophagojejunostomy • hand-sewn anastomosis, mechanical anastomosis • complications

For citation: Toneev EA, Berestov NA, Prokhorov DD, Sypalo MA, Nevedomskaia PA, Rysaev AF, Mitina EA. Evaluation of Long-Term Outcomes After Total Gastrectomy for Gastric Cancer: A Comparative Analysis of Hand-Sewn Versus Mechanical Esophagojejunostomy. International Journal of Biomedicine. 2026;16(1):41-45. doi:10.21103/Article16(1)_OA4

Introduction

Gastric cancer remains one of the leading causes of cancer-related mortality worldwide, ranking fifth in incidence and fourth in mortality among malignant tumors.[1] Despite a decline in incidence in several countries, the prognosis for advanced-stage disease remains unfavorable.[2] In Russia, gastric cancer consistently ranks among the ten most common oncological diseases.[3] Surgical treatment remains the main and essential component of multimodal therapy, providing acceptable long-term oncological outcomes. One of the radical treatment options is total gastrectomy. A crucial aspect of gastrectomy is the creation of the esophagojejunostomy, whose technique and reliability determine both early surgical outcomes and long-term functional results.[2] The use of mechanical stapling devices has standardized techniques and

reduced operative time. However, the discussion regarding the advantages of the hand-sewn technique versus mechanical anastomosis remains open, particularly with respect to long-term quality-of-life outcomes.[4] This study aimed to evaluate and compare long-term functional outcomes and quality of life in patients undergoing total gastrectomy with either hand-sewn or mechanical esophagojejunostomy.

Materials and Methods

The retrospective study of total gastrectomy was conducted in 153 patients at the Ulyanovsk Regional Clinical Oncology Dispensary from 01.01.2019 to 01.09.2025.

The study included patients with morphologically confirmed gastric adenocarcinoma who underwent total gastrectomy, were aged 18 to 85 years, had no distant metastases, and had provided written informed consent. Exclusion criteria: patients who underwent emergency surgery, had high anesthetic risk (ASA IV–V), had a history of prior gastric surgery, or refused to participate.

Patients were divided into two groups based on the method of esophagojejunostomy formation: mechanical (using a circular stapler) (Group 1) and hand-sewn (Grpip 2), as described in the proposed technique. An esophagojejunostomy using a mechanical circular stapler was performed according to standard technique. After preparation of the Roux limb, a jejunojejunostomy was performed; the limb was passed through an avascular window in the transverse mesocolon, and the esophagojejunostomy was created with a circular stapler. The staple line was additionally reinforced with 4–5 interrupted esophagojejunal sutures using PDS 3-0. The hand-sewn esophagojejunostomy was formed using the authors' patented technique (Russian Federation).[5] An absorbable braided PGA 3-0 suture (MiM, Russia) with an atraumatic needle was used as follows: After completing a gastrectomy and D2 lymphadenectomy, a Roux limb was created to restore gastrointestinal continuity. The jejunal loop was transected 20–25 cm distal to the ligament of Treitz. A mobile Roux limb 60 cm in length was formed according to anatomical considerations. After choosing the appropriate length, a side-to-side jejunojejunostomy was created. During the transection of the stomach from the esophagus, a Satinsky clamp was applied to the esophagus. The esophagus was transected in stages (adventitia/muscular layer, followed by submucosal–mucosal layer) under the clamp. Two fixation sutures were placed on the blind end of the jejunum 2–3 cm from the edge, approximating the loop to the lateral surfaces of the esophagus. A small enterotomy (5–7 mm) was created 3–4 mm from the first suture line. The posterior wall was created with a row of five full-thickness interrupted sutures oriented "mucosa to mucosa." Two "transition" stitches were then placed at the junction of the posterior and anterior lips, with needle entry and exit from the mucosal side of the jejunum and the esophagus. The anterior wall was constructed with seromuscular interrupted sutures: entry from the serosal side of the jejunum, then through the esophageal mucosa near its edge, and cranially exiting onto the adventitia. The final step was invagination of the anastomotic line using "saddle-shaped" P-sutures: needle entry from the serosa of the jejunum, perpendicularly engaging the esophageal adventitia, and a third needle entry again through the serosa of the jejunum. As a result, the first row of anterior interrupted sutures was buried beneath the row of P-sutures. Assessment of long-term outcomes.

The primary endpoint was quality of life at 12 months, assessed using the EORTC QLQ-C30 and QLQ-STO22 questionnaires.

Secondary endpoints included postoperative complications (Clavien–Dindo classification) and endoscopic findings according to the Los Angeles classification (at 12 months).

Statistical analysis was performed using R version 4.2.2 and StatTech v. 4.1.2 (StatTech LLC, Russia). Baseline characteristics were summarized as frequencies and percentages for categorical variables and mean±standard deviation (SD) for continuous variables. Means of 2 continuous normally distributed variables were compared by an independent samples Student's t-test. The frequencies of categorical variables were compared using the chi-square test or Fisher's exact test (2-tailed), when appropriate. A value of $P < 0.05$ was considered significant.

Results

A comparative analysis of clinical and demographic characteristics, as well as intraoperative data, for patients with mechanical and hand-sewn esophagojejunostomies is presented in Table 1. When comparing the two groups, statistically significant differences were identified in operative duration (185.3±24.7 min vs. 224.8±29.4 min, $P<0.001$), blood loss (281.5±78.2 mL vs. 318.7±88.9 mL, $P=0.007$), and anastomosis formation time (18.2±4.8 min vs. 34.7±7.9 min, $P<0.001$), indicating the advantages of the mechanical technique. The rate of anastomotic leakage was higher in the mechanical group (3.8% vs. 0%). However, the difference did not reach statistical significance ($P=0.246$).

The frequency and pattern of complications according to the Clavien–Dindo classification did not differ significantly between the groups (Table 2). Most patients in both cohorts experienced no postoperative complications.

Quality-of-life indicators in patients after gastrectomy differed significantly between those who received a mechanical and those who received a hand-sewn anastomosis (Table 3). Patients in the hand-sewn anastomosis group demonstrated higher levels of physical and role functioning, as well as better overall quality of life. In addition, these patients experienced significantly lower rates of nausea/vomiting and pain. To assess specific symptoms related to the disease and surgical intervention, the EORTC QLQ-STO22 module was used. A comparative analysis of the indicators in the mechanical and hand-sewn anastomosis groups is presented in Table 4.

Patients with a hand-sewn anastomosis demonstrated significantly lower levels of dysphagia, reflux symptoms, dietary restrictions, and pain, which reflects a more favorable long-term quality of life. The incidence of esophagitis according to the Los Angeles classification in the long-term follow-up period is presented in Table 5.

Table 1.

Clinical and demographic characteristics.

Parameter		Group1 (n=79)	Group 2 (n=74)	*P*-value
Age, years (M±SD)		66.5±12.8	61.8±12.2	0.021
Sex	Male, n (%)	59 (74.7%)	48 (64.9%)	0.218
	Female, n (%)	27 (34.2%)	26 (35.1%)	
The ASA physical status classification system	I, n (%)	8 (10.1%)	6 (8.1%)	0.782
	II–III, n (%)	71 (89.9%)	68 (91.9%)	
Diabetes mellitus, n (%)		12 (15.2%)	6 (8.1%)	0.214
Ischemic heart disease, n (%)		28 (35.4%)	20 (27.0%)	0.298
Hypertension, n (%)		52 (65.8%)	43 (58.1%)	0.405
Charlson index (M±SD)		2.0±0.7	1.8±0.4	0.031
BMI (M±SD)		27.8±5.0	26.1±4.6	0.030
Tumor location, n (%)	Distal part	32 (40.5%)	37 (50.0%)	0,488
	Body	18 (22.8%)	15 (20.3%)	
	Cardia (Siewert III)	29 (36.7%)	22 (29.7%)	
T stage, n (%)		T1 8 (10,1%)	T1 3 (4.1%)	0.401
		T2 9 (11,4%)	T2 4 (5.4%)	
		T3a 25 (31,6%)	T3a 28 (37.8%)	
		T3b 16 (20,3%)	T3b 21 (28.4%)	
		T4a 12 (15,2%)	T4a 10 (13.5%)	
		T4b 9 (11,4%)	T4b 8 (10.8%)	
N stage, n (%)		N0 28 (35.4%)	N0 30 (40.5%)	0.341
		N1 18 (22.8%)	N1 22 (29.7%)	
		N2 27 (34.2%)	N2 20 (27.0%)	
		N3 6 (7.6%)	N3 2 (2.7%)	
M stage, n		M0 79 (100%)	M0 74 (100%)	1.000
		M1 0 (0%)	M1 0 (0%)	
Completed 4 cycles of neoadjuvant chemotherapy, n (%)		62 (78.5%)	65 (87.8%)	0.137
Operation time, min (M±SD)		185.3±24.7	224.8±29.4	<0.001
Blood loss. mL (M±SD)		281.5±78.2	318.7±88.9	0.007
Anastomosis time, min (M±SD)		18.2±4.8	34.7±7.9	<0.001
Anastomotic leakage, n (%)		3 (3.8%)	0 (0%)	0.246

Table 2.

Complications according to the Clavien–Dindo classification.

Grade	Group 1 (n=79)	Group 2 (n=74)	*P*-value
Grade 0–I	61 (77.2%)	56 (75.7%)	0.851
Grade II	12 (15.2%)	10 (13.5%)	0.821
Grade IIIA	2 (2.53%)	3 (4.05%)	0.673
Grade IIIB	1 (1.27%)	2 (2.70%)	0.610
Grade IVA	0 (0.0%)	2 (2.70%)	0.232
Grade IVB	1 (1.27%)	0 (0.0%)	1.000
Grade V	2 (2.53%)	1 (1.35%)	1.000

Table 3.

Quality of life according to the EORTC QLQ-C30 at 12 months after surgery.

Scale	Group 1 (n=42)	Group 2 (n=38)	*P*-value
Physical functioning	76.8±15.1	82.3±13.5	0.024
Role functioning	73.2±18.4	79.8±16.7	0.041
Global quality of life	70.9±17.4	77.1±15.6	0.034
Nausea/vomiting	26.2±12.5	19.7±10.8	0.002
Pain	23.4±10.2	17.9±8.7	0.001

Table 4.

Quality of life according to the EORTC QLQ-STO22 at 12 months after surgery.

Scale	Group 1 (n=42)	Group 2 (n=38)	*P*-value
Reflux symptoms	21.4±10.7	14.6±8.3	0.002
Dietary restrictions	24.3±12.8	18.9±10.4	0.043
Specific pain	20.1±10.3	15.7±8.9	0.045

Table 5.

Endoscopic assessment according to the Los Angeles classification.

Esophagitis grade	Group 1 (n=70)	Group 2 (n=68)	*P*-value
N (normal)	48 (68.6%)	41 (60.3%)	0.212
A (mild)	12 (17.1%)	15 (22.1%)	0.386
B (moderate)	6 (8.6%)	8 (11.8%)	0.532
C (severe)	3 (4.3%)	3 (4.4%)	0.988
D (very severe)	1 (1.4%)	1 (1.5%)	0.973
Any A–D	22 (31.4%)	27 (39.7%)	0.212
Clinically significant (C–D)	4 (5.7%)	4 (5.9%)	0.974

No statistically significant differences were found between the groups in terms of the frequency or severity of esophagitis. Most patients in both groups showed no signs of esophagitis, and clinically significant changes (grades C-D) were observed only in a small number of cases.

Discussion

The results of the present study demonstrate that long-term quality-of-life outcomes after gastrectomy in patients with gastric cancer are no less important than the immediate surgical results.[6,7] A comparative analysis of clinical and demographic characteristics confirmed comparability between the groups on key parameters (age, sex, functional status), thereby excluding the influence of systematic differences on the results. At the same time, the use of mechanical anastomosis was associated with a statistically significant reduction in operative time and intraoperative blood loss, consistent with results reported by other authors.[8,9] These advantages make stapling technologies convenient for surgeons, as they are highly reproducible and reduce operative trauma; however, their impact on long-term outcomes remains a matter of debate.[10]

Analysis of complications according to the Clavien-Dindo classification showed no statistically significant differences between the groups.[11] The rate of severe complications was low, which is consistent with international data.[12,13] Russian publications also emphasize that the surgical center's experience and standardized technique are key factors in reducing postoperative mortality.[14] Nevertheless, studies report statistically significantly higher complication rates in the hand-sewn anastomosis group.[15]

Currently, quality of life is considered an important indicator of treatment effectiveness. Great attention is paid to this aspect to improve patient well-being, functional capacity, and overall quality of life. Standardized questionnaires allow direct comparison of treatment outcomes across different surgical centers and techniques.[16] The differences observed in the EORTC QLQ-C30 domains in our study are consistent with findings reported by other authors: the severity of symptoms and subjective outcomes after gastrectomy significantly depend on the type of reconstruction and the anatomical configuration of the anastomosis. In several variants, more frequently stapled ones, more pronounced gastrointestinal symptoms (reflux, discomfort) have been described, whereas global functional indicators may remain comparable.[17] This confirms that the technical simplicity of a procedure is not always associated with better subjective outcomes.

The QLQ-STO22 results further clarified the picture, demonstrating statistically more severe reflux symptoms and dietary restrictions in patients with mechanical anastomosis.[18,19] Endoscopic evaluation using the Los Angeles classification revealed a low incidence of severe esophagitis, with no significant differences between the groups. However, the correlation between endoscopic findings and questionnaire results (QLQ-STO22) suggests that functional disorders (dysphagia, reflux symptoms, and others) may have greater clinical significance for the patient than morphological changes. This observation is also reflected in several Russian and international publications.[20-24] The use of multiple questionnaires to assess subjective patient-reported outcomes, combined with instrumental diagnostic methods such as upper endoscopy, enables a comprehensive evaluation of quality of life and ultimately provides a complete picture of the effectiveness of the proposed anastomotic technique.

Thus, the results of the study demonstrate that the choice of anastomosis technique affects long-term functional outcomes. The hand-sewn technique showed better quality-of-life indicators, as assessed by both subjective and objective methods, making it preferable when long-term outcomes are prioritized, namely, a minimal risk of anastomosis-related complications, including anastomotic leakage and reflux esophagitis. At the same time, mechanical anastomosis remains valuable due to reduced operative time and blood loss, which may be critically important for frail patients. In clinical practice, the choice of technique should be determined not only by the surgical center's technical capabilities but also by the anticipated impact on long-term quality-of-life outcomes.

In conclusion, when comparing hand-sewn and mechanical methods of anastomosis formation, both demonstrated comparable early postoperative outcomes; however, in the long-term period, the hand-sewn method provides superior quality of life.

Ethical Statement

The study was performed in accordance with the principles of the Declaration of Helsinki and approved by the local ethics committee (No. 12, dated 10.01.2025). All patients signed informed consent for the procedure.

References

1. Sung H, Ferlay J, Siegel RL, Laversanne M, Soerjomataram I, Jemal A, Bray F. Global Cancer Statistics 2020: GLOBOCAN Estimates of Incidence and Mortality Worldwide for 36 Cancers in 185 Countries. CA Cancer J Clin. 2021 May;71(3):209-249. doi: 10.3322/caac.21660.
2. Lordick F, Carneiro F, Cascinu S, Fleitas T, Haustermans K, Piessen G, Vogel A, Smyth EC; ESMO Guidelines Committee. Gastric cancer: ESMO Clinical Practice Guideline for diagnosis, treatment and follow-up. Ann Oncol. 2022 Oct;33(10):1005-1020. doi: 10.1016/j.annonc.2022.07.004. PMID: 35914639.
3. Kaprin AD, Starinsky VV, Shakhzadova AO (eds.). Malignant neoplasms in Russia in 2021 (morbidity and mortality). Moscow: Hertsen Moscow Oncology Research Institute – Branch of the National Medical Research Radiology Centre, Ministry of Health of Russia, 2022. [In Russian].
4. Honório FCC, Tustumi F, Pinheiro Filho JEL, Marques SSB, Glina FPA, Henriques AC, Dias AR, Waisberg J. Esophagojejunostomy after total gastrectomy: A systematic review and meta-analysis comparing hand-sewn and stapled anastomosis. J Surg Oncol. 2022 Jul;126(1):161-167. doi: 10.1002/jso.26909. PMID: 35689590.
5. Toneev EA, Firsov AA, Martynov AA, Keshyan EA. Patent RU № 2836347. 2025. [In Russian].
6. Weimann A, Braga M, Carli F, Higashiguchi T, Hübner M, Klek S, et al. ESPEN practical guideline: Clinical nutrition in surgery. Clin Nutr. 2021 Jul;40(7):4745-4761. doi: 10.1016/j.clnu.2021.03.031. PMID: 34242915.
7. Pinheiro RN, Mucci S, Zanatto RM, Picanço Junior OM, Bottino AAG, Fontoura RP, Lopes Filho GJ. Quality of life as a fundamental outcome after curative intent gastrectomy for adenocarcinoma: lessons learned from patients. J Gastrointest Oncol. 2019 Oct;10(5):989–998. doi:10.21037/jgo.2019.06.05. PMID: 31602337.
8. Zhou ZG, Hu M, Li Y, et al. Stapled vs hand-sewn gastroenteric anastomosis after gastrectomy: randomized controlled trial. World J Gastroenterol. 2003;9(4):772–774.
9. Degiuli M, Elmore U, De Carli S, et al. Mechanical vs hand-sewn anastomosis after gastrectomy for cancer: a multicenter comparison. World J Surg Oncol. 2014;12:292.
10. Kvist E, Helminen O, Helmiö M, Huhta H, Jalkanen A, Junttila A, et al.; FINEGO group. Stapled vs handsewn anastomosis and anastomotic leaks in gastric cancer surgery-a population-based nationwide study in Finland. J Gastrointest Surg. 2024 Jun;28(6):820-823. doi: 10.1016/j.gassur.2024.03.005. PMID: 38599994.
11. Dindo D, Demartines N, Clavien PA. Classification of surgical complications: a new proposal with evaluation in a cohort of 6336 patients and results of a survey. Ann Surg. 2004 Aug;240(2):205-13. doi: 10.1097/01.sla.0000133083.54934.ae. PMID: 15273542; PMCID: PMC1360123.
12. Katai H, Ishikawa T, Akazawa K, Isobe Y, Miyashiro I, Oda I, et al. Short-term surgical outcomes from the nationwide registry of the Japanese Gastric Cancer Association. Gastric Cancer. 2018;21(4):665–674.
13. Sano T, Sasako M, Yamamoto S, Nashimoto A, Kurita A, Hiratsuka M, et al. Mortality and morbidity after D2 gastrectomy for gastric cancer: an analysis of 2,500 patients. Br J Surg. 2004;91(8):1099–1104.
14. Toneev EA, Firstov AA, Keshyan EA, Pikin OV, Danilova LA, Martynov AA, Zhinov AV. Immediate surgical results of gastrectomies for gastric cancer: Experience of the regional oncology center. Novosti Khirurgii [News of Surgery]. 2023;31(6):502–512. [In Russian].
15. Uprak TK, Ekdal DC, Ergenç M, Attaallah W, et al. "Hand-sewn versus Stapled Anastomosis for Billroth II Gastrojejunostomy After Distal Gastrectomy: Comparison of Short-term Outcomes." İstanbul Med J. 2023;24(2):181-185.
16. van Amelsfoort RM, van der Sluis K, Schats W, Jansen EPM, van Sandick JW, Verheij M, Walraven I. Health-Related Quality of Life in Locally Advanced Gastric Cancer: A Systematic Review. Cancers (Basel). 2021 Nov 25;13(23):5934. doi: 10.3390/cancers13235934.
17. Yang K, Zhang WH, Liu K, Chen XZ, Zhou ZG, Hu JK. Comparison of quality of life between Billroth-I and Roux-en-Y anastomosis after distal gastrectomy for gastric cancer: A randomized controlled trial. Sci Rep. 2017 Sep 12;7(1):11245. doi: 10.1038/s41598-017-09676-2. Erratum in: Sci Rep. 2018 Apr 25;8(1):6783. doi: 10.1038/s41598-018-24612-8. PMID: 28900096; PMCID: PMC5595810.
18. Park KB, Park JY, Lee SS, Chung HY, Kwon OK. Chronological changes in quality of life and body composition after gastrectomy for locally advanced gastric cancer. Ann Surg Treat Res. 2020 May;98(5):262-269. doi: 10.4174/astr.2020.98.5.262.
19. Ito Y, Yoshikawa T, Fujiwara M, Kojima H, Matsui T, Mochizuki Y, et al. Quality of life and nutritional consequences after aboral pouch reconstruction following total gastrectomy for gastric cancer: randomized controlled trial CCG1101. Gastric Cancer. 2016 Jul;19(3):977-85. doi: 10.1007/s10120-015-0529-5. Epub 2015 Aug 14. PMID: 26272278.
20. Im MH, Kim DY, Kim YJ, Kim SH, Kim CW, Choi SH, et al. The impact of esophageal reflux-induced symptoms on quality of life after gastrectomy for gastric cancer. J Gastric Cancer. 2014;14(3):207–214. doi:10.5230/jgc.2014.14.3.207. PMID: 25364383; PMCID: PMC3996245.
21. Park SH, Man Yoon H, Ryu KW, Kim YW, Han M, Eom BW. Long-term Functional and Patient-reported Outcomes Between Intra-corporeal Delta-shaped Gastroduodenostomy and Gastrojejunostomy After Laparoscopic Distal Gastrectomy. J Gastric Cancer. 2023 Oct;23(4):561-573. doi: 10.5230/jgc.2023.23.e35. PMID: 37932223; PMCID: PMC10630562.
22. Maev IV, Andreev DN, Kucheryavy YuA. Gastroesophageal reflux disease: current concepts of pathogenesis, diagnosis, and treatment. Lechashchiy Vrach (The Attending Physician). 2004;(4):12–17. [In Russian].
23. Solovyova GA, Ilchenko AA, Filippov YuV, Andreev DN. Development and validation of the Russian version of the GERD-HRQL questionnaire for assessing quality of life in patients with gastroesophageal reflux disease. Kachestvennaya Klinicheskaya Praktika (Quality Clinical Practice). 2020;(2):45–51. [In Russian].
24. Sheptulin AA, Storonova OA, Rumyantseva SA. Classifications of reflux esophagitis and their clinical significance. Endoskopicheskaya Praktika (Endoscopic Practice). 2015;(2):34–39. [In Russian].

***Corresponding author**: Evgeniy A. Toneev, PhD. E-mail: e.toneev@inbox.ru*

International Journal of Biomedicine 16(1) (2026) 46-52
http://dx.doi.org/10.21103/Article16(1)_OA5

ORIGINAL ARTICLE

Oncology

INTERNATIONAL JOURNAL OF BIOMEDICINE

Efficacy and Safety of PD-1 Inhibitor-Based Treatment in Advanced Cervical Cancer

Shunqin Hu[1], Xiuying Li[2*]

[1]*Department of Gynecology and Obstetrics, the First Affiliated Hospital of Kunming Medical University, Kunming, China*
[2]*Faculty of Life Science and Technology, Kunming University of Science and Technology, Kunming, China*

Abstract

Background: This meta-analysis aimed to assess the clinical efficacy and safety of PD-1 inhibitor-based treatment in advanced cervical cancer patients.
Methods and Results: PubMed and Web of Science were systematically searched for relevant studies. This meta-analysis comprises 14 studies involving 1504 patients. The pooled results of ORR (objective response rate) and DCR (disease control rate) are as follows, respectively: 1) 16% and 53% in patients who were treated with a PD-1 inhibitor; 2) 26% and 56% in patients who were treated with a PD-1 plus a CTLA-4 inhibitor; 3) 68% and 92% in patients who were treated with a PD-1 inhibitor plus an antiangiogenic agent. Patients treated with a PD-1 inhibitor, a PD-1 inhibitor plus an antiangiogenic agent, or single-agent pembrolizumab experienced ≥ grade 3 adverse events at rates of 21%, 50%, and 10%, respectively.
Conclusion: Although the therapeutic efficacy of a PD-1 inhibitor plus an antiangiogenic agent is superior to PD-1 inhibitor monotherapy or the combination of a PD-1 and CTLA-4 inhibitor, this combination is more toxic than other treatment strategies. Further evidence from large-scale randomized controlled trials is needed to validate the current results.(**International Journal of Biomedicine. 2026;16(1):46-52.**)

Keywords: cervical cancer • immunotherapy • efficacy • safety

For citation: Hu S, Li X. Efficacy and Safety of PD-1 Inhibitor-Based Treatment in Advanced Cervical Cancer. International Journal of Biomedicine. 2026;16(1):46-52. doi:10.21103/Article16(1)_OA5

Abbreviations

AEs, adverse events; **DCR**, disease control rate; **ORR**, objective response rate; **OS**, overall survival; **PFS**, progression-free survival.

Introduction

Cervical cancer remains a major public health problem in women. Increasing rates of human papillomavirus prophylactic vaccination and well-organized screening programs in recent years have led to a decline in the incidence and mortality of cervical cancer. However, globally, many women lack access to screening programs, prophylactic vaccines, and high-quality interventional treatments when required.[1]

For cervical cancer, different stages have different treatment options. Early-stage cervical cancer may be cured by surgery with tailored adjuvant therapy. Although treatment strategies have continuously evolved over the past several years, the treatment choice for locally advanced cancer is quite limited, and the prognosis of recurrence or advanced cervical cancer remains dismal.[2] In this scenario, immunotherapy has attracted significant attention as a potential strategy to improve clinical outcomes of recurrence or advanced cervical cancer. Pembrolizumab was approved for the treatment of PD-L1-positive, persistent, recurrent, or advanced cervical cancer in 2020.[3]

To date, multiple clinical trials have been conducted to investigate the effect of PD-1 inhibitor-based immunotherapy in advanced cervical cancer, and some have reported final or midterm results.[4,5] There is still a lack of supported evidence

***Corresponding author:** Xiuying Li, e-mail: Xiuyingli2013@kust.edu.cn

that PD-1 inhibitor-based immunotherapy in advanced cervical cancer is effective and safe. Therefore, we conducted this meta-analysis of existing studies to assess the efficacy and safety of PD-1 inhibitor-based immunotherapy in patients with advanced cervical cancer.

Patients and Methods

Study Strategy

All relevant studies published before 12 Mar 2025 were identified through the electronic databases PubMed and Web of Science. The following terms were used as the specific search strategy: cervical and (serplulimab or balstilimab or pembrolizumab or camrelizumab or sintilimab or nivolumab or cemiplimab or PD-1 or immune checkpoint inhibitor) and (neoplasia or tumor or malignancy or cancer or carcinoma or neoplasm) and patients. Additionally, the reference lists of relevant articles were manually examined to identify further potentially relevant studies.

Inclusion and Exclusion Criteria

The inclusion criteria were as follows: 1) The association between PD-1 inhibitor-based immunotherapy and efficacy/safety was investigated in prospective clinical studies or retrospective studies; 2) Sample size was greater than or equal to 20 patients; 3) The included patients confirmed with advanced/persistent/recurrent/metastatic cervical cancer; 4) The patients were treated with PD-1 inhibitor, both single-agent therapy or in combination with other agents; 5) Studies reported outcome, such as either efficacy and/or safety end points, including the ORR (objective response rate), DCR (disease control rate), PFS (progression-free survival), OS (overall survival), and adverse events (AEs) with 95% confidence interval (CI) or data to calculate them; 6) Literature in English was considered. If authors published several studies using the same data, the comprehensive or most recent study was included.

The exclusion criteria were as follows: 1) Meeting abstracts, case reports, letters, reviews, and comments; 2) Duplicated publications; 3) Studies lacked the necessary data for analysis; 4) Ongoing clinical trials for which the results have not been published; 5) Animal studies.

Data Extraction

Two investigators independently extracted data from the eligible articles according to the inclusion and exclusion criteria. A consensus was achieved for any discrepancies through discussion. The extracted data included basic information, such as first author, publication year, sample size, age, disease status, study type, intervention, recruitment, case review period, data cutoff, and follow-up time.

Quality Assessment

We evaluated the quality of randomized controlled trials (RCTs) using the modified Jadad scale.[6] Methodological Index for Non-Randomized Studies (MINORS) criteria are used to assess the quality of comparative and non-comparative studies.[7] The retrospective studies without a comparison group were assessed by the JBI Critical Appraisal Checklist.[8]

Statistical analysis

This meta-analysis was performed using Stata 12.0 (Stata Corporation). All results were reported as pooled RRs (risk ratios) and 95% CIs. The Cochran's Q test[9] and Higgins' I2 statistic[10] were applied to assess the heterogeneity among the included studies. The chi-square *P*-value >0.10 or I2 >50% suggested the existence of heterogeneity; a random-effect model was used; otherwise, the fixed-effect model was used. The effect size was reported as the 95% CI. Sensitivity analyses were performed to reflect the influence of individual data on the pooled results. Additionally, Begg's and Egger's tests were used to assess the potential publication bias of the enrolled studies. Values of $P<0.05$ were considered statistically significant.

Results

Study Selection and Characteristics

Supplementary Figure 1 shows the literature screening process. One retrospective study[11] and 13 prospective studies [4,5,12-22] with 1504 patients were included in this meta-analysis. The study by Lorusso et al.[22] included two cohorts by treatment; we treated this study as two reports in our analysis. The eligible studies were published from 2017 to 2025. The sample sizes ranged from 20 to 304. The general characteristics of each included study were described in Supplementary Table 1.

Table 1.

The clinical response.

Objective response rate	Events	No. of studies	Pooled RR (95%CI)	*P*	Effects model	Heterogeneity		Publication bias	
						I^2 (%)	Ph	Egger's	Begg's
PD-1 inhibitor	1004	10	0.16 (0.14-0.18)	0.000	Random	88.4	0.000	0.210	0.391
PD-1 inhibitor plus antiangiogenic agent	316	4	0.68 (0.63-0.73)	0.000	Random	87.0	0.000	0.089	0.025
PD-1 plus CTLA-4 inhibitor	180	2	0.26 (0.20-0.33)	0.000	Fixed	0.0	0.815	–	–
Pembrolizumab	410	5	0.16 (0.13-0.15)	0.000	Random	93.3	0.000	0.086	0.419
Disease control rate									
PD-1 inhibitor	945	9	0.53 (0.50-0.56)	0.000	Random	92.7	0.000	0.754	0.472
PD-1 inhibitor plus antiangiogenic agent	316	4	0.92 (0.89-0.95)	0.000	Random	66.9	0.028	0.089	0.118
PD-1 plus CTLA-4 inhibitor	180	2	0.56 (0.48-0.63)	0.000	Fixed	0.0	0.613	–	–
Pembrolizumab	351	4	0.50 (0.45-0.55)	0.000	Random	96.9	0.000	0.734	0.525
Nivolumab	45	2	0.56(0.17-0.94)	0.004	Random	87.8	0.004	–	–

Quality Assessment

Supplementary Table 2 indicates the quality assessment of included studies. The retrospective study was assessed using the JBI Critical Appraisal Checklist and included in this study. Ten single-arm studies were evaluated using the MINORS index and scored 13-15 points, which were acceptable for the present meta-analysis. According to the Jadad scale, the included RCT studies were of high quality.

Tumor Response

The ORR and DCR were assessed according to Response Evaluation Criteria in Solid Tumors (RECIST version 1.1). ORR included CR (complete response) and PR (partial response). DCR included CR, PR, and SD (stable disease). The pooled results of ORR and DCR were as follows, respectively: 1) 16% and 53% in patients who were treated with PD-1 inhibitor; 2) 68% and 92% in patients who were treated with PD-1 inhibitor plus antiangiogenic agent; 3) 26% and 50% in patients who were treated with PD-1 plus CTLA-4 inhibitor; 4) 16% and 56% in patient who were treated with single pembrolizumab (Figure 1b and Table 1).

Progression-Free Survival

PFS was analyzed according to treatment agents. The pooled median PFS was 3.02 months in patients treated with a single PD-1 inhibitor, 2.91 months in patients treated with a single pembrolizumab, and 11.00 months in patients treated with a PD-1 inhibitor plus antiangiogenic agents (Table 2). Supplementary Table 3 shows the results of the pooled 6- and 12-month PFS rates.

Overall Survival

OS was also analyzed according to treatment agents. The pooled median OS was 11.66 months in patients treated with a single-agent PD-1 inhibitor, and 11.48 months in patients treated with a single-agent pembrolizumab (Table 2). The pooled 6- and 12-month OS rates are indicated in Supplementary Table 3.

Safety

The adverse events were graded according to the National Cancer Institute Common Terminology Criteria for Adverse Events. The results are indicated in Supplementary Table 4.

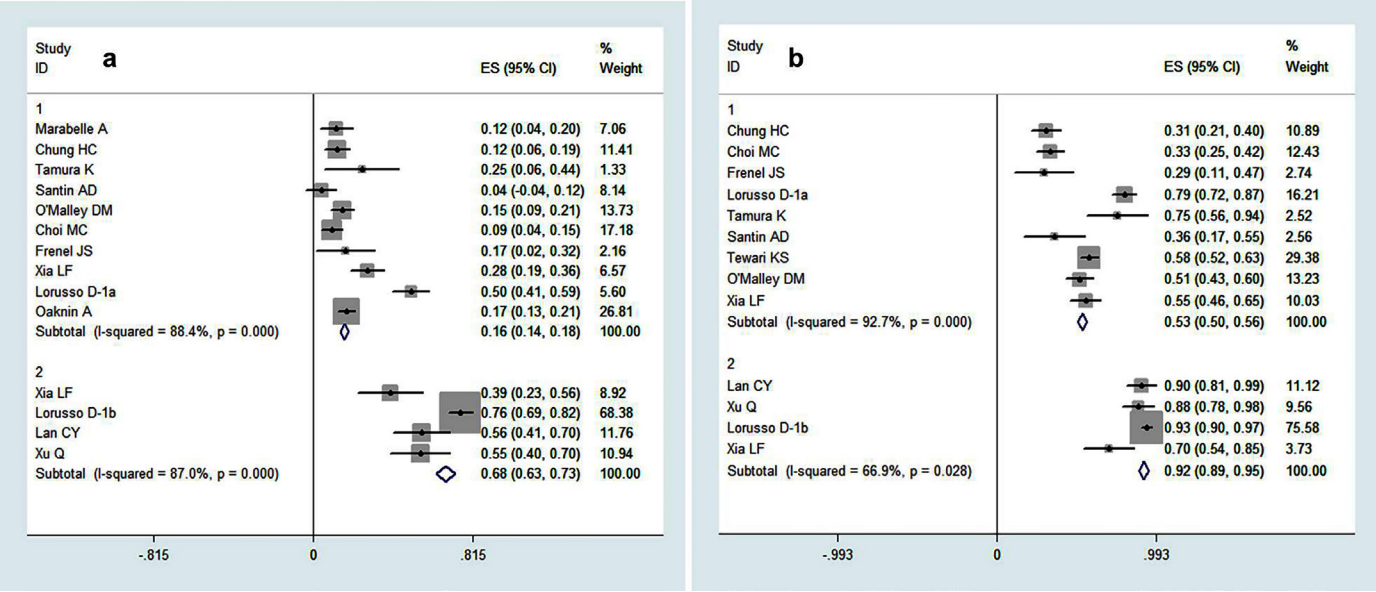

Figure 1. *Pooled results of objective response rate (ORR) (a). [1]Patients were treated with a single anti-PD-1 antibody. [2]Patients were treated with an anti-PD-1 antibody plus antiangiogenic agent. Pooled results of disease control rate (DCR) (b).[1]Patients were treated with a single anti-PD-1 antibody.[2]Patients were treated with an anti-PD-1 antibody plus antiangiogenic agent.*

Table 2.

Median PFS and OS.

Median PFS	Events	No. of studies	Pooled RR (95%CI)	*P*	Effects model	Heterogeneity		Publication bias	
						I^2 (%)	Ph	Begg's	Egger's
PD-1 inhibitor	456	5	3.02 (1.92-4.72)	0.000	Random	97.9	0.000	0.806	0.969
Pembrolizumab	351	4	2.91 (1.78-4.75)	0.000	Random	98.4	0.000	1.00	0.983
PD-1 inhibitor plus antiangiogenic agent	268	3	11.0(7.82-15.47)	0.000	Random	50.9	0.131	1.000	0.837
Median OS									
PD-1 inhibitor	665	5	11.66 (9.04-15.05)	0.000	Random	76.8	0.002	1.000	0.500
Pembrolizumab	351	4	11.48(7.84-16.81)	0.000	Random	81.7	0.001	1.000	0.387

Sensitivity Analysis and Publication Bias

The sensitivity analysis was performed to assess the robustness of the results. For ORR (Supplementary Figure 2a) and DCR (Supplementary Figure 3a), the pooled results were not significantly affected by omitting trials one by one. This demonstrated that the results were robust and reliable.

To assess publication bias, funnel plots of studies reporting ORR (Supplementary Figure 2b) and DCR (Supplementary Figure 3b) were generated. Egger's and Begg's tests for ORR, DCR, PFS, OS, and AEs were performed to recognize publication bias in this study. No obvious publication bias was observed in the current study (Tables 1 and 2, Supplementary Tables 3 and 4).

Discussion

Cervical cancer is the most common female gynecological malignancy. Although about 90% of early-stage patients can be cured through proper therapeutic strategies, the treatment for the advanced-stage patients still faces challenges.[1] The introduction of immunotherapy has revolutionized the treatment landscape in cervical cancer.[23] Study indicated that the expression level of PD-L1 in cervical cancer patients is relatively high, ranging from 34.4% to 96.0%, which suggests that cervical cancer patients can benefit from PD-1/PD-L1 inhibitors.[24] Nivolumab has been proven to have clinical activity in both PD-L1-positive and PD-L1-negative cervical cancer patients.[5,25]

Several strategies have been investigated to improve the clinical efficacy of PD-1 inhibitors, including combining them with other agents. Studies have demonstrated that the ability of antigen presentation was increased after the blockade of cytotoxic T-lymphocyte associated protein 4 (CTLA-4) axis, resulting in an expanded cytotoxic T-cell response.[26] Due to limited efficacy as monotherapy, CTLA-4 inhibitors were combined with other regimens in clinical trials. The combination of PD-1 and CTLA-4 inhibitors has a synergist effect on the activation of the antitumor immune response.[4,5] Studies suggested that anti-angiogenic agents may exert an immunostimulatory effect in the tumor microenvironment through multiple mechanisms.[27,28]

This meta-analysis systematically assessed the efficacy and safety of PD-1 inhibitor-based treatment in advanced cervical cancer. Thirteen clinical trials and one retrospective study, involving 1504 patients, were included. The results indicated that the clinical efficacy of a PD-1 inhibitor in combination with antiangiogenic agents was superior to PD-1 inhibitor monotherapy or to the combination of PD-1 and CTLA-4 inhibitors. Still, the combination of a PD-1 inhibitor plus antiangiogenic agents was more toxic.

Admittedly, our study has some limitations. First, the number of included studies was small, despite a comprehensive and systematic search of mainstream databases. Second, most of the studies included were non-controlled trials, and the sample sizes of some trials were limited; therefore, we cannot make a direct comparison to assess whether PD-1 inhibitor-based treatment has advantages. Therefore, more clinical studies are needed to validate the current results.

Conflicts of Interest

The authors declare that they have no competing interests.

References

1. Rimel BJ, Kunos CA, Macioce N, Temkin SM. Current gaps and opportunities in screening, prevention, and treatment of cervical cancer. Cancer. 2022 Dec 1;128(23):4063-4073. doi: 10.1002/cncr.34487. Epub 2022 Oct 14. PMID: 36239009.
2. Grau JF, Farinas-Madrid L, Garcia-Duran C, Garcia-Illescas D, Oaknin A. Advances in immunotherapy in cervical cancer. Int J Gynecol Cancer. 2023 Mar 6;33(3):403-413. doi: 10.1136/ijgc-2022-003758. PMID: 36878562.
3. Monk BJ, Enomoto T, Kast WM, McCormack M, Tan DSP, Wu X, et al. Integration of immunotherapy into treatment of cervical cancer: Recent data and ongoing trials. Cancer Treat Rev. 2022 May;106:102385. doi: 10.1016/j.ctrv.2022.102385. Epub 2022 Mar 31. PMID: 35413489; PMCID: PMC10697630.
4. Chung HC, Ros W, Delord JP, Perets R, Italiano A, Shapira-Frommer R, et al. Efficacy and Safety of Pembrolizumab in Previously Treated Advanced Cervical Cancer: Results From the Phase II KEYNOTE-158 Study. J Clin Oncol. 2019 Jun 10;37(17):1470-1478. doi: 10.1200/JCO.18.01265. Epub 2019 Apr 3. PMID: 30943124.
5. Santin AD, Deng W, Frumovitz M, Buza N, Bellone S, Huh W, et al. Phase II evaluation of nivolumab in the treatment of persistent or recurrent cervical cancer (NCT02257528/NRG-GY002). Gynecol Oncol. 2020 Apr;157(1):161-166. doi: 10.1016/j.ygyno.2019.12.034. Epub 2020 Jan 7. PMID: 31924334; PMCID: PMC7127981.
6. Bañares R, Albillos A, Rincón D, Alonso S, González M, Ruiz-del-Arbol L, et al. Endoscopic treatment versus endoscopic plus pharmacologic treatment for acute variceal bleeding: a meta-analysis. Hepatology. 2002 Mar;35(3):609-15. doi: 10.1053/jhep.2002.31354. PMID: 11870374.
7. Slim K, Nini E, Forestier D, Kwiatkowski F, Panis Y, Chipponi J. Methodological index for non-randomized studies (minors): development and validation of a new instrument. ANZ J Surg. 2003 Sep;73(9):712-6. doi: 10.1046/j.1445-2197.2003.02748.x. PMID: 12956787.
8. Baldwin S, Bick D. First-time fathers' needs and experiences of transition to fatherhood in relation to their mental health and wellbeing: a qualitative systematic review protocol. JBI Database System Rev Implement Rep. 2017 Mar;15(3):647-656. doi: 10.11124/JBISRIR-2016-003031. PMID: 28267026.
9. COCHRAN WG. The role of mathematics in the medical sciences. N Engl J Med. 1961 Jul 27;265:176. doi: 10.1056/NEJM196107272650406. PMID: 13694214.
10. Higgins JP, Thompson SG. Quantifying heterogeneity in a meta-analysis. Stat Med. 2002 Jun 15;21(11):1539-58. doi: 10.1002/sim.1186. PMID: 12111919.
11. Choi MC, Kim YM, Lee JW, Lee YJ, Suh DH, Lee SJ, et al. Real-World Experience of Pembrolizumab Monotherapy in Patients with Recurrent or Persistent Cervical Cancer: A Korean Multi-Center Retrospective Study (KGOG1041).

Cancers (Basel). 2020 Oct 29;12(11):3188. doi: 10.3390/cancers12113188. PMID: 33138190; PMCID: PMC7693862.
12. Marabelle A, Fakih M, Lopez J, Shah M, Shapira-Frommer R, Nakagawa K, et al. Association of tumour mutational burden with outcomes in patients with advanced solid tumours treated with pembrolizumab: prospective biomarker analysis of the multicohort, open-label, phase 2 KEYNOTE-158 study. Lancet Oncol. 2020 Oct;21(10):1353-1365. doi: 10.1016/S1470-2045(20)30445-9. Epub 2020 Sep 10. PMID: 32919526.
13. Lan C, Lu H, Zhou L, Liao K, Liu J, Xie Z, et al. Long-term survival outcomes and immune checkpoint inhibitor retreatment in patients with advanced cervical cancer treated with camrelizumab plus apatinib in the phase II CLAP study. Cancer Commun (Lond). 2024 Jun;44(6):654-669. doi: 10.1002/cac2.12547. Epub 2024 May 13. PMID: 38741375; PMCID: PMC11194449.
14. O'Malley DM, Neffa M, Monk BJ, Melkadze T, Huang M, Kryzhanivska A, et al. Dual PD-1 and CTLA-4 Checkpoint Blockade Using Balstilimab and Zalifrelimab Combination as Second-Line Treatment for Advanced Cervical Cancer: An Open-Label Phase II Study. J Clin Oncol. 2022 Mar 1;40(7):762-771. doi: 10.1200/JCO.21.02067. Epub 2021 Dec 21. PMID: 34932394; PMCID: PMC8887945.
15. Xu Q, Wang J, Sun Y, Lin Y, Liu J, Zhuo Y, et al. Efficacy and Safety of Sintilimab Plus Anlotinib for PD-L1-Positive Recurrent or Metastatic Cervical Cancer: A Multicenter, Single-Arm, Prospective Phase II Trial. J Clin Oncol. 2022 Jun 1;40(16):1795-1805. doi: 10.1200/JCO.21.02091. Epub 2022 Feb 22. PMID: 35192397; PMCID: PMC9148684.
16. O'Malley DM, Oaknin A, Monk BJ, Selle F, Rojas C, Gladieff L, et al. Phase II study of the safety and efficacy of the anti-PD-1 antibody balstilimab in patients with recurrent and/or metastatic cervical cancer. Gynecol Oncol. 2021 Nov;163(2):274-280. doi: 10.1016/j.ygyno.2021.08.018. Epub 2021 Aug 25. PMID: 34452745.
17. Frenel JS, Le Tourneau C, O'Neil B, Ott PA, Piha-Paul SA, Gomez-Roca C, et al. Safety and Efficacy of Pembrolizumab in Advanced, Programmed Death Ligand 1-Positive Cervical Cancer: Results From the Phase Ib KEYNOTE-028 Trial. J Clin Oncol. 2017 Dec 20;35(36):4035-4041. doi: 10.1200/JCO.2017.74.5471. Epub 2017 Nov 2. PMID: 29095678.
18. Zhao Y, Ma Y, Zang A, Cheng Y, Zhang Y, Wang X, et al. First-in-human phase I/Ib study of QL1706 (PSB205), a bifunctional PD1/CTLA4 dual blocker, in patients with advanced solid tumors. J Hematol Oncol. 2023 May 8;16(1):50. doi: 10.1186/s13045-023-01445-1. PMID: 37158938; PMCID: PMC10169367.
19. Tamura K, Hasegawa K, Katsumata N, Matsumoto K, Mukai H, Takahashi S, et al. Efficacy and safety of nivolumab in Japanese patients with uterine cervical cancer, uterine corpus cancer, or soft tissue sarcoma: Multicenter, open-label phase 2 trial. Cancer Sci. 2019 Sep;110(9):2894-2904. doi: 10.1111/cas.14148. Epub 2019 Sep 3. PMID: 31348579; PMCID: PMC6726684.
20. Oaknin A, Monk BJ, de Melo AC, Kim HS, Kim YM, Lisyanskaya AS, et al. Cemiplimab in recurrent cervical cancer: Final analysis of overall survival in the phase III EMPOWER-Cervical 1/GOG-3016/ENGOT-cx9 trial. Eur J Cancer. 2025 Feb 5;216:115146. doi: 10.1016/j.ejca.2024.115146. Epub 2025 Jan 10. PMID: 39798514.
21. Xia L, Wang J, Wang C, Zhang Q, Zhu J, Rao Q, et al. Efficacy and safety of zimberelimab (GLS-010) monotherapy in patients with recurrent or metastatic cervical cancer: a multicenter, single-arm, phase II study. Int J Gynecol Cancer. 2023 Dec 4;33(12):1861-1868. doi: 10.1136/ijgc-2023-004705. PMID: 37875323; PMCID: PMC10804044.
22. Lorusso D, Colombo N, Dubot C, Cáceres MV, Hasegawa K, Shapira-Frommer R, et al. Pembrolizumab plus chemotherapy for advanced and recurrent cervical cancer: final analysis according to bevacizumab use in the randomized KEYNOTE-826 study. Ann Oncol. 2025 Jan;36(1):65-75. doi: 10.1016/j.annonc.2024.10.002. Epub 2024 Oct 10. PMID: 39393777.
23. Cha JH, Chan LC, Li CW, Hsu JL, Hung MC. Mechanisms Controlling PD-L1 Expression in Cancer. Mol Cell. 2019 Nov 7;76(3):359-370. doi: 10.1016/j.molcel.2019.09.030. Epub 2019 Oct 24. PMID: 31668929; PMCID: PMC6981282.
24. Liu Y, Wu L, Tong R, Yang F, Yin L, Li M, et al. PD-1/PD-L1 Inhibitors in Cervical Cancer. Front Pharmacol. 2019 Feb 1;10:65. doi: 10.3389/fphar.2019.00065. PMID: 30774597; PMCID: PMC6367228.
25. Naumann RW, Hollebecque A, Meyer T, Devlin MJ, Oaknin A, Kerger J, et al. Safety and Efficacy of Nivolumab Monotherapy in Recurrent or Metastatic Cervical, Vaginal, or Vulvar Carcinoma: Results From the Phase I/II CheckMate 358 Trial. J Clin Oncol. 2019 Nov 1;37(31):2825-2834. doi: 10.1200/JCO.19.00739. Epub 2019 Sep 5. PMID: 31487218; PMCID: PMC6823884.
26. Sobhani N, Tardiel-Cyril DR, Davtyan A, Generali D, Roudi R, Li Y. CTLA-4 in Regulatory T Cells for Cancer Immunotherapy. Cancers (Basel). 2021 Mar 22;13(6):1440. doi: 10.3390/cancers13061440. PMID: 33809974; PMCID: PMC8005092.
27. Di Tacchio M, Macas J, Weissenberger J, Sommer K, Bähr O, Steinbach JP, et al. Tumor Vessel Normalization, Immunostimulatory Reprogramming, and Improved Survival in Glioblastoma with Combined Inhibition of PD-1, Angiopoietin-2, and VEGF. Cancer Immunol Res. 2019 Dec;7(12):1910-1927. doi: 10.1158/2326-6066.CIR-18-0865. Epub 2019 Oct 9. PMID: 31597643.
28. Dimopoulos MA, Dytfeld D, Grosicki S, Moreau P, Takezako N, Hori M, et al. Elotuzumab plus Pomalidomide and Dexamethasone for Multiple Myeloma. N Engl J Med. 2018 Nov 8;379(19):1811-1822. doi: 10.1056/NEJMoa1805762. PMID: 30403938.

Supplementary Material

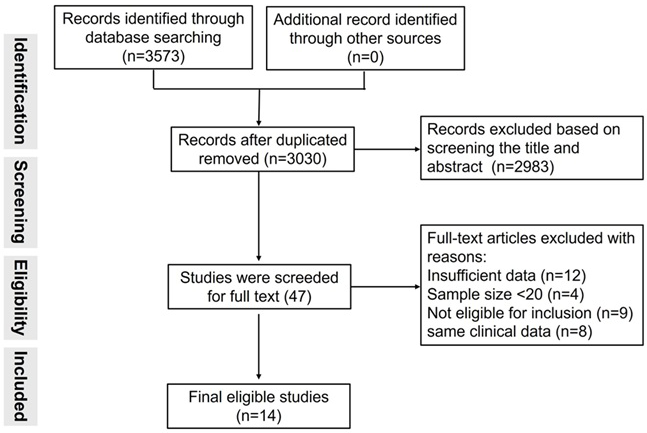

Supplementary Figure 1. *Flow chart of the study selection process.*

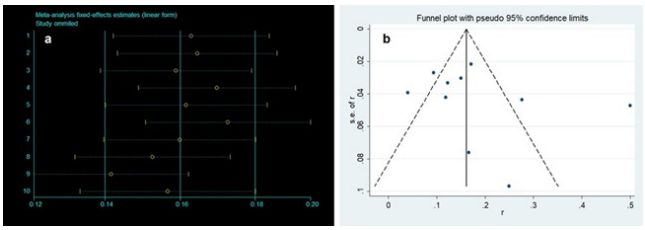

Supplementary Figure 2. *Sensitivity analysis and publication bias.* **(***a) Sensitivity analysis for ORR. (b) Funnel plot of ORR.*

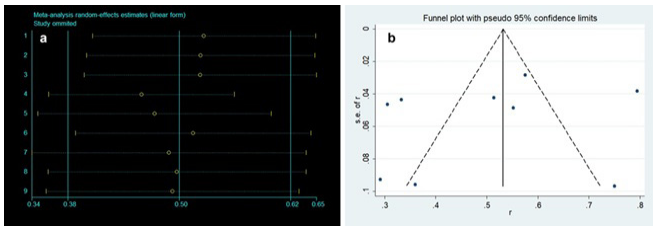

Supplementary Figure 3. *Sensitivity analysis and publication bias. (a) Sensitivity analysis for DCR. (b) Funnel plot of DCR.*

Supplementary Table 1.
The characteristics of all included studies.

Author	Year	Age	Study type	Sample size	Recruitment/ case review period	Data cutoff	Follow-up (months)	Intervention
Marabelle A et al.	2020	61(55-68)	phase II	75	Jan 15, 2016, to Jun 25, 2019	Jun 27, 2019	37.1 (IQR 35.0-38.3)	Pembrolizumab
Chung HC et al.	2019	46(24-75)	phase II	98	Jan27, 2016, to Aug 18, 2016	Jan 15, 2018	10.2(0.6-22.7)	Pembrolizumab
O'Malley DM et al.	2022	50(24-76)	phase II	125	Aug 27, 2018, to May 7, 2020	Apr 29, 2021	21(11.8-32.1)	Balstilimab plus zalifrelimab
Xu Q et al.	2022	53(36-67)	phase II	42	Dec 2019 to Dec 2020	Jul 13, 2021	10.9 (0.03-19.2)	Sintilimab plus anlotinib
O'Malley DM et al.	2021	53(25-81)	phase II	161	Nov 20, 2017, to Apr 16, 2020	Feb 11, 2021	14.6(9.9-38.8)	Balstilimab
Choi MC, et al.	2020	53(28-79)	retrospective	117	Jan 2016 to March 2020	31 Mar, 2020	4.9 (0.2–35.3)	Pembrolizumab
Frenel JS et al.	2017	42(26-62)	phase Ib	24	NA	NA	11.0(1.3-32.2)	Pembrolizumab
Zhao YY et al.	2023	53(20-81)	phase Ib	55	March 2020 to July 2021	Mar 31, 2021	89.5	PSB205 (QL1706)
Santin AD et al.	2020	45	phase II	25	May 2015 to June 2016	NA	32 (2-41.5)	Nivolumab
Tamura K et al.	2019	50(32-68)	phase II	20	NA	Aug 18, 2017	8.6 (1.4-13.7)	Nivolumab
Oaknin A et al.	2025	18.2(6.0-38.2)	phase III	304	Jul 2017 to Aug2020	Apr 20, 2023	47.3	Cemiplimab
Xia L et al.	2023	51 (31-75)	phase II	105	Jun 11, 2020, to Apr 29, 2021	Apr 29, 2022	16.9 (6.3-18.4)	Zimberelimab
Lorusso D et al. (1a)	2025	52.5 (30-82)	phase III	112	Nov 20, 2018, to Jan 31, 2020	Oct 3, 2022	39.1 (32.1-46.5)	Pembrolizumab
Lorusso D et al. (1b)	2025	51 (25-82)	phase III	196	Nov 20, 2018, to Jan 31, 2020	Oct 3, 2022	39.1 (32.1-46.5)	Pembrolizumab plus bevacizumab
Lan C et al.	2024	51 (33-67)	phase II	45	Jan 21 to Aug 2019	Jul 31, 2023	NA	Camrelizumab plus apatinib

Supplementary Table 2.
Quality assessment.

JBI Critical Appraisal Checklist for included retrospective study											
Study	Q1	Q2	Q3	Q4	Q5	Q6	Q7	Q8	Q9	Q10	Overall appraisal
Choi MC et al. (2020)	yes	yes	yes	unclear	yes	yes	yes	yes	yes	yes	included
B. MINORS index for included non-randomized studies											
Study		I	II	III	IV	V	VI	VII	VIII	Total	
Marabelle A et al. (2020)		2	1	2	2	2	2	0	2	13	
Lan CY et al. (2020)		2	1	2	2	2	2	2	2	15	
O'Malley DM et al. (2022)		2	1	2	2	2	2	0	2	13	
Tamura K et al. (2019)		2	1	2	2	2	2	2	2	15	
Chung HC et al. (2019)		2	1	2	2	2	2	2	2	15	
Xu Qet al. (2022)		2	1	2	2	1	2	2	2	14	
Zhao YY et al. (2023)		2	1	2	2	1	2	2	2	14	
O'Malley DM et al. (2021)		2	1	2	2	2	2	2	2	15	
Santin AD et al. (2020)		2	1	2	2	1	2	2	2	14	
Frenel JS et al. (2017)		2	1	2	2	1	2	2	2	14	
Xia LF et al. (2023)		2	1	2	2	2	2	0	2	13	
Lan CY et al. (2024)			2	1	2	2	1	2	2	14	
Jadad scale for included RCT study											
Study		Randomization		Concealment of allocation		Double blinding		Withdrawals and dropouts		Quality grade	
Tewari KS et al. (2022)		2		2		1		2		7	
Oaknin A et al. (2025)		2		2		1		2		7	
Lorusso D et al. (2024)		2		2		2		2		8	

Numbers I-VIII in the heading signify: I, a clearly stated aim; II, inclusion of consecutive patients; III, prospective collection of data; IV, endpoints appropriate to the aim of the study; V, unbiased assessment of the study endpoint; VI, follow-up period appropriate to the aim of the study; VII, loss of follow up less than 5%; VIII, prospective calculation of the study size.
Numbers Q1-Q10 in the heading signify: Q1: Were there clear criteria for inclusion in the case series? Q2: Was the condition measured in a standard, reliable way for all participants included in the case series? Q3: Were valid methods used for the identification of the condition for all participants included in the case series? Q4: Did the case series have consecutive inclusion of participants? Q5: Did the case series have complete inclusion of participants? Q6: Was there transparent reporting of the demographics of the participants in the study? Q7: Was there transparent reporting of clinical information of the participants? Q8, were the outcomes or follow-up results of cases clearly reported?
Q9: Was there transparent reporting of the presenting site(s)/clinic(s) demographic information? Q10: Was the statistical analysis appropriate?

Supplementary Table 3.
6-month and 12-month rates of PFS and OS

6-month rate of PFS	Events	No. of studies	Pooled RR (95%CI)	*P*	Effects model	Heterogeneity		Publication bias	
						I^2 (%)	Ph	Begg's	Egger's
Pembrolizumab	239	3	0.27 (0.21-0.32)	0.000	Fixed	0.0	0.579	0.296	0.480
6-month rate of OS									
PD-1 inhibitor	259	4	0.66 (0.45-0.87)	0.000	Random	92.0	0.000	0.734	0.668
Pembrolizumab	239	3	0.61 (0.36-0.85)	0.000	Random	93.3	0.000	1.000	0.943
12-month rate of PFS									
PD-1 inhibitor	246	3	0.16(0.11-0.20)	0.000	Random	87.9	0.000	1.000	0.818
12-month rate of OS									
PD-1 inhibitor	227	3	0.49(0.42-0.55)	0.000	Random	69.9	0.036	1.000	0.731
PD-1 inhibitor plus antiangiogenic agent	72	2	0.67(0.57-0.78)	0.000	Random	58.6	0.120	–	–

Supplementary Table 4.
Treatment-related adverse events (AEs).

Treatment	Events	No. of studies	Pooled RR (95%CI)	*P*	Effects model	Heterogeneity		Publication bias	
						I^2 (%)	Ph	Egger's	Begg's
PD-1 inhibitor	947	10	0.21(0.19-0.23)	0.000	Random	97.6	0.000	0.089	0.595
PD-1 inhibitor plus angiogenesis	779	4	0.50(0.47-0.53)	0.000	Random	98.7	0.000	0.734	0.408
Pembrolizumab	281	4	0.10(0.06-0.13)	0.000	Fixed	43.7	0.148	0.089	0.056

International Journal of Biomedicine 16(1) (2026) 53-58
http://dx.doi.org/10.21103/Article16(1)_OA6

ORIGINAL ARTICLE

Oncology

INTERNATIONAL JOURNAL OF BIOMEDICINE

TRPS1 Expression in Triple-Negative Breast Cancer and Its Association with the Efficacy of Neoadjuvant Chemotherapy

N. V. Krakhmal[1,2*], S. V. Vtorushin[1,2]

[1]*Siberian State Medical University, Tomsk, Russian Federation*
[2]*Cancer Research Institute, Tomsk National Research Medical Center of the RAS, Tomsk, Russian Federation*

Abstract

Background. Triple-negative breast cancer (TNBC) is characterized by pronounced biological heterogeneity and variable sensitivity to neoadjuvant chemotherapy, underscoring the need for additional diagnostic and predictive biomarkers. TRPS1, a GATA family transcription factor, has been identified as a highly sensitive marker of mammary differentiation; however, its clinical relevance in TNBC remains insufficiently explored.

Methods and Results. The aim of this study was to evaluate TRPS1 expression in TNBC and to assess its association with clinicopathological features, stromal tumor-infiltrating lymphocytes, and the efficacy of neoadjuvant chemotherapy. This single-center retrospective study included 54 patients with invasive TNBC treated with neoadjuvant chemotherapy. TRPS1 expression was assessed by immunohistochemistry using an H-score-based approach. Stromal tumor-infiltrating lymphocytes were evaluated on hematoxylin and eosin-stained tumor slides. Response to neoadjuvant chemotherapy was assessed by the rate of pathological complete response and the Residual Cancer Burden classification. High TRPS1 expression was detected in 53.7% of cases and was associated with a significantly higher pathological complete response rate (51.7% vs. 20.0%, P=0.016), a more favorable distribution of Residual Cancer Burden categories, and higher levels of stromal tumor-infiltrating lymphocytes. Overall, TRPS1 expression in TNBC was associated with improved response to neoadjuvant chemotherapy.

Conclusions. TRPS1 expression in TNBC is associated with enhanced sensitivity to neoadjuvant chemotherapy and may be considered not only a diagnostic marker of mammary differentiation but also a potential predictive marker of treatment response. (**International Journal of Biomedicine. 2026;16(1):53-58.**)

Keywords: TRPS1 • triple-negative breast cancer • neoadjuvant chemotherapy • pathological complete response • residual cancer burden

For citation: Krakhmal NV, Vtorushin SV. TRPS1 Expression in Triple-Negative Breast Cancer and Its Association with the Efficacy of Neoadjuvant Chemotherapy. International Journal of Biomedicine. 2026;16(1):53-58. doi:10.21103/Article16(1)_OA5

Abbreviations

IHC, immunohistochemistry; **NACT,** neoadjuvant chemotherapy; **pCR,** pathological complete response; **RCB,** residual cancer burden; **sTILs,** stromal tumor-infiltrating lymphocytes; **TNBC,** triple negative breast cancer.

Introduction

Triple-negative breast cancer (TNBC) represents a clinically, morphologically, and biologically heterogeneous group of tumors characterized by the absence of estrogen and progesterone receptor expression and the lack of HER2 protein overexpression or gene amplification.[1,2] Despite a uniform immunophenotypic definition, TNBC demonstrates marked variability in morphological features, sensitivity to systemic therapy, and clinical outcomes, highlighting the ongoing need for additional diagnostic and predictive biomarkers.[3]

Neoadjuvant chemotherapy (NACT) constitutes a standard component of treatment for patients with locally advanced TNBC. Achievement of a pathological complete response (pCR) is associated with a more favorable prognosis; however, pCR rates remain limited, and the depth of response to

***Corresponding author**: Nadezhda V. Krakhmal, PhD. E-mail: krakhmal@mail.ru*

therapy varies substantially even with the use of contemporary treatment regimens.[4,5]

The tumor microenvironment plays a crucial role in modulating therapeutic response. Previous studies have demonstrated that the level of stromal tumor-infiltrating lymphocytes (sTILs) represents a significant prognostic and predictive factor in TNBC.[6,7] Nevertheless, immune-related parameters alone do not fully capture the biological characteristics of tumor cells and require complementary tissue-based markers reflecting tumor differentiation status.

TRPS1 (tricho-rhino-phalangeal syndrome type 1), a GATA family transcription factor, is currently regarded as one of the most sensitive immunohistochemical markers of mammary tissue differentiation. Several studies have reported preserved TRPS1 expression in the vast majority of TNBC cases, including poorly differentiated and metaplastic variants, with higher sensitivity compared with conventional markers such as GATA3 and SOX10.[8-11] In addition to its diagnostic utility, TRPS1 is involved in the regulation of cellular differentiation and the maintenance of phenotypic stability in tumor cells.

Despite increasing interest in TRPS1 data, its clinical and predictive significance in TNBC remains limited. In particular, the association between TRPS1 expression and clinicopathological characteristics, as well as response to NACT, including the extent of pathological response, remains insufficiently investigated. Therefore, the aim of the present study was to evaluate TRPS1 expression in TNBC and to assess its diagnostic and potential predictive significance.

Methods

Study Design and Patients

A single-center retrospective study was conducted. The analysis included 54 cases of invasive breast carcinoma with a triple-negative molecular profile; all patients were treated at a single specialized oncological center (Cancer Research Institute, Tomsk National Research Medical Center of the Russian Academy of Sciences).

The study material consisted of diagnostic core needle biopsy specimens obtained prior to the initiation of NACT, as well as surgical specimens of breast tumor tissue and axillary lymph nodes collected after completion of systemic treatment. All patients received a full course of NACT followed by surgical intervention, allowing for a comprehensive assessment of tumor morphology before treatment and evaluation of pathological response after therapy. NACT was administered in accordance with current clinical guidelines for the treatment of TNBC. Standard regimens including anthracycline- and taxane-based protocols were used. 36 patients (66.7%) received a sequential anthracycline-taxane regimen, while platinum-containing agents were additionally included in the treatment regimen of 18 patients (33.3%). The choice of chemotherapy regimen and treatment duration were determined based on clinical indications in accordance with the current guidelines of the Ministry of Health of the Russian Federation.

Histopathological Evaluation

Histological verification and classification of tumors were performed according to the World Health Organization Classification of Tumours of the Breast (WHO, 5th edition). Morphological evaluation of tumor core biopsy specimens included assessment of histological subtype, histological grade according to the Nottingham grading system, and the presence and extent of tumor necrosis. Triple-negative status was confirmed by immunohistochemistry (IHC) in all cases and defined as the absence of estrogen and progesterone receptor expression (<1% of tumor cells) and lack of HER2 overexpression or amplification (HER2 score 0-1+ by IHC or HER2 score 2+ with a negative *in situ* hybridization result).

Assessment of sTILs

In the study, sTILs were evaluated on hematoxylin and eosin-stained slides of diagnostic core biopsy specimens obtained prior to treatment. sTILs were assessed as the percentage of stromal area occupied by mononuclear inflammatory cells in accordance with the recommendations of the International TILs Working Group.[12] Areas of necrosis, artifacts, and intraductal tumor components were excluded from the analysis.

Immunohistochemistry

Evaluation of TRPS1 expression was performed on formalin-fixed paraffin-embedded sections of diagnostic core biopsy specimens. Staining was carried out using an automated immunohistochemistry stainer (Bond-Max, Leica Biosystems) according to the manufacturer's standard protocol. TRPS1 expression was detected using a monoclonal antibody against TRPS1 (clone QR099, Rabbit, RTU; Quartett). TRPS1 expression was assessed based on nuclear staining of tumor cells. Semi-quantitative evaluation was performed using the H-score, calculated by taking into account both the percentage of positively stained tumor cells and staining intensity. For analytical purposes, all tumor samples were stratified into two groups: tumors with high TRPS1 expression (TRPS1-high; H-score ≥150) and tumors with low or absent TRPS1 expression (TRPS1-low/negative; H-score <150).

Additionally, in a subset of cases, immunohistochemical analysis was performed using antibodies against GATA3 (clone L50-823, Rabbit, RTU; Cell Marque), SOX10 (clone EP268, Rabbit, RTU; Cell Marque), and androgen receptor (AR; clone AR441, Mouse, RTU; Cell Marque) to compare TRPS1 expression with other markers of mammary differentiation.

Assessment of Response to NACT

The efficacy of NACT was evaluated based on histopathological examination of surgical specimens of breast tumor tissue obtained after completion of systemic therapy. Pathological complete response (pCR) was defined as the absence of invasive carcinoma in the breast and regional lymph nodes (ypT0/is ypN0). In addition, quantitative assessment of residual tumor burden was performed in all cases using the Residual Cancer Burden (RCB) system, with classification of patients into RCB-0, RCB-I, RCB-II, and RCB-III categories according to the methodology proposed by Symmans et al.[13]

Statistical processing of the obtained data was performed using Statistica 10.0 (StatSoft Inc., USA). Quantitative indicators are presented as median and interquartile range (IQR). To compare quantitative variables between two independent groups, the nonparametric Mann-Whitney test was used. Qualitative indicators were compared using the

Pearson χ^2 test or Fisher's exact test (for expected values less than 5). To evaluate factors associated with achieving a complete pathomorphological response, univariate logistic regression was used to estimate the odds ratio (OR) and 95% confidence interval (95% CI). Differences were considered statistically significant at $P<0.05$.

Results

The study included 54 patients with TNBC. The median age was 52 years (interquartile range [IQR], 45-61 years). At the initiation of NACT, most patients presented with locally advanced disease: tumors classified as cT2 or higher were observed in 72.2% of cases, and metastatic involvement of regional lymph nodes was detected in 57.4%.

From a morphological standpoint, invasive carcinoma of no special type (NST) predominated, accounting for 85.2% of cases, whereas metaplastic carcinomas accounted for 14.8%. High histological grade (Nottingham grade 3) was identified in 75.9% of patients. The median sTIL level was 30% (IQR, 15-45%). Detailed clinicopathological characteristics of the study cohort are summarized in Table 1. pCR to NACT was achieved in 37.0% of cases (n=20). According to the RCB classification, patients with complete response (RCB-0) accounted for 37.0%, RCB-I for 16.7%, whereas 46.3% of patients demonstrated substantial residual tumor burden (RCB-II and RCB-III) (Table 1).

Table 1.
Clinicopathological characteristics of patients with TNBC (n = 54).

Parameter	Value, n (%)
Menopausal status	
Premenopausal	29 (53.7)
Postmenopausal	25 (46.3)
cT ≥2	39 (72.2)
cN+	31 (57.4)
Histological type of breast tumor	
Invasive carcinoma of no special type (NST)	46 (85.2)
Metaplastic carcinoma	8 (14.8)
Histological grade (Nottingham)	
Garde 1	-
Grade 2	13 (24.1)
Grade 3	41 (75.9)
Distribution of cases according to Residual Cancer Burden (RCB)	
RCB-0	20 (37.0)
RCB-I	9 (16.7)
RCB-II	17 (31.5)
RCB-III	8 (14.8)
pCR	20 (37.0)

TRPS1 Expression and Clinicopathological Associations

Immunohistochemical analysis revealed TRPS1 expression in 87.0% of cases (n=47/54). In most tumors, TRPS1 showed diffuse nuclear staining with moderate to high intensity. Based on semi-quantitative evaluation using the H-score, all cases were stratified into two groups: tumors with high TRPS1 expression (TRPS1-high; H-score ≥150) and tumors with low or absent TRPS1 expression (TRPS1-low/negative; H-score <150).

The TRPS1-high group comprised 29 patients (53.7%), whereas 25 patients (46.3%) demonstrated low or absent TRPS1 expression. Notably, TRPS1 expression was preserved in a subset of tumors lacking immunoreactivity for other markers of mammary differentiation, including GATA3 and SOX10, underscoring its additional diagnostic value.

Analysis of associations between TRPS1 expression and morphological parameters revealed several significant findings. Tumors with high TRPS1 expression were significantly less likely to exhibit high histological grade (Grade 3) compared with TRPS1-low/negative tumors. Similarly, metaplastic breast carcinoma variants were significantly less frequent in the TRPS1-high group, indicating an association between reduced TRPS1 expression and morphologically less differentiated tumor phenotypes.

Association between TRPS1 Expression and Tumor Microenvironment

sTIL levels were significantly higher in the TRPS1-high group. Median sTIL values in this group exceeded those observed in TRPS1-low/negative tumors. Representative morphological and immunohistochemical features of a tumor with high TRPS1 expression and prominent stromal lymphocytic infiltration are shown in Figure 1.

Androgen receptor expression was detected more frequently in TRPS1-high tumors; however, this association did not reach statistical significance. Detailed data on the relationships between TRPS1 expression and clinicopathological and immunohistochemical characteristics of TNBC are presented in Table 2.

TRPS1 Expression and Response to NACT

Analysis of the association between TRPS1 expression and response to NACT demonstrated that pCR occurred significantly more often in the TRPS1-high group. The pCR rate in this group was 51.7%, compared with 20.0% in the TRPS1-low/negative group (Figure 2A, Table 3).

Evaluation of RCB distribution revealed that tumors with high TRPS1 expression were significantly more likely to be classified as RCB-0 or RCB-I, reflecting absence or minimal residual tumor burden. In contrast, the RCB-II and RCB-III categories, indicative of substantial residual disease following NACT, predominated among patients in the TRPS1-low/negative group ((Figure 2B, Table 3).

Predictors of pCR

In univariate logistic regression analysis, pathological complete response was significantly associated with high TRPS1 expression and elevated sTIL levels. Inclusion of

platinum-based agents in NACT regimens was associated with a trend toward increased pCR rates; however, this association did not reach statistical significance. The results of the univariate analysis of factors associated with pCR are summarized in Table 4.

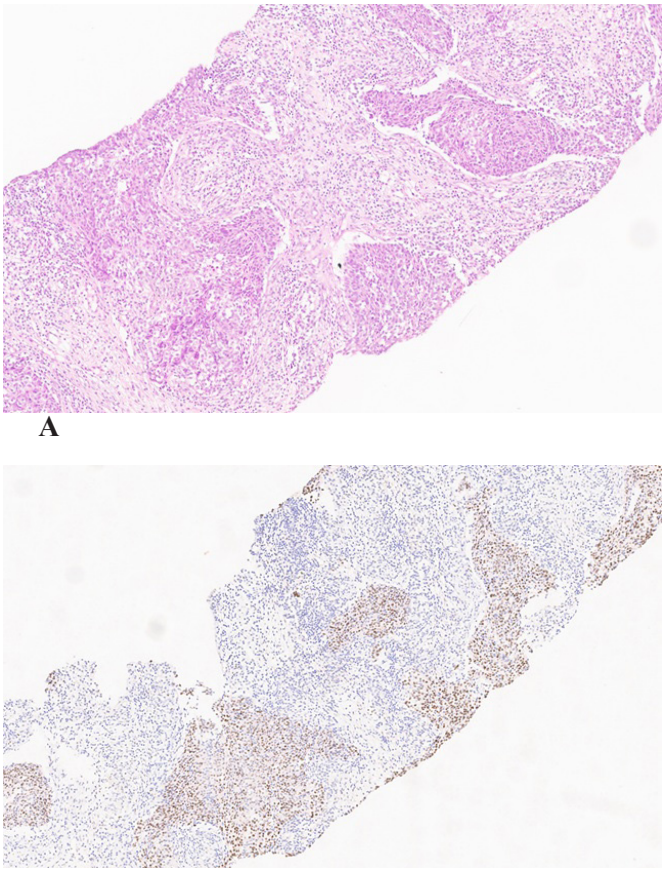

Figure 1. *Morphological and immunohistochemical features of TNBC with high TRPS1 expression.*
A - Core needle biopsy specimen showing prominent sTILs; hematoxylin and eosin staining. B - Diffuse nuclear TRPS1 expression in tumor cells; IHC staining. Original magnification ×4. Digital images were acquired using an Aperio AT2 *scanner.*

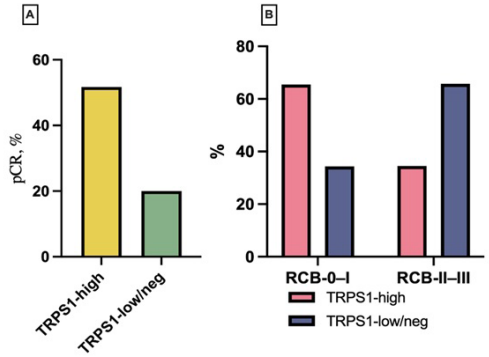

Figure 2. *Association between TRPS1 expression and the efficacy of NACT in TNBC. A - Rate of pCR in the TRPS1-high and TRPS1-low/negative groups. B - Distribution of RCB categories according to TRPS1 expression level.*

Table 2.

Association between TRPS1 expression and morphological and immunohistochemical characteristics of TNBC.

Parameter	TRPS1-high (n = 29)	TRPS1-low/negative (n = 25)	*P*-value
Histological Grade 3	19 (65.5%)	22 (88.0%)	0.054
sTILs, %, median (IQR)	35 (25-50)	20 (10-30)	0.006
Metaplastic TNBC	2 (6.9%)	6 (24.0%)	0.077

Table 3.

Association between TRPS1 expression and pathological response to NACT (pCR and RCB) in TNBC.

Parameter	TRPS1-high (n=29)	TRPS1-low/negative (n=25)	*P*-value
pCR	15 (51.7%)	5 (20.0%)	0.016
RCB-0 and RCB-I	20 (69.0%)	9 (36.0%)	0.015
RCB-II and RCB-III	9 (31.0%)	16 (64.0%)	0.015

Table 4.

Factors associated with achievement of pCR to NACT (univariate analysis).

Variable	OR	95% CI	*P*-value
TRPS1-high	4.3	1.3-14.2	0.017
sTILs (>30%)	3.9	1.2-12.7	0.021
Inclusion of platinum-based agents in NACT	2.1	0.7-6.1	0.18
Histological Grade 3	0.6	0.2-1.9	0.39

Discussion

The present study confirms the high frequency of TRPS1 expression in TNBC and underscores its significance as a diagnostic marker of mammary differentiation in the setting of loss of hormone receptor and HER2 expression. In the studied cohort, TRPS1 was detected in most cases, consistent with data from large immunohistochemical series and supporting its superior sensitivity compared with traditionally used markers such as GATA3 and SOX10. Notably, TRPS1 expression was preserved in a subset of tumors that lacked immunoreactivity for other mammary markers, underscoring its additional diagnostic value, particularly in the evaluation of biopsy specimens and metastatic tumor tissue.

Analysis of clinicopathological associations demonstrated that high TRPS1 expression was linked to less aggressive morphological features. Tumors in the TRPS1-high group showed a significantly lower frequency of metaplastic

carcinoma variants and high Nottingham histological grade, suggesting an association between reduced TRPS1 expression and loss of epithelial differentiation. These findings are consistent with current concepts regarding the role of TRPS1 in maintaining the epithelial phenotype and suppressing epithelial-mesenchymal transition. Accordingly, decreased TRPS1 expression may be regarded as a morphological indicator of biologically more aggressive, poorly differentiated TNBC.

Of particular interest is the observed association between TRPS1 expression and tumor microenvironment characteristics. In the present study, tumors with high TRPS1 expression exhibited significantly higher levels of sTILs. Given the well-established prognostic and predictive significance of sTILs in TNBC, this observation suggests that TRPS1-expressing tumors may exhibit enhanced immune reactivity, potentially contributing to improved responses to systemic therapy. At the same time, the relationship between TRPS1 expression and sTILs levels likely reflects a complex interplay between tumor cell state and the immune microenvironment rather than a simple linear dependency.

The most clinically relevant finding of this study is the association between TRPS1 expression and NACT efficacy. pCR and minimal residual tumor burden (RCB-0 and RCB-I) were observed significantly more frequently in the TRPS1-high group, whereas tumors with low or absent TRPS1 expression predominantly exhibited higher RCB categories (RCB-II and RCB-III). These results indicate a potential predictive role for TRPS1 not only in achieving pCR but also in the depth of therapeutic response.

The biological interpretation of these findings may be related to the multifaceted role of TRPS1 in regulating cell cycle control, DNA damage response, and epithelial-mesenchymal transition. Preserved TRPS1 expression may reflect a more differentiated epithelial phenotype associated with increased sensitivity to cytotoxic chemotherapy. Conversely, reduced TRPS1 expression may be accompanied by activation of cellular plasticity programs and DNA damage resistance, resulting in reduced chemotherapy efficacy and greater residual tumor burden. In this context, TRPS1 may be considered an integrative marker reflecting the combined influence of morphological, molecular, and immune tumor characteristics.

It should be noted that inclusion of platinum-based agents in NACT regimens was associated only with a trend toward increased pCR rates and did not reach statistical significance in this study. This may be attributable to the relatively limited sample size and heterogeneity of treatment regimens. Nevertheless, the observed association between TRPS1 expression and response to NACT, regardless of the specific treatment regimen, suggests that this marker may have universal predictive value.

Several limitations of the present study should be acknowledged, including its retrospective design, relatively small cohort size, and lack of molecular stratification of TNBC subtypes. In addition, TRPS1 expression was assessed in diagnostic biopsy material, which does not fully account for potential intratumoral heterogeneity. However, evaluation of pre-treatment biopsy specimens provides the greatest clinical relevance for the practical application of TRPS1 as a predictive biomarker.

In summary, the results of this study support the consideration of TRPS1 not only as a highly sensitive diagnostic marker of mammary differentiation in TNBC but also as a potential predictive factor for the efficacy of neoadjuvant chemotherapy. Further prospective studies incorporating comprehensive molecular characterization of tumors are warranted to clarify the role of TRPS1 within personalized treatment strategies for TNBC.

Ethical Considerations

The study was conducted in accordance with the ethical principles of the Declaration of Helsinki. It was approved by the Local Ethics Committee of the Oncology Institution (Protocol No. 13 dated 12.21, 2020). Given the retrospective nature of the study and the use of anonymized archival materials, informed consent from patients was not required.

Competing Interests

The authors declare that they have no competing interests.

References

1. Ding Q, Huo L, Peng Y, Yoon EC, Li Z, Sahin AA. Immunohistochemical Markers for Distinguishing Metastatic Breast Carcinoma from Other Common Malignancies: Update and Revisit. Semin Diagn Pathol. 2022 Sep;39(5):313-321. doi: 10.1053/j.semdp.2022.04.002. PMID: 35461734.

2. Sangoi AR, Shrestha B, Yang G, Mego O, Beck AH. The Novel Marker GATA3 is Significantly More Sensitive Than Traditional Markers Mammaglobin and GCDFP15 for Identifying Breast Cancer in Surgical and Cytology Specimens of Metastatic and Matched Primary Tumors. Appl Immunohistochem Mol Morphol. 2016 Apr;24(4):229-237. doi: 10.1097/PAI.0000000000000186. PMID: 25906123; PMCID: PMC5610542.

3. Kandalaft PL, Simon RA, Isacson C, Gown AM. Comparative Sensitivities and Specificities of Antibodies to Breast Markers GCDFP-15, Mammaglobin A, and Different Clones of Antibodies to GATA-3: A Study of 338 Tumors Using Whole Sections. Appl Immunohistochem Mol Morphol. 2016 Oct;24(9):609-614. doi: 10.1097/PAI.0000000000000237. PMID: 26447897.

4. Du T, Pan L, Zheng C, Chen K, Yang Y, Chen J, Chao X, Li M, Lu J, Luo R, Zhang J, Wu Y, He J, Jiang D, Sun P. Matrix Gla protein (MGP), GATA3, and TRPS1: a novel diagnostic panel to determine breast origin. Breast Cancer Res. 2022 Oct;24(1):70. doi: 10.1186/s13058-022-01569-1. PMID: 36284362; PMCID: PMC9598034.

5. Ai D, Yao J, Yang F, Huo L, Chen H, Lu W, Soto LMS, Jiang M, Raso MG, Wang S, Bell D, Liu J, Wang H, Tan D, Torres-Cabala C, Gan Q, Wu Y, Albarracin C, Hung MC, Meric-Bernstam F, Wistuba II, Prieto VG, Sahin AA, Ding

Q. TRPS1: a highly sensitive and specific marker for breast carcinoma, especially for triple-negative breast cancer. Mod Pathol. 2021 Apr;34(4):710-719. doi: 10.1038/s41379-020-00692-8. PMID: 33011748; PMCID: PMC12010768.
6. Kong C, Yu B, Bi R, Xu X, Cheng Y, Yang W, Shui R. TRPS1, a sensitive marker for different histological and molecular types of breast cancer. Diagn Pathol. 2024 Sep;19(1):121. doi: 10.1186/s13000-024-01542-w. PMID: 39243111; PMCID: PMC11378484.
7. Hashmi AA, Brogi E, Wen HY. Trichorhinophalangeal syndrome type 1 (TRPS1) in breast pathology: diagnostic utility and pitfalls. Diagn Pathol. 2025 Mar;20(1):26. doi: 10.1186/s13000-025-01623-4. PMID: 40025593; PMCID: PMC11872298.
8. Yoon EC, Wang G, Parkinson B, Huo L, Peng Y, Wang J, Salisbury T, Wu Y, Chen H, Albarracin CT, Resetkova E, Middleton LP, Krishnamurthy S, Gan Q, Sun H, Huang X, Shen T, Chen W, Parwani AV, Sahin AA, Li Z, Ding Q. TRPS1, GATA3, and SOX10 expression in triple-negative breast carcinoma. Hum Pathol. 2022 Jul;125:97-107. doi: 10.1016/j.humpath.2022.04.006. PMID: 35413381.
9. Parkinson B, Chen W, Shen T, Parwani AV, Li Z. TRPS1 Expression in Breast Carcinomas: Focusing on Metaplastic Breast Carcinomas. Am J Surg Pathol. 2022 Mar;46(3):415-423. doi: 10.1097/PAS.0000000000001824. PMID: 35175968.
10. Lennartz M, Löhr N, Höflmayer D, Dwertmann Rico S, von Bargen C, Kind S, Reiswich V, Viehweger F, Lutz F, Bertram V, Fraune C, Gorbokon N, Weidemann S, Blessin NC, Hube-Magg C, Menz A, Schlichter R, Krech T, Hinsch A, Burandt E, Sauter G, Simon R, Kluth M, Marx AH, Lebok P, Dum D, Minner S, Jacobsen F, Clauditz TS, Bernreuther C, Steurer S. TRPS1 is a Highly Sensitive Marker for Breast Cancer: A Tissue Microarray Study Evaluating More Than 19,000 Tumors From 152 Different Tumor Entities. Am J Surg Pathol. 2024 Jun;48(6):637-651. doi: 10.1097/PAS.0000000000002213. PMID: 38647255; PMCID: PMC11093513.
11. Baban F, Koepplin JW, Ahmad M, Clarke-Brodber AL, Bois MC, Hartley CP, Sturgis CD. TRPS1 outperforms GATA3 in pleural effusions with metastatic breast carcinoma versus mesothelioma. Diagn Cytopathol. 2023 Aug;51(8):488-492. doi: 10.1002/dc.25148. PMID: 37096814.
12. Salgado R, Denkert C, Demaria S, Sirtaine N, Klauschen F, Pruneri G, Wienert S, Van den Eynden G, Baehner FL, Penault-Llorca F, Perez EA, Thompson EA, Symmans WF, Richardson AL, Brock J, Criscitiello C, Bailey H, Ignatiadis M, Floris G, Sparano J, Kos Z, Nielsen T, Rimm DL, Allison KH, Reis-Filho JS, Loibl S, Sotiriou C, Viale G, Badve S, Adams S, Willard-Gallo K, Loi S; International TILs Working Group 2014. The evaluation of tumor-infiltrating lymphocytes (TILs) in breast cancer: recommendations by an International TILs Working Group 2014. Ann Oncol. 2015 Feb;26(2):259-271. doi: 10.1093/annonc/mdu450. PMID: 25214542; PMCID: PMC6267863.
13. Symmans WF, Peintinger F, Hatzis C, Rajan R, Kuerer H, Valero V, Assad L, Poniecka A, Hennessy B, Green M, Buzdar AU, Singletary SE, Hortobagyi GN, Pusztai L. Measurement of residual breast cancer burden to predict survival after neoadjuvant chemotherapy. J Clin Oncol. 2007 Oct;25(28):4414-4422. doi: 10.1200/JCO.2007.10.6823. PMID: 17785706.

International Journal of Biomedicine 16(1) (2026) 59-63
http://dx.doi.org/10.21103/Article16(1)_OA7

ORIGINAL ARTICLE

Otorhinolaryngology

INTERNATIONAL JOURNAL OF BIOMEDICINE

Nature of Nasal Polyps among Adults in Al Kharj City: A Retrospective Study

Ali Hassan A. Ali[1*], Wafaey Badawy[2], Turki Aldriweesh[3], Soltan Emad Eldeen H. Alkhaldi[4], Saud Lafai Alsulami[4], Abdullah F. Alanazi[4], Ahmed Eidhah Almalki[4], Mohammed Abdullah Alharbi[4], Saleh Abdullatif Almunyif[4], Raghad Abdullah Aldosari[4], Shouq Bader S. Alotaibi[4], Rasil Nasser Alqahtani[4], Mohammed Ahmed Saad Almalki[5], Raghad Shudayyid R. Almutairi[6]

[1]*Basic Medical Science Department, College of Medicine, Prince Sattam bin Abdulaziz University, Al-Kharj 11942, Saudi Arabia*
[2]*Department of Pathology, Military Industries Hospital, Al-Kharj, Saudi Arabia*
[3]*Department of Otolaryngology-Head and Neck Surgery College of Medicine, Prince Sattam bin Abdulaziz University, Al-Kharj 11942, Saudi Arabia*
[4]*College of Medicine, Prince Sattam bin Abdulaziz University, Al-Kharj 11942, Saudi Arabia*
[5]*College of Medicine, Imam Mohammed Ibn Saud Islamic University, Riyadh, Saudi Arabia*
[6]*Faculty of Medicine, Almaarefa University, Riyadh, Saudi Arabia*

Abstract

Background: Clinical and radiographic criteria are used to diagnose nasal polyps, but histopathologic examination is necessary for a definitive diagnosis. There are numerous categories for the histological classification of nasal polyps. The aim of this study was to identify the histological subtypes of nasal polyps in adult patients in Al Kharj city.
Material and Methods: Fifty-one individuals who had surgery to remove nasal polyps between January 2024 and June 2025, and whose diagnoses were verified by histological analysis, were the subject of a retrospective study based on hospital information. Males made up more than half (58.8%) of the patients. Inflammatory or allergic polyps were found in most cases (52.9%). Inverted papilloma was found in 21 cases (41.2%). Of the 51 cases, only 3 were malignant.
Conclusion: Uupon histological inspection, the nasal polyps primarily exhibit an inflammatory or allergic pattern. Histopathological examination of a resected nasal polyp is often necessary to establish the definitive diagnosis, as it is challenging to detect the pathology of a nasal mass clinically.(**International Journal of Biomedicine. 2026;16(1):59-63.**)

Keywords: nasal polyps • histopathology • retrospective study

For citation: Ali AHA, Badawy W, Aldriweesh T, Alkhaldi SEEH, Alsulami SL, Alanazi AF, Almalki AE, Alharbi MA, Almunyif SA, Aldosari RA, Alotaibi SBS, Alqahtani RN, Almalki MAS, Almutairi RSR. Nature of Nasal Polyps among Adults in Al Kharj City: A Retrospective Study. International Journal of Biomedicine. 2026;16(1):59-63. doi:10.21103/Article16(1)_OA7

Introduction

Nasal polyposis is a benign hyperplastic growth of the nasal mucosa. It is the outcome of a complicated process that some people experience. Some people have it, including those with cystic fibrosis, rhinitis, and chronic sinusitis. Clinical and radiographic criteria are used to diagnose nasal polyps, but histopathologic examination is crucial for precise diagnosis.[1] Nasal polyposis is present in 25–30% of patients with chronic rhinosinusitis and in 1%–4% of the general population.[2] Numerous pathologic processes and etiologic factors have been implicated in the development of nasal polyps. The causes of nasal polyps remain unclear. Nasal polyps have a complex etiology, including allergies, primary ciliary dyskinesia, cystic fibrosis, persistent infections, and some systemic vasculitides. Aspirin sensitivity and asthma are well known to be associated

***Corresponding author:** Prof. Ali Hassan A. Ali. E-mail: alihassan3750@yahoo.com, a.ali@psau.edu.sa*

with the development of nasal polyps.[3] Every nasal polyp excised during surgery should be routinely referred for histological analysis. Currently, otolaryngologists cannot agree on the necessity of routinely examining nasal polyps. Pathological findings often alter patient management, and microscopic analysis of nasal polyp specimens typically aligns well with prior clinical impressions. It was discovered that the accumulation of extracellular fluid, a moderate inflammatory process, and the growth of mucosa and submucosa within the turbinates or paranasal sinus were the causes. Nasal polyps are more common in adults than in children.[4]

Polyps originating from the mucosa can be sessile (no stalk), sessile-semipedunculated, or pedunculated (with a stalk). These benign, painless, and often translucent, grey-colored growths are usually found near the ethmoid sinuses. There are inflammatory or granulomatous polyps, linked to a persistent naso-sinusoidal infection, and the other types, linked to nasal allergy and multiple eosinophilic infiltrations of the stroma.[5]

Nasal obstruction, congestion, anosmia, nasal discharge, rhinorrhea, facial pain, and headache are all clinical signs of nasal polyps.[6] The complete knowledge of stromal alterations and of epithelial cells, particularly of several populations of inflammatory cells implicated in the pathophysiology of this disease, is made possible by histological examination.[7] Accurate classification of nasal polyps is challenging due to their overlapping histological features.

The aim of this study was to identify the histological subtypes of nasal polyps in adult patients in Al Kharj city.

Materials and Methods

The research design used in this study was a retrospective design. The Military Industries Hospital served as the location. This study comprised the hospital records of every patient who had nasal polyp removal surgery at the histopathology department at Al Kharj Military Industries Hospital between January 2024 and June 2025. Histopathological analysis was performed on all nasal polyp specimens obtained from patients of various ages and genders during the study period. Patients with nasal polyps who were older than 12 and whose diagnosis was verified by histological examination met the inclusion criteria. Nevertheless, only instances with sufficient tissue samples and comprehensive clinical data were taken into consideration for analysis. Additionally, patients with congenital nasal polyps and a history of previous surgery were not involved in the research study. The pathology department's histopathology section received all of the specimens in 10% formalin along with significant clinical data, including age and sex. The usual biopsy processing protocol for paraffin-embedded sections was followed for all tissue sections. Eosin and hematoxylin stains were applied following the fabrication of sections that were three to five microns thick. To ensure diagnostic consistency, each slide was examined under a light microscope by two separate trained pathologists. They used standard morphological criteria to categorize the polyps as allergic, inflammatory, and other forms based on their histological characteristics. For this study, information was gathered from patients' medical records. Data analysis was done using SPSS statistics 22.0.

Results

Males accounted for more than half (58.8%) of patients, and 21 (41.2%) were female. The patients ranged in age from 12 to 76. The largest proportion (23/45.1%) of participants in the current study were aged 31-40. The next most frequent age group affected was 41 to 50 years old (Table 1)

Table 1.

Lesion distribution according to histology, age, and gender (n=51).

Parameter	Category	N	Percentage
Gender	Male	30	58.8%
	Female	21	41.2%
Age	12-30	3	5.9%
	31-40	23	45.1%
	41-50	18	35.3%
	51-60	5	9.8%
	≥61	2	3.9%
Type of lesion (Polyp)	Non-neoplastic		
	Inflammatory or allergic	27	52.9%
	Neoplastic		
	Benign inverted papilloma	21	41.2%
	Malignant lesion	3	5.9%

Only 3 of the 51 instances were malignant; 27 were non-neoplastic (52.9%), and 24 were benign neoplastic polyps (47.1%). Nearly all cases had varying numbers of eosinophils, in addition to other inflammatory or allergic polyps. Sheets of mononuclear cells and eosinophils were also visible. All allergic and inflammatory polyps exhibited edema and a noticeable alteration in vascularity. The stroma of these polyps also contained fibroblasts, inflammatory cells, and fluid that formed pseudocystic gaps. There was typically a moderate number of inflammatory cells. Additionally, dilated arteries and hyperplasia of seromucinous glands were discovered. (Figures 1A,B,C,D & 2A,B,C,D)

A benign epithelial growth in the nasal cavity and the paranasal sinuses' underlying stroma is called an inverted papilloma. In 21 (41.2%) cases, it was identified. Histological analysis revealed polypoid tissue coated in pseudostratified columnar ciliated epithelium with mixed mucocytes in the hematoxylin and eosin-stained section. (Figures 3A,B,C,D & 4A,B,C,D)

An 18-year-old patient had a little nasal nodule. It typically manifests in early childhood or at birth. solitary skin-colored papule with a maximum size of less than 1 cm. It displays more developed vellus hair follicles in close proximity. (Figure 5A,B,C,D)

It was determined that the malignant specimen was nasopharyngeal cancer. A biopsy performed in the clinic revealed that the three patients' unilateral nasal tumors were nasal polyps. Histologically, nasopharyngeal carcinoma was identified as a nonkeratinizing undifferentiated type, characterized by clusters of tumor cells with vesicular nuclei, large central nucleoli, and indistinct cell borders. Plasma cells and background lymphocytes were frequently observed. (Figure 6A,B,C,D)

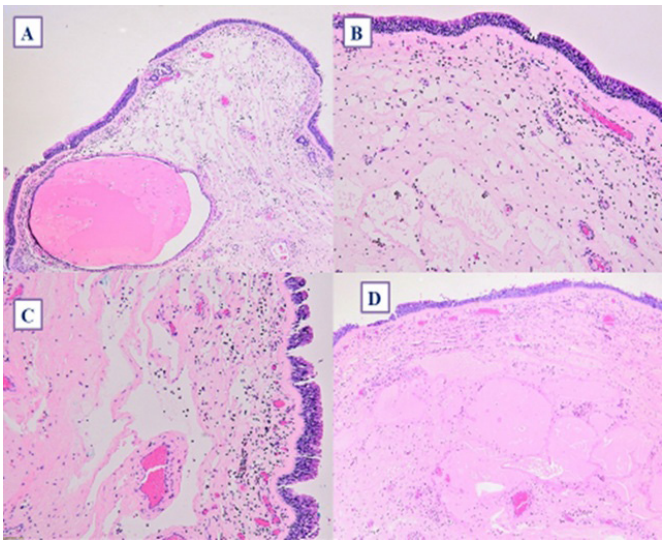

Fig. 1. *Different images of allergic and inflammatory nasal polyps stained with Hematoxylin and Eosin. A) Thrombotic stratification is observed in cavernous-like structures.B) Acute and chronic inflammatory cells, together with a few fibroblasts and tiny blood vessels, are mixed together in the edematous stroma. C) The respiratory epithelium exhibits stromal edema hyperplasia in a polyp with seromucinous gland hyperplasia, and the basal membrane that divides the epithelium from the edematous stroma thickens. D) The surface is covered in pseudostratified columnar epithelium, and the stroma is loose and edematous. (A, B X 200). (C, D X 400)*

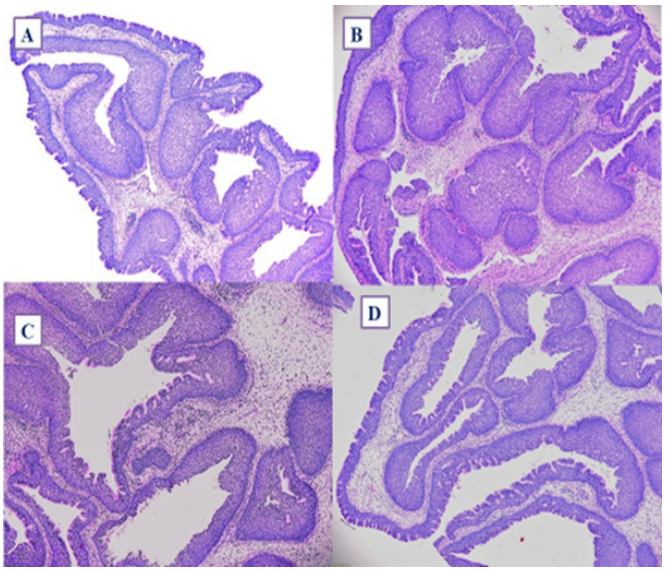

Fig. 3. *Different images of inverted papillomas stained with Hematoxylin and Eosin. A) demonstrates an endophytic or inverted growth pattern with noticeably thicker squamous epithelial proliferation that descends into the connective tissue stroma underneath. B) Has an inverted growth pattern with pseudostratified ciliated columnar epithelium that is noticeably thicker and grows downward into the underlying stroma. C) Low-power inverted papilloma. Typical form and pattern that should not be mistaken for common nasal polyps. D) Noticeable downward endophytic proliferation of smooth-surfaced, spherical to long, linked epithelial nests. (A, B, C & D X 200)*

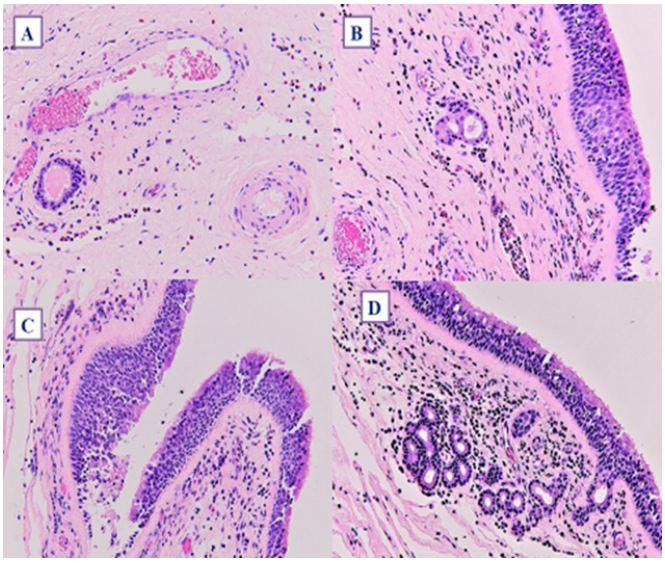

Fig. 2. *Different images of allergic and inflammatory nasal polyps stained with Hematoxylin and Eosin. A) Inflammatory cell infiltration, including eosinophils, lymphocytes, and plasma cells. B) Neutrophil transmigration is observed with stroma edema, and the epithelium is hyperplastic and of a squamous type. C) There are tiny intraepithelial mucin cysts. Both an exophytic and an inverted growth pattern are present in these polyps. D) Many seromucinous glands and ductal structures in an edematous stroma are visible in polyps with seromucinous gland hyperplasia. (A, B, C & D X 400)*

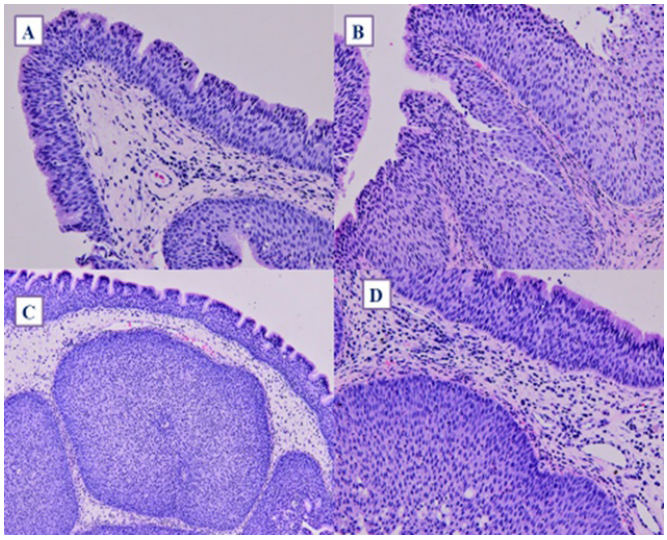

Fig. 4. *Different images of inverted papillomas stained with Hematoxylin and Eosin. A) High magnification reveals that the epithelium is made up of intraepithelial mucin microcysts and pseudostratified columnar cells intermingled with mucocytes (goblet cells). B) Markedly thickened squamous epithelial proliferation. C) Multiple layers of eosinophilic columnar cells, occasionally ciliated, make up the epithelium. D) Sinonasal papilloma, inverted type, ethmoid. The squamous mucosa has dysplasia. (A, B, C & D X 400)*

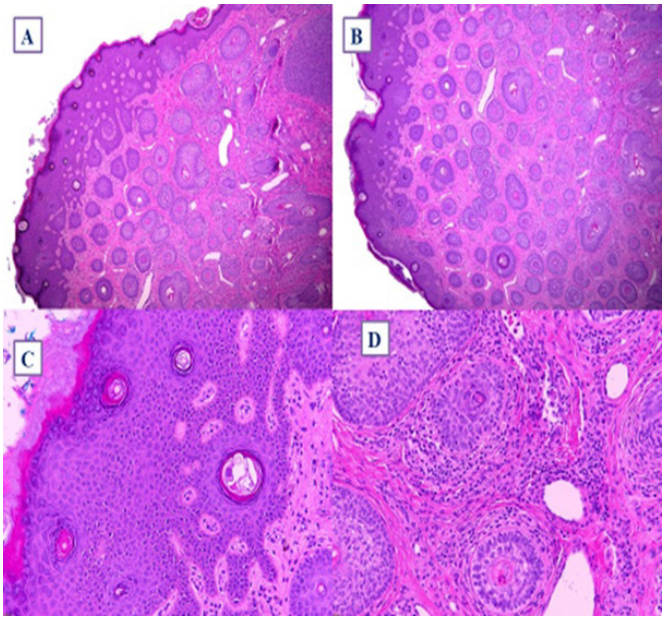

Fig. 5. *Different images of nasal ala small nodule in the vestibule stained with Hematoxylin and Eosin. A) Lower power magnification of mesoderm-derived fibroadipose tissue surrounded by pilosebaceous units and squamous epithelium derived from ectoderm. B) Epidermal stratified squamous epithelium with sebaceous glands and hair follicles. C) Aberrant squamous cells encroaching on the surrounding tissue. D) Increased numbers of closely spaced mature vellus hair follicles are seen at high magnification. (A, B X 200). (C, D X 400).*

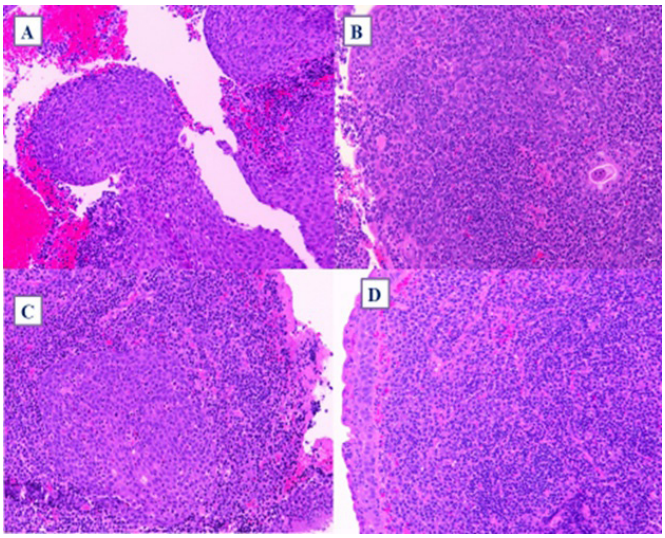

Fig. 6. *Different images of nasopharyngeal cancer stained with Hematoxylin and Eosin. A) Sheets of undifferentiated cancer cells with necrotic patches invade the mucosa. B) A concentrated build-up of lymphocytes, plasma cells, and epithelioid cells without necrosis. C) Undifferentiated nonkeratinizing carcinoma. D) Keratinizing squamous cell carcinoma (A, B X 200). (C, D X 400).*

Discussion

A range of disorders, from benign to malignant nasal lesions, can also present as nasal polyps; however, most nasal polyps submitted for histology are inflammatory, attributable to infection, allergy, or idiopathic causes. It has been suggested that allergies and inflammation contribute to nasal polyps, and approximately 30% of patients with nasal polyps test positive for environmental allergens.[8] We discovered that men are impacted more often than women. It was consistent with a prior study that found a higher frequency among men.[9,10] The histopathological variety of nasal polyps has important clinical implications in addition to helping with accurate diagnosis. Every nasal polyp excised during surgery should be routinely referred for histological analysis. Currently, otolaryngologists cannot agree on the necessity of routinely examining nasal polyps. If all tissues retrieved from the sinonasal tract after surgery are not sent for histological analysis, the diagnosis may be missed, and the proper course of treatment may be delayed.[11] A simple nasal mass might be mistaken for a number of illnesses, from benign lesions to malignant nasal tumors. Therefore, it is nearly impossible to diagnose a nasal mass clinically.

To arrive at the correct diagnosis, histopathology and nasal endoscopy should be used in tandem. As a result, the real diagnosis is often dependent on the histological analysis of a resected nasal polyp. According to earlier research, middle-aged men are most likely to have nasal polyps. Patients in the fourth and fifth decades are often more likely to have non-neoplastic nasal masses, but those in the fifth or sixth decades are more likely to have neoplastic masses.[12,13] More allergic and inflammatory polyps were found in the current investigation. This result is consistent with another study that found that 60.32% of nasal polyps were allergy-related. [9] Three malignant nasopharyngeal carcinoma lesions were found in the current investigation. Rarely, malignant tumors of the sinonasal region account for about 3% of all upper respiratory tract cancers.

Conclusion

Upon histological inspection, the nasal polyps primarily exhibit an inflammatory or allergic pattern. Histopathological examination of a resected nasal polyp is often necessary to establish the definitive diagnosis, as it is challenging to detect the pathology of a nasal mass clinically.

Competing Interests

The authors declare that they have no conflicts of interest.

Acknowledgements

The authors are grateful to the Deanship of Scientific Research, Prince Sattam bin Abdulaziz University, Al-Kharj, Saudi Arabia, for its support and encouragement in conducting the research and publishing this report.

Ethical Approval

All steps implemented in this study complied with the Ethics Committee of the Institutional Review Board of Prince Sattam bin Abdulaziz University (SCBR-501/2025).

References

1. Allen JS, Eisma R, LaFreniere D, Leonard G, Kreutzer D. Characterization of the eosinophil chemokine RANTES in nasal polyps. Ann Otol Rhinol Laryngol. 1998 May;107(5 Pt 1):416-20. doi: 10.1177/000348949810700510. PMID: 9596221.
2. Fokkens WJ, Lund VJ, Hopkins C, Hellings PW, Kern R, Reitsma S, et al. European Position Paper on Rhinosinusitis and Nasal Polyps 2020. Rhinology. 2020 Feb 20;58(Suppl S29):1-464. doi: 10.4193/Rhin20.600. PMID: 32077450.
3. Fan Y, Jiao Q, Zhou A, Liu J. [Correlation between chronic sinusitis subtypes and basophil levels in peripheral blood]. Lin Chuang Er Bi Yan Hou Tou Jing Wai Ke Za Zhi. 2023 Apr;37(4):293-296;301. Chinese. doi: 10.13201/j.issn.2096-7993.2023.04.011. PMID: 36987961; PMCID: PMC10406586.
4. Hellings PW, Borrelli D, Pietikainen S, Agache I, Akdis C, Bachert C, Bewick M, Botjes E, Constantinidis J, Fokkens W, Haahtela T, Hopkins C, Illario M, Joos G, Lund V, Muraro A, Pugin B, Seys S, Somekh D, Stjärne P, Valiulis A, Valovirta E, Bousquet J. European Summit on the Prevention and Self-Management of Chronic Respiratory Diseases: report of the European Union Parliament Summit (29 March 2017). Clin Transl Allergy. 2017 Dec 27;7:49. doi: 10.1186/s13601-017-0186-3. PMID: 29299230; PMCID: PMC5745781.
5. Lathi A, Syed MM, Kalakoti P, Qutub D, Kishve SP. Clinico-pathological profile of sinonasal masses: a study from a tertiary care hospital of India. Acta Otorhinolaryngol Ital. 2011 Dec;31(6):372-7. PMID: 22323848; PMCID: PMC3272868.
6. Valera FC, Anselmo-Lima WT. Evaluation of efficacy of topical corticosteroid for the clinical treatment of nasal polyposis: searching for clinical events that may predict response to treatment. Rhinology. 2007 Mar;45(1):59-62. PMID: 17432072.
7. Enache I, IoniȚĂ E, Mitroi M, Anghelina F, MogoantĂ C, Ciolofan S, CĂpitĂnescu A, Stepan A, Simionescu C. Histopathological Features of Chronic Rhinosinusitis with Nasal Allergic Polyps. Curr Health Sci J. 2020 Jan-Mar;46(1):66-71. doi: 10.12865/CHSJ.46.01.09. Epub 2020 Mar 31. PMID: 32637167; PMCID: PMC7323723.
8. Bernstein JM, Gorfien J, Noble B. Role of allergy in nasal polyposis: a review. Otolaryngol Head Neck Surg. 1995 Dec;113(6):724-32. doi: 10.1016/s0194-5998(95)70012-9. PMID: 7501384.
9. Abdulla MS, Janardhan K, Lakshmi VP, John R. A Retrospective Study on Histomorphological Analysis of Sinonasal Polyps at A Tertiary Care Centre in A Rural Area of South India. Int J Trop Med. 2024 May 2;18:83-9.
10. Lanza DC, Kennedy DW. Current concepts in the surgical management of nasal polyposis. J Allergy Clin Immunol. 1992 Sep;90(3 Pt 2):543-5; discussion 546. doi: 10.1016/0091-6749(92)90182-2. PMID: 1527347.
11. Chen SH, Wu CS, Chan KH, Hongh YT, Shun CT, Liu CM. Primary sinonasal non-Hodgkin's lymphoma masquerading as chronic rhinosinusitis: an issue of routine histopathological examination. J Laryngol Otol. 2003 May;117(5):404-7. doi: 10.1258/002221503321626483. PMID: 12803794.
12. Kirtsreesakul V. Nasal polyps: the relationship to allergy, sinonasal infection and histopathological type. J Med Assoc Thai. 2004 Mar;87(3):277-82. PMID: 15117044.
13. Kitapçi F, Muluk NB, Atasoy P, Koç C. Role of mast and goblet cells in the pathogenesis of nasal polyps. J Otolaryngol. 2006 Apr;35(2):122-32. doi: 10.2310/7070.2005.5004. PMID: 16527032.

International Journal of Biomedicine 16(1) (2026) 64-70
http://dx.doi.org/10.21103/Article16(1)_OA8

ORIGINAL ARTICLE

Radiology

INTERNATIONAL JOURNAL OF BIOMEDICINE

Utilizing Ultrasound for Estimating Liver Size in Patients with Fatty Liver Disease: A Study in Jeddah, Saudi Arabia

Salem Alghamdi[1], Abdulrahman Tajaldeen[1*], Rowa Aljondi[1], Abdulrzzag Alghamdi[1], Hamza Showlag[1], Abdulaziz Helabi[1], Samer Ahmed[1], Saeed Al-Malki[1], Talal Al-Omari[1]

[1]*Applied Radiologic Technology Department, College of Applied Medical Sciences, University of Jeddah, Jeddah, Saudi Arabia*

Abstract

Background: Ultrasound is widely used to evaluate liver morphology in nonalcoholic fatty liver disease (NAFLD), yet the relationships between ultrasound-derived liver size and patient characteristics remain incompletely described in Saudi populations. This study assessed the association between right-lobe liver size and demographic/anthropometric variables among adults with ultrasound-confirmed NAFLD in Jeddah, Saudi Arabia.

Methods and Results: This retrospective, cross-sectional, two-center study included 212 adults (≥18 years) with NAFLD documented on ultrasound reports from 2 tertiary hospitals in Jeddah between 2020 and 2025. The primary outcome was right-lobe liver size (cm) extracted from ultrasound reports and/or PACS measurements. Predictors included sex, age, BMI, and hospital site. Of 212 participants, 114 (53.8%) were female; mean age was 49.5 years, and mean BMI was 31.6 kg/m², with most participants classified as overweight or obese. Mean right-lobe liver size was similar between Hospital A and Hospital B (15.98±2.02 vs 16.07±2.03 cm; P=0.763). Females had numerically larger right-lobe measurements than males in both hospitals, but differences were not statistically significant overall (16.18±2.07 vs 15.84±1.94 cm; P=0.218). Liver size correlated inversely and weakly with age (r=−0.160, P=0.019) and weakly and positively with weight (r=0.221, P=0.001) and BMI (r=0.180, P=0.009). In multivariable regression adjusting for sex, BMI, and hospital, age remained independently associated with liver size (β=−0.023 cm/year; P=0.026), while BMI did not retain significance (β=0.043 cm per kg/m²; P=0.110); sex and hospital were not significant predictors.

Conclusion: In adults with ultrasound-reported NAFLD in Jeddah, right-lobe liver size showed modest associations with age and adiposity, with age remaining an independent predictor after adjustment. Sex-based differences were small and non-significant, and measurements were consistent across two hospitals. Standardized acquisition and inclusion of objective NAFLD severity measures (e.g., elastography and laboratory markers) are needed to refine the interpretation of routine ultrasound liver size metrics in regional NAFLD populations.(**International Journal of Biomedicine. 2026;16(1):64-70.**)

Keywords: nonalcoholic fatty liver disease • ultrasound • liver size • right lobe • body mass index • B-mode

For citation: Alghamdi S, Tajaldeen A, Aljondi R, Alghamdi A, Showlag H, Helabi A, Ahmed S, Al-Malki S, Al-Omari T. Utilizing Ultrasound for Estimating Liver Size in Patients with Fatty Liver Disease: A Study in Jeddah, Saudi Arabia. International Journal of Biomedicine. 2026;16(1):64-70. doi:10.21103/Article16(1)_OA8

Introduction

Ultrasound (US) is a diagnostic imaging modality that uses high-frequency sound waves to produce real-time images; it is also referred to as ultrasonography, sonography, and real-time echography.[1] It is preferably used as a diagnostic modality because it is non-invasive, cost-effective, non-ionizing, and widely accessible across medical and clinical settings.[2-4] A sonographer, a person who operates an ultrasound machine, typically uses a handheld probe called a transducer that both emits and receives sound waves.[5] The transducer is placed directly on the patient's skin and moved over the area of interest, emitting sound waves; a computer converts the returning echoes into visual grey-scale images.[3] Diagnostic ultrasound is primarily used to visualize subcutaneous structures and soft tissues, including tendons, muscles, joints, vessels, and internal organs, to

***Corresponding author:** Dr. Abdulrahman Tajaldeen. E-mail: aatajaldeen@uj.edu.sa*

detect potential pathology or lesions.[6] Air can be a source of artifact during ultrasound imaging, especially in hairy individuals, because it can trap between the transducer and the body; therefore, a water-based gel is used to couple the ultrasound transducer to the patient.[3]

The liver is a large, dense organ situated mainly in the right hypochondrium, spanning the epigastric region and extending into the left hypochondrium toward the left lateral line. Typical liver weight ranges from about 1,400–1,600 g in males and 1,200–1,400 g in females.[7,8] Liver size can vary across many clinical conditions. It may be enlarged in diseases such as hepatitis, alcoholic liver disease, heart failure, and certain metabolic/storage disorders, or decreased in acute fulminant hepatitis and cirrhosis; in some cases, it remains normal. Overall, measuring liver size is a useful diagnostic marker.[7,9] Liver size showed significant associations with sex, age, body mass index (BMI), the presence of fatty liver, and hepatic steatosis grade.[10]

Nonalcoholic fatty liver disease (NAFLD) is among the most prevalent metabolic conditions globally, characterized by abnormal fat buildup in liver cells and potentially progressing to serious complications, including fibrosis, cirrhosis, and hepatocellular carcinoma (HCC).[11-13] NAFLD affects approximately 25% of the global population. Its prevalence is highest in the Middle East (31.79%) and South America (30.45%), while the lowest rates have been reported in Africa (13.48%).[14,15] In 2017, the estimated NAFLD burden was 8,451,000 cases (25.7%) in Saudi Arabia and 255,000 cases (25%) in the UAE. By 2030, NAFLD cases are expected to increase by 48% in Saudi Arabia, reaching 12,534,000, and by 46% in the UAE, reaching 372,000.[16] NAFLD occurs across all sexes, age groups, and ethnicities, and is most strongly associated with obesity, hyperlipidemia, diabetes mellitus, and metabolic syndrome driven by insulin resistance.[17,18]

Ultrasound is an important imaging modality used to assess liver volume, particularly in NAFLD patients.[11,19] It offers a non-invasive approach for evaluating liver size and fat content.[11] Additionally, it enables visualization of liver size and parenchymal texture. Measurements are obtained in multiple planes to ensure accurate liver volume.[17] Studies have demonstrated that B-mode US is effective for identifying moderate-to-severe steatosis, with sensitivity and specificity varying with the degree of fat accumulation.[11,20-24]

Ultrasound B-mode imaging enables a subjective assessment of the extent of fatty infiltration in the liver.[11] The grading of liver steatosis is typically determined using several US features, including liver brightness, liver–kidney contrast, the US appearance of intrahepatic vessels, liver parenchyma, and the diaphragm.[2,11,25] Steatosis is graded as follows: Absent (score 0) when the liver echotexture is normal; mild (score 1), when there is a slight, diffuse increase in liver echogenicity with normal visualization of the diaphragm and the portal vein wall; moderate (score 2), when liver echogenicity is moderately increased with mildly reduced visualization of the portal vein wall and the diaphragm; severe (score 3), when liver echogenicity is markedly increased with poor or absent visualization of the portal vein wall, diaphragm, and the posterior portion of the right liver lobe.[26-29]

This study aims to examine the association between liver size and demographic variables, including gender, age, and BMI, among patients with NAFLD attending healthcare centers in Jeddah, Saudi Arabia. By evaluating ultrasound findings in a representative sample, the study seeks to expand the evidence base on liver disease within the Saudi population. Furthermore, the results may support improved early detection and assist healthcare professionals in developing management strategies tailored to individual patient characteristics.

Methods

Study Design and Setting

This retrospective, cross-sectional study evaluated adult patients who underwent liver ultrasound examinations at two tertiary hospitals in Jeddah, Western Saudi Arabia. Ultrasound and clinical record data were retrieved for examinations performed between 2020 and 2025.

The study included 212 adults aged 18 years or older with ultrasound-based evidence of NAFLD documented in the imaging report.

Inclusion criteria:

Age ≥18 years.

Liver ultrasound performed during 2020–2025 at one of the participating hospitals.

NAFLD reported on ultrasound.

Availability of right lobe liver measurement and core demographic/anthropometric variables (sex, age, weight, height, or BMI).

Exclusion criteria: records indicated alternative causes of hepatic steatosis or liver size alteration (e.g., significant alcohol use if documented, viral hepatitis, known chronic liver disease of other etiology, focal liver mass affecting measurement, prior hepatic surgery/transplantation), pregnancy, or incomplete/uninterpretable ultrasound images/measurements.

Ultrasound Acquisition and Measurement Protocol

All ultrasound examinations were performed as part of routine clinical care at the two participating hospitals. Images and reports were archived in the Picture Archiving and Communication System (PACS). Because this was a retrospective study, a prespecified research acquisition protocol was not implemented, and detailed acquisition parameters (e.g., transducer frequency, exact respiratory phase, and standardized measurement landmarks) were inconsistently documented and therefore could not be fully verified. Right-lobe liver size was extracted from the original clinical documentation (ultrasound report and/or PACS annotations), reflecting the measurements recorded at the time of the examination. When more than one right-lobe measurement was documented, the value labeled as the right-lobe length in the report was used; if multiple right-lobe length values were recorded, the largest documented value was selected for analysis.

Data Sources and Data Collection

Study variables were collected using a structured data extraction sheet. Imaging measurements were obtained from PACS, while demographic and anthropometric data were

retrieved from the hospital's electronic medical record system (Oasis). Trained data collectors extracted the data following a predefined coding manual to reduce variability and improve reproducibility.

Variables

Outcome variable: right lobe liver size (cm).

Predictor variables: gender (male/female), age (years), and BMI (kg/m²).

Anthropometric inputs used to compute BMI (when not recorded): weight (kg) and height (m).

Data Management and Quality Control

All data were de-identified before analysis and stored in password-protected files accessible only to the study team. Data cleaning included range checks (e.g., biologically plausible limits for height/weight/BMI and liver size), duplicate removal, and verification of outliers against source records (PACS/EMR). A predefined dataset dictionary was used to ensure uniform data entry.

Statistical Analysis

Statistical analyses were performed using the Statistical Package for Social Sciences SPSS v26. Continuous variables (right-lobe liver size, age, weight, height, and BMI) were summarized as mean ± standard deviation (SD), while categorical variables (sex, age categories, weight categories, height categories, and BMI classifications) were summarized as frequency and percentage. Mean right-lobe liver size was compared between males and females within each hospital (Hospital A and Hospital B) using the independent-samples t-test. Associations between right-lobe liver size and continuous variables (age, weight, height, and BMI) were examined using Pearson's correlation coefficient (r) with two-tailed P-values. A *P*-value <0.05 was considered statistically significant. Records with missing values for the primary outcome (right-lobe measurement) were excluded. For covariates, analyses were performed using complete-case analysis for the variables included in the study.

Results

A total of 212 adults with ultrasound-reported NAFLD were included. As shown in Table 1, Hospital A contributed 109 patients (63/57.8% female and 46/42.2% male), and Hospital B contributed 103 patients (51/49.5% female and 52/50.5% male). Age distribution differed slightly between hospitals; patients aged ≥60 years comprised 19.27% of Hospital A compared with 32.03% of Hospital B (Table 1).

The cohort demonstrated a high metabolic risk profile, with an overall mean BMI of 31.56±7.53 kg/m² (Table 2). Consistent with this, the majority of participants were classified as overweight or obese (Table 1). Specifically, obesity was more frequent in Hospital A (56.88%) than in Hospital B (46.60%), whereas overweight status was more frequent in Hospital B (37.86%) than in Hospital A (24.77%) (Table 1, Figure 1).

Right-lobe liver size estimates by sex and hospital are summarized in Table 3 and visualized in Figure 2. In Hospital A, females demonstrated a larger mean right-lobe liver size than males (16.24±1.77 cm vs. 15.63±2.28 cm), although this difference was not statistically significant (mean difference 0.61 cm, 95% CI −0.19 to 1.41, *P*=0.135). In Hospital B, mean liver size was comparable between females and males (16.11±2.40 cm vs. 16.02±1.59 cm; mean difference 0.08 cm, 95% CI −0.72 to 0.88, *P*=0.836) (Table 3).

Table 1.

Demographic characteristics of patients in Hospital (H) A and B.

Variable	Categories	H-A (n)	H-A (%)	H-B (n)	H-B (%)	Total n(%)
Age (years)	< 20	0	0.00%	1	0.97%	1(0.47%)
	20-29	7	6.42%	3	2.91%	10(4.72%)
	30-39	24	22.02%	19	18.45%	43(20.28%)
	40-49	31	28.44%	29	28.16%	60(28.3%)
	50-59	26	23.85%	18	17.48%	44(20.75%)
	60+	21	19.27%	33	32.03%	54(25.48%)
Total		109	100%	103	100%	212(100%)
Gender	Male	46	42.20%	52	50.49%	98(46.23%)
	Female	63	57.80%	51	49.51%	114(53.77%)
Total		109	100%	103	100%	100%
Weight (kg)	40-49.9	1	0.92%	0	0.00%	1(0.47%)
	50-59.9	5	4.59%	12	11.65%	17(8.02%)
	60-69.9	21	19.27%	16	15.54%	37(17.45%)
	70-79.9	22	20.18%	26	25.24%	48(22.64%)
	80-89.9	23	21.10%	21	20.39%	44(20.76%)
	90-99.9	19	17.43%	11	10.68%	30(14.15%)
	100+	18	16.51%	17	16.50%	35(16.51%)
Total		109	100%	103	100%	212(100%)
Height (m)	1.5-1.599	48	44.0%	40	38.83%	88(41.51%)
	1.6-1.699	36	33.0%	41	39.81%	77(36.32%)
	1.7-1.799	21	19.3%	20	19.42%	41(19.34%)
	1.8-1.899	4	3.7%	2	1.94%	6(2.83%)
Total		109	100%	103	100%	212(100%)
BMI (kg/m²)	Underweight	1	0.92%	0	0.00%	1(0.47%)
	Normal	19	17.43%	16	15.54%	35(16.51%)
	Overweight	27	24.77%	39	37.86%	66(31.13%)
	Obese	62	56.88%	48	46.60%	110(51.89%)
Total		109	100%	103	100%	212(100%)

Table 2.

Continuous variables (mean ± SD) in Hospital A and Hospital B.

Variable	Hospital A	Hospital B
Age (years)	47.94 ± 12.55	51.16 ± 14.13
Weight (kg)	83.18 ± 18.28	81.96 ± 21.12
Height (m)	1.62 ± 0.09	1.62 ± 0.09
BMI (kg/m²)	31.69 ± 6.97	31.41 ± 8.12
Right-lobe liver size (cm)	15.98 ± 2.02	16.07 ± 2.03

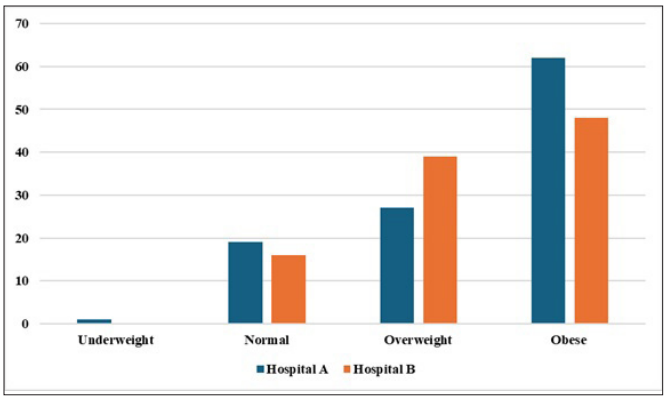

Figure 1. *BMI category distribution by hospital.*

Table 3.

Right-lobe liver size (cm) by sex and hospital, with sex comparisons using independent-samples t-tests.

Comparison	Female (n)	Male (n)	Female mean (cm)	Male mean (cm)	Mean diff (F-M) [95% CI]	*P*-value
Hospital A: Female vs Male	63	46	16.24	15.63	0.61 [-0.19, 1.41]	0.135
Hospital B: Female vs Male	51	52	16.11	16.02	0.08 [-0.72, 0.88]	0.836
Overall: Female vs Male	114	98	16.18	15.84	0.34 [-0.20, 0.89]	0.218

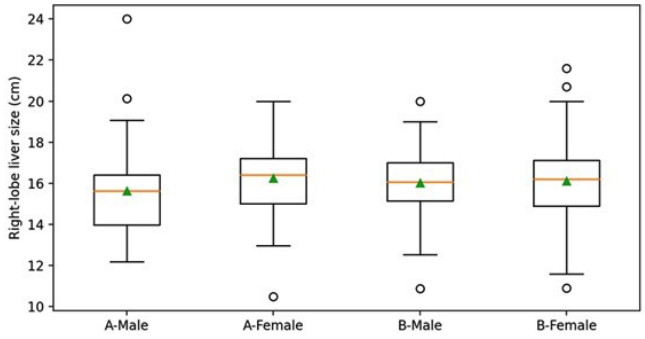

Figure 2. *Right-lobe liver size by sex and hospital (boxplot).*

When both hospitals were pooled, females continued to show a numerically larger mean liver size than males (16.18±2.07 cm vs. 15.84±1.94 cm); however, the between-sex difference remained non-significant (mean difference 0.34 cm, 95% CI −0.20 to 0.89, *P*=0.218) (Table 3).

Across the full sample, mean right-lobe liver size did not differ between hospitals (15.98±2.02 cm in Hospital A vs. 16.07±2.03 cm in Hospital B; *P*=0.763). This finding was consistent in sex-stratified analyses, with no statistically significant hospital-related differences among males (*P*=0.329) or females (*P*=0.746) (hospital comparison output).

As shown in Table 4 and Figure 3, Pearson correlation analysis demonstrated a weak but statistically significant inverse association between age and liver size (r=−0.160, *P*=0.019). Liver size correlated positively and weakly with body weight (r=0.221, *P*=0.001) and BMI (r=0.180, *P*=0.009), while height was not associated with liver size (r=0.031, *P*=0.658) (Table 4).

Table 4.

Pearson correlation between right-lobe liver size and age, weight, height, and BMI.

Predictor	r	*P*-value
Age (years)	-0.16	0.0194
Weight (kg)	0.221	0.0012
Height (m)	0.031	0.6583
BMI (kg/m²)	0.18	0.0087

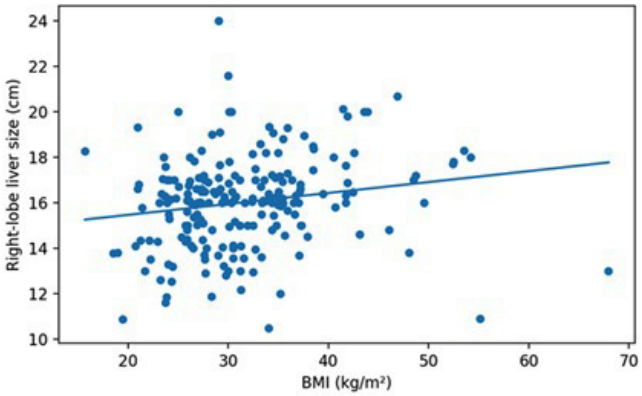

Figure 3. *Association between BMI and right-lobe liver size (scatter plot).*

Multivariable linear regression results are shown in Table 5. After adjustment for sex, BMI, and hospital, age remained independently associated with liver size (β=−0.023 cm/year, 95% CI −0.044 to −0.003, *P*=0.026). BMI showed a positive coefficient but did not reach statistical significance in the adjusted model (β=0.043 cm per 1 kg/m², 95% CI −0.010 to 0.097, *P*=0.110). Sex and hospital were not significant predictors after adjustment (female versus male: P=0.560; Hospital B versus A: *P*=0.515) (Table 5). The model explained a modest proportion of variance in liver size (R^2=0.058, adjusted R^2=0.040).

Table 5.

Multivariable linear regression for predictors of right-lobe liver size (sex, age, BMI, and hospital).

Predictor	Beta (cm)	SE	95% CI	*P*-value
Intercept	15.619	1.052	[13.557, 17.681]	<0.001
Sex (Female vs Male)	0.164	0.281	[-0.387, 0.715]	0.5598
Hospital (B vs A)	0.184	0.282	[-0.369, 0.736]	0.5149
Age (per 1 year)	-0.023	0.01	[-0.044, -0.003]	0.0263
BMI (per 1 kg/m²)	0.043	0.027	[-0.010, 0.097]	0.1095

Discussion

This retrospective two-center study evaluated ultrasound-derived right-lobe liver size in 212 adults with ultrasound-reported NAFLD in Jeddah, Saudi Arabia, and examined

associations with sex and demographic/anthropometric variables. The key findings were: (i) females demonstrated numerically larger mean right-lobe measurements than males in both hospitals, although sex differences were not statistically significant; (ii) liver size showed significant positive correlations with weight and BMI and a small inverse correlation with age; and (iii) in multivariable regression including sex, age, BMI, and hospital, age remained independently associated with liver size, whereas BMI did not remain significant after adjustment. These results highlight that ultrasound-measured right-lobe size in NAFLD varies modestly with patient characteristics, and that sex differences may be small and cohort-dependent.

In our cohort, females had a higher mean right-lobe size than males at Hospital A (16.24 vs 15.63 cm) and Hospital B (16.11 vs 16.02 cm), but these between-sex differences were not statistically significant. This contrasts with several studies reporting larger liver dimensions in males, including Dorostghol et al.[10] and earlier reports by Patell et al.,[30] Cruz et al.,[31] and Kratzer et al.[32] Heterogeneity across studies is expected in imaging-based NAFLD research and may reflect differences in cohort composition (age distribution, obesity burden, metabolic comorbidities, and NAFLD severity), as well as variability in ultrasound measurement definitions and technique.[32,33-35] Even when "liver size" is reported, studies may use different planes, landmarks, and respiratory phases, or report linear dimensions rather than volume surrogates, all of which can influence observed sex differences and limit direct comparability.[10,33] Therefore, our results do not necessarily contradict prior evidence but suggest that sex-related differences in ultrasound-measured right-lobe size may not be consistent across NAFLD populations and may be sensitive to both clinical and technical factors.[33,35]

We observed significant positive correlations between liver size and both weight and BMI, aligning with the established relationship between adiposity and NAFLD-related liver enlargement.[10,18,36] However, BMI did not remain statistically significant in the multivariable model, whereas age remained independently associated. This divergence between unadjusted and adjusted analyses is common in clinical datasets and likely reflects shared variance between anthropometric measures and other covariates, as well as residual confounding from unmeasured clinical factors (e.g., diabetes, dyslipidemia, medication exposure, and NAFLD severity).[37] In NAFLD, liver size may reflect not only steatosis-related enlargement but also disease remodeling across the spectrum; without fibrosis staging (e.g., elastography) or biochemical indices, the independent contribution of BMI may be attenuated after adjustment.[33,36] From an imaging standpoint, these findings support interpreting linear liver measurements as part of a broader assessment rather than as a stand-alone marker of disease severity.[18]

Age showed a small inverse association with liver size and remained significant after adjustment. While the effect size was modest, this suggests that liver size may not increase linearly with age in NAFLD cohorts.[10] Age-related variation could reflect differences in metabolic phenotype, disease duration, or the distribution of fibrosis stages.[18,36] For example, advanced fibrosis and architectural remodeling could potentially alter gross liver morphology and may not be captured by a single linear right-lobe measurement.[36] Because fibrosis staging and laboratory markers were not available in this dataset, causal explanations cannot be confirmed; nonetheless, the finding underscores the value of incorporating objective severity assessment (e.g., elastography) in future imaging studies of NAFLD.[33,36]

A strength of this study is the inclusion of two tertiary hospitals and the adjustment for hospital site in the analysis. The findings, therefore, reflect real-world clinical ultrasound reporting across two centers. This cross-site consistency supports the robustness of the observed associations and suggests that the findings are not driven by a single institutional case mix. However, ultrasound measurements remain operator-dependent and can be affected by patient body habitus, transducer selection, scanning plane, and respiratory phase.[10,33,35-36] Future work would be strengthened by explicit reporting of acquisition parameters, a standardized measurement protocol, and reproducibility assessment (intra- and inter-observer agreement), which are particularly valued in imaging journals and facilitate comparison across centers and studies.[33,36]

Clinical Relevance

Ultrasound remains widely used as a first-line imaging modality for suspected hepatic steatosis because it is accessible, noninvasive, and low-cost; however, its sensitivity for mild steatosis is limited, and it cannot stage fibrosis without additional techniques.[10,26,33,34,36-38] In routine abdominal ultrasound reporting, right-lobe size is often available and may provide a supportive context when interpreted alongside steatosis grade, clinical risk profile, and (when available) fibrosis risk stratification tools.[33,36] Our findings suggest that sex-based expectations of liver size may be unreliable in some NAFLD cohorts and underscore the importance of standardized measurement and cautious interpretation, particularly in light of patient-specific characteristics.

Limitations

Several limitations should be acknowledged. First, the retrospective design limited control over ultrasound acquisition conditions and may introduce measurement variability. Second, NAFLD was defined based on ultrasound report documentation without histological confirmation or elastography staging, introducing heterogeneity in disease severity and limiting inference regarding fibrosis-related morphological change. Third, the outcome was a single linear right-lobe measurement rather than true liver volume; linear dimensions may not fully represent three-dimensional liver size. Fourth, important clinical covariates (e.g., diabetes status, lipid profile, liver enzymes, medications, and fibrosis markers) were not available, limiting adjustment for confounding and severity. Finally, although exclusions were intended to reduce alternative causes of hepatomegaly, incomplete documentation is an inherent limitation of retrospective record review.

Future Directions

Prospective multicenter studies in Saudi Arabia should implement standardized ultrasound measurement protocols, document acquisition parameters, and evaluate reproducibility. Integrating elastography with laboratory markers would enable stratification by fibrosis stage and clarify the relationship between linear right-lobe measurements and disease severity. Larger datasets would also allow formal testing of interaction effects (e.g., sex-by-BMI) and development of adjusted reference ranges or prediction models tailored to regional NAFLD populations.[33,34] Where feasible, comparison with MRI- or CT-based volumetry could further validate ultrasound-derived size estimates and improve interpretability in clinical pathways.

Conclusion

In this retrospective two-center study of 212 adults with ultrasound-reported NAFLD in Jeddah, Saudi Arabia, ultrasound-derived right-lobe liver size showed measurable associations with patient characteristics. Mean right-lobe liver size was numerically higher in females than in males in both hospitals; however, sex differences were not statistically significant. Liver size showed a significant but weak correlation with weight and BMI and a weak inverse correlation with age. In multivariable analysis adjusting for sex, BMI, and hospital, age remained independently associated with liver size, whereas BMI did not remain statistically significant. No significant differences in mean liver size were observed between the two hospitals. These findings support the utility of routine ultrasound-based right-lobe measurements as a practical indicator that should be interpreted in the context of demographic and anthropometric factors, and they highlight the need for future multicenter prospective studies incorporating standardized acquisition protocols and objective NAFLD severity measures (e.g., elastography and laboratory markers) to refine clinical interpretation and risk stratification.

Ethical Considerations

The study was conducted in accordance with institutional policies and the Declaration of Helsinki. Ethical approval was obtained from the appropriate institutional review board, and a waiver of informed consent was requested due to the retrospective design and use of de-identified data.

Acknowledgements

First and foremost, we thank Allah for His countless blessings. We also express our sincere gratitude to the University of Jeddah and the College of Applied Medical Sciences for their support. We are especially grateful to Dr. Salem Alghamdi, Dr. Abdulrahman Taj Alden, and Dr. Elbagir Hamza for their valuable guidance and assistance. The authors also thank the technical personnel and staff of the ultrasound departments at all participating hospitals for their support in data collection. Finally, we extend our appreciation to Mr. Meshal Alotaibi for his assistance.

AI Statement

During the preparation of this manuscript, the authors used ChatGPT (OpenAI) for language editing and to articulate research insights effectively. All AI-assisted content was reviewed, verified, and revised by the authors, who take full responsibility for the accuracy, integrity, and final content of the manuscript.

Funding Statement

This work was funded by the Deanship of Research and Innovation at the University of Jeddah, Jeddah, Saudi Arabia, under grant No. UJ-22-DR-119.

Competing Interests

The authors declare that they have no conflicts of interest.

References

1. Demirturk Kocasarac H, Angelopoulos C. Ultrasound in Dentistry: Toward a Future of Radiation-Free Imaging. Dent Clin North Am. 2018 Jul;62(3):481-489. doi: 10.1016/j.cden.2018.03.007. PMID: 29903563.
2. Ribeiro R, Sanches J. Fatty liver characterization and classification by ultrasound. Lecture Notes in Computer Science. 2009: 354–361).
3. Azhari H. Ultrasound: medical imaging and beyond (an invited review). Curr Pharm Biotechnol. 2012 Sep;13(11):2104-16. doi: 10.2174/138920112802502033.
4. Wells PN. Physics and engineering: milestones in medicine. Med Eng Phys. 2001 Apr;23(3):147-53. doi: 10.1016/s1350-4533(01)00042-x. PMID: 11410379.
5. Said H. Principles of ultrasonography. J Natl Med Assoc. 1974 May;66(3):205-7, 231.
6. Rumack CM, Levine D. Published by Elsevier Enhanced Digital Version Copyright© 2024. Print ISBN: 9780323877954
7. Singh T, Singla B. Clinical and sonographic estimation of liver span in normal healthy adults. International Journal of Medical Research & Health Sciences. 2017; 6(1): 94-97.
8. Chaurasia BD. Human anatomy: regional and applied upper limb and thorax. CBS Publishers & Distributors. 1984.
9. Rosenfield AT, Laufer I, Schneider PB. The significance of a palpable liver. A correlation of clinical and radioisotope studies. Am J Roentgenol Radium Ther Nucl Med. 1974 Oct;122(2):313-7. doi: 10.2214/ajr.122.2.313.
10. Dorostghol M, Gharibvand MM, Hanafi MG, Motamedfar A. Comparison of size of the liver between patients with non-alcoholic fatty liver disease and healthy controls. J Family Med Prim Care. 2024 Feb;13(2):425-430. doi: 10.4103/jfmpc.jfmpc_94_23.
11. Petzold G. Role of Ultrasound Methods for the Assessment of NAFLD. J Clin Med. 2022 Aug 5;11(15):4581. doi: 10.3390/jcm11154581. PMID: 35956196; PMCID: PMC9369745.
12. European Association for the Study of the Liver (EASL); European Association for the Study of Diabetes (EASD); European Association for the Study of Obesity (EASO). EASL-EASD-EASO Clinical Practice Guidelines for the management of non-alcoholic fatty liver disease. J Hepatol. 2016 Jun;64(6):1388-402. doi: 10.1016/j.jhep.2015.11.004.
13. Simon TG, Roelstraete B, Khalili H, Hagström H,

Ludvigsson JF. Mortality in biopsy-confirmed nonalcoholic fatty liver disease: results from a nationwide cohort. Gut. 2021 Jul;70(7):1375-1382. doi: 10.1136/gutjnl-2020-322786.
14. Chalasani N, Younossi Z, Lavine JE, Charlton M, Cusi K, Rinella M, Harrison SA, Brunt EM, Sanyal AJ. The diagnosis and management of nonalcoholic fatty liver disease: Practice guidance from the American Association for the Study of Liver Diseases. Hepatology. 2018 Jan;67(1):328-357. doi: 10.1002/hep.29367. Epub 2017 Sep 29. PMID: 28714183.
15. Younossi ZM, Koenig AB, Abdelatif D, Fazel Y, Henry L, Wymer M. Global epidemiology of nonalcoholic fatty liver disease-Meta-analytic assessment of prevalence, incidence, and outcomes. Hepatology. 2016 Jul;64(1):73-84. doi: 10.1002/hep.28431. Epub 2016 Feb 22. PMID: 26707365.
16. Alswat K, Aljumah AA, Sanai FM, Abaalkhail F, Alghamdi M, Al Hamoudi WK, Al Khathlan A, Al Quraishi H, Al Rifai A, Al Zaabi M, Babatin MA, Estes C, Hashim A, Razavi H. Nonalcoholic fatty liver disease burden - Saudi Arabia and United Arab Emirates, 2017-2030. Saudi J Gastroenterol. 2018 Jul-Aug;24(4):211-219. doi: 10.4103/sjg.SJG_122_18. Erratum in: Saudi J Gastroenterol. 2018 Jul-Aug;24(4):255. doi: 10.4103/1319-3767.237645.
17. Alsabaani AA, Mahfouz AA, Awadalla NJ, Musa MJ, Al Humayed SM. Non-Alcoholic Fatty Liver Disease among Type-2 Diabetes Mellitus Patients in Abha City, South Western Saudi Arabia. Int J Environ Res Public Health. 2018 Nov 11;15(11):2521. doi: 10.3390/ijerph15112521.
18. Younossi ZM. Review article: current management of non-alcoholic fatty liver disease and non-alcoholic steatohepatitis. Aliment Pharmacol Ther. 2008 Jul;28(1):2-12. doi: 10.1111/j.1365-2036.2008.03710.x.
19. Tamaki N, Ajmera V, Loomba R. Non-invasive methods for imaging hepatic steatosis and their clinical importance in NAFLD. Nat Rev Endocrinol. 2022 Jan;18(1):55-66. doi: 10.1038/s41574-021-00584-0.
20. van Werven JR, Marsman HA, Nederveen AJ, Smits NJ, ten Kate FJ, van Gulik TM, Stoker J. Assessment of hepatic steatosis in patients undergoing liver resection: comparison of US, CT, T1-weighted dual-echo MR imaging, and point-resolved 1H MR spectroscopy. Radiology. 2010 Jul;256(1):159-68. doi: 10.1148/radiol.10091790.
21. Petzold G, Lasser J, Rühl J, Bremer SCB, Knoop RF, Ellenrieder V, et al. Diagnostic accuracy of B-Mode ultrasound and Hepatorenal Index for graduation of hepatic steatosis in patients with chronic liver disease. PLoS One. 2020 May 1;15(5):e0231044. doi: 10.1371/journal.pone.0231044.
22. de Moura Almeida A, Cotrim HP, Barbosa DB, de Athayde LG, Santos AS, Bitencourt AG, de Freitas LA, Rios A, Alves E. Fatty liver disease in severe obese patients: diagnostic value of abdominal ultrasound. World J Gastroenterol. 2008 Mar 7;14(9):1415-8. doi: 10.3748/wjg.14.1415.
23. Lee SS, Park SH, Kim HJ, Kim SY, Kim MY, Kim DY, Suh DJ, Kim KM, Bae MH, Lee JY, Lee SG, Yu ES. Non-invasive assessment of hepatic steatosis: prospective comparison of the accuracy of imaging examinations. J Hepatol. 2010 Apr;52(4):579-85. doi: 10.1016/j.jhep.2010.01.008.
24. Palmentieri B, de Sio I, La Mura V, Masarone M, Vecchione R, Bruno S, Torella R, Persico M. The role of bright liver echo pattern on ultrasound B-mode examination in the diagnosis of liver steatosis. Dig Liver Dis. 2006 Jul;38(7):485-9. doi: 10.1016/j.dld.2006.03.021.
25. Dogra VS, Rubens DJ. Ultrasound secrets. Elsevier Health Sciences, 2004.
26. Ferraioli G, Soares Monteiro LB. Ultrasound-based techniques for the diagnosis of liver steatosis. World J Gastroenterol. 2019 Oct 28;25(40):6053-6062. doi: 10.3748/wjg.v25.i40.6053. PMID: 31686762; PMCID: PMC6824276.
27. Kim SH, Lee JM, Kim JH, Kim KG, Han JK, Lee KH, et al. Appropriateness of a donor liver with respect to macrosteatosis: application of artificial neural networks to US images--initial experience. Radiology. 2005 Mar;234(3):793-803. doi: 10.1148/radiol.2343040142.
28. Hernaez R, Lazo M, Bonekamp S, Kamel I, Brancati FL, Guallar E, et al. Diagnostic accuracy and reliability of ultrasonography for the detection of fatty liver: a meta-analysis. Hepatology. 2011 Sep2;54(3):1082-1090. doi:10.1002/hep.24452.
29. Dasarathy S, Dasarathy J, Khiyami A, Joseph R, Lopez R, McCullough AJ. Validity of real time ultrasound in the diagnosis of hepatic steatosis: a prospective study. J Hepatol. 2009 Dec;51(6):1061-7. doi: 10.1016/j.jhep.2009.09.001. Epub 2009 Sep 20. PMID: 19846234; PMCID: PMC6136148.
30. Patell R, Dosi R, Joshi H, Sheth S, Shah P, Jasdanwala S. Non-Alcoholic Fatty Liver Disease (NAFLD) in Obesity. J Clin Diagn Res. 2014 Jan;8(1):62-6. doi: 10.7860/JCDR/2014/6691.3953.
31. Cruz JF, Cruz MA, Machado Neto J, de Santana DS, Oliveira CC, Lima SO. Prevalence and sonographic changes compatible with fatty liver disease in patients referred for abdominal ultrasound examination in Aracaju, SE. Radiol Bras. 2016 Jan-Feb;49(1):1-5. doi: 10.1590/0100-3984.2014.0124.
32. Kratzer W, Fritz V, Mason RA, Haenle MM, Kaechele V; Roemerstein Study Group. Factors affecting liver size: a sonographic survey of 2080 subjects. J Ultrasound Med. 2003 Nov;22(11):1155-61. doi: 10.7863/jum.2003.22.11.1155.
33. Ozturk A, Kumar V, Pierce TT, Li Q, Baikpour M, Rosado-Mendez I, et al. The Future Is Beyond Bright: The Evolving Role of Quantitative US for Fatty Liver Disease. Radiology. 2023 Nov;309(2):e223146. doi: 10.1148/radiol.223146. .
34. Fetzer DT, Pierce TT, Robbin ML, Cloutier G, Mufti A, Hall TJ, et al. US Quantification of Liver Fat: Past, Present, and Future. Radiographics. 2023 Jul;43(7):e220178. doi: 10.1148/rg.220178. PMID: 37289646.
35. Ballestri S, Romagnoli D, Nascimbeni F, Francica G, Lonardo A. Role of ultrasound in the diagnosis and treatment of nonalcoholic fatty liver disease and its complications. Expert Rev Gastroenterol Hepatol. 2015 May;9(5):603-27. doi: 10.1586/17474124.2015.1007955.
36. Mishra P, Younossi ZM. Abdominal ultrasound for diagnosis of nonalcoholic fatty liver disease (NAFLD). Am J Gastroenterol. 2007 Dec;102(12):2716-7. doi: 10.1111/j.1572-0241.2007.01520.x. PMID: 18042105.
37. European Association for the Study of the Liver (EASL); European Association for the Study of Diabetes (EASD); European Association for the Study of Obesity (EASO). EASL-EASD-EASO Clinical Practice Guidelines for the management of non-alcoholic fatty liver disease. J Hepatol. 2016 Jun;64(6):1388-402. doi: 10.1016/j.jhep.2015.11.004.
38. Chalasani N, Younossi Z, Lavine JE, Charlton M, Cusi K, Rinella M, et al. The diagnosis and management of nonalcoholic fatty liver disease: Practice guidance from the American Association for the Study of Liver Diseases. Hepatology. 2018 Jan;67(1):328-357. doi: 10.1002/hep.29367.

International Journal of Biomedicine 16(1) (2026) 71-77
http://dx.doi.org/10.21103/Article16(1)_OA9

ORIGINAL ARTICLE

Radiology

INTERNATIONAL JOURNAL OF BIOMEDICINE

Intrarenal Hemodynamic Alterations and Their Biochemical Correlates in Type 2 Diabetes: A Doppler Ultrasound Study

Marwa Mohammed Shareif Farah[1], Awadia Gareeballah[2*], Moawia Gameraddin[2], Marzoug Ahmed Ali Hussaun[3], Mogahid M. A. Zidan[4], Elrashid AbdElrahim[5], Raga Ahmed Abouraida[6], Amna Mohamed Ahmed[6], Nisreen Hassan[7], Ala M. A. Elgyoum[4]

[1]*Faculty of Radiology, College of Graduate Studies, Karary University, Khartoum, Sudan*
[2]*Department of Diagnostic Radiology, College of Applied Medical Sciences, Taibah University, Al-Madinah Al-Munawwarah, Kingdom of Saudi Arabia*
[3]*Al Mukhtar Hospital, Alhdyda, Yemen*
[4]*Faculty of Radiology and Nuclear Medicine Sciences, The National Ribat University, Khartoum, 11111, Sudan*
[5]*College of Applied Medical Sciences, Radiological Sciences Department, Taif University, Taif, Kingdom of Saudi Arabia*
[6]*Department of Radiological Sciences, College of Applied Medical Sciences, King Khalid University, Abha, Kingdom of Saudi Arabia*
[7]*AlGhad college For Applied Medical Sciences, Riyadh, Kingdom of Saudi Arabia*

Abstract

Background: Diabetic nephropathy (DN) is a major cause of chronic kidney disease (CKD) and end-stage renal disease worldwide. While biochemical markers such as blood urea nitrogen, serum creatinine, estimated glomerular filtration rate (eGFR), and albuminuria are routinely used, early and subclinical renal dysfunction may be missed. Renal Doppler ultrasound, particularly the resistive index (RI) and pulsatility index (PI), provides a noninvasive tool for assessing intrarenal hemodynamics. This study aimed to explore the association between common biochemical markers and renal Doppler ultrasound parameters in diabetic patients and to evaluate how factors such as glycemic control and disease duration influence these measures.
Methods and Results: A cross-sectional study was conducted on type 2 diabetes (T2D). Biochemical markers and Doppler indices were measured. Appropriate statistical tests were performed to examine relationships between biochemical and Doppler ultrasound findings. Of the 150 patients (mean age of 51.2±8.4 years), 41.3% had poor glycemic control (HbA1c > 8%). Both RI and PI exhibited significant negative correlations with eGFR (P<0.001) and significant positive correlations with blood urea and serum creatinine. RI and PI values were noticeably higher in patients with poorer glycemic control and longer duration of diabetes. Peak systolic velocity (PSV) and end-diastolic velocity (EDV) had no significant correlation with biochemical markers (P>0.05).
Conclusion: In patients with T2D, there is a strong correlation between biochemical markers of renal dysfunction and renal Doppler ultrasound parameters, particularly RI and PI. These parameters worsen with poor glycemic control and longer disease duration. (**International Journal of Biomedicine. 2026;16(1):71-77.**)

Keywords: diabetes • Doppler ultrasound • resistive index • pulsatility index • eGFR

For citation: Farah MMS, Gareeballah A, Gameraddin M, Hussaun MAA, Zidan MMA, AbdElrahim E, Abouraida RA, Ahmed AM, Hassan N, Elgyoum AMA. Intrarenal Hemodynamic Alterations and Their Biochemical Correlates in Type 2 Diabetes: A Doppler Ultrasound Study. International Journal of Biomedicine. 2025;16(1):71-77. doi:10.21103/Article16(1)_OA9

Key Points

• High intrarenal Doppler indices (RI, PI) correlate with worse eGFR stages and higher albuminuria in T2D patients.
• Poor glycemic control and longer duration of diabetes both predict more pronounced renal dysfunction on Doppler.
• Renal Doppler ultrasound holds promise as an adjunct tool for early detection and ongoing assessment of diabetic nephropathy.

Abbreviations

BMI, body mass index; **BUN**, blood urea nitrogen; **CKD**, chronic kidney disease; **DN**, diabetic nephropathy; **eGFR**, estimated glomerular filtration rate; **EDV**, end-diastolic velocity; **LK**, left kidney; **PSV**, peak systolic velocity; **PI**, pulsatility index; **RI**, resistive index; **RK**, right kidney; **T2D**, type 2 diabetes.

Introduction

Diabetes mellitus is becoming more common worldwide, which makes it a major health concern. Globally, there are currently 537 million people with diabetes mellitus. By 2045, that number is predicted to rise to 783 million.[1]Advanced age, obesity, unhealthy lifestyle choices like inactivity, and poor diet quality are all blamed for the rising incidence of disease. Countries with lower and middle incomes have a higher burden of disease.[2] In 2017, the estimated prevalence of diabetes mellitus in Africa was 3.3%, with Sudan being one of the nations with a prevalence of over 12%.[3] The most frequent causes of end-stage renal disease are diabetes. About 30% of people with diabetes develop diabetic nephropathy, one of the most common microvascular complications of the disease. One of the first indicators that diabetic nephropathy will develop is microalbuminuria.[4]

Renal ultrasonography and Doppler studies are non-invasive and are frequently used to measure kidney size, assess renal parenchymal echogenicity and vascular alterations, and rule out potential obstructive uropathy.[5] Renal Doppler imaging provides informative data on renal and intrarenal arterial flow. The renal resistive index (RI) and pulsatility index (PI), measured via non-invasive Doppler ultrasound, are considered valuable indicators for early detection of diabetic nephropathy (DN). These indices explore the blood flow resistance in the renal arteries.[6] Sugiura et al.[7] reported that an increase in renal RI has been linked with vascular lesions, tubulointerstitial damage, and glomerulosclerosis. The PI is another Doppler parameter that has not been extensively studied; most previous studies focused on RI alone. Studies conducted in Sudan have assessed Doppler imaging's utility for diagnosing diabetic nephropathy in patients with type 2 diabetes (T2D), but have not examined its correlation with other clinical and biochemical parameters. This study aimed to investigate the relationships between Doppler indices (RI, PI, PSV, and EDV) and clinical and biochemical parameters in patients with T2D, including body mass index (BMI), diabetes duration, albuminuria, HbA1C, and GFR. The outcomes of this study would aid early diagnosis and treatment of diabetic nephropathy and provide more thorough insight into its pathophysiology.

Materials and Methods

Study Design and Study Population

This hospital-based, cross-sectional study was conducted among adult diabetic patients from April 2021 to March 2023. The sample included adults aged 18 years or older with a known diagnosis of T2D and who attend diabetes or nephrology clinics in the study area. Any patient with congenital kidney abnormalities or other primary renal pathologies unrelated to diabetes and those with acute renal injury or ongoing use of nephrotoxic drugs that could confound renal function measurements were excluded. A convenience sample of 150 consecutive diabetic patients who met the inclusion criteria was enrolled.

Clinical and Demographic Data

The demographic and clinical data include age, sex, body mass index (BMI), Duration of diabetes mellitus, and Glycemic control as measured by hemoglobin A1c (HbA1c).

Biochemical Investigations

Blood Urea Nitrogen (BUN) and Serum Creatinine (Cr): Measured using automated methods in the hospital laboratory.

Estimated Glomerular Filtration Rate (eGFR): Calculated using the CKD-EPI equation.

Albuminuria: Classified as normoalbuminuria (<30 mg/day), microalbuminuria (30–300 mg/day), or macroalbuminuria (>300 mg/day).

Ultrasound Examinations

Grayscale and renal Doppler ultrasound were applied. For conventional B-mode ultrasound, the kidney dimensions (length, width, and parenchymal thickness) and cortico-medullary differentiation were assessed using a 3.5 MHz convex probe. Subsequently, intrarenal vessels (interlobar or arcuate arteries) were sampled to measure Doppler indices. The peak systolic velocity (PSV), end-diastolic velocity (EDV), and acceleration time (AT) were recorded (Figure 1). Normal RI was defined as ≤0.70; High RI was defined as >0.70, and normal PI was considered ≤1.1; High PI was defined as >1.1.

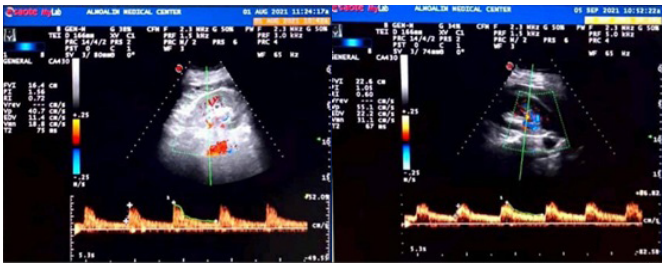

A B

Fig. 1. *Doppler ultrasound showing high (A) and normal (B) Resistive Index (RI) and Pulsatility Index (PI)*

Statistical Analysis

The data were analyzed using SPSS version 27 and the DATAtab online statistical calculator. In descriptive statistics, mean ± standard deviation (SD) and standard error of the mean (SEM) were used for continuous variables, and frequencies and percentages were used for categorical variables. Then the patients were stratified by eGFR stages (1–3), albuminuria categories (normo-, micro-, macroalbuminuria), glycemic control (HbA1c <7%, 7–8%, >8%), and diabetes duration (<5 years, 5–10 years, >10 years). Comparisons of means and Pearson's correlation were used to assess differences in gray-scale ultrasound parameters and Doppler indices across groups. Multiple comparisons were performed with one-way ANOVA and a post-hoc Tukey HSD test.The probability value of $P<0.05$ was considered statistically significant.

Results

A total of 150 adult T2D patients, with a mean age of 51.2 ± 8.4 years, were included in the study. Females slightly predominated (55.3%). Regarding diabetes duration, 62.7% were in the first 10 years, 25.3% in 11-20 years, and 12.3% in more than 20 years. (Table 1).

Table 1.

Baseline characteristics of the study patients.

Characters		Frequency	Percent
Age, years	30-40	23	15.3
	41-50	43	28.7
	51-60	84	56.0
Gender	Female	83	55.3
	Male	67	44.7
BMI	Underweight	19	12.7
	Normal	104	69.3
	Overweight	5	3.3
	Obese	22	14.7
T2D duration, years	0-10	94	62.7
	11-20	38	25.3
	More than 20	18	12.0
Total		150	100.0

Blood urea nitrogen (BUN) averaged 27.7±10.0 mg/dL. Serum creatinine averaged 0.90±0.33 mg/dL. Urine albumin levels averaged 25.5 ± 53.0 mg/dL, corresponding to normoalbuminuric in 82.0%, microalbuminuria in 14.7%, and macroalbuminuria in 3.3%. Based on eGFR, 64.0% of subjects were in Stage 1, 22.7% in Stage 2, and 13.3% in Stage 3 CKD. 41.3% of patients show poor glycemic control, and 55.3% show elevated BUN. (Table 2, Table 3).

Table 2.

Laboratory tests and biomarkers of the study patients.

Lab test and biomarkers	Categories	N	%
eGFR, mL/min/1.73 m²	Normal (More than 90)	96	64.0
	Stage two (60-89)	34	22.7
	Stage 3 (less than 60)	20	13.3
Albuminuria, mg/day	Normal (<30)	123	82.0
	Microalbuminuria (30-300)	22	14.7
	Macroalbuminuria (>300)	5	3.3
HbA1C, %	4-6 (excellent control)	19	12.7
	7-8 (Good control)	69	46
	> 8 (Poor)	62	41.3
Urea, mg/dL	Low	1	0.7
	Normal	66	44.0
	Elevated	83	55.3
Total		150	100.0

Table 3.

Descriptive statistics of Doppler indices in the study patients.

Parameters	Mean± SD
Age, years	51.25±8.43
BMI, kg/cm²	23.15±4.57
Duration of DM, years	11.02±7.52
Urea, mg/dL	27.72±10.23
Creatinine (cr), mg/dL	0.90±.33
eGFR, mL/min/1.73 m²	101.34±30.86
HbA1C, %	8.17±1.88
RK length, cm	10.02±.76
RK volume, cm³	147.72±43.21
R PSV, cm/sec	43.59±15.60
R EDV, cm/sec	13.72±6.64
R RI	0.70±.065
R PI	1.42±.33
R AT, msec	59.25±23.56
LK length, cm	10.11±.79
LK volume, cm³	158.02±44.45
L PSV, cm/sec	42.76±18.07
L EDV, cm/sec	13.40±5.38
L RI	0.69±.07
L PI	1.37±.30

R -right, L-left.

On Doppler assessment, the mean right RI was 0.69±0.06, and the left side was 0.68±0.06. The PI measures averaged 1.41±0.32 (right) and 1.36 ± 0.30 (left) (Table 3).

The RI and PI revealed significant positive correlations with biomarkers of renal function, such as urea and creatinine (for RI: r=0.498 and r=0.5 [RK] and r=0.488 and r=0.495 [LK], respectively (P<0.0001 in all cases), while for PI: r=0.508 and r=0.553 [RK] and r=0.481 and r=0.501 [LK], respectively, P<0.001 in all cases)). A significant negative correlation between the indices (RI, PI) and eGFR was observed in both kidneys (P<0.001). Furthermore, the age of T2D patients shows a weak positive correlation with Doppler PI and RI (Table 4, Figures 2 and 3). There was no significant correlation between PSV, AT, and the duration of T2D, urea, Cr, GFR, and HbA1C (Table 4).

Regarding the relationship between kidney gray-scale measurements in T2D with normal and decreased eGFR, it was found that as eGFR decreased, kidney size and volume decreased slightly. At the same time, PSV and AT slightly increased with each reduction in eGFR. These variations were insignificant. The parameters most affected by reduced kidney function were PI and RI, which were significantly higher in patients with eGFR<90 mL/min/1.73 m² than in those with eGFR ≥90 mL/min/1.73 m² (P<0.001) (Table 5).

The study found a weak positive linear association between RI and Cr (R^2=0.25 for both kidneys) (Figure 5), as well as between RI and urea (R^2=0.24 for RK and R^2=0.23 for LK) (Figure 6). There was an inverse weak linear association between GFR and RI in both kidneys (R^2=0.25 for LK and R^2=0.24 for RK) (Figure 7).

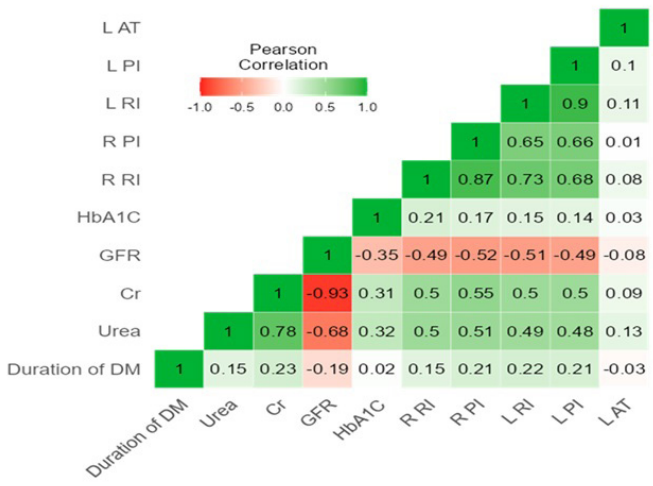

Fig.2. *Correlation heatmap to assess the relationship between duration, lap profile, and Doppler parameters in the T2D group.*

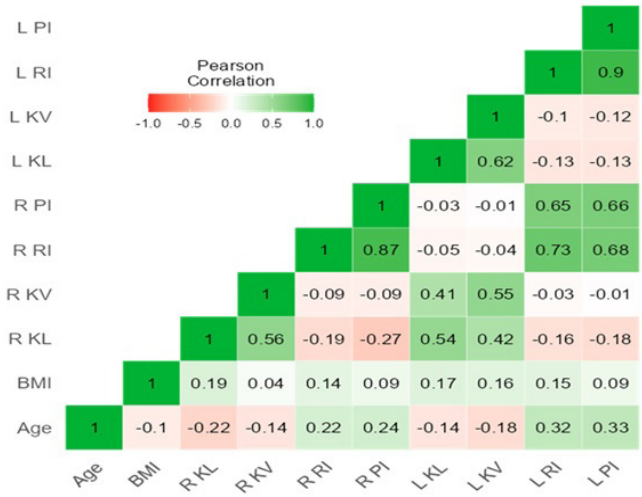

Fig.3. *Correlation heatmap to assess the relationship between gray-scale ultrasound and Doppler parameters in the T2D group.*

Table 4.

Results of the correlation analysis.

		Duration of T2D	Urea	Cr	GFR	HbA1C
R PSV	Pearson Correlation	-0.012	0.084	0.013	-0.010	0.093
	Sig. (2-tailed)	0.880	0.308	0.879	0.908	0.256
L PSV	Pearson Correlation	-0.132	-0.008	-0.068	0.035	0.000
	Sig. (2-tailed)	0.106	0.923	0.409	0.671	0.999
R RI	Pearson Correlation	0.150	**0.498**	**0.500**	**-0.489**	**0.205**
	Sig. (2-tailed)	0.067	<0.001	<0.001	<0.001	0.012
R PI	Pearson Correlation	**0.209**	**0.508**	**0.553**	**-0.524**	**0.174**
	Sig. (2-tailed)	0.010	<0.001	<0.001	<0.001	0.033
R AT	Pearson Correlation	-0.040	0.030	-0.009	0.023	0.010
	Sig. (2-tailed)	0.624	0.719	0.908	0.779	0.904
L RI	Pearson Correlation	**0.216**	**0.488**	**0.495**	**-0.507**	0.146
	Sig. (2-tailed)	0.008	<0.001	<0.001	<0.001	0.074
L PI	Pearson Correlation	**0.215**	**0.481**	**0.501**	**-0.490**	0.143
	Sig. (2-tailed)	0.008	<0.001	<0.001	<0.001	0.081
L AT	Pearson Correlation	-0.026	0.131	0.086	-0.078	0.029
	Sig. (2-tailed)	0.750	0.109	0.297	0.342	0.722

R – right, L – left, Weak Pearson correlation, Moderate Pearson correlation

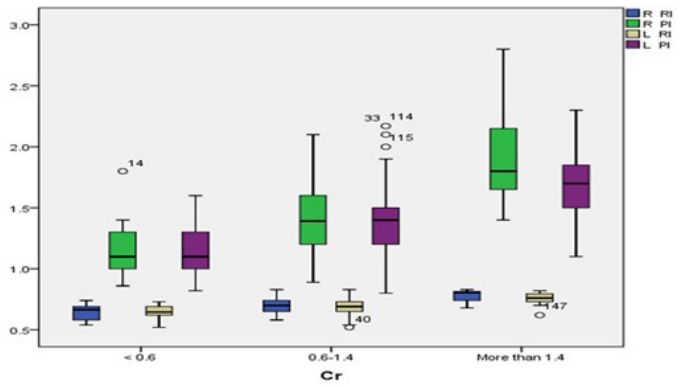

Fig. 4. *Plot box for comparing mean kidney measurements and Doppler indices among T2D patients with normal, low, and elevated Cr levels.*

Table 5.

Kidney measurements and Doppler indices in T2D patients with normal and low eGFR (mL/min/1.73 m²).

Parameters	eGFR	N	Mean	SD	SEM	*P*-value
RK length, cm	≥90	96	10.031	0.7624	0.0778	0.744
	<90	54	9.989	0.7615	0.1036	
RK volume, cm^3	≥90	96	146.876	46.0301	4.6979	0.740
	<90	54	149.206	38.0462	5.1774	
R PSV, cm/sec	≥90	96	43.304	14.9719	1.5281	0.771
	<90	54	44.106	16.7952	2.2855	
R RI	≥90	96	0.6822	0.06315	0.00645	<.001
	<90	54	0.7289	0.05881	0.00800	
R PI	≥90	96	1.3203	0.26431	0.02698	<.001
	<90	54	1.5898	0.35347	0.04810	
R AT, msec	≥90	96	58.90	23.468	2.395	0.810
	<90	54	59.87	23.928	3.256	
LK length, cm	≥90	96	10.169	0.8278	0.0845	0.199
	<90	54	10.002	0.7178	0.0977	
LK volume, cm^3	≥90	96	159.668	48.4076	4.9406	0.515
	<90	54	155.083	36.6076	4.9817	
L PSV, cm/sec	≥90	96	42.526	17.8538	1.8222	0.835
	<90	54	43.178	18.6090	2.5324	
L RI	≥90	96	0.6675	0.06209	0.00634	<0.001
	<90	54	0.7196	0.05798	0.00789	
L PI	≥90	96	1.2871	0.27132	0.02769	<0.001
	<90	54	1.5148	0.29908	0.04070	
L AT, msec	≥90	96	57.48	21.500	2.194	0.229
	<90	54	62.57	29.816	4.057	

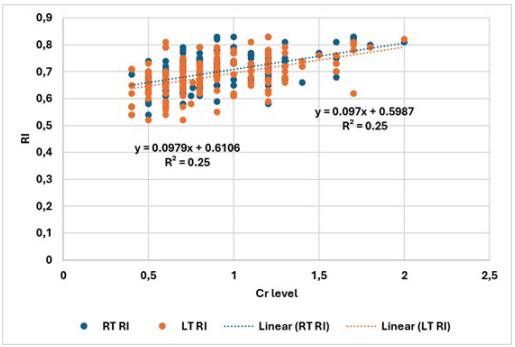

Fig. 5. *Relationship between RI and Cr level.*

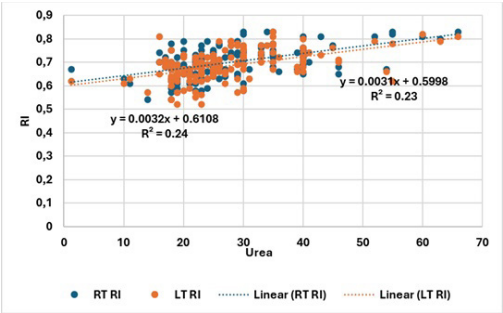

Fig. 6. *Relationship between RI and urea level.*

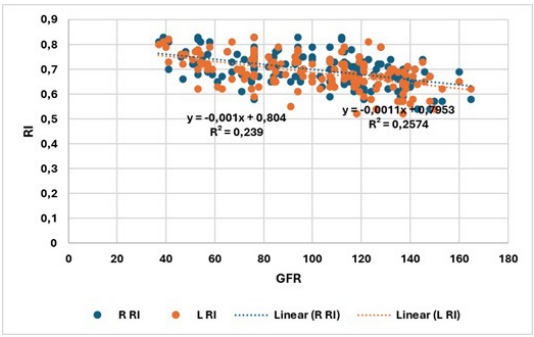

Fig. *7. Relationship between RI and eGFR.*

The study found that as albuminuria increased, Doppler RI and PI increased significantly (P<0.001 (Table 6).

Discussion

Numerous renal diseases, including obstructive kidney disease,[8] renovascular hypertension,[9] and parenchymal renal disease,[10] have been examined using Doppler imaging sonography. We noninvasively examined intrarenal hemodynamic changes in patients with T2D using sonography and Doppler imaging. It was found that T2D patients with nephropathy, characterized by elevated albuminuria and renal insufficiency, exhibited intrarenal hemodynamic alterations. Kidney diseases have been evaluated using the intrarenal RI and PI, measures of renal vascular alterations. Most previous studies used only RRI to evaluate renal artery flowmetry. The significance of this study is that it uses all Doppler parameters (RI, PI, PSV, EDV, and AT), which are associated with a faster decline in renal function.

Table 6.

Kidney measurements and Doppler indices among T2D patients with different albuminuria ranges.

Albuminuria		R RI	*P*-value	R PI	*P*-value	L RI		L PI	*P*-value
<30 mg/day n=123 [1]	Mean	0.68	F=43.8495 P=0.0000 P^{1-2}=0.0000 P^{1-3}=0.4259	1.34	F=25.2487 P=0.0000 P^{1-2}=0.0000 P^{1-3}=0.4483	0.67	F=40.2075 P=0.0000 P^{1-2}=0.0000 P^{1-3}=0.9081	1.30	F=30.9016 P=0.0000 P^{1-2}=0.0000 P^{1-3}=0.0991
	SD	0.05		0.29		0.05		0.25	
30-300 mg/day n=22 [2]	Mean	0.77		1.73		0.76		1.66	
	SD	0.04		0.25		0.04		0.25	
> 300 mg/day n=5 [3]	Mean	0.80		1.9		0.77		1.92	
	SD	0.04		0.32		0.03		0.35	
Total	Mean	0.70		1.42		0.67		1.37	
	SD	0.07		0.32		0.06		0.30	

The study found that the RI and PI of the renal arteries in diabetic patients correlated significantly with biomarkers of renal function, such as urea and creatinine. It was also observed that both RI and PI were negatively correlated with GFR. In agreement with this finding, a previous study reported that serum creatinine and HbA1c were statistically significantly positively correlated with both RI and PI.[11] Additionally, Khalifa reported that the RI had a significant positive correlation with albuminuria, urea, creatinine, and HbA1c.[5] Ishimura et al.[12] reported that RRI values were significantly affected by creatinine clearance and duration of DM. The changes in PI and RI indicate severe renal hemodynamic dysfunction. These changes are caused by advanced microvascular damage, decreased renal compliance, and increased vascular stiffness.[13]

The present study found a strong negative relationship between Doppler parameters (RI and PI) and eGFR in both kidneys. Consistently, Guarav et al. reported a significant inverse relationship between RRI and eGFR.[14] Soyoye et al.[15] also reported a negative relationship between eGFR and PI and RI. Both PI and RI were significantly elevated when eGFR<90 mL/min/1.73 m². This elevation in RI reflects intrarenal vascular resistance, indicating increased renal vascular resistance and microvascular alterations linked to diabetic nephropathy. This correlation may be used as an early objective indicator of renal impairment. Therefore, both PI and RI are helpful, non-invasive methods for tracking disease course and assessing risk in diabetic patients.

The other Doppler parameters, PSV and EDV, showed no significant association with eGFR in our study. In agreement with this finding, Chen et al. reported that eGFR was not significantly correlated with PSV or EDV.[16] They reported that the PSV increased significantly with CKD progression.

Some studies found moderate-to-strong correlations between PSV, EDV, and eGFR, whereas others reported no significant association.[17,18] This could be attributed to variations in patient populations, study methodologies, and the specific arteries measured (renal artery vs. intrarenal arteries). While renal artery PSV and EDV may be influenced by factors such as age and may not directly correlate with eGFR as intrarenal Doppler parameters do, some studies suggest that interlobar EDV is a powerful indicator of renal function.

Uncontrolled diabetes affects kidney vascularity and can be detected by elevated RI and PI. In this study, the RI and PI increased significantly with HbA1C, showing a positive linear correlation. In agreement with this finding, Sharma et al. reported that RI and PI exhibited a statistically significant positive connection with HbA1c.[11] Additionally, Miyoshi et al. reported a positive correlation of RI with HbA1c.[19] In contrast, Lotfinejad and Khan reported that RI was not significantly correlated with HbA1c.[20,21]

The study found significant positive correlations between T2D duration and PI, as well as between T2D duration and RI. Nasir et al.[22] also found a significant correlation between renal RI and T2D duration. Additionally, Youseff and Fawzy [23] reported that the increase in RI correlated significantly with the duration of DM.Most of these studies focused on the impact of renal RI rather than PI. However, our study found that PI has the same impact, and when used together, they could provide accurate results and a better evaluation of renal vascularity in diabetic patients.

The study found that the renal artery RI and PI increased significantly in patients with macroalbuminuria compared to those with microalbuminuria and no albuminuria, as reported by Hamano et al.[24] Consistent with our findings, they also found that the RI values were higher in DM patients with albuminuria than in those without albuminuria. Nosadini et al.[25] reported that increased renal RI can predict progression of renal function in T2D with microalbuminuria, even when GFR remains normal.

In general, this study supports the use of renal Doppler ultrasonography as a useful supplement to biochemical evaluation in DN. The consistent associations between RI and PI and indicators such as creatinine, urea, HbA1c, albuminuria, and eGFR highlight that kidney vascular alterations can be identified before any obvious biochemical decline. Together with data from earlier studies, these results suggest that incorporating Doppler parameters into clinical practice may improve the early detection of renal impairment, especially in patients with long disease duration or poor glycemic control. Renal Doppler assessment, when used in conjunction with standard laboratory testing, offers a more thorough understanding of the course of diabetic kidney disease and may help direct prompt interventions to reduce its burden.

This study has some limitations that should be considered. Firstly, the relationship between the biochemical markers and the Doppler indices might be affected by temporal changes and disease progression. In addition, the study was conducted at a single tertiary care center and used a convenience sample of 150 patients, which further limits the generalizability of the results. In addition, the potential confounding factors of co-existing hypertension, use of nephrotoxic drugs, and other microvascular changes may not be adequately controlled. Also, the inter- and intra-observer variability of Doppler measurements could affect the reproducibility of some results. Further longitudinal multi-center studies with larger, more representative, and more diverse populations are needed to generalize the study findings.

Conclusion

Our study highlights the significant correlations between biochemical markers of renal function (especially eGFR and albuminuria) and Doppler ultrasound findings (RI and PI) in diabetic patients. Poor glycemic control and longer disease duration are each linked to higher Doppler indices and worse biochemical profiles, underscoring the multifactorial nature of DN progression. These results support the adjunctive value of renal Doppler in early detection and monitoring of DN, encouraging clinicians to combine biochemical and Doppler imaging assessments to optimize patient outcomes.

Ethical Considerations

This study received ethical approval for publication from the Ethics Committee at College of Graduate Studies, Karary

University (Khartoum, Sudan). All participants received a clear explanation of the study's purpose and objectives and provided verbal approval to participate.

Availability of Data and Materials

The data of this study are available from the corresponding author upon a justifiable request.

Conflicts of Interest

The authors declare no conflict of interest in this study.

References

1. Forouhi NG, Wareham NJ. Epidemiology of diabetes. Medicine (Abingdon). 2014 Dec;42(12):698-702. doi: 10.1016/j.mpmed.2014.09.007.
2. Al-Jawaldeh A, Abbass MMS. Unhealthy Dietary Habits and Obesity: The Major Risk Factors Beyond Non-Communicable Diseases in the Eastern Mediterranean Region. Front Nutr. 2022 Mar 16;9:817808. doi: 10.3389/fnut.2022.817808. PMID: 35369054; PMCID: PMC8970016.
3. IDF diabetes atlas. 8th ed. Brussels: International Diabetes Federation; 2017 [cited 2025 Aug 30]. Available from: https://fmdiabetes.org/wp-content/uploads/2018/03/IDF-2017.pdf
4. Vedaraju KS, Benegal DS. Correlation of Renal Artery Resistive Index with Albuminuria and Other Risk Factors in Type 2 Diabetes Mellitus Patients. International Journal of Contemporary Medicine, Surgery and Radiology. 2019 Jan;4(1).
5. Khalifa AGM, Sweed I, Shalaby AI, El Alfy A. Renal Ultrasound and Renal Duplex Ultrasonography for Prediction of Diabetic Nephropathy in Correlation to Biochemical Markers & Glomerular Filtration Rate. The Egyptian Journal of Hospital Medicine. 2025 Apr 1;99(1):1744–50.
6. KCT, Das SK, Shetty MS. Renal Resistive Index: Revisited. Cureus. 2023 Mar 13;15(3):e36091. doi: 10.7759/cureus.36091.
7. Sugiura T, Nakamori A, Wada A, Fukuhara Y. Evaluation of tubulointerstitial injury by Doppler ultrasonography in glomerular diseases. Clin Nephrol. 2004 Feb;61(2):119-26. doi: 10.5414/cnp61119. PMID: 14989631.
8. Platt JF. Duplex Doppler evaluation of native kidney dysfunction: obstructive and nonobstructive disease. AJR Am J Roentgenol. 1992 May;158(5):1035-42. doi: 10.2214/ajr.158.5.1566663. PMID: 1566663.
9. Veglio F, Frascisco M, Melchio R, Provera E, Rabbia F, Oliva S, Chiandussi L. Assessment of renal resistance index after captopril test by Doppler in essential and renovascular hypertension. Kidney Int. 1995 Nov;48(5):1611-6. doi: 10.1038/ki.1995.455. PMID: 8544422.
10. Platt JF, Ellis JH, Rubin JM, DiPietro MA, Sedman AB. Intrarenal arterial Doppler sonography in patients with nonobstructive renal disease: correlation of resistive index with biopsy findings. AJR Am J Roentgenol. 1990 Jun;154(6):1223-7. doi: 10.2214/ajr.154.6.2110732.
11. Sharma K, Thakur MK, Mahela S, Konwar R, Varma D, Ullah IK, et al. Role of renal doppler ultrasonography in evaluating renal haemodynamics in diabetic patients and its correlation with laboratory parameters (serum HbA1C and serum creatinine). International Journal of Research in Medical Sciences. 2023 May 29;11(6):2174–80.
12. Ishimura E, Nishizawa Y, Kawagishi T, Okuno Y, Kogawa K, Fukumoto S, et al. Intrarenal hemodynamic abnormalities in diabetic nephropathy measured by duplex Doppler sonography. Kidney Int. 1997 Jun;51(6):1920-7. doi: 10.1038/ki.1997.261.
13. O'Neill WC. Renal resistive index: a case of mistaken identity. Hypertension. 2014 Nov;64(5):915-7. doi: 10.1161/HYPERTENSIONAHA.114.04183. Epub 2014 Aug 25. Erratum in: Hypertension. 2015 Aug;66(2):e9. doi: 10.1161/HYP.0000000000000032. PMID: 25156171.
14. Gaurav K, Yalavarthy U, Chamberlain N, Pugh S, Panda M. Correlation between Renal Resistive Index and Estimated Glomerular Filtration Rate in Patients with Hypertension. Journal for Vascular Ultrasound. 2008 Jun;32(2):82–4.
15. Soyoye DO, Dawha SD, Ayoola OO, Ibitoye BO, Ikem RT, Adedeji TA. Relationship between Renal Doppler Indices and Biochemical indices of Renal Function in Type 2 Diabetes Mellitus. West Afr J Med. 2018 Sep-Dec;35(3):189-194.
16. Chen Q, He F, Feng X, Luo Z, Zhang J, Zhang L, et al. Correlation of Doppler parameters with renal pathology: A study of 992 patients. Exp Ther Med. 2014 Feb;7(2):439-442. doi: 10.3892/etm.2013.1442.
17. Baz AA, Abdeen EM, Helmy MY, Al-Bohy AEM. Diagnostic utility of renal shear wave elastography and renal Doppler findings in diabetic nephropathy: a case–control study. Egyptian Journal of Radiology and Nuclear Medicine. 2024 Mar 15;55(1).
18. Abe M, Akaishi T, Miki T, Miki M, Funamizu Y, Araya K, et al. Influence of renal function and demographic data on intrarenal Doppler ultrasonography. PLoS One. 2019 Aug 27;14(8):e0221244. doi: 10.1371/journal.pone.0221244.
19. Miyoshi K, Okura T, Nagao T, Jotoku M, Enomoto D, Irita J, et al. HbA1c is an Independent Determinant of Renal Vascular Resistance Estimated by Doppler Sonography in Non-Diabetic Hypertensive Patients. Clinical medicine Endocrinology and diabetes. 2008 Jan;1:CMED.S936.
20. Lotfinejad M, Rashedi A, Amirkhanlou S. The Survey of Relationship Between Resistance Index of Renal Artery and Albuminuria in Diabetic Patients Referring to Shahid Sayyad Shirazi Hospital, 2017 to 2018. Iran J Kidney Dis. 2020 Sep;14(5):358-364. PMID: 32943590.
21. Khan A, Ahmed A, Bhutta MR, Zafar I, Khan MNN, Ehsan J. Correlation Between Resistive Index and Serum Creatinine in Patients with Diabetic Nephropathy. Pakistan Armed Forces Medical Journal. 2023 Apr 18;73(2):435–8.
22. Nasir M, Maryam S, Abdul Qadir S, Fatima M. Correlation Between Renal Artery Resistive Index and Renal Function Tests in Type II Diabetic Patients. Avicenna Journal of Health Sciences. 2024 Jul;1(3):62–6.
23. Youssef DM, Fawzy FM. Value of renal resistive index as an early marker of diabetic nephropathy in children with type-1 diabetes mellitus. Saudi J Kidney Dis Transpl. 2012 Sep;23(5):985-92. doi: 10.4103/1319-2442.100880.
24. Hamano K, Nitta A, Ohtake T, Kobayashi S. Associations of renal vascular resistance with albuminuria and other macroangiopathy in type 2 diabetic patients. Diabetes Care. 2008 Sep;31(9):1853-7. doi: 10.2337/dc08-0168. Epub 2008 Jun 19. PMID: 18566339; PMCID: PMC2518358.
25. Nosadini R, Velussi M, Brocco E, Abaterusso C, Carraro A, Piarulli F, et al. Increased renal arterial resistance predicts the course of renal function in type 2 diabetes with microalbuminuria. Diabetes. 2006 Jan;55(1):234-9.

***Corresponding author**: Dr. Awadia Gareeballah, E-mail: awadhia1978@gmail.com*

International Journal of Biomedicine 16(1) (2026) 78-82
http://dx.doi.org/10.21103/Article16(1)_OA10

ORIGINAL ARTICLE

Pediatrics

INTERNATIONAL JOURNAL OF BIOMEDICINE

Metabolic Biomarkers Behind Stunting: The Role of Serum Leptin and Adiponectin in Early Childhood Growth

Putriatri Krimasusini Senudin[1,2], Irwanto[3*], Nur Aisiyah Widjaja[3], Sulistiawati[4]

[1]*Doctoral Program of Medical Science, Faculty of Medicine, Universitas Airlangga, Surabaya, Indonesia*
[2]*Department of Midwifery, Faculty of Health Science, Universitas Katolik Indonesia Santu Paulus, Ruteng, Indonesia*
[3]*Department of Child Health, Faculty of Medicine, Universitas Airlangga, Dr. Soetomo General Academic Hospital, Surabaya, Indonesia*
[4]*Department of Public Health and Preventive Medicine, Faculty of Medicine, Universitas Airlangga, Surabaya, Indonesia*

Abstract

Background: Stunting is a nutritional problem that often affects children worldwide. Leptin and adiponectin are essential in modulating bone metabolism and, consequently, skeletal growth and height. This study aims to analyse leptin and adiponectin levels in stunted children and normal children and to determine the threshold values of leptin and adiponectin as early biomarkers of stunting.

Methods and Results: A case-control study was conducted in the working area of Kota Ruteng Primary Health Center Care, in Manggarai Regency, East Nusa Tenggara, Indonesia, from September to December 2024. The subjects were randomly selected from children aged 24-60 months. A total of 80 children, including 38 boys and 42 girls, were enrolled and divided into a stunting group (n=40) and a non-stunting group (n=40).

Multivariate analysis demonstrated that age 2–3 years, premature birth, low birth weight, and height were significant determinants of stunting, while leptin and adiponectin were independently associated with increased risk. ROC analysis showed that leptin had moderate discriminatory ability (AUC = 0.630; cut-off <2.18 ng/mL), whereas adiponectin yielded an AUC of 0.266 with a cut-off <29.5 ng/mL

Conclusion: Stunted children have higher leptin levels, and their height and adiponectin levels are lower than those of non-stunted children. Leptin and adiponectin levels can be used as early biomarkers of stunting.(**International Journal of Biomedicine. 2026;16(1):78-82.**)

Keywords: stunting • leptin • adiponectin • child growth • early childhood

For citation: Senudin PK, Irwanto, Widjaja NA, Sulistiawati. Metabolic Biomarkers Behind Stunting: The Role of Serum Leptin and Adiponectin in Early Childhood Growth. International Journal of Biomedicine. 2026;16(1):78-82. doi:10.21103/Article16(1)_OA10

Abbreviations

HAZ, height-for-age z-score; **LAZ**, length-for-age z-score; **LBW**, low birth weight.

Introduction

Infancy and childhood are periods of rapid growth, requiring a high intake of energy-rich foods. Inadequate food intake, both in terms of quality and quantity, leads to stunting.[1] Stunting has a severe impact on children's future, such as cognitive impairment, chronic diseases, and even mortality.[2] The causes of stunting are multifactorial, including malnutrition, infection, and chronic inflammation.[3]

In addition to growth hormone, adipokines (leptin and adiponectin) also influence child growth and development, energy regulation, and glucose homeostasis.[4] Leptin and adiponectin play a role in regulating metabolic function and growth rate in children, such as weight and height.[5] Most previous studies have examined the relationship between leptin and adiponectin and obesity, such as cohort studies in Korea,[6] Brazil,[7] and Spain.[8] Conversely, there is still little research evidence examining leptin and adiponectin in stunted children, such as in the Philippines[9] and Bangladesh,[10] in different populations, such as fetuses, one-month-old, and 6-month-old children, and the results are still controversial, so further research is needed.

Although adipokines such as leptin and adiponectin are known to influence growth, there is still a significant gap in understanding their specific relationship with stunting in children in underdeveloped areas. Most studies have focused on urban populations or developed countries, making research in rural and marginalized communities a priority, as stunting is most prevalent in these areas. Addressing this gap could provide valuable insights into preventing and managing stunting in vulnerable populations. The relationship between serum leptin and adiponectin levels and stunting in children aged 24–60 months is still poorly understood. Given their role in regulating metabolism and growth, these adipokines may be valuable biomarkers for predicting stunting. This study aims to explore the relationships among leptin, adiponectin, and stunting in children aged 24–60 months, and to identify the threshold values of leptin and adiponectin that can serve as predictive biomarkers for stunting.

Methods

Study Population

This study was a case-control study in children aged 24-60 months in the working area of the Kota Ruteng Primary Health Center Care, Manggarai, Indonesia, spread across eleven sub-districts (Laci, Carep, Compang Carep, Bangka Nekang, Karot, Mbaumuku, Pitak, Pocomal, Satar Tacik, Tadong, and Watu) from September to December 2024. The subjects were randomly selected, with a sample size of 80 (40 stunted and 40 normal children). The inclusion criteria for the case group in this study were: parents willing to serve as research respondents and children with a height-for-age z-score < -2SD. The inclusion criteria for the control group were parents willing to serve as research respondents and children with height-for-age z-scores ≥ -2SD. This study excluded children with parental heights (father and mother) ≤145 cm, children with congenital abnormalities, and children who were ill at the time of the study.

Anthropometric Measurements

Respondents' body weight was measured using a SECA 334 standing baby scale or a SECA 813 standing scale (Hamburg, Germany) and recorded in grams. Respondents' height/length was measured using a SECA 416 infantometer or SECA 213 stadiometer (Hamburg, Germany) and recorded in centimeters. HAZ/LAZ of each respondent was calculated based on height/length, using the WHO child growth standards. Stunting was determined if the HAZ/LAZ z-score was less than -2SD.

Blood Chemistry Measurements

Blood samples were collected and processed by a professional laboratory. 5 mL of venous blood was collected from respondents into EDTA tubes, centrifuged for 10 minutes at 4000 rpm, and immediately quenched. Aliquots were stored at -20°C until analysis. All biomarkers were analyzed using commercially available enzyme-linked immunosorbent assay (ELISA) kits from Diagnostic Biochem Canada (DBC) according to the manufacturer's instructions. Leptin ELISA Kit (CAN-L-4260, DBC, Inc., London, Canada) and adiponectin ELISA kit (CAN-APN-5000, DBC, Inc., London, Canada). Results were read using an ELSA microplate reader series 17539 in the Institute of Tropical Diseases, Airlangga University, Surabaya. Concentrations were calculated against standards for each biomarker.

Predictive Analytics Approach

To enhance the analytical value, logistic regression results and ROC curves were used to identify predictive thresholds for implementation in digital health dashboards or decision-support systems. The model's performance indicators (AUC, sensitivity, and specificity) were assessed to evaluate their potential for stunting risk classification.

Statistical analysis

Statistical analysis was performed using IBM SPSS version 20.0. The normality of the data distribution was tested using the Shapiro-Wilk test for continuous data (P>0.05). Baseline characteristics were summarized as frequencies and percentages for categorical variables and mean ± standard deviation (SD) for continuous variables. Bivariate analysis used the Chi-Square test or Fisher's Exact Test for categorical variables, while continuous variables used the independent t-test for normally distributed data or the Mann–Whitney U test for non-normal distributions. Variables with P-value < 0.25 at the bivariate stage were then entered into a multivariate logistic regression model. The probability value of P-value <0.05 was considered statistically significant. Receiver operating characteristic (ROC) curves were used to determine leptin and adiponectin cut-off values in predicting stunting.

Results

There were 80 children in total, 40 of whom experienced stunting and 40 healthy children, consisting of 38 boys and 42 girls. The characteristics of the respondents are summarized in Table 1. There was a difference in age between groups (P=0.000). Stunted children significantly had a history of premature birth (P=0.018) and low birth weight (P=0.002). As expected, stunted children experienced a significant decrease in body weight (10.56±1.92 vs. 14.18±2.11 kg; P=0.000) and a significantly shorter height (83.69±6.74 vs. 95.47±6.20 cm; P=0.000) compared to the control group. Leptin levels (2.234±1.978 vs 1.278 ± 0.928 ng/mL; P=0.045) were higher in stunted children than in controls. In contrast, compared to controls, adiponectin levels (26.822±10.194 vs 37.939±15.624 ng/mL; P=0.000) were lower in stunted children.

Table 1.

Demographic characteristics and biochemical parameters.

Characteristics	Group		*P*-value
	Stunting (n=40)	Normal (n=40)	
Age 2-3 years >3 – 5 years	 18 (45.0%) 22 (55.0%)	 19 (47.5%) 21 (52.5%)	0.000[a]
Birth History Premature Normal	 6 (15.0%) 34 (85.0%)	 0 40 (100.0%)	0.018[b]
Birth Weight LBW Normal	 10 (25.0%) 30 (75.0%)	 0 40 (100.0%)	0.002[b]
Body Weight, kg	10.56 ± 1.92	14.18 ± 2.11	0.000[c]
Height, cm	83.69 ± 6.74	95.47 ± 6.20	0.000[c]
Leptin (ng/mL)	2.234 ± 1.978	1.278 ± 0.928	0.045[c]
Adiponectin (ng/mL)	26.822 ± 10.194	37.939 ± 15.624	0.000[c]

[a] *Chi-square test;* [b] *Fisher's Exact Test;* [c] *Mann-Whitney U.*

The multivariate model was developed using the Forward Wald method. The Hosmer–Lemeshow goodness-of-fit test indicated that the model fit the data well (P=0.879). Multivariate logistic regression (Table 2) showed that children aged 2–3 years had a higher risk of stunting (OR=0.302; *P*=0.006), while premature birth remained a significant predictor (OR=0.455; *P*=0.001). Low birth weight indicated a tendency toward increased risk (OR=0.786; *P*=0.019), and height demonstrated a protective effect (OR=0.683; *P*=0.045). Leptin (OR=2.728; *P*=0.025) and adiponectin (OR=4.925; *P*=0.001) were both significantly associated with elevated stunting risk. These findings indicate that birth characteristics, anthropometric status, and metabolic biomarkers collectively influence stunting in children.

Table 2.

Logistic regression risk factor with stunting.

Variables	*P*-value	OR	95% CI	
			Lower	Upper
Age >3 – 5 years (Reff) 2-3 years	0.006	0.302	0.027	1.044
Birth History Normal (Reff) Premature	0.001	0.455	0.334	1.506
Birth Weight Normal (Reff) LBW	0.019	0.786	0.404	1.214
Body Weight, kg	0.991	1.0302	1.044	1.062
Height, cm	0.045	0.683	0.470	2.065
Leptin (ng/mL)	0.025	2.728	1.072	4.784
Adiponectin (ng/mL)	0.001	4.925	0,882	6.970

OR = Odds Ratio; CI = Confidence Interval.

Based on the area under the curve (AUC), leptin can predict stunting with an AUC of 0.630 (95% CI=0.509-0.0752). The cut-off value of leptin in detecting stunting is <2.18 ng/mL (sensitivity 37.5% and specificity 85.0%, *P*=0.045) (Figure 1). Based on the area under the curve (AUC), adiponectin can be predicted at 0.266 (95% CI=0.158-0.375). The cut-off value of adiponectin in detecting stunting is <29.5 ng/mL (sensitivity 32.5% and specificity 67.5%, *P*=0.000) (Figure 2).

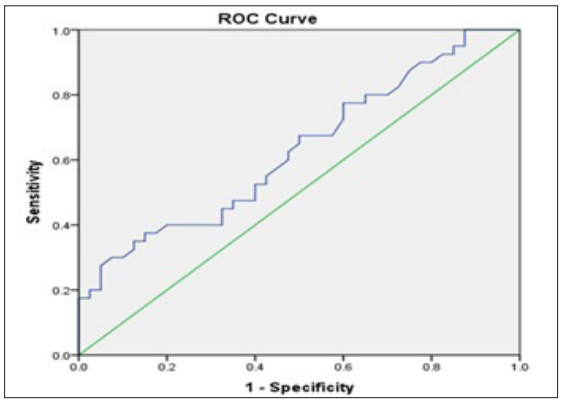

Figure 1. *The ROC curve for the diagnostic accuracy of leptin in detecting stunting.*

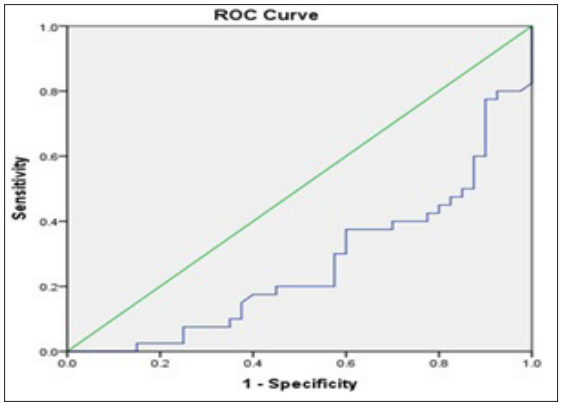

Figure 2. *The ROC curve for the diagnostic accuracy of adiponectin in detecting stunting.*

Discussion

Premature births and LBW children experience short stature in the first 5 years of life and experience a 10% decrease in height until adulthood. This is caused by abnormalities in growth hormones, such as insulin-like growth factor (IGF), and by the accumulation of network adipose tissue.[11] In addition, children with premature births will experience the phenomenon of catching up on growth in infancy, so that the accumulation of fat mass is faster than muscle mass in childhood.[12] Leptin circulation in the blood can regulate food intake and nutrient metabolism, impacting nutritional status. Leptin regulates glucogenesis and gluconeogenesis, maintains metabolic homeostasis, suppresses appetite, and increases energy expenditure.

Adequate, stable energy balance generally maintains healthy leptin levels. The average leptin levels of stunted children aged 6-8 years were higher than those of non-stunted children.[13,14] Our study supports this data, as leptin levels were higher in stunted children.

The cut-off value of leptin in stunted children was <2.18 ng/mL. This finding supports the evidence that low leptin levels are closely associated with impaired linear growth. The role of leptin in growth regulation is more complex than its function as an indicator of fat mass; it also acts as an energy-metabolism regulator and influences bone development, including the epiphyseal growth plate, which is essential for height gain.[15] A low cut-off value may reflect deficits in adipose tissue and energy reserves, conditions that can disrupt hormonal signaling required for linear growth and reduce the potential for catch-up growth in stunted children.[16] Therefore, future interventions aimed at improving leptin levels may contribute to more effective stunting prevention and management.

Adiponectin also plays a critical role in metabolic regulation, energy homeostasis, and the link between fat metabolism and bone health. Disruptions in fat oxidation are associated with an increased risk of fat accumulation, thereby increasing vulnerability to a high-fat diet among stunted adolescents.[17] Low-fat and energy intake during childhood can reduce growth factors, such as IGF hormones, and loss of fat mass can result in low adiponectin levels.[18]

The establishment of an adiponectin cut-off value of <29.5 ng/mL in the present study suggests that children aged 24–60 months with reduced adiponectin levels may be at increased risk of stunting. This relationship is biologically plausible, as adiponectin plays a central role in regulating energy homeostasis, insulin sensitivity, and lipid metabolism, all of which are integral to linear growth and bone tissue development. Lower circulating adiponectin may impair anabolic pathways involved in chondrocyte maturation, osteoblast activity, and overall skeletal growth, thereby contributing to growth faltering.[19,20] These findings support the potential use of adiponectin as an adjunctive biomarker for early identification of stunting risk. Incorporating adiponectin measurement into routine screening could complement conventional anthropometric assessment, particularly in regions with high stunting prevalence or in settings where standardized equipment for height and weight measurement is limited. This biomarker-based approach may enhance the detection of growth disturbances at earlier stages, allowing for more timely and targeted interventions.

The strengths of this study include its focus on a specific population of stunted children and its contribution of significant regional data to the worldwide literature on stunting. The strategic use of leptin and adiponectin as biomarkers is a reasonable approach to understanding the mechanisms underlying child stunting. Using ROC curves to find optimal cut-off values adds complexity, but, more importantly, ROC analysis helps identify the threshold that maximizes overall sensitivity and specificity. Meanwhile, this study also has several limitations. First, data collection in this study was conducted on a single occasion without a follow-up period, which can introduce bias in the observations because it cannot account for seasonal variations or changes in children's lifestyles over time. Observations conducted over a longer period can yield more representative results. Second, this study is a single-center study with a small sample size. It was also performed at a community health center. Finally, this study did not measure body fat mass in stunted children, so it cannot identify the causes and risk factors that affect leptin and adiponectin levels.

Conclusion

Leptin levels are significantly higher in stunted children, while adiponectin levels are considerably lower than in non-stunted children. Low adiponectin levels are more likely to stymie than high leptin levels. The findings demonstrate the potential to integrate leptin and adiponectin biomarker analysis into predictive-analytic frameworks for early stunting detection.

Funding

This study did not receive any specific grant from funding agencies in the public, commercial, or not-for-profit sectors.

Ethical Statement

This study received approval from the Health Research Ethics Committee of the Faculty of Medicine, Airlangga University, Surabaya, with No. Ref 203/EC/KEPK/FKUA/2024.

Competing Interests

The authors declare that they have no conflicts of interest.

References

1. Janawisuta H, Gunawan PH. Early Detection of Stunting in Indonesian Toddlers: A Machine Learning Approach. International Conference on Data Science and Its Applications. 2024;12–16. doi :10.1109/ICoDSA62899.2024.10651637
2. Montenegro CR, Gomez G, Hincapie O, Dvoretskiy S, DeWitt T, Gracia D, Misas JD. The pediatric global burden of stunting: Focus on Latin America. Lifestyle Medicine. 2022;3(3). doi: 10.1002/lim2.67
3. Hafid F, Nasrul N, Amsal A, Ramadhan K, Taufiqurahman T, Sariman S. Low Birth Weight, Child Gender, Number of Children, and Maternal Education as Risk Factors for Stunting in Palu City-Indonesia. Amerta Nutrition.2024;8(2SP):75–84. doi: 10.20473/amnt.v8i2SP.2024.75-84
4. Mantzoros CS, Rifas-Shiman SL, Williams CJ, Fargnoli JL, Kelesidis T, Gillman MW. Cord blood leptin and adiponectin as predictors of adiposity in children at 3 years of age: a prospective cohort study. Pediatrics. 2009 Feb;123(2):682-9. doi: 10.1542/peds.2008-0343. PMID:

19171638; PMCID: PMC2761663.
5. Aydin HI, Eser A, Kaygusuz I, Yildirim S, Celik T, Gunduz S, Kalman S. Adipokine, adropin and endothelin-1 levels in intrauterine growth restricted neonates and their mothers. J Perinat Med. 2016 Aug 1;44(6):669-76. doi: 10.1515/jpm-2014-0353. PMID: 26352058.
6. Park JE, Choi HJ, Kim IK, Lee HJ, Kang JH, Song J. Influence of serum leptin levels on future overweight risk in Korean children. Nutr Metab Cardiovasc Dis. 2012 Mar;22(3):260-8. doi: 10.1016/j.numecd.2010.08.010. Epub 2010 Dec 28. PMID: 21193296.
7. Diamond FB Jr, Cuthbertson D, Hanna S, Eichler D. Correlates of adiponectin and the leptin/adiponectin ratio in obese and non-obese children. J Pediatr Endocrinol Metab. 2004 Aug;17(8):1069-75. doi: 10.1515/jpem.2004.17.8.1069. PMID: 15379417.
8. Jois A, Navarro P, Ortega-Senovilla H, Gavela-Pérez T, Soriano-Guillén L, Garcés C. Relationship of high leptin levels with an adverse lipid and insulin profile in 6-8 year-old children in Spain. Nutr Metab Cardiovasc Dis. 2015 Dec;25(12):1111-6. doi: 10.1016/j.numecd.2015.09.005. Epub 2015 Sep 25. PMID: 26610652.
9. Park S, Vargas Z, Zhao A, Baltazar PI, Friedman JF, McDonald EA. Cord blood adiponectin and leptin are associated with a lower risk of stunting during infancy. Sci Rep. 2022 Sep 6;12(1):15122. doi: 10.1038/s41598-022-19463-3. PMID: 36068284; PMCID: PMC9448758.
10. Hossain M, Nahar B, Haque MA, Mondal D, Mahfuz M, Naila NN, Gazi MA, Hasan MM, Haque NMS, Haque R, Arndt MB, Walson JL, Ahmed T. Serum Adipokines, Growth Factors, and Cytokines Are Independently Associated with Stunting in Bangladeshi Children. Nutrients. 2019 Aug 7;11(8):1827. doi: 10.3390/nu11081827. PMID: 31394828; PMCID: PMC6723106.
11. Nakano Y. Adult-Onset Diseases in Low Birth Weight Infants: Association with Adipose Tissue Maldevelopment. J Atheroscler Thromb. 2020 May 1;27(5):397-405. doi: 10.5551/jat.RV17039. Epub 2019 Dec 20. PMID: 31866623; PMCID: PMC7242223.
12. Anam MS, Mexitalia M, Panunggal B, Sidhartani M, Rachmawati B, Subagio HW. Leptin levels in childhood tuberculosis and its correlation with body mass index, IFN-γ, and TNF-α in an Indonesian population. Indian J Tuberc. 2024 Jan;71(1):35-40. doi: 10.1016/j.ijtb.2023.03.012. Epub 2023 Mar 31. PMID: 38296389.
13. Ciptaninggita HD, Theodorean CF, Djais AA, Idrus E, Bachtiar EW. [Analisis Hubungan Antara Kadar Leptin pada Saliva Anak Usia 6-8 Tahun Dengan Status Stunting di NTT]. Univesitas Indonesia; 2022. Available at https://lib.ui.ac.id/detail?id=9999920517468&lokasi=lokal [Article in Indonesian].
14. Surmita S, Megawati G, Fatimah SN, Rakhmawati Y. [Indeks Massa Tubuh dan Massa Lemak serta Kadar Adiponektin Remaja Perawakan Pendek (Body Mass and Fat Mass Indexes and Adiponectin Levels of Stunting Adolescents)]. Indonesia Journal Human Nutrition. 2016 Dec 29; 3(2): 69–74. Doi: 10.21776/ub.ijhn.2016.003.02.2 [Article in Indonesian].
15. Eryando T, Sipahutar T, Budhiharsana MP, Siregar KN, Nur Aidi M, Minarto M, Utari DM, Rahmaniati M, Hendarwan H. Spatial analysis of stunting determinants in 514 Indonesian districts/cities: Implications for intervention and setting of priority. Geospat Health. 2022 May 17;17(1). doi: 10.4081/gh.2022.1055. PMID: 35579253.
16. Al Fatiah N, Ari Yuniastuti A, WH N, Lisdiana. Kadar Leptin Balita Stunting yang Diberi Makanan Tambahan Berbasis Daun Kelor dan Ikan Laut. *Life Science* .2024; 13(1): 35-43.
17. Hoffman DJ, Sawaya AL, Verreschi I, Tucker KL, Roberts SB. Why are nutritionally stunted children at increased risk of obesity? Studies of metabolic rate and fat oxidation in shantytown children from São Paulo, Brazil. Am J Clin Nutr. 2000 Sep;72(3):702-7. doi: 10.1093/ajcn/72.3.702. PMID: 10966887.
18. Brand C, Gaya ACA, Dias AF, Agostinis-Sobrinho C, Farinha JB, Boeno FP, Mota J, Reischak de Oliveira A, Gaya AR. Relationship between insulin resistance and adipocytokines: the mediator role of adiposity in children. Ann Hum Biol. 2020 May;47(3):244-249. doi: 10.1080/03014460.2020.1740320. Epub 2020 Apr 13. PMID: 32279531.
19. Kroll C, Farias DR, Kac G, de França PHC, Mastroeni MF. Adiponectin and leptin gene variants and their effects on body weight trajectories in children from birth to 6 years of age: the PREDI Study. Br J Nutr. 2021 Feb 14;125(3):241-250. doi: 10.1017/S0007114520002780. Epub 2020 Jul 22. PMID: 32693844.
20. Mexitalia M, Perdani P, Saputra E, Saputra GI. Cut-Off Levels of Insulin Like Growth Factor-1, Leptin and Adiponectin Umbilical Cord Blood in Low Birth Weight Babies. Medica Hospitalia Journal of Clinical Medicine. 2022;9(3):286–291. doi:10.36408/mhjcm.v9i3.765

***Corresponding author**: Prof. Irwanto, MD, PhD. E-mail: irwanto@fk.unair.ac.id*

International Journal of Biomedicine 16(1) (2026) 83-89
http://dx.doi.org/10.21103/Article16(1)_OA11

ORIGINAL ARTICLE

Pediatrics

INTERNATIONAL JOURNAL OF BIOMEDICINE

Associations of Childhood Overweight and Obesity with Sociodemographic Characteristics and Parental Chronic Health Conditions in Albania

Jolanda Hyska[1,2], Elida Peka[3], Dorina Toçi[2], Ervin Toçi[1*]

[1]*Department of Public Health, Faculty of Medicine, University of Medicine, Tirana, Albania*
[2]*Institute of Public Health, Tirana, Albania*
[3]*Department of Clinical Subject, Faculty of Medical and Technical Sciences, University of Medicine, Tirana, Albania*

Abstract

Background: Childhood overweight and obesity are major public health concerns, yet evidence on key sociodemographic and familial risk factors in Albania is limited. This study examined associations between overweight (including obesity) and sex, residence, parental education, and parental chronic health conditions among children aged 8–9 years.
Methods: Data were drawn from the nationally representative Assessment of Childhood Obesity and Impact of the COVID-19 Pandemic on the Daily Routine and Behaviors of School-Aged Children in Albania, conducted within WHO COSI Round 6. A one-stage stratified cluster sampling of primary schools was applied. Anthropometric measurements were collected, and parents reported chronic health conditions. Logistic regression analyses assessed associations between overweight/obesity and sociodemographic and parental health factors, adjusting for confounders.
Results: Among 3,058 children (50.3% boys; 62.6% urban), overweight prevalence was higher in boys, urban residents, and children of parents with medium or higher education. Parental chronic conditions, including hypertension, diabetes, and high cholesterol, were associated with increased odds of child overweight. Adjusted analyses confirmed male sex (OR=1.40), urban residence (OR=1.34), and parental multimorbidity (OR up to 1.47) as significant predictors.
Conclusion: Childhood overweight in Albania is shaped by sex, urbanization, parental education, and parental chronic health conditions, reflecting combined lifestyle, environmental, and intergenerational influences.(**International Journal of Biomedicine. 2026;16(1):83-89.**)

Keywords: cross-sectional study • parental multimorbidity • childhood overweight • urbanization

For citation: Hyska J, Peka E, Toçi D, Toçi E. Associations of Childhood Overweight and Obesity with Sociodemographic Characteristics and Parental Chronic Health Conditions in Albania. International Journal of Biomedicine. 2026;16(1):83-89. doi:10.21103/Article16(1)_OA11

Introduction

Childhood overweight and obesity represent one of the most serious and persistent public health challenges of the 21st century. Globally, the prevalence of excess body weight among children and adolescents has increased markedly over recent decades, reaching levels that justify its classification as a public health pandemic.[1-3]

In Europe, surveillance data consistently demonstrate high prevalence rates of childhood overweight and obesity, with only limited evidence of stabilization in some countries.[4,5] Data from the WHO European Childhood Obesity Surveillance Initiative (COSI) provide robust and comparable evidence on the magnitude and distribution of childhood overweight and obesity across the WHO European Region.[4] Findings from the sixth round of data collection (2022–2024) confirm that childhood overweight and obesity remain widespread, with substantial variation across countries and population subgroups, underscoring the need for sustained surveillance and targeted prevention strategies.[6] Importantly, COSI data

***Corresponding author**: Assoc. Prof. Ervin Toçi, MD, IMPH, PhD. E-mail: ervintoci@yahoo.com*

indicate that obesity-related inequalities emerge early in life and tend to persist over time, contributing to long-term health and socioeconomic burdens.

Sex differences constitute a well-established dimension of childhood obesity epidemiology. Across many European countries, boys exhibit higher prevalence rates of overweight and obesity compared with girls, although the magnitude and direction of these differences vary by context and age group.[4,5] Emerging evidence further suggests that gender-specific differences in dietary behaviors, physical activity, and sedentary lifestyles may contribute to these disparities.[7,8]

Place of residence represents another key determinant of childhood overweight and obesity. Numerous studies have documented significant rural–urban differences in obesity prevalence, physical activity, dietary patterns, and food security among children and adolescents.[9-12] In many settings, children residing in rural areas face a higher risk of overweight and obesity than their urban counterparts, potentially reflecting structural disadvantages related to access to healthy foods, opportunities for physical activity, and health-promoting environments.[13]

Socioeconomic position, particularly parental education, is among the most consistent predictors of childhood overweight and obesity. Lower parental educational attainment has been repeatedly associated with higher obesity prevalence among children across Europe and globally, reflecting inequalities in health literacy, dietary quality, and capacity to support healthy behaviors within the household.[2,4,14]

Beyond sociodemographic factors, increasing attention has been directed to the role of parental health status in shaping the risk of childhood obesity. Evidence suggests that parental chronic health conditions, including hypertension, diabetes, hypercholesterolemia, and metabolic syndrome, are associated with a higher likelihood of overweight and obesity in offspring, likely due to a combination of genetic susceptibility and shared environmental and behavioral factors.[15-19] Despite the growing international evidence base, comprehensive analyses examining the combined influence of sex, rural–urban residence, parental education, and parental chronic health conditions on childhood overweight and obesity remain limited in several countries, including Albania. Addressing this gap is essential to informing equitable, context-specific public health interventions.

The aim of the present study was therefore to examine the association between childhood overweight (including obesity) and key sociodemographic factors (sex, place of residence, and parental education level), as well as parental chronic health conditions (high blood pressure, diabetes, and high cholesterol), among Albanian children aged 8–9 years, using nationally representative data from the Assessment of Childhood Obesity and Impact of the COVID-19 Pandemic on the Daily Routine and Behaviors of School-Aged Children in Albania, conducted within the framework of the WHO European Childhood Obesity Surveillance Initiative (COSI). [6,20]

Methods

Participants

This study is a secondary, in-depth analysis of data derived from the Assessment of Childhood Obesity and the Impact of the COVID-19 Pandemic on the Daily Routine and Behaviors of School-Aged Children in Albania,[19] conducted within the framework of the WHO European Childhood Obesity Surveillance Initiative (COSI), Round 6, and implemented in accordance with a standardized protocol developed by the WHO Regional Office for Europe.[21]

The study population consisted of children attending the second and third grades of the nine-year compulsory education system in Albania. For the purposes of this analysis, only children aged 8.00–8.99 years were included, in line with the COSI protocol and to ensure comparability with previous survey rounds.[21] A one-stage stratified cluster sampling design was applied, with primary schools serving as the primary sampling units. Schools were stratified by region and selected with probability proportional to size. Within each participating school, one second-grade and one third-grade class were randomly selected.

Although anthropometric measurements were collected from a larger cohort during fieldwork, the final analytical sample included only children aged 8.00–8.99 years who were present on the day of measurement, whose parents or guardians provided informed consent, who had valid anthropometric measurements, and whose parents completed the questionnaire on chronic health conditions.

A detailed description of the COSI survey methodology as implemented in Albania is available elsewhere.[20]

Instruments

Data were collected using standardized instruments developed by the World Health Organization for the COSI study.[21] These instruments included a child record form, completed by trained examiners to collect anthropometric measurements, and a voluntary family questionnaire completed by parents or caregivers.

The family questionnaire collected information on child behavioral characteristics, as well as household sociodemographic and health characteristics, including parental education level and parental chronic health conditions (elevated blood pressure, diabetes, and high cholesterol). These variables constitute the primary exposures examined in the present analysis.

Procedure and study variables

Outcome variables: The primary outcome was child overweight, including obesity, defined using WHO body mass index (BMI)-for-age z-scores for children aged over 5 years. Overweight was defined as a BMI-for-age > +1 standard deviation (SD), and obesity as a BMI-for-age > +2 SD, in accordance with WHO growth references.[22,23] For analysis, overweight and obesity were combined into a single category.

Exposure variables: Sociodemographic characteristics of the children included sex, place of residence (urban/rural), and parental education level. Parental education was categorized as low (both parents with lower education), medium (one parent with lower education and one with higher education), or high (both parents with higher education). Lower education was defined as completion of primary education, lower secondary education, or upper secondary/post-secondary non-tertiary education, while higher education included short-

cycle tertiary, bachelor's, master's, or doctoral degrees. In single-parent households, parental education classification was based on the education level of the responding parent, in line with the COSI analytical framework.[24]

Statistical Analysis

Data were analyzed using SPSS software, version 21. Descriptive statistics were used to summarize the characteristics of participating children and their parents. Associations between child overweight (including obesity) and sociodemographic characteristics, as well as parental chronic health conditions, were examined using logistic regression analyses. Both crude (unadjusted) and multivariable-adjusted odds ratios (ORs) with 95% confidence intervals (CIs) were estimated. Statistical significance was defined as $P \leq 0.05$. A separate logistic regression analysis was conducted to identify predictors of overweight (including obesity) after excluding underweight children (n = 100; 3.2% of the total sample). In this restricted sample, both crude and multivariable-adjusted binary logistic regression models were applied to assess associations with (a) demographic and socioeconomic factors and (b) parental chronic health conditions.

Results

General Characteristics of Participants

Among the participating children, 50.3% were boys, and 62.6% had urban residence. More than two-thirds of parents (67.8%) had a high level of education, about 14% had a medium level of education, and 18.3% had a low level of education. The Prevalence of overweight (including obesity) was significantly higher among boys than girls (55.2% vs. 44.8%, respectively), among urban than rural residents (67.9% vs. 32.1%), and among children of low education parents (63%) compared to medium (16.4%) and high education level parents (20.6%) (Table 1).

The prevalence of parental high blood pressure, high cholesterol, and diabetes was 21%, 19.7% and 23.1%, respectively, with about 19% of parents having 1 chronic condition and 2-3 chronic conditions each. The prevalence of overweight was significantly higher among children of parents with high blood pressure, high cholesterol, diabetes, and 1 or more chronic conditions (Table 1).

Association of Overweight with Demographic and Socioeconomic Factors

In unadjusted logistic regression analyses (Table 2, upper panel), several demographic and socioeconomic characteristics were significantly associated with overweight (including obesity). Boys were 1.33 times more likely to be overweight compared with girls (OR=1.33, 95% CI: 1.14–1.55, $P<0.001$). Likewise, urban residence was associated with a 1.4-fold higher likelihood of being overweight compared with rural residence (OR=1.40, 95% CI: 1.19–1.64, $P<0.001$).

Medium and high parental education level was associated with a statistically significant increase in the likelihood of obesity by 1.42 and 1.33 times, respectively, compared to parents with a low level of education (OR=1.42, 95% CI: 1.12-1.79, $P=0.003$ and OR=1.33, 95% CI: 1.08-1.65, $P=0.008$, respectively).

Table 1.

Characteristics of participating children and their parents.

Variable	Total	Normal (N=2103)	Overweight (N=955)	*P*-value
Gender				
Boy	1537 (50.3)	1010 (65.7)*	527 (34.3)	<0.001
Girl	1521 (49.7)	1093 (71.9)	428 (28.1)	
Residence				
Urban	1913 (62.56)	1265 (66.1)	648 (33.9)	<0.001
Rural	1145 (37.44)	838 (73.2)	307 (26.8)	
Parental education				
Low	1817 (18.2)	1295 (71.3)	522 (28.7)	0.001
Medium	374 (14.0)	238 (63.6)	136 (36.4)	
High	489 (67.8)	318 (65.0)	171 (35.0)	
Parental high blood pressure				
No	2037 (79.0)	1434 (70.4)	603 (29.6)	0.007
Yes	542 (21.0)	348 (64.2)	194 (35.8)	
Parental high cholesterol				
No	2136 (80.3)	1513 (70.8)	623 (29.2)	<0.001
Yes	525 (19.7)	322 (61.3)	203 (38.7)	
Parental diabetes				
No	1983 (76.9)	1394 (70.3)	589 (29.7)	0.010
Yes	597 (23.1)	386 (64.7)	211 (35.3)	
Parental number of chronic conditions				
None	1528 (62.5)	1096 (71.7)	432 (28.3)	<0.001
1 condition	461 (18.9)	302 (65.5)	159 (34.5)	
2-3 conditions	455 (18.6)	284 (62.4)	171 (37.6)	

*Overweight (including obesity);*Numbers and row percentages (in parentheses). For the total, column percentages. Any discrepancy with the total number is due to missing data; P-value according to chi-square test. For a 2x2 table, the P-value according to Fisher's Exact Test.*

Table 2.

Association of overweight (including obesity) with demographic and socioeconomic characteristics of the children; crude (unadjusted) odds ratios (OR) from binary logistic regression models.

Upper panel: Crude (unadjusted) ORs			
Variable	OR*	95%CI*	*P**
Gender			
Boy	1.33	1.14-1.55	<0.001
Girl	1.00	reference	
Residence			
Urban	1.40	1.19-1.64	<0.001
Rural	1.00	reference	
Parental education			0.002 (2)†
Low	1.00	reference	-
Medium	1.42	1.12-1.79	0.003
High	1.33	1.08-1.65	0.008
Lower panel: Multivariable adjusted ORs			
Variable	OR*	95%CI*	*P**
Gender			
Boy	1.40	1.19-1.65	<0.001
Girl	1.00	reference	
Residence			
Urban	1.34	1.12-1.60	0.002
Rural	1.00	reference	
Parental education			0.002 (2)†
Low	1.00	reference	-
Medium	1.32	1.04-1.68	0.021
High	1.22	1.0.98-1.53	0.074

**Odds ratios (OR: overweight including obesity vs. normal weight), 95% confidence intervals (95%CIs) and P-values from binary logistic regression† Overall P-value and degrees of freedom (in parenthesis).*

After simultaneous adjustment for all demographic variables (gender, place of residence, and parental education), the associations remained largely consistent (Table 2, lower panel). Male gender remained a strong predictor (OR=1.40, 95% CI: 1.19–1.65, P<0.001), indicating a 40% increased likelihood of overweight/obesity among boys compared to girls. Urban residence continued to be significantly associated with overweight/obesity (OR=1.34, 95% CI: 1.12–1.60, P=0.002).

Regarding parental education, after adjusting for gender and place of residence, the association with obesity weakened slightly but remained statistically significant overall and for the medium education level, whereas it was only borderline significant for the high education level.

Association of Overweight with Parental Chronic Health Conditions

In the unadjusted models, overweight/obesity in children was significantly associated with several parental chronic health conditions (Table 3, upper panel). Children of parents with high blood pressure (OR=1.33, 95% CI: 1.09–1.62, P=0.006), high cholesterol (OR=1.30, 95% CI: 1.07–1.57, P=0.009), and diabetes (OR=1.53, 95% CI: 1.26–1.87, P<0.001) had significantly higher odds of being overweight.

Table 3.

Association of overweight (including obesity) with parental chronic health conditions of the children; crude (unadjusted) odds ratios (OR) from binary logistic regression models.

Upper panel: Crude (unadjusted) ORs			
Variable	OR*	95%CI*	P*
Parental high blood pressure			
No	1.00	reference	0.006
Yes	1.33	1.09-1.62	
Parental high cholesterol			
No	1.00	reference	0.009
Yes	1.29	1.07-1.57	
Parental diabetes			
No	1.00	reference	<0.001
Yes	1.53	1.26-1.87	
Parental number of chronic conditions			<0.001 (2)†
None	1.00	reference	-
1 condition	1.34	1.07-1.67	0.011
2-3 conditions	1.53	1.23-1.90	<0.001
Lower panel: Multivariable adjusted ORs			
Variable	OR*	95%CI*	P*
Parental high blood pressure			
No	1.00	reference	0.032
Yes	1.25	1.02-1.54	
Parental high cholesterol			
No	1.00	reference	0.018
Yes	1.27	1.04-1.55	
Parental diabetes			
No	1.00	reference	<0.001
Yes	1.51	1.24-1.86	
Parental number of chronic conditions			0.001 (2)†
None	1.00	reference	-
1 condition	1.29	1.03-1.61	0.029
2-3 conditions	1.47	1.18-1.85	0.001

**Odds ratios (OR: overweight including obesity vs. normal weight), 95% confidence intervals (95%CIs), and P-values from binary logistic regression.† Overall p-value and degrees of freedom (in parentheses).*

Moreover, a dose–response pattern was evident for the number of parental chronic health conditions: with increasing parental health conditions, the likelihood of being overweight increased significantly. Children whose parents had two or three chronic health conditions had 53% higher odds of overweight/obesity (OR=1.53, 95% CI: 1.23–1.90), while those with one condition had 34% higher odds (OR=1.34, 95% CI: 1.07–1.67), compared with children whose parents had no chronic health conditions (overall P<0.001).

After adjusting for the child's gender, residence, and parental education, all associations retained statistical significance but weakened slightly across all variables (Table 3, lower panel).

Discussion

This national cross-sectional study, conducted among a large sample of school-aged children in Albania, identified several key sociodemographic and parental health factors associated with childhood overweight and obesity. The results indicate that male sex and urban residence were associated with a significantly higher likelihood of being overweight compared with female sex and residence in rural areas. Furthermore, children whose parents had medium or high educational attainment showed a significantly increased likelihood of being overweight. Notably, parental chronic health conditions, including hypertension, hypercholesterolemia, diabetes, and multimorbidity, were each significantly associated with a higher likelihood of childhood overweight, and these associations remained robust after adjustment for sociodemographic confounders. Moreover, the association between childhood overweight and parental multimorbidity followed a graded pattern, with the likelihood of childhood overweight increasing significantly as the number of parental morbidities increased.

Our findings are consistent with a substantial body of international evidence. In particular, the higher risk of overweight observed among boys in our study aligns with well-documented global and European patterns. The WHO European Childhood Obesity Surveillance Initiative (COSI) has consistently reported a higher prevalence of overweight among boys compared with girls in 31 out of 37 participating countries, including Albania and several neighboring countries, such as Italy, Greece, Croatia, Montenegro, and North Macedonia, as well as other former communist countries like Poland and Romania.[6]

Earlier pooled analyses based on three rounds of COSI data collected between 2007 and 2013, covering more than 630,000 children aged 6–9 years across 21 European countries, also demonstrated that the prevalence of severe obesity was generally higher among boys than girls.[5] Similar sex-specific patterns have been confirmed in later analyses examining trends in childhood overweight and obesity across Europe between 2007 and 2017.[4]

At the global level, a recent systematic review and meta-analysis including data from 154 countries and over 45 million children and adolescents reported a significantly higher prevalence of obesity among boys than girls,[1] reinforcing

the robustness and consistency of this sex differential across regions and income levels.

The higher prevalence of overweight among boys observed in Albania and its concordance with international findings may reflect gendered patterns in lifestyle behaviors that are relatively consistent across countries. These include differences in physical activity, sedentary behaviors (e.g., screen time), dietary habits, and broader family lifestyle influences. For example, the global meta-analysis by Zhang et al.[1] reported higher levels of screen time and sedentary behavior among boys across several settings. Empirical evidence from Italy showed that boys are significantly more likely than girls to consume energy-dense foods such as commercial cookies.[7] Similarly, data from Germany indicated that although boys tend to be more physically active, girls score higher on multiple indicators of diet quality and nutrition habits.[8] Differences in dietary patterns persist into young adulthood, with a recent study among university students reporting significantly higher consumption of butter, red meat, sweetened beverages, and alcoholic beverages among men than among women.[25] Consistently, the COSI Round 6 report showed that, in most participating countries, boys consumed sugar-sweetened beverages more frequently than girls (more than three days per week).[6]

In addition to sex differences, we found that urban residence was significantly associated with childhood overweight, in line with evidence from several middle-income countries undergoing rapid nutritional and lifestyle transitions. Studies from Turkey, Serbia, and Romania have reported higher prevalences of childhood overweight and obesity in urban settings, coinciding with increased fast-food consumption and shifts away from traditional dietary patterns.[10-12] Urban environments are typically characterized by greater availability of calorie-dense foods, reduced opportunities for spontaneous physical activity, higher traffic density, and increased sedentary behavior.

Quantitative evidence supports these mechanisms: children spending two or more hours per day on computers had more than twofold the prevalence of obesity compared with those spending less than two hours per day (11.9% vs. 5.5%, respectively).[1] A cross-sectional study in India, including children aged 5–12 years, similarly reported higher obesity prevalence among boys and urban children, alongside higher consumption of sugary beverages and lower physical activity levels in urban areas.[9] Long-term global analyses have shown that overweight and obesity increase more rapidly in urbanized populations, largely due to the higher likelihood of exposure to obesogenic environments.[26-28]

While some studies from high-income countries such as the United States and Sweden report higher obesity prevalence in rural areas, these patterns are often explained by context-specific factors, including rural poverty and food insecurity.[13,29,30] In Albania, however, our findings suggest that the effects of urbanization currently outweigh the protective influence of traditional rural dietary patterns, which remain closer to home-prepared meals and Mediterranean-type diets.

Regarding parental education, our results indicate that higher parental education is associated with a higher likelihood of childhood overweight. This finding contrasts with evidence from most high-income countries, where lower parental education and socioeconomic status are well-established risk factors for childhood obesity.[13,29] However, our findings are consistent with reports from middle-income and transitioning countries, in which higher socioeconomic status, including education, is often associated with greater access to energy-dense diets and more sedentary lifestyles.[14] In such contexts, higher socioeconomic groups are typically the first to be exposed to obesogenic environments, before the burden gradually shifts toward lower socioeconomic groups as the obesity epidemic matures.[2,3]

The simultaneous association of male sex, urban residence, and higher parental education with childhood overweight in our study suggests a clustering of risk factors within more affluent households. This pattern is consistent with theoretical and empirical models of obesity transitions in developing and middle-income countries, in which high-SES groups are initially most affected by lifestyle and dietary changes associated with modernization and urbanization.[27,2] Finally, we observed significant associations between parental chronic conditions (diabetes, hypertension, and hypercholesterolemia) and childhood overweight. Moreover, the likelihood of childhood overweight increased with the number of parental comorbidities. These findings are consistent with previous studies demonstrating intergenerational clustering of cardiometabolic risk, mediated through shared genetic predisposition, common dietary patterns, physical inactivity, and broader household environments.[15-17] The coexistence of parental multimorbidity and childhood overweight may also reflect cumulative household-level stressors and lifestyle constraints, particularly in urban settings undergoing rapid socioeconomic change.[18,19]

Conclusions

Childhood overweight and obesity in Albania appear to be strongly influenced by multiple elements of the family environment. Specifically, male sex, urban residence, and higher parental education were associated with an increased likelihood of overweight among children. These findings suggest that lifestyle modernization, urbanization, and higher socioeconomic status are contributing significantly to the emerging obesity epidemic in this post-communist context. Furthermore, parental chronic health conditions were also associated with elevated risk of childhood overweight, indicating the complex interplay of genetic predisposition, shared lifestyle and behavioral patterns, and household environment.

Future research should prioritize longitudinal studies to elucidate causal pathways underlying these associations, with cohort designs being particularly appropriate. Complementary qualitative investigations are warranted to explore cultural perceptions and practices regarding diet, physical activity, and other lifestyle factors across diverse socioeconomic groups. Additionally, intervention studies, particularly those targeting families or high-risk geographic areas such as urban centers, are needed to evaluate the effectiveness of preventive strategies and mitigate the ongoing obesity epidemic in Albania.

Limitations of the Study

This study has several limitations. First, its cross-sectional design precludes establishing causal relationships. Second, parental chronic health conditions were self-reported, which may introduce information bias (e.g., recall bias or under-reporting); however, there is no evidence suggesting systematic misreporting. Third, important confounders beyond parental education were not adjusted for, suggesting that residual confounding may have influenced the observed associations.

Despite these limitations, this study also has notable strengths. It included a large sample size, thereby enhancing statistical power to detect true associations. Underweight children were excluded to enable a more focused analysis on overweight and obesity. Finally, adjustment for multiple confounding factors strengthened the validity of the identified predictors of childhood overweight.

Funding

The data used were obtained through the project Assessment of Childhood Obesity and Impact of the COVID-19 Pandemic on the Daily Routine and Behaviors of School-Aged Children in Albania, which was funded by the World Health Organization (WHO), UNICEF, and the Institute of Public Health, Albania.

Ethical Statement

The Assessment of Childhood Obesity and Impact of the COVID-19 Pandemic on the Daily Routine and Behaviors of School-Aged Children in Albania study was conducted in accordance with the International Ethical Guidelines for Biomedical Research Involving Human Subjects. Ethical approval for this national survey was granted by the Ethics Committee at the Ministry of Health and Social Protection (Decision No. 131/39, July 26, 2022).

Competing Interests

The authors declare that they have no competing interests.

References

1. Zhang X, Liu J, Ni Y, Yi C, Fang Y, Ning Q, et al. Global Prevalence of Overweight and Obesity in Children and Adolescents: A Systematic Review and Meta-Analysis. JAMA Pediatr. 2024 Aug 1;178(8):800-813. doi: 10.1001/jamapediatrics.2024.1576. PMID: 38856986; PMCID: PMC11165417.

2. Wang Y, Lim H. The global childhood obesity epidemic and the association between socio-economic status and childhood obesity. Int Rev Psychiatry. 2012 Jun;24(3):176-88. doi: 10.3109/09540261.2012.688195. PMID: 22724639; PMCID: PMC4561623.

3. Popkin BM, Adair LS, Ng SW. Global nutrition transition and the pandemic of obesity in developing countries. Nutr Rev. 2012 Jan;70(1):3-21. doi: 10.1111/j.1753-4887.2011.00456.x. PMID: 22221213; PMCID: PMC3257829.

4. Buoncristiano M, Spinelli A, Williams J, Nardone P, Rito AI, García-Solano M, Grøholt EK, Gutiérrez-González E, Klepp KI, Starc G, Petrauskienė A, Kunešová M, Hassapidou M, Pérez-Farinós N, Pudule I, Kelleher CC, Duleva V, Rakovac I, Chatterjee S, Breda J. Childhood overweight and obesity in Europe: Changes from 2007 to 2017. Obes Rev. 2021 Nov;22 Suppl 6:e13226. doi: 10.1111/obr.13226. Epub 2021 Aug 10. PMID: 34378305.

5. Spinelli A, Buoncristiano M, Kovacs VA, Yngve A, Spiroski I, Obreja G, Starc G, Pérez N, Rito AI, Kunešová M, Sant'Angelo VF, Meisfjord J, Bergh IH, Kelleher C, Yardim N, Pudule I, Petrauskiene A, Duleva V, Sjöberg A, Gualtieri A, Hassapidou M, Hyska J, Burazeri G, Petrescu CH, Heinen M, Takacs H, Zamrazilová H, Bosi TB, Sacchini E, Pagkalos I, Cucu A, Nardone P, Gately P, Williams J, Breda J. Prevalence of Severe Obesity among Primary School Children in 21 European Countries. Obes Facts. 2019;12(2):244-258. doi: 10.1159/000500436. Epub 2019 Apr 26. PMID: 31030201; PMCID: PMC6547273.

6. World Health Organization. WHO European Childhood Obesity Surveillance Initiative (COSI): Sixth Round Report 2022–2024. Copenhagen: WHO Regional Office for Europe; 2025

7. Silenzi A, Giona L, Zanchi G, Tammaro A, Monteleone V, D'Archivio M, Santangelo C, Masella R, Scazzocchio B, Varì R. Gender differences in eating habits and lifestyles of young students: observational evaluation from MaestraNatura program. Front Nutr. 2025 Nov 19;12:1653154. doi: 10.3389/fnut.2025.1653154. PMID: 41346677; PMCID: PMC12672309.

8. Bucksch J, Häußler A, Schneider K, Finne E, Schmidt K, Dadacynski K, Sudeck G. Physical activity and dietary habits of older children and adolescents in Germany - Cross-sectional results of the 2017/18 HBSC study and trends. J Health Monit. 2020 Sep 16;5(3):21-36. doi: 10.25646/6900. PMID: 35146271; PMCID: PMC8734148.

9. Pradeep P. Prevalence and risk factors of childhood obesity in urban and rural settings: a cross-sectional study. Int J Early Child Spec Educ. 2021;13:1125–1131

10. Pop TL, Maniu D, Rajka D, Lazea C, Cismaru G, Ştef A, Căinap SS. Prevalence of Underweight, Overweight and Obesity in School-Aged Children in the Urban Area of the Northwestern Part of Romania. Int J Environ Res Public Health. 2021 May 13;18(10):5176. doi: 10.3390/ijerph18105176. PMID: 34068152; PMCID: PMC8152956.

11. Marković L, Đorđić V, Trajković N, Božić P, Halaši S, Cvejić D, Ostojić SM. Childhood Obesity in Serbia on the Rise. Children (Basel). 2021 May 18;8(5):409. doi: 10.3390/children8050409. PMID: 34070022; PMCID: PMC8157883.

12. Yavuz CM. Prevalence and trends of overweight and obesity among children and adolescents in Turkey: A meta-analysis. Int J Hum Health Sci. 2023;7:20–30

13. Crouch E, Abshire DA, Wirth MD, Hung P, Benavidez GA. Rural-Urban Differences in Overweight and Obesity, Physical Activity, and Food Security Among Children and Adolescents. Prev Chronic Dis. 2023 Oct 19;20:E92. doi: 10.5888/pcd20.230136. PMID: 37857462; PMCID: PMC10599326.

14. Moradi G, Mostafavi F, Azadi N, Esmaeilnasab N, Ghaderi E. Socioeconomic Inequality in Childhood Obesity. J Res Health Sci. 2017 Aug 15;17(3):e00391. PMID: 28878109.
15. Liu J, Sekine M, Tatsuse T, Hamanishi S, Fujimura Y, Zheng X. Family history of hypertension and the risk of overweight in Japanese children: results from the Toyama Birth Cohort Study. J Epidemiol. 2014;24(4):304-11. doi: 10.2188/jea.je20130149. Epub 2014 May 24. PMID: 24857956; PMCID: PMC4074635.
16. Lee NY, Han K, Lee Y, Kim S, Lee S, Choi Y, et al. Association between Parent's Metabolic Syndrome and 12- to18-Year-Old Offspring's Overweight: Results from the Korea National Health and Nutrition Examination Survey (K-NHANES) 2009-2016. Int J Endocrinol. 2020 Oct 30;2020:8737912. doi: 10.1155/2020/8737912. PMID: 33178270; PMCID: PMC7648677.
17. Linares Segovia B, Gutiérrez Tinoco M, Izquierdo Arrizon A, Guízar Mendoza JM, Amador Licona N. Long-term consequences for offspring of paternal diabetes and metabolic syndrome. Exp Diabetes Res. 2012;2012:684562. doi: 10.1155/2012/684562. Epub 2012 Nov 5. PMID: 23193389; PMCID: PMC3501830.
18. Webber-Ritchey KJ, Habtezgi D, Wu X, Samek A. Examining the Association Between Parental Factors and Childhood Obesity. J Community Health Nurs. 2023 Apr-Jun;40(2):94-105. doi: 10.1080/07370016.2022.2125809. PMID: 36920112; PMCID: PMC10020867.
19. Wang Y, Min J, Khuri J, Li M. A Systematic Examination of the Association between Parental and Child Obesity across Countries. Adv Nutr. 2017 May 15;8(3):436-448. doi: 10.3945/an.116.013235. PMID: 28507009; PMCID: PMC5421118.
20. UNICEF Albania. Assessment of Childhood Obesity and Impact of the COVID-19 Pandemic on the Daily Routine and Behaviors of School-Aged Children in Albania. UNICEF; 2021
21. World Health Organization. WHO COSI Manual of Data Collection Procedures 2021–2023. WHO Regional Office for Europe; 2021
22. de Onis M, Onyango AW, Borghi E, Siyam A, Nishida C, Siekmann J. Development of a WHO growth reference for school-aged children and adolescents. Bull World Health Organ. 2007 Sep;85(9):660-7. doi: 10.2471/blt.07.043497. PMID: 18026621; PMCID: PMC2636412.
23. World Health Organization. WHO AnthroPlus for Personal Computers: Software for Assessing Growth of the World's Children and Adolescents. WHO; 2009
24. Ramos Salas X, Buoncristiano M, Williams J, Kebbe M, Spinelli A, Nardone P, et al. Parental Perceptions of Children's Weight Status in 22 Countries: The WHO European Childhood Obesity Surveillance Initiative: COSI 2015/2017. Obes Facts. 2021;14(6):658-674. doi: 10.1159/000517586. Epub 2021 Nov 5. PMID: 34818257; PMCID: PMC8739931.
25. Malara M, Widłak P, Tomczyk Ł. Gender differences in diet and health promoting nutrition among university students. Sci Rep. 2025 Nov 19;15(1):40778. doi: 10.1038/s41598-025-24604-5. PMID: 41257958; PMCID: PMC12630838.
26. Wang Y, Lobstein T. Worldwide trends in childhood overweight and obesity. Int J Pediatr Obes. 2006;1(1):11-25. doi: 10.1080/17477160600586747. PMID: 17902211.
27. Pirgon Ö, Aslan N. The Role of Urbanization in Childhood Obesity. J Clin Res Pediatr Endocrinol. 2015 Sep;7(3):163-7. doi: 10.4274/jcrpe.1984. PMID: 26831548; PMCID: PMC4677549.
28. Askari M, Heshmati J, Shahinfar H, Tripathi N, Daneshzad E. Ultra-processed food and the risk of overweight and obesity: a systematic review and meta-analysis of observational studies. Int J Obes (Lond). 2020 Oct;44(10):2080-2091. doi: 10.1038/s41366-020-00650-z. Epub 2020 Aug 14. PMID: 32796919.
29. Jonsson F, Goicolea I, San Sebastian M. Rural-urban differences in health among youth in northern Sweden: an outcome-wide epidemiological approach. Int J Circumpolar Health. 2019 Dec;78(1):1640015. doi: 10.1080/22423982.2019.1640015. PMID: 31282296; PMCID: PMC7595226.
30. Liang R, Goto R, Okubo Y, Rehkopf DH, Inoue K. Poverty and Childhood Obesity: Current Evidence and Methodologies for Future Research. Curr Obes Rep. 2025 Apr 11;14(1):33. doi: 10.1007/s13679-025-00627-x. PMID: 40210845; PMCID: PMC11985678.

International Journal of Biomedicine 16(1) (2026) 90-94
http://dx.doi.org/10.21103/Article16(1)_OA12

ORIGINAL ARTICLE

Pediatrics

INTERNATIONAL JOURNAL OF BIOMEDICINE

Pediatric High Body Mass Index and Urinary Tract Infections: The Clinical and Microbiological Association

Aseel S. Almallakhdeer[1], Safaa Mahmood Sultan[2], Ali Adel Shareef[1,3]

[1]*Department of Pediatrics, College of Medicine, Ninevah University, Mosul, Iraq*
[2]*Department of Community Health Techniques, Mosul Medical Technical Institute, Northern Technical University, Mosul, Iraq.*
[3]*Al-Khansaa Maternity and Children's Teaching Hospital, Mosul, Iraq*

Abstract

Background: Both increased body mass index (BMI) and urinary tract infections (UTI) are common pediatric problems. Being overweight or obese is a risk factor for pediatric UTI, but it has not been extensively studied. This study aimed to investigate the clinical and microbiological associations between overweight and obesity and UTI among hospitalized children.
Methods and Results: This cross-sectional analytical study involved hospitalized children at Al-Khansaa Pediatric Hospital in Mosul, northern Iraq. A total of 74 patients aged ≤15 years of both sexes were included in the study from October 2023 to September 2024. Upper UTI was documented by urine culture and ultrasonography. The mean age of patients was 6.88±4.49 years. Males accounted for 37.8%, females for 62.2%, and 77% of patients were from urban areas. Patients were divided into three groups based on BMI: normal weight, overweight, and obese. Most patients (43.2%) had a normal weight, 18.9% were overweight, and 37.8% were obese. Overweight and obesity were more prevalent among UTI children than among normal children, according to the current data (P=0.03 and P=0.000, respectively). *E. coli* was the main causative organism among the normal weight group (31%), while *Candida* species dominated among the overweight and obese groups (38% and 35%). There was increasing resistance to antibiotics with the increase in BMI among the obese group, with a significant Spearman correlation (R^2 =0.14, P=0.045).
Conclusion: According to this study, overweight and obesity are possible risk factors for pediatric UTI. Increases in BMI beyond the normal range shift the causative microorganisms of UTI from *E. coli* to *Candida* species and increase antibiotic resistance. (**International Journal of Biomedicine. 2026;16(1):90-94.**)

Keywords: children • obesity • overweight • urinary tract infection

For citation: Almallakhdeer AS, Sultan SM, Shareef AA. Pediatric High Body Mass Index and Urinary Tract Infections: The Clinical and Microbiological Association. International Journal of Biomedicine. 2026;16(1):90-94. doi:10.21103/Article16(1)_OA12

Introduction

Febrile UTI is a leading cause of doctor visits and hospitalizations in pediatric patients. Reports from meta-analyses of 36 studies published between 200 and 2021 documented a global prevalence of UTI of 16% among girls and 10% among boys aged <18 years, with *Escherichia coli* identified as the leading causative microorganism in up to 58% of cases.[1,2] On the other hand, it is also estimated that the global prevalence of pediatric overweight and obesity is considerably high in both sexes, with a pooled rate of 14.8% and 22.2%, respectively.[3] A much higher rate of childhood obesity (49.4%) was reported in the Middle East and North African countries.[4] In Iraq, higher than the global rates of pediatric UTI were observed in different regions, ranging from 14.7% in Baghdad school-aged children to as high as 43.3% in Erbil hospitalized children.[5,6] It has been reported that the prevalence of overweight and obesity in Iraq ranges from 11.14% and 11.74%, respectively, in Mosul to as high as 25.3% and 28.7% in Kirkuk.[7-9] Increased BMI is now considered a risk factor for UTI in the pediatric population, and such risk increases by 45% in some studies; furthermore, the odds ratio of overweight and obesity is approximately double among UTI children. Excess abdominal fat can put pressure on the bladder and urethra, impairing complete bladder emptying and causing urinary stasis, which creates an ideal environment for bacterial growth and increases the risk of UTI.[10,11] The habit of infrequent voiding and reduced

urinary tract flushing due to bacterial colonization among such children further contributes to the higher risk of UTI.[12] In addition to these, obesity contributes to chronic low-grade inflammation and alters the body's immune response.[13] Some studies also suggest that overweight and obesity may increase the incidence of vesicoureteral reflux, which acts as another risk factor for UTI among children.[14]

Methods

This cross-sectional analytical study involved hospitalized children at Al-Khansaa Pediatric Hospital in Mosul, northern Iraq. A total of 74 patients (28 males and 46 females) aged ≤15 years of both sexes were included in the study from October 2023 to September 2024. Upper UTI was documented by urine culture and ultrasonography.

In this study, the sample size was calculated based on the global average UTI prevalence (7%) at a 90% confidence level and a 5% margin of error. All patients were admitted to pediatric wards for management of fever, with or without urinary symptoms. Written parental consent was obtained for each participant. Patient demographic and clinical data were recorded using a specific questionnaire. The BMI for each patient was calculated and plotted on the appropriate Centers for Disease Control and Prevention (CDC) growth charts to determine the corresponding percentile. Participants with a BMI <5% were classified as underweight and excluded from the study; those with a BMI> 5% and <85% were classified as having normal BMI, ≥85% as overweight, and ≥95% as obese. A clean-catch midstream urine collection method was used for toilet-trained children, and a catheterized urine sample collection method was used for non-toilet-trained children. Urine cultures were performed and evaluated by a different person who was blinded to the patients' identities. Cystine-Lactose-Electrolyte Deficient (CLED) and Sabouraud Dextrose (SAD) agars were used to culture the urine samples and identify the causative microorganism. Every other patient diagnosed with UTI was selected in an alternate manner to ensure randomization.

Statistical analysis was performed using the statistical software package SPSS version 27.0 (SPSS Inc, Armonk, NY: IBM Corp). Chi-square and two proportions Z test, and Spearman correlation tests were used for statistical analysis. A significant *P*-value was set at ≤0.05.

Results

The mean age of patients was 6.88±4.49 years. Males accounted for 37.8%, females for 62.2%, and 77% of patients were from urban areas. Patients were divided into three groups based on BMI: normal weight (43.2%), overweight (18.9%), and obese (37.8%) (Table 1).

Regarding the clinical manifestations of UTI, a significantly higher number of normal weight children, 23(71.8%), were complaining of dysuria, while decreased food intake was more common among obese children, 21(75%), than among the other groups (Table 2). The three groups did not show a significant difference with the other clinical manifestations of UTI, like abdominal pain, fever, and vomiting, as well as being an uncircumcised male. On the other hand, the three groups did not show significant differences in the microscopic examination of urine with respect to the number of WBC or viable bacteria per high-power field (HPF).

Table 1.

Baseline characteristics of the study patients.

Variable		Patients (n=74)
Mean age (years)		6.88 ±4.49
Gender	Male	28 (37.8%)
	Female	46 (62.2%)
Residence	Urban	57 (77.0%)
	Rural	17 (33.0%)
BMI	Normal weight	32 (43.2%)
	Overweight	14 (18.9%)
	Obese	28 (37.8%)

Table 2.

Clinical and laboratory features among the three groups [n(%)]

Variable		Normal weight (n= 32)	Over-weight (n=14)	Obese (n=28)	*P*-value
Clinical features	Abdominal pain	22 (68.7)	13 (93)	25 (89.2)	0.59
	Dysuria	23 (71.8)	9 (64.3)	8 (28.5)	0.002
	Fever	26 (31.25)	12 (85.7)	25 (89.2)	0.86
	Nausea	7 (21.8)	7 (50)	9 (32.1)	0.16
	Vomiting	17 (53.1)	7 (50)	7 (25)	0.07
	Low appetite	9 (28.1)	2 (14.3)	21 (75)	0.000
	Uncircum-cised male	11 (34.4)	3 (21.4)	13 (46.4)	0.27
≥ 5 Pus cells per HPF on GUE	Positive	24 (75)	10 (71.4)	24 (85.7)	0.47
	Negative	8 (25)	4 (28.5)	4 (14.3)	
Bacteria on GUE	Positive	27 (84.4)	11 (78.6)	18 (64.3)	0.18
	Negative	5 (15.6)	3 (21.4)	10 (35.7)	

Figure 1 shows the results of urine culture among the three groups. It is clear that *E.coli* followed by *Staphylococcus* species were the most frequent among normal weight patients in a frequency of 31% and 25% respectively, while among overweight children, *Candida* species followed by *Staphylococcus* species were the most frequent (38% and 31%, respectively), however *Candida* species followed *E.coli* were most frequent among obese group (35% and 31%). *Candida* species become the dominant causative microorganisms when BMI exceeds the normal range.

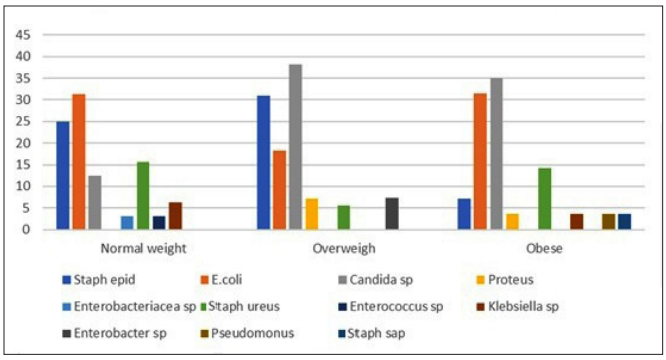

Fig. 1. *Results of urine culture.*

The sensitivity results (Figure 2) showed that amikacin, followed by nitrofurantoin and nalidixic acid, had the highest sensitivity rates among normal-weight children as antibacterial agents, and nystatin, followed by itraconazole and fluconazole, as antifungal agents (62%, 59%,35%, 59%, 47% and 31%, respectively). The same order of antibiotic sensitivity, with lower frequencies, is observed in the overweight group. This pattern differs in the obese children group, with the order shifting to meropenem, followed by amikacin and ciprofloxacin (50%, 47%, and 25%, respectively) as antibacterial agents, whereas the antifungal agents shift to miconazole, followed by nystatin and ketoconazole (52%, 49% and 48%, respectively). When we examined the correlation between increased BMI percentile and the number of antibiotics to which resistance was detected on urine culture, only the obese group showed a significant Spearman correlation (R^2 =0.14, *P*=0.045) (Figure 3). A higher BMI in this group is associated with a greater number of such antibiotics.

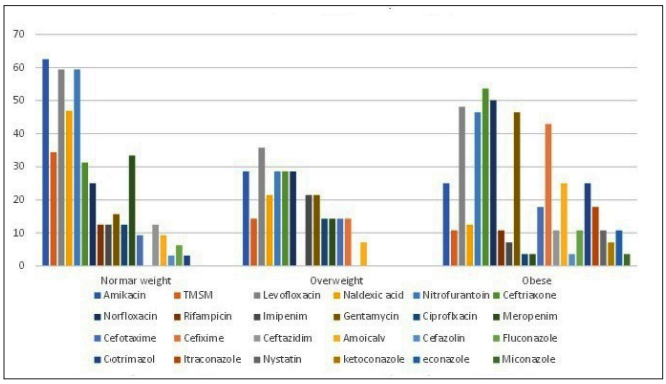

Fig. 2. *Antibiotic sensitivity on urine culture.*

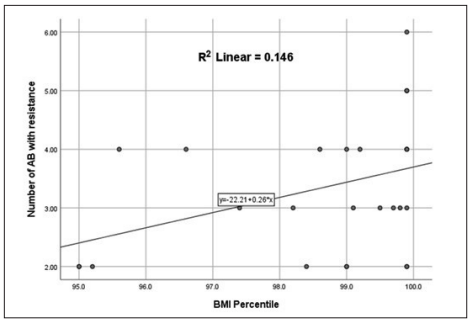

Fig. 3. *Correlation of BMI with the number of AB with resistant action among obese children.*

Discussion

Pediatric overweight, obesity, and UTI are relatively common and challenging problems for the health institutes and medical care providers everywhere in the world. According to the current literature reports, about one-fifth of the pediatric population suffers from either overweight or obesity.[3,15] Recently, Alqishawi et al. reported a prevalence of overweight and obesity in children aged 2-18 years in Mosul city as 11.14 and 11.74, respectively.[8] Using two proportion Z tests, we found that there was a significantly higher prevalence of overweight and obesity among our sample children with UTI (*P*=0.034 and *P*=0.000, respectively), supporting our hypothesis that there is an association between these two types of pediatric morbidities. We believe that the pelvic muscle dysfunction due to the increased intra-abdominal pressure in overweight and obese children will predispose them to urination problems and consequently increase the risk of UTI. In addition to that, there are many studies about the association of obesity with the malfunction of the body's immune system to explain the increased risk of infections, including UTI, among obese and overweight children. Elevated TNF-α and leptin levels, and a disrupted infection-related immune response in macrophages, monocytes, and lymphocytes, are likely responsible for the increased risk.[16] As in this study, Yang et al.[17] reported a high odds ratio for obesity in their sample of children with UTI.It has been reported that obese patients experience UTI symptoms more frequently than normal-weight individuals.[18] The current study did not show a significant difference in symptoms, except for a lower appetite level among obese patients than among the normal weight group (*P*=0.000), who experienced a higher frequency of dysuria than the other groups (*P*=0.002). It is well established that obesity is characterized by a chronic inflammatory state, with elevated baseline levels of the cytokines TNF-α and IL-6, as well as the cytokine-like substance leptin, and by a marked surge during infections. These cytokines have appetite-suppressing effects.[19,20] It is also reported that obese adult patients may have more severe UTIs than normal subjects, which might be an additional reason for such a lower appetite level. The chronicity of bladder inflammation and higher frequency of overactive bladder, and possible resultant reduction in pain sensation, may explain the lower frequency of dysuria among overweight and obese patients with UTIs.[21]

A variety of studies across pediatric age groups have established that *E. coli* is the leading cause of UTI, accounting for one-half to three-quarters of such infections.[22,23] Studies of Iraqi children also reported similar findings.[24,25] The current study results are the same for the normal weight group. The reason is that *E. coli* is the most common gut flora and possesses characteristics that enable it to colonize the urinary tract and exhibit specialized virulence traits.[26] Although not statistically significant (*P*=0.07), *Candida* species were the dominant organisms among overweight and obese children (38% and 35%, respectively) compared with the normal-weight group (12.5%) in this study. It has been reported that being overweight and obese are both risk factors for fungal infections due to an altered body immunity and associated

hyperglycemia, but we couldn't find such a study to support that for UTI in children.[27,28]

Generally, the antibiotic resistance and sensitivity patterns also showed special characteristics in association with an increase in the BMI, specifically among the obese group. Correlations showed that there is a significant increase in the number of ineffective antibiotics as the BMI increases in the obese group (P=0.045). The pharmacokinetics of antibiotics, particularly hydrophilic agents such as aminoglycosides and β-lactams, are significantly altered by high BMI and increased blood volume, resulting in more diluted and less effective concentrations in the circulation. It has also been noted that obesity alters the body's immune function in response to infections.[29,30] Although many adult studies report results consistent with ours, studies in pediatric age groups are scarce.[31-34] However, pediatric studies linking antibiotic resistance with abnormally high BMI support our findings.[35]

In conclusion, the frequency of being overweight and obese is significantly higher among children with UTI than among those who do not have UTI. Interestingly, this study reports that high BMI is associated with an increased risk for fungal UTI and increased resistance to antibiotics.

Competing Interests

The authors declare that they have no conflicts of interest.

References

1. Jamshidbeigi T, Adibi A, Hashemipour SMA, Sarokhani D, Hasanpour Dehkordi A, Fakhri M, Alaienezhad S. A systematic review and meta-analysis of prevalence of urinary tract infection in childhood. J Renal Inj Prev. 2023; 12(4): e32160. doi: 10.34172/jrip.2023.32160.
2. Agrawal P, Paunikar VM. Urinary Tract Infection in Children: A Narrative Review. Cureus. 2024 Jan 1;16(1):e51469. doi: 10.7759/cureus.51469. PMID: 38298274; PMCID: PMC10828737.
3. Zhang X, Liu J, Ni Y, Yi C, Fang Y, Ning Q, Shen B, Zhang K, Liu Y, Yang L, Li K, Liu Y, Huang R, Li Z. Global Prevalence of Overweight and Obesity in Children and Adolescents: A Systematic Review and Meta-Analysis. JAMA Pediatr. 2024 Aug 1;178(8):800-813. doi: 10.1001/jamapediatrics.2024.1576. PMID: 38856986; PMCID: PMC11165417.
4. Alruwaili BF, Bayyumi DF, Alruwaili OS, Alsadun RS, Alanazi AS, Hadi A, Alruwaili NKS, Thirunavukkarasu A, Aldaghmani NF, Alrayes AA. Prevalence and Determinants of Obesity and Overweight Among Children and Adolescents in the Middle East and North African Countries: An Updated Systematic Review. Diabetes Metab Syndr Obes. 2024 May 21;17:2095-2103. doi: 10.2147/DMSO.S458003. PMID: 38799280; PMCID: PMC11127655.
5. Saeed CH, AL-Otraqchi KIB, Mansoor IY. Prevalence of urinary tract infections and antibiotics susceptibility pattern among infants and young children in Erbil city. Zanco Journal of Medical Sciences (Zanco J Med Sci). 2015;19(1), 915_922. doi: 10.15218/zjms.2015.0012
6. Abdulameer AJ, Abdulla DE. Prevalence of urinary tract infection and its related factors in a sample of school age children from Baghdad, Iraq. Pediatr Neonat Biol. 2022;7(2):000167.
7. Al-Delaimy AK, Sarhan YT, Al-Taha MA, Yahyaa BT, Al-Rawi RA. Occurrence of overweight, obesity and their associated risk factors among primary school pupils in Samarra/Iraq: a cross-sectional study. J Pak Med Assoc. 2024 Oct;74(10 (Supple-8)):S127-S131. doi: 10.47391/JPMA-BAGH-16-28. PMID: 39434287.
8. Alqishawi MAY, Mhmood RH, Mohammed RI. The Prevalence of Overweight and Obesity Among Children and Adolescents in Mosul City. Sci J Med Res. 2024;8(29):18-24.
9. Mohamed O, Mahmood EH, Awad SK, Abas AJ, Mohamed D. Prevalence of Obesity in Primary School Children in Kirkuk: Children obesity. INTERNATIONAL JOURNAL OF MEDICAL SCIENCES. 2025; 8(2):16–26
10. Grier WR, Kratimenos P, Singh S, Guaghan JP, Koutroulis I. Obesity as a Risk Factor for Urinary Tract Infection in Children. Clin Pediatr (Phila). 2016 Sep;55(10):952-6. doi: 10.1177/0009922815617974. Epub 2016 Jan 24. PMID: 26810625.
11. Hsu PC, Chen SJ. Obesity and risk of urinary tract infection in young children presenting with fever. Medicine (Baltimore). 2018 Dec;97(49):e13006. doi: 10.1097/MD.0000000000013006. PMID: 30544371; PMCID: PMC6310556.
12. Yim HE, Han KD, Kim B, Yoo KH. Impact of early-life weight status on urinary tract infections in children: a nationwide population-based study in Korea. Epidemiol Health. 2021;43:e2021005. doi: 10.4178/epih.e2021005. Epub 2020 Dec 29. PMID: 33445823; PMCID: PMC8060518.
13. Renko M, Salo J, Ekstrand M, Pokka T, Pieviläinen O, Uhari M, Tapiainen T. Meta-analysis of the Risk Factors for Urinary Tract Infection in Children. Pediatr Infect Dis J. 2022 Oct 1;41(10):787-792. doi: 10.1097/INF.0000000000003628. Epub 2022 Jul 6. PMID: 35788126; PMCID: PMC9508987.
14. Byun HJ, Ha JY, Jung W, Kim BH, Park CH, Kim CI. The impact of obesity on febrile urinary tract infection and renal scarring in children with vesicoureteral reflux. J Pediatr Urol. 2017 Feb;13(1):67.e1-67.e6. doi: 10.1016/j.jpurol.2016.08.018. Epub 2016 Oct 1. PMID: 28087230.
15. GBD 2021 Adolescent BMI Collaborators. Global, regional, and national prevalence of child and adolescent overweight and obesity, 1990-2021, with forecasts to 2050: a forecasting study for the Global Burden of Disease Study 2021. Lancet. 2025 Mar 8;405(10481):785-812. doi: 10.1016/S0140-6736(25)00397-6. Epub 2025 Mar 3. PMID: 40049185; PMCID: PMC11920006.
16. Şen S, Kızılay D Özalp , Ersoy B. Urinary tract infections in obese children and adolescents with their outcomes and clinical aspects. Hong Kong J Pediatr Res 2021; 4(1):6-11.
17. Yang TH, Yim HE, Yoo KH. Obesity and a febrile urinary tract infection: dual burden for young children? Urology. 2014 Aug;84(2):445-9. doi: 10.1016/j.urology.2014.03.032. Epub 2014 May 10. PMID: 24824410.
18. Amous Y, Isefan S, Hamarsheh K, Hijaz H, Amer R, Shawahna R. Lower urinary tract symptoms among normal-weight, overweight, and obese palestinians: a study of prevalence and impact on the quality of life. BMC Urol. 2024 Sep 13;24(1):199. doi: 10.1186/s12894-024-01587-5. PMID:

39272085; PMCID: PMC11396118.
19. Khanna D, Khanna S, Khanna P, Kahar P, Patel BM. Obesity: A Chronic Low-Grade Inflammation and Its Markers. Cureus. 2022 Feb 28;14(2):e22711. doi: 10.7759/cureus.22711. PMID: 35386146; PMCID: PMC8967417.
20. Kiernan K, MacIver NJ. The Role of the Adipokine Leptin in Immune Cell Function in Health and Disease. Front Immunol. 2021 Jan 29;11:622468. doi: 10.3389/fimmu.2020.622468. PMID: 33584724; PMCID: PMC7878386.
21. Hsu LN, Hu JC, Chen PY, Lee WC, Chuang YC. Metabolic Syndrome and Overactive Bladder Syndrome May Share Common Pathophysiologies. Biomedicines. 2022 Aug 12;10(8):1957. doi: 10.3390/biomedicines10081957. PMID: 36009505; PMCID: PMC9405560.
22. Krishna Mandal A, Kumar Jana J, Chatterjee Y, Pradhan M, Mahata D, Mallick MSA. Clinical and Microbiological Profiles of Urinary Tract Infections in Febrile Children Aged Six Months to Five Years Attending a Tertiary Care Hospital in India. Cureus. 2024 Jan 8;16(1):e51903. doi: 10.7759/cureus.51903. PMID: 38333508; PMCID: PMC10850440.
23. Agrawal P, Paunikar VM. Urinary Tract Infection in Children: A Narrative Review. Cureus. 2024 Jan 1;16(1):e51469. doi: 10.7759/cureus.51469. PMID: 38298274; PMCID: PMC10828737.
24. Abdul Raheem RS, Hussein MA, Al-Din NI. Causative organism of urinary tract infection and drug resistance in children at child's Central Teaching Hospital in Baghdad City. J Pak Med Assoc. 2019 Aug;69(Suppl 3)(8):S59-S63. PMID: 31603879.
25. Hadi ZJ, Alkhayyat AS, Bashbosh AE. OCCURRENCE OF AMINOGLYCOSIDES RESISTANCE GENES ACC(6)-IB AND ACC(3)-II AMONG GRAM-NEGATIVE ISOLATES CAUSING URINARY TRACT INFECTION IN PEDIATRIC PATIENTS, NAJAF, IRAQ. Wiad Lek. 2023;76(2):297-304.
26. Bunduki GK, Heinz E, Phiri VS, Noah P, Feasey N, Musaya J. Virulence factors and antimicrobial resistance of uropathogenic Escherichia coli (UPEC) isolated from urinary tract infections: a systematic review and meta-analysis. BMC Infect Dis. 2021 Aug 4;21(1):753. doi: 10.1186/s12879-021-06435-7. PMID: 34348646; PMCID: PMC8336361.
27. Pugliese G, Liccardi A, Graziadio C, Barrea L, Muscogiuri G, Colao A. Obesity and infectious diseases: pathophysiology and epidemiology of a double pandemic condition. Int J Obes (Lond). 2022 Mar;46(3):449-465. doi: 10.1038/s41366-021-01035-6. Epub 2022 Jan 21. PMID: 35058571.
28. Holt RIG, Cockram CS, Ma RCW, Luk AOY. Diabetes and infection: review of the epidemiology, mechanisms and principles of treatment. Diabetologia. 2024 Jul;67(7):1168-1180. doi: 10.1007/s00125-024-06102-x. Epub 2024 Feb 20. PMID: 38374451; PMCID: PMC11153295.
29. Stahlmann R, Lode H. Pharmakokinetik von Antibiotika bei Übergewichtigen und kritisch Kranken [Pharmacokinetics of antibiotics in obese and critical care patients]. Dtsch Med Wochenschr. 2015 Feb;140(4):271-6. German. doi: 10.1055/s-0041-100443. Epub 2015 Feb 19. PMID: 25704524.
30. Milner JJ, Beck MA. The impact of obesity on the immune response to infection. Proc Nutr Soc. 2012 May;71(2):298-306. doi: 10.1017/S0029665112000158. Epub 2012 Mar 14. PMID: 22414338; PMCID: PMC4791086.
31. Fromer DL, Luck ME, Cheng WY, Mahendran M, da Costa WL, Pinaire M, Duh MS, Preib MT, Ellis JJ. Risk Factors for Empiric Treatment Failure in US Female Outpatients with Uncomplicated Urinary Tract Infection: an Observational Study. J Gen Intern Med. 2025 Mar;40(4):862-870. doi: 10.1007/s11606-024-09029-6. Epub 2024 Oct 2. Erratum in: J Gen Intern Med. 2024 Dec 16. doi: 10.1007/s11606-024-09265-w. PMID: 39356448; PMCID: PMC11914431.
32. Greissman S, Mattiazzi A, Mendoza M, Natori Y, Grady M, Quinonez J, Zukerman R, Camargo JF, Morris MI, Simkins J, Guerra G, Abbo LM. Antimicrobial resistance and recurrent bacterial urinary tract infections in hospitalized patients following kidney transplantation: A single-center experience. Transpl Infect Dis. 2020 Aug;22(4):e13337. doi: 10.1111/tid.13337. Epub 2020 Jun 9. PMID: 32452596.
33. Ali G, Riaz-Ul-Hassan S, Shah MA, Javid MQ, Khan AR, Shakir L. Antibiotic susceptibility and drug prescription pattern in uropathogenic Escherichia coli in district Muzaffarabad, Azad Jammu and Kashmir, Pakistan. J Pak Med Assoc. 2020 Nov;70(11):2039-2042. doi: 10.5455/JPMA.10831. PMID: 33341855.
34. Shareef AA, Alsuwayfee KI, Almallakhdeer AS. Association of Overweight and Obesity with Monosymptomatic Nocturnal Enuresis in 5-15 Years Old Children. International Journal of Biomedicine. 2024;14(1):30-35. doi:10.21103/Article14(1)_OA3
35. Kutasy B, Coyle D, Fossum M. Urinary Tract Infection in Children: Management in the Era of Antibiotic Resistance-A Pediatric Urologist's View. Eur Urol Focus. 2017 Apr;3(2-3):207-211. doi: 10.1016/j.euf.2017.09.013. Epub 2017 Sep 29. PMID: 28965960.

International Journal of Biomedicine 16(1) (2026) 95-100
http://dx.doi.org/10.21103/Article16(1)_OA13

ORIGINAL ARTICLE

Infectious Diseases

INTERNATIONAL JOURNAL OF BIOMEDICINE

Seroprevalence of HIV, HBV, HCV, and Syphilis Among Blood Donors in Omdurman, Sudan (2019–2022): A Retrospective Study

Eithar Zain Elaabdeen Mohammed Ahmed[1], Elharam Ibrahim Abdallah[2,1], Abdel Rahim Mahmoud Muddathir[3], Wala Eldin Osman Elradi[4,1], Fawzia Awad Elhassan Ali[5], Habab Merghani Yassin[6], Nasir Abdelrafie Hamad[7,8], Alaa Eltayeb Omer[9], Lienda Bashier Eltayeb[9*]

[1]*Medical Laboratory Science (Hematology and Blood Transfusion Department), Alzaiem Alazhari University, Khartoum, Sudan*
[2]*Department of Medical Laboratory Sciences, College of Applied Medical Sciences, Qassim University, Buraydah, Saudi Arabia*
[3]*Department of Medical Laboratory Technology, Faculty of Applied Medical Sciences Taibah University, Medina, Saudi Arabia*
[4]*Department of health information management, College of Applied Medical Sciences, Buraydah Private Colleges, 51418, Buraydah, Saudi Arabia*
[5]*Computer Department, Imam Abdulrahman Bin Faisal University, Dammam, Saudi Arabia*
[6]*Department of Biology, College of Science, King Khalid university, Abha, Saudi Arabia*
[7]*Department of Biochemistry, Faculty of Medicine, National University of Sciences and Technology, Sohar, Oman*
[8]*Department of biochemistry, Faculty of Medicine, Al-Neelain University, Khartoum Sudan*
[9]*Department of Medical Laboratory Sciences, College of Applied Medical Sciences, Prince Sattam Bin Abdulaziz University, Al-Kharj, 11942, Saudi Arabia*

Abstract

Background: Transfusion-transmitted infection (TTI) poses significant risks to blood transfusion safety and represents a major public health challenge in Sudan. However, current data on TTI prevalence among blood donors is limited. This study aimed to assess the prevalence of TTI among male blood donors at the Blood Bank of Nao Teaching Hospital, Omdurman, Sudan, from January 2019 to December 2022.

Methods and Results: A retrospective 4-year descriptive cross-sectional study was conducted using blood donation records to examine the prevalence of TTI, including human immunodeficiency virus (HIV), hepatitis B (HBV), hepatitis C (HCV), and syphilis. Data were analyzed for trends over the four-year period. The study identified a total TTI prevalence of 8.8% (302 of 3401 donors). Among TTI, HBV had the highest prevalence at 4.29%, followed by syphilis at 3.91%. HIV prevalence was 0.56%, and HCV prevalence was 0.12%. No cases of co-infection were reported. The overall TTI prevalence declined from 10.2% in 2019 to 6.9% in 2022.

Conclusion: The findings emphasize the importance of ongoing monitoring and improved screening measures to enhance blood safety in Sudan. The high prevalence of HBV and syphilis underscores the need for targeted public health campaigns to raise awareness and promote safe blood donation practices.(**International Journal of Biomedicine. 2026;16(1):95-100.**)

Keywords: transfusion-transmitted infection • HBV • HCV • HIV • syphilis

For citation: Ahmed EZEM, Abdallah EI, Muddathir ARM, Elradi WEO, Ali FAE, Yassin HM, Hamad NA, Omer AE, Eltayeb LB. Seroprevalence of HIV, HBV, HCV, and Syphilis Among Blood Donors in Omdurman, Sudan (2019–2022): A Retrospective Study. International Journal of Biomedicine. 2026;16(1):95-100. doi:10.21103/Article16(1)_OA13

Abbreviations

CI, confidence interval; **HBV**, hepatitis B virus; **HCV**, hepatitis C virus; **HIV**, human immunodeficiency virus; **TTI**, transfusion-transmitted infection.

Introduction

Blood transfusion is a vital therapeutic procedure and remains indispensable in countries such as Sudan, where the need for donated blood is heightened due to the widespread occurrence of infectious diseases like malaria, persistent nutritional deficiencies, and frequent obstetric emergencies. Despite its life-saving role, transfusion carries an inherent risk of transmitting infectious pathogens, including hepatitis B virus (HBV), hepatitis C virus (HCV), human immunodeficiency virus (HIV), and syphilis. Current estimates suggest that around 1% of transfusion events may lead to complications, including transfusion-transmitted infection (TTI). Although advances in transfusion technology and laboratory diagnostics have improved blood safety, ensuring a consistently secure blood supply remains a major challenge in low-resource settings, where comprehensive, routine TTI screening is still not universally practiced.[1] Transfusion-transmitted infection—particularly those caused by HIV, HBV, HCV, and syphilis—continue to pose substantial public health threats across sub-Saharan Africa. Limited epidemiological data compounds this challenge, as the World Health Organization recommends systematic screening for all blood donors. In addition, infections with HIV, HBV, and Treponema pallidum are also transmitted through sex, resulting in rapid, pervasive dissemination through communities and compounding the problems caused by unsafe blood transfusion practices.[2,3] HIV and viral hepatitis continue to impose a considerable global health burden, affecting millions of people and occurring together in the liver at a rate that hastens injury and worsens clinical outcomes.[4] Sudan is a known high-endemic region for both HBV and HCV, with prevalence rates different among important groups such as donors and pregnant women.[5,6] Syphilis is another lingering public health issue, due to a strong connection with greater vulnerability to HIV; however, the availability of epidemiological data on its distribution in Sudan is limited.[7] Transfusion-transmitted infection is a serious issue for blood safety in Sudan due to the paucity of national surveillance at the national level. Accordingly, the burden of TTI is vital in identifying asymptomatic infection, improving donor screening techniques, and directing public health interventions. In this light, the current study aimed to establish the prevalence of HIV, HBV, HCV, and syphilis among blood donors who underwent visits to Nao Teaching Hospital, Omdurman, for the period 2019 to 2022.

Materials and Methods

Study Design

This study employed a retrospective, descriptive cross-sectional design conducted over a four-year period at the Blood Bank of Nao Teaching Hospital in Omdurman, Sudan. The study timeframe extended from January 2019 to December 2022, during which 3,401 male blood donors were screened. Relevant data were extracted from existing blood bank records. All donors provided written informed consent and completed a standardized questionnaire used to assess their eligibility for blood donation. Confidentiality was strictly maintained for seropositive subjects, and consent procedures were obtained at the time of blood collection. The study included voluntary blood donors aged 18–65 years, weighing over 45 kg, and with hemoglobin levels above 13 g/dL. Donors were required to meet the Sudan National Blood Transfusion Protocol standards, including normal vital signs (blood pressure, temperature, pulse) and absence of significant medical or surgical history.

Inclusion and Exclusion Criteria

Participants who fulfilled the eligibility criteria were included. Exclusion criteria encompassed individuals at high risk, such as those with chronic illnesses, substance abuse, pregnancy, dialysis dependence, donors deferred due to abnormal hemoglobin or blood pressure, and those with incomplete records.

Data Collection and Laboratory Testing

Two milliliters of blood were collected from each donor using plain vacutainer tubes, and serum was separated for serological analysis. All samples were screened for HIV, HBV, HCV, and syphilis. HIV testing was performed using the HIV (Ag/Ab) ELISA kit (Fortress Diagnostics, UK) to detect both HIV-1 and HIV-2 antibodies. HBV detection was performed using the HS HBsAg ELISA kit (Fortress Diagnostics, UK), while HCV was screened using the microwell ELISA kit (ABIA, AB Diagnostic Systems, Germany). Syphilis antibodies were identified using the ABIA Treponema Ab ELISA test (ABIA, AB Diagnostic Systems, Germany).

Data were analyzed using IBM SPSS Statistics V22.0. The chi-square test was used to examine the relationship between certain diseases and different years. A *P*-value was set at less than 0.05 to be statistically significant.

Results

The study included 3,401 voluntary male blood donors aged 18–65 years. Most were between 31 and 45 years old (37.5%), with the remainder distributed across the 18–30 and 46–65 age groups. Nearly half (45.0%) weighed 56–70 kg, and the majority had hemoglobin levels between 14.1 and 16 g/dL (52.5%). Blood group distribution showed group B as the most common (35.0%), followed by O (30.0%), AB (25.0%), and A (10.0%). Overall, donors met the required national standards for safe blood donation, as illustrated in Table 1.

Table 2 demonstrates the prevalence of TTI among seropositive donors from 2019 to 2022. Out of 3,401 donors, 302 TTI were detected (8.88%), with HBV being the most common (48.3%), followed by syphilis (44%), HIV (6.3%), and HCV (1.3%). Yearly TTI rates were 10.2% in 2019, 7.89% in 2020, 9.4% in 2021, and 6.9% in 2022, with HBV and syphilis predominating each year.

Table 3 summarizes the prevalence of specific TTI among 3,401 blood donors from 2019 to 2022. HIV was detected in 0.56% of donors, HBV in 4.29%, HCV in 0.12%, and syphilis in 3.91%. Yearly prevalence showed minor fluctuations: HIV ranged from 0.2% to 1%, HBV from 2.5% to 5.6%, HCV remained below 0.3%, and syphilis ranged from 2.5% to 4.4%, indicating that HBV and syphilis were the

most common infections, while HIV and HCV remained low throughout the period.

Table 4 presents the annual prevalence of TTI with 95% CI and adjusted true prevalence.

Table 1.

Demographic data for study participants

Characteristic	Category	Number (%)
Age (years)	18–30	1.020 (30.0%)
	31–45	1.275 (37.5%)
	46–65	1.106 (32.5%)
Sex	Male	3.401 (100%)
	Female	0 (0%)
Weight (kg)	45–55	815 (24.0%)
	56–70	1.530 (45.0%)
	>70	1.056 (31.0%)
Hemoglobin (g/dL)	13–14	1.020 (30.0%)
	14.1–16	1.785 (52.5%)
	>16	596 (17.5%)
Donation type	Voluntary	3.401 (100%)
	Unvoluntary	0 (0%)
ABO blood group	A	340 (10.0%)
	B	1.190 (35.0%)
	AB	851 (25.0%)
	O	1.020 (30.0%)

Table 2.

Annual frequency of HIV, HBV, HCV, and syphilis cases among seropositive donors.

Year	HIV	HBV	HCV	Syphilis	Total
2019	3 (1.9%)	85 (55.2%)	0 (0%)	66 (42.6%)	154 (10.2%)
2020	6 (11.3%)	17 (32.1%)	2 (3.8%)	28 (52.8%)	53 (7.89%)
2021	4 (10.3%)	16 (41%)	0 (0%)	19 (48.7%)	39 (9.4%)
2022	6 (10.7%)	28 (50%)	2 (3.6%)	20 (35.7%)	56 (6.9%)
Total	19 (6.3%)	146 (48.3%)	4 (1.3%)	133 (44%)	302 (8.88%)
P-value	0.08	0.02	0.71	0.00	

Table 3.

Annual true prevalence of TTI among all blood donors.

Year	Total number	HIV	HBV	HCV	Syphilis
2019	1507	3 (0.2%)	85 (5.6%)	0 (0%)	66 (4.4%)
2020	671	6 (0.9%)	17 (2.5%)	2 (0.3%)	28 (4.2%)
2021	415	4 (1%)	16 (3.9%)	0 (0%)	19 (4.6%)
2022	808	6 (0.7%)	28 (3.5%)	2 (0.2%)	20 (2.5%)
Total	3401	19 (0.56%)	146 (4.29%)	4 (0.12%)	133 (3.91%)
P-value	-	0.08	0.02	0.71	0.00

Table 4.

Annual prevalence of TTI with 95% CI and adjusted true prevalence.

Year	HIV % (95% CI)	HBV % (95% CI)	HCV % (95% CI)	Syphilis % (95% CI)
2019	0.20 [0.07–0.58]	5.64 [4.58–6.92]	0.00 [0.00–0.25]	4.38 [3.46–5.53]
2020	0.89 [0.41–1.94]	2.53 [1.59–4.02]	0.30 [0.08–1.08]	4.17 [2.90–5.97]
2021	0.96 [0.38–2.45]	3.86 [2.39–6.17]	0.00 [0.00–0.92]	4.58 [2.95–7.04]
2022	0.74 [0.34–1.61]	3.47 [2.41–4.96]	0.25 [0.07–0.90]	2.48 [1.61–3.79]

Figure 1 demonstrates the trend analysis, which shows that the positivity rates of the screening tests fluctuated over time. Blood transfusion-transmissible infections were 154/1507 (10.2%) in 2019, then decreased to 53/671 (7.89%) in 2020, increased to 39/415 (9.4%) in 2021, and decreased to 56/808 (6.9%) in 2022. From screened TTI, seropositivity for HBV and syphilis decreased from 2019 to 2021 and increased again from 2021 to 2022. However, HIV positivity rates gradually increased from 2019 to 2021 and decreased in 2022. HCV positivity was consistently low over the four years, with no positive cases in 2019 and 2021.

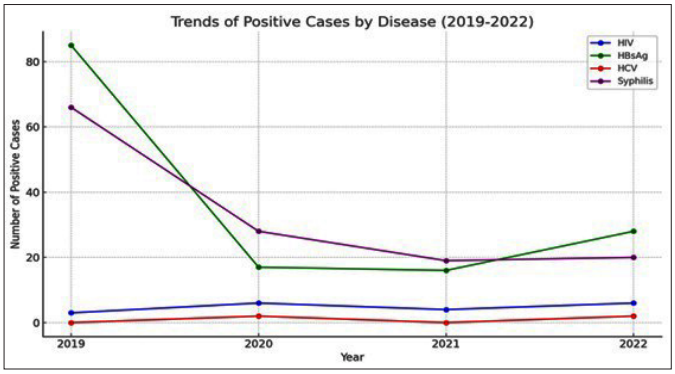

Figure 1. *Trend of positive cases according to different years.*

Discussion

Transfusion-transmitted infection continues to pose a significant challenge to safe blood transfusion practices. Each unit of blood carries an estimated 1% risk of transfusion-related complications, including TTIs, highlighting the critical importance of thorough donor screening to prevent potential biohazards.[8]

The present study examined the prevalence of TTIs among blood donors at the Blood Bank of Nao Teaching Hospital in Omdurman over a four-year period from 2019 to 2022. Notably, all donors included in this study were male. This predominance may be explained by several factors, including physiological differences between the sexes, cultural beliefs, pregnancy and lactation in women, and the higher prevalence of iron-deficiency anemia among female populations. Additionally, societal perceptions that men are

generally healthier than women likely contribute to the higher proportion of male donors.

Over the study period, the overall prevalence of TTIs among donors was 302 out of 3,401 (8.8%). This rate is higher than the 5.6% prevalence reported by Ahmed et al.[9] in Khartoum and exceeds international findings from Saudi Arabia (7.4%),[10] Ethiopia (5.43%),[11] Eritrea (3.6%),[12] and India (1.58%).[13] Conversely, the prevalence observed in this study is lower than that documented in Kosti (22.52%),[14] Port Sudan (20.1%),[15] and White Nile State (15.91%),[16] as well as studies in Ghana (16.1%)[17] and South Sudan (22.1%).[18]

The considerable variation in TTI prevalence across different regions may reflect differences in diagnostic techniques, the sensitivity and specificity of testing reagents, geographical and temporal variations in disease burden, and disparities in healthcare infrastructure and access. These findings underscore the ongoing need for rigorous donor screening, continuous monitoring of infection trends, and tailored public health interventions to enhance the safety of the blood supply in Sudan and comparable settings. Over the four-year study period, the prevalence of HIV among blood donors at Nao Teaching Hospital fluctuated, with an overall rate of 0.56%. This rate is lower than previously reported figures from Kosti (1.77%),[14] Port Sudan (1.4%),[15] White Nile State (2.61%),[16] Ghana (1.6%),[17] and South Sudan (6.7%).[18] Conversely, it is higher than the prevalence documented in Khartoum (0.4%),[9] Saudi Arabia (0.06%),[10] Ethiopia (0.34%),[11] India (0.16%),[13] and Eritrea (0.3%).[12]

Hepatitis B virus (HBV) remains one of the most widespread infectious diseases globally, with approximately two billion people having been infected at some point, and it is considered hyper-endemic in sub-Saharan Africa and parts of Asia.[19] Sudan has historically been classified as a high HBV endemic country, with a prevalence of 8% reported by the World Health Organization in 1996.[20] In the present study, HBV was the most prevalent TTI, affecting 4.29% of donors. This prevalence is lower than that reported in Kosti (6.07%),[14] Port Sudan (11.7%),[15] White Nile State (5.57%),[16] Khartoum (6%),[9] Saudi Arabia (6.1%),[10] and South Sudan (22.1%).[18] However, it exceeds the rates observed in Ethiopia (2.1%),[11] Ghana (3.1%),[17] India (0.77%),[13] and Eritrea (2%).[12] The prevalence of HCV in this study was notably low at 0.12%, considerably lower than figures reported in other regions, including Kosti (1.4%),[14] Port Sudan (0.4%),[15] White Nile State (1.4%),[16] and Khartoum (0.2%).[9] Neighboring countries also reported higher prevalence, such as Saudi Arabia (0.4%),[10] Ethiopia (0.8%),[11] Eritrea (0.7%),[12] Ghana (5%),[17] and South Sudan (8.9%).[18] In contrast, our finding is like the 0.11% rate reported in India.[13] These differences may be explained by variations in study populations, geographic factors, and laboratory screening methods. The relatively lower prevalence of HCV compared to HBV may reflect its more restricted transmission routes, primarily limited to blood-to-blood contact, whereas HBV can be transmitted through multiple pathways, including sexual contact and vertical transmission.

Syphilis continues to represent a major global public health concern, particularly in developing countries. In this study, the prevalence of syphilis among blood donors was 3.91%, making it the second most common TTI observed. This rate is lower than those reported in Kosti (11.87%),[14] Port Sudan (6.6%),[15] White Nile State (5.72%),[16] Khartoum (5.4%),[9] and Ghana (6.4%).[17] Conversely, it exceeds prevalence rates reported internationally, including Saudi Arabia (0.34%),[10] Ethiopia (1.4%),[11] India (0.53%),[13] and Eritrea (0.6%).[12] These findings indicate that syphilis remains a significant concern in various regions, with differences in prevalence likely influenced by local transmission dynamics, healthcare infrastructure, and public health interventions.

Notably, no cases of co-infections were observed in the present study, in contrast to previous reports where co-infection rates ranged from 0.1% in Eritrea[12] to 1.67% in Kosti,[14] with intermediate rates reported in Port Sudan (1.1%), [15] White Nile State (0.59%),[16] and Khartoum (0.65%).[9]

Analysis of TTI trends from 2019 to 2022 revealed a general decline in seroprevalence, decreasing from 10.2% in 2019 to 6.9% in 2022, with a notable dip in 2020 (7.89%). This decline is likely related to the COVID-19 pandemic, which affected both donor turnout and the capacity of healthcare services to perform routine screenings. Similar patterns were observed internationally, such as in Saudi Arabia, where Minshawi et al.[10] reported a decline from 1.5% in 2019 to 0.9% in 2020, followed by a slight rise to 1.1% in 2021. In contrast, studies in Kosti[14] and Ghana[17] reported fluctuating trends, with temporary increases and decreases in TTI prevalence.

Specifically, HIV seroprevalence in our study increased from 0.2% in 2019 to 0.9% in 2020, peaking at 1.0% in 2021 before slightly declining to 0.7% in 2022. HBV prevalence declined steadily from 5.6% in 2019 to 2.5% in 2020, stabilizing at 3.9% in 2021 and 3.5% in 2022. HCV prevalence remained consistently low, ranging from 0% to 0.3%, resulting in an overall rate of 0.12%, reflecting effective screening and control measures. Syphilis rates remained relatively stable at approximately 4% from 2019 to 2021, with a slight decrease to 2.5% in 2022, suggesting improvements in donor screening and a reduction in transmission.

Overall, the fluctuations in TTI prevalence during 2020 and 2021 appear to have been largely influenced by the COVID-19 pandemic, which disrupted routine healthcare services and reduced donor participation. The resumption of normal healthcare operations and an increase in donor numbers by 2022 contributed to the stabilization of seroprevalence rates across all TTIs.

The observed variations in TTI prevalence across different studies can be attributed to multiple factors. Demographic characteristics, including age, gender, and sexual behaviors, along with differences in healthcare access, public awareness, education, cultural norms, and social stigma, play significant roles. Methodological differences, such as the type of screening tests used and the frequency of testing, also influence reported prevalence rates. Furthermore, regional disease outbreaks, public health policies, socioeconomic conditions, and the robustness of healthcare infrastructure contribute to these discrepancies. The COVID-19 pandemic likely affected prevalence estimates by reducing donor turnout and limiting routine

screening, as reflected in this study and others. Additionally, the retrospective design of this study and variations in study periods and donor numbers in previous investigations may have contributed to differences in TTI prevalence. Collectively, these factors help explain the wide range of prevalence rates reported across diverse regions and timeframes.

Conclusion

This study identified a TTI prevalence of 8.8%, underscoring the persistent risk of blood transfusion in the region. Among the infections assessed, HBV was the most prevalent, affecting 4.29% of donors, followed by syphilis at 3.91%. The prevalence of HIV (0.56%) and HCV (0.12%) was comparatively low, and no cases of co-infections were observed. Additionally, the study observed a declining trend in TTI seroprevalence over the four-year period, emphasizing the critical role of continued vigilance and robust donor screening practices to ensure blood safety.

Limitations and Future Directions

This study has several limitations that should be considered when interpreting the findings. Its single-center design and the inclusion of only male donors restrict the generalizability of the results to the broader Sudanese population, particularly female donors. Additionally, the retrospective nature of the study limited the availability of certain variables, and the screening protocol did not include other regionally relevant infections such as malaria. The absence of confirmatory testing and advanced diagnostic methods, such as nucleic acid testing (NAT), may also have affected the accuracy of TTI detection due to an overestimation of some TTI prevalence rates, particularly for HBV and syphilis. Therefore, future research should adopt a multi-center approach, include both genders, and incorporate more comprehensive screening panels with confirmatory and molecular methods. Expanding surveillance systems and integrating donor education and awareness programs are also recommended to strengthen blood transfusion safety in Sudan.

Ethical Considerations

The study received ethical clearance from the research board at the Faculty of Medical Laboratory Sciences, Alzaiem Alazhari University. The study applied previously collected data, and no study participants were included at any point. Informed consent was not sought as the study was performed on secondary data; however, consent was obtained from the head of the Blood Bank.

Acknowledgments

This publication was supported by the Deanship of Scientific Research at Prince Sattam bin Abdulaziz University.

The authors acknowledge OpenAI ChatGPT (GPT-4) for providing proofreading support during the writing process.

Conflicts of Interest

The authors declare that they have no competing interests.

References

1. Widman FK, editor. Technical manual. American Association of Blood Banks; 1985.
2. Bisetegen FS, Bekele FB, Ageru TA, Wada FW. Transfusion-Transmissible Infections among Voluntary Blood Donors at Wolaita Sodo University Teaching Referral Hospital, South Ethiopia. Can J Infect Dis Med Microbiol. 2016;2016:8254343. doi: 10.1155/2016/8254343. Epub 2016 Aug 15. PMID: 27597875; PMCID: PMC5002453.
3. Soares CC, Georg I, Lampe E, Lewis L, Morgado MG, Nicol AF, Pinho AA, Salles RC, Teixeira SL, Vicente AC, Viscidi RP, Gomes SA. HIV-1, HBV, HCV, HTLV, HPV-16/18, and Treponema pallidum infections in a sample of Brazilian men who have sex with men. PLoS One. 2014 Aug 1;9(8):e102676. doi: 10.1371/journal.pone.0102676. PMID: 25083768; PMCID: PMC4118852.
4. UNAIDS. Fact sheet - Latest statistics on the status of the AIDS epidemic. 2017.
5. Badawi MM, Atif MS, Mustafa YY. Systematic review and meta-analysis of HIV, HBV and HCV infection prevalence in Sudan. Virol J. 2018 Sep 25;15(1):148. doi: 10.1186/s12985-018-1060-1. PMID: 30253805; PMCID: PMC6157049.
6. McCarthy MC, Hyams KC, el-Tigani el-Hag A, el-Dabi MA, el-Sadig el-Tayeb M, Khalid IO, George JF, Constantine NT, Woody JN. HIV-1 and hepatitis B transmission in Sudan. AIDS. 1989 Nov;3(11):725-9. doi: 10.1097/00002030-198911000-00006. PMID: 2515878.
7. Olokoba AB, Olokoba LB, Salawu FK, Danburam A, Desalu OO, Midala J, et al. Syphilis in voluntary blood donors in North-Eastern, Nigeria. European Journal of Scientific Research.2009;31(3):335-340.
8. Garg S, Mathur DR, Garg DK. Comparison of seropositivity of HIV, HBV, HCV and syphilis in replacement and voluntary blood donors in western India. Indian J Pathol Microbiol. 2001 Oct;44(4):409-12. PMID: 12035351.
9. Ahmed NOA, Omer ED, Mohammed MAA. Sero-prevalence of transfusion-transmissible infections among blood donors in Khartoum, Central Sudan. Eur Acad Res. 2016;IV(3):2566.
10. Minshawi F, Abdulshakoor AA, Alwakil EM, Basfar GT, Kabrah S, Aslam A, Almasmoum H, Mujalli A, Moaminah RH, Almoalad GA, Alwadani MA, Alzahrani MG, Alsehemi KA, Refaat B. Seroprevalence of transfusion-transmitted infections among blood donors in Makkah, Saudi Arabia. J Infect Dev Ctries. 2024 Jun 30;18(6):957-963. doi: 10.3855/jidc.19559. PMID: 38991002.
11. Aliyo A, Ashenafi G, Adem S. Evaluation of Transfusion Transmissible Infections Prevalence and Trend Among Blood Donors Attended at Bule Hora Blood Bank, West Guji, South

Ethiopia. Health Serv Res Manag Epidemiol. 2022 Nov 3;9:23333928221136717. doi: 10.1177/23333928221136717. PMID: 36337767; PMCID: PMC9634199.
12. Siraj N, Achila OO, Issac J, Menghisteab E, Hailemariam M, Hagos S, Gebremeskel Y, Tesfamichael D. Seroprevalence of transfusion-transmissible infections among blood donors at National Blood Transfusion Service, Eritrea: a seven-year retrospective study. BMC Infect Dis. 2018 Jun 7;18(1):264. doi: 10.1186/s12879-018-3174-x. PMID: 29879912; PMCID: PMC5992706.
13. Sharma HB, Bansal M, Sharma R, Kumar N, Munjal D. Seroprevalence of Transfusion Transmitted Diseases in a Tertiary Care Hospital of Northern India: A Five Year Retrospective Study. Natl J Lab Med. 2022;11(2).
14. Almugadam BS, Ibrahim OMA, Ahmed YMA. Seroprevalence of the Serological Markers of Transfusion-Transmissible Infections among Volunteer Blood Donors of Kosti Obstetrics and Gynecology Hospital. Medicines (Basel). 2021 Oct 29;8(11):64. doi: 10.3390/medicines8110064. PMID: 34822361; PMCID: PMC8619909.
15. Mohamed B, Gibreel MO, Badaneen M. Prevalence of transfusion-transmissible infections among blood donors in Port Sudan. East Mediterr Health J. 2019;44:72.
16. Ahmed EB, Essa AA, Almugadam BS, Ahmed QM, Hussein MM. Transfusion transmitted infections among male blood donors of White Nile State, Sudan: Screening of the current seroprevalence and distribution. BMC Res Notes. 2020 Nov 30;13(1):549. doi: 10.1186/s13104-020-05333-6. PMID: 33256839; PMCID: PMC7708122.
17. Hadfield PY, Vechey GA, Bansah E, Nyahe M, Khuzwayo N, Tarkang EE. Transfusion-Transmissible Infections Among Blood Donors in a Regional Hospital in Ghana: A 6-Year Trend Analysis (2017-2022). J Int Assoc Provid AIDS Care. 2024 Jan-Dec;23:23259582241274305. doi: 10.1177/23259582241274305. PMID: 39175401; PMCID: PMC11342317.
18. Ratib D, Lako R, Umar B, Yahiya O, Picozzi K. Viral transfusion transmissible infections among blood donors in Maridi County Hospital, South Sudan. South Sudan Med J. 2014;7:4-6.
19. Fessehaye N, Naik D, Fessehaye T. Transfusion transmitted infections - a retrospective analysis from the National Blood Transfusion Service in Eritrea. Pan Afr Med J. 2011;9:40. doi: 10.4314/pamj.v9i1.71219. Epub 2011 Aug 18. PMID: 22145069; PMCID: PMC3215562.
20. World Health Organization. Expanded program on immunization, hepatitis B vaccine, making global progress: EPI update. Geneva, Switzerland: WHO; 1996.

***Corresponding author:** Dr. Linda Eltayeb. E-mail: lindarose009@hotmail.com*

International Journal of Biomedicine 16(1) (2026) 101-106
http://dx.doi.org/10.21103/Article16(1)_OA14

ORIGINAL ARTICLE

Dentistry

INTERNATIONAL JOURNAL OF BIOMEDICINE

Enhancing Dentin Bonding of Fifth-Generation Adhesive Through Experimental 10-MDP Primer: A Pilot Study on Human Teeth

Timur V. Melkumyan[1,2*], Zurab S. Khabadze[2], Maria K. Makeeva[2], Marina U. Dashtieva[2], Fikret V. Badalov[2], Shahnoza K. Musashaykhova[1], Hayrullo I. Hamidov[3], Sultan X. Suleymanov[4], Natalya A. Kulagina[4], Dato How Kim Chuan[5], Gerhard K. Seeberger[6], Bedros Y. Sakuk[7], Julietta Y. Rau[8], Nuriddin Kh. Kamilov[1], Angela D. Dadamova[1]

[1]*Tashkent State Medical University, Tashkent, Uzbekistan*
[2]*Peoples' Friendship University of Russia (RUDN University), Moscow, Russia*
[3]*Navoi State University of Mining and Technologies, Uzbekistan*
[4]*Institute of Materials Science of Uzbekistan Academy of Sciences, Uzbekistan*
[5]*State Medical University of Malaysia, Malasia*
[6]*Order of Physicians and Dentists of the Province of Cagliari, Sardinia, Italy*
[7]*NYU College of Dentistry, USA*
[8]*Institute of the "Structure of Matter" of the Italian National Research Council, Rome, Italy*

Abstract

Background: The study aimed to evaluate the effectiveness of an experimental primer (EP) based on the 10-MDP monomer when used with the fifth-generation adhesive system.

Methods and Results: Tests were performed on tooth samples from wisdom teeth and premolars extracted for orthodontic purposes. The EP consisted of 10-MDP monomer (10%), ethanol (40%), propanol-2 (30%), water (18%), and a camphorquinone-based photoinitiator system (2%). The pH of the EP was 2.4. The adhesive resin of the fifth-generation OptiBond Solo Plus (OSP) and the universal composite Herculite XRV were the materials of choice. Two adhesive techniques were tested: the traditional total-etch technique with OSP application, and the optional technique with sequential EP and OSP applications using a selective-etch approach. Adhesive bond strength was assessed in two groups using the ultra-test technique (Ultradent Products, Inc., USA). All samples in each group underwent two sequential shear bond strength (SBS) tests. The quality of the resin composite adhesion was assessed on four specimens using an FE-SEM (Thermo Fisher Scientific Apreo 2S LoVac). Microleakage assessment was made on 10 teeth. In each tooth, two artificial cavities of similar size were prepared. Fillings were placed using two techniques in each tooth. Depth of dye penetration at tooth-composite interface was assessed using nonparametric scores. The phase composition of the dentin surface was assessed on six tooth samples divided into three groups of two using thin-film X-ray diffraction (TF-XRD). Samples from the control group were used for XRD of the dentin surface. Samples of Group 1 were used to apply EP to the dentin surface; samples of Group 2 were used for sequential application of EP and OSB to the dentin surface.

A significant difference of more than three times (P=0.000) was observed between the SBS values of the first and second tests in samples from Group 1 compared with those from Group 2. SEM of the filling-to-dentin interface in samples with sequential application of EP and OSP using a selective etch approach showed a more uniform hybrid layer than with OSP application with the total-etch technique. Microleakage analysis of the dentin-composite interface revealed a significantly higher dye penetration rate in samples with the traditional OSP application. The presence of the 10-MDP calcium salt peak at diffraction angle of 2θ=2.54º after sequential application of EP and OSP corresponded to the longest d-spacing (3.48 nm) of the nanolayered structure on the surface of tooth dentin.(**International Journal of Biomedicine. 2026;16(1):101-106.**)

Keywords: tooth dentin• adhesive monomers • 10-MDP-Ca salts • shear bond strength • microleakage

For citation: Melkumyan TV, Khabadze ZS, Makeeva MK, Dashtieva MU, Badalov FV, Musashaykhova SK, Hamidov HI, Suleymanov SX, Kulagina NA, Chuan DHK, Seeberger GK, Sakuk BY, Rau JY, Kamilov NKh, Dadamova AD. Enhancing Dentin Bonding of Fifth-Generation Adhesive Through Experimental 10-MDP Primer: A Pilot Study on Human Teeth. International Journal of Biomedicine. 2026;16(1):101-106. doi:10.21103/Article16(1)_OA14

Abbreviations

DP, dye penetration; **EP**, experimental primer; **FE-SEM**, field emission scanning electron microscopy; **OSP**, OptiBond Solo Plus; **SBS**, shear bond strength; **TF-XRD**, thin-film X-ray diffraction.

Introduction

Strong and stable adhesion to tooth dentin is a pressing issue in modern restorative dentistry that, despite the availability of numerous adhesive systems, remains unresolved. Currently, there are two main concepts for bonding materials to tooth enamel and dentin. These have been implemented in total-etch and self-etch adhesive systems.[1,2]

The total-etch concept means acid etching of both enamel and dentin. Among the positive aspects of this technique are the formation of microporosities on the enamel surface, removal of debris, smear layer, and plugs from the dentin surface, opening of the dentinal tubule orifices, and the formation of niches on the surface of peritubular dentin, which can serve as retention sites for adhesive resin monomers during hybrid layer formation.[2]

Unlike enamel, dentin has a different three-dimensional organization and composition. Acid etching of dentin exposes the organic matrix, which, after losing its mineral component, can maintain its spatial structure only in the presence of moisture. The collapse of the collagen matrix, caused by drying of the etched dentin, is the main reason for its ineffective impregnation with adhesive resin monomers and the formation of a weak hybrid layer. The inconsistency in hybrid layer quality and the magnitude of polymer stress that occur in the bulk of the composite material during photoactivation lead to postoperative sensitivity, micro-gap formation, and many possible complications associated with an absence of a tight seal around the composite restoration.[3]

Considering the serious shortcomings of the total-etch technique and the urgent need for an alternative approach, adhesive systems with functional acidic monomers capable of forming chemical bonds with tooth hydroxyapatite began to be used in tooth restoration.[4,5] The mechanism of their bonding to enamel and dentin is based less on micromechanical retention and more on the chemical bond of functional monomers with the hydroxyapatite on the tooth surface. The resulting ionic bond ensures strong, stable adhesion of the composite material to the tooth.[6,7]

Among three commonly used functional monomers (10-MDP, 4-MET, and Phenyl-P), 10-MDP has been found to be the most effective at forming ionic bonds with hydroxyapatite. This chemical interaction results in the formation of MDP–Ca salts in a nanolayered structure on enamel and dentin surfaces. It is generally accepted that the pronounced hydrophobicity of this nanolayer determines the chemical stability of the composite material-tooth interface and prevents its hydrolytic degradation.[7,8]

One significant drawback of the 10-MDP monomer is its relatively large molecular size, which can negatively affect the mechanical stability of the adhesive bond. One solution to this issue is to add monomethacrylates and dimethacrylates of low molecular weight, such as HEMA (2-hydroxyethyl methacrylate) and TEGDMA (triethylene glycol dimethacrylate), to form a composition. These compounds are necessary for cross-linking linear polymers and increasing their strength. However, HEMA and TEGDMA each have shortcomings. The first, despite their ability to adsorb to the surfaces of tooth enamel and dentin in a competitive manner with other compounding monomers, has hydroxyl groups that are unable to form ionic bonds with the mineralized portion of a tooth. The second, being hydrophilic, HEMA and TEGDMA promote water absorption, leading to hydrolytic degradation of the adhesive and hybrid layers, which is the main reason for a reduction in bond strength between the restoration and the tooth over time.[9,10]

Considering the positive and negative aspects of short-chain monomers, the prior application of 10-MDP monomer to initially form an uninterrupted, waterproof nanolayer on the surface of enamel and dentin, and subsequently adding it for the cross-linking of 10-MDP monomer, might offer significant practical value.[10,11]

Also, because most total-etch adhesive systems contain HEMA and TEGDMA and lack functional monomers capable of chemically reacting with tooth hydroxyapatite, this pilot study aimed to evaluate the effectiveness of an EP based on the 10-MDP monomer when used with a fifth-generation adhesive system.

Methods

In the study we used caries-free wisdom teeth and premolars, which were extracted for orthodontic purposes. 10-MDP monomer was synthesized in the laboratory of the Joint Research Institute of Chemistry of RUDN University. The EP consisted of 10-MDP monomer (10%), ethanol (40%), propanol-2 (30%), water (18%), and a camphorquinone-based photoinitiator system (2%). The pH of the EP was 2.4. The adhesive resin of the fifth-generation Optibond Solo Plus (OSP) and the universal composite Herculite XRV (Kerr, Italy) were the materials of choice.

The adhesive bond strength was assessed on 20 samples prepared using the ultra-test technique (Ultradent Products, Inc., USA). To achieve a uniform level of roughness, the dentin surface was treated with sandpaper grits ranging from 300 to 600 units (Figure 1).

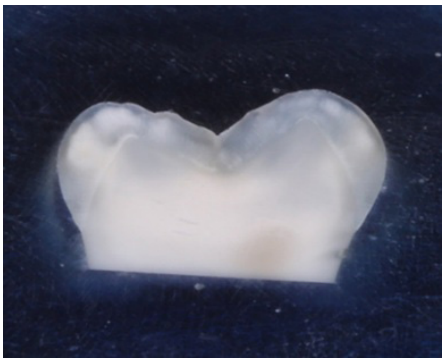

Fig. 1. *Tooth sample for adhesion of composite buildups on dentin.*

Composite cylindrical buildups on the dentin surface were made by fixing the tooth sample in a bonding clamp and polymerizing the material in a plastic mold. Photoactivation was performed using VALO X (Ultradent Products, Inc., USA) in the standard mode according to the manufacturer's instructions for the materials used.

In line with the study's aim, tooth samples for the shear bond strength (SBS) test were divided into two groups. In Group 1 (n=10), acid etching of the dentin was performed for 15 seconds, followed by rinsing the surface with distilled water for the same amount of time. OSP was applied according to the wet adhesive protocol and the manufacturer's instructions. In Group 2 (n=10), the acid etching step was replaced by rubbing EP into the dentin surface for 15 seconds. After application, the EP was air-thinned on the dentin surface to remove excess material and evaporate the solvent. Subsequently, the OSP was applied and air-thinned.

The strength of adhesion of the composite material to tooth dentin was assessed using the shear force in an UltraTester Bond Strength Testing Machine (Ultradent Products, Inc., USA). Tests were conducted at a speed of 1 mm/min to determine peak load capacity. In each sample, two areas on the dentin adhesive surface were selected for the sequential placement of cylindrical buildups and testing of bond strength (Figure 2). Thus, the total number of tests in each group was 20. The bond strength of the composite buildup to the tooth dentin was recorded in pounds (lb).

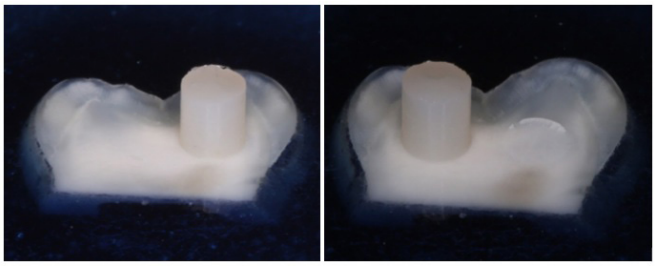

Fig. 2. *Tooth sample for performing 2 consecutive SBS tests.*

The quality of the resin composite adhesion was assessed on four specimens using a FE-SEM (Thermo Fisher Scientific Apreo 2S LoVac). To prepare the specimens, only the coronal portion of the teeth was used, which was sectioned into two halves using diamond discs along the central fissure under copious water cooling. The vestibular and oral enamel surfaces were also ground to expose a flat portion of midcoronal dentin. The resulting four tooth slabs were randomly divided into two groups of two specimens each.

In Group 1 samples, enamel and dentin surfaces were acid-etched (37.5% Phosphoric Acid Gel, Kerr) for 30 seconds and 15 seconds, respectively. After they were rinsed in distilled water for 30 seconds, excess moisture was removed, and OSP was applied. In Group 2 samples, only the enamel was acid-etched. After rinsing with water and air-drying, EP and OSP were sequentially applied to the enamel and dentin surfaces in accordance with the principles of sample preparation for the SBS test.

The application and polymerization of the resin composite were performed using an incremental freehand technique until the adhesive surfaces were completely laminated. The thickness of the composite laminate varied from 1.3 to 1.5 mm. The laminated tooth slabs were cut into two halves and embedded in epoxy resin. Further sample processing was performed using abrasives and polishing pastes with grit sizes ranging from 300 to 1200.

After rinsing under running water, the samples (Figure 3) were cleaned in an ultrasonic bath with distilled water for five minutes. Before scanning, the samples were coated with a 10nm gold layer using a Quorum magnetron (Q150R ES, England) sputtering system.

Fig. 3. *Tooth samples for SEM.*

Microleakage assessment of two adhesive regimens was performed on 10 teeth. Round artificial cavities (4 mm in diameter, 1 mm deep) were prepared on two approximal surfaces of each tooth, with half of the margin in enamel and the other half in root dentin. Mesial proximal surfaces were assigned for the traditional total-etch regimen and application of OSP, and distal proximal surfaces were assigned for the selective etching of enamel and consecutive application of EP and OSP. All cavities were filled with composite using a similar technique. After this, the fillings were polished, and the tooth samples were subjected to thermocycling (5000 cycles in separate water baths of 5°C and 55°C±2°C with a dwell time of 10 seconds in each bath and a transfer time of 1 second). Next, the apices of tooth samples were sealed with sticky wax and coated with nail varnish to exclude fillings with a 1 mm distance around them. The teeth were stained in 1% methylene blue solution for 24 hours and sectioned through the centers of restorations. Microleakage at the enamel and dentin margins was considered (Figure 4).

Fig. 4*. Microleakage assessment.*

Enamel and dentin dye penetration (DP) was assessed using the following scale of 0-3 scoring system: 0 - no DP; 1 - DP up to one-half of the cavity wall length; 2 - DP up to the full length of the cavity wall, not including the axial wall; 3 - DP to the full extent of the cavity wall, including the axial wall.

The phase composition of the dentin surface was assessed on six tooth samples divided into three groups of two using TF-XRD (Figure 5). The analysis was performed using an Empyrean instrument (Malvern Panalytical, Netherlands) operating at an accelerating voltage of 45 kV and a current of 40 mA with a fixed incident X-ray beam angle of 0.3° and a scan rate of 0.02°/s for 2θ scanning. The specimen surfaces were ground and polished according to the principles of sample preparation for SEM analysis. However, after polishing, the dentin surface of all specimens was abraded with an erythritol-based air-abrasive mixture (14 μm, Air-Flow Plus, EMS, Nyon, Switzerland) with a constant particle flow at 0.25 MPa for 10 seconds. The nozzle was held at 3-5 mm from the surface and at 45° angulation to it. After this, the prepared surfaces were thoroughly washed with an air-water spray for 30 seconds and dried.

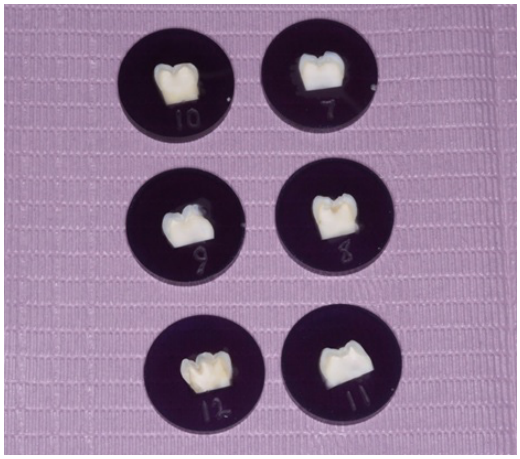

Fig. 5. *Tooth samples for TF-XRD.*

Samples from the control group were used for XRD of the dentin surface. Group 1 samples were used to detect diffraction peaks from the dentin surface after the application of EP; Group 2 samples were used to identify changes, such as the diffraction peaks, after sequential application of EP and OSP to the dentin surface.

Statistical analysis was performed using StatSoft Statistica v6.0. The probability value of $P<0.05$ was considered statistically significant.

Results

A comparative analysis of the obtained data (Table 1) revealed that applying EP to the dentin surface before OSP did not significantly affect bond strength. However, a significant difference of more than three times ($P<0.0001$) was observed between the first and second test values in samples of Group 1 than in Group 2.

Table 1.

Influence of experimental 10-MDP primer (EP) pretreatment on shear bond strength of Optibond Solo Plus (OSP) to dentin.

Group	Group 1 (n=10) (Total-etch, OSP)			Group 2 (n=10) (Selective-etch, EP-OSP)		
SBS test	1st test	2nd test	Δ^*_1	1st test	2nd test	Δ^*_2
Bond strength, lb	25.0 29.4 27.3 28.2 31.1 25.1 21.2 26.4 24.3 28.2	28.9 25.8 24.1 24.1 27.4 27.8 23.5 29.3 21.1 32.1	3.9 3.6 3.2 4.1 3.7 2.7 2.3 2.9 3.2 3.9	26.4 27.3 28.1 29.1 25.4 20.1 27.2 25.2 27.5 29.8	26.5 28.3 26.9 28.7 24.3 20.3 29.6 25.4 24.9 30.1	0.1 1.0 1.2 0.4 1.1 0.2 2.4 0.2 2.6 0.3
M ± SD	26.6±2.8	26.4±3.3	3.4±0.6	26.6±2.7	26.5±2.9	1.0±0.9
P-value	0.728			0.936		
$P^*<0.0001$ (between Δ^*_1 and Δ^*_2)						

SEM of resin-composite-to-dentin interfaces in Group 1 samples (Figure 6A) revealed an uneven hybrid layer width, with varying depths of adhesive resin penetration into dentinal tubules. In some areas, signs of penetration were completely absent, while in others, the adhesive tags reached 10-12 μm.

On the other hand, SEM of the filling-to-dentin interface surface in Group 2 samples (Figure 6B) demonstrated the presence of a uniform hybrid layer and comparatively better obturation of the dentinal tubules.

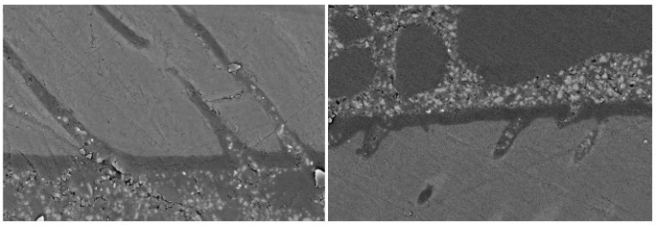

A B

Fig. 6. *A - Sector of the filling-to-dentin interface of the Group 1 sample; B- Sector of the filling-to-dentin interface of the Group 2 sample.*

SEM images of the dental composite-to-enamel interface in both groups of samples (Figure 7A,B) were of similar quality, reflecting the presence of both a tight adhesion and loose marginal adaptation.

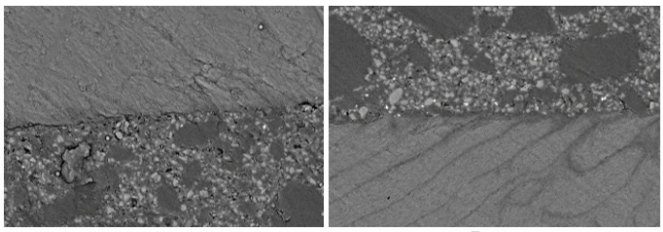

A B

Fig. 7. *A - Sector of the filling-to-enamel interface of the Group 1 sample; B – Sector of the filling-to-enamel interface of the Group 2 sample.*

As for microleakage, examination of sections from tooth samples in both groups showed no significant difference in the degree of DP between the composite filling and the enamel margin. However, a microscopic examination of the interface between the composite filling and dentin (Figure 4) revealed a significantly higher leakage rate in Group 1 samples (Tables 2 and 3). Instead, Group 2 samples showed reliable adhesion of the biomaterial to dentin in 80% of cases.

Table 2.

Frequency table of the microleakage scores in groups

Site of microleakage	Enamel-filling interface	Dentin-filling interface
Nonparametric scale (score)	0 1 2 3 4	0 1 2 3 4
Total-etch mode (OSP)	7 2 1 0 0	4 1 2 2 1
Selective-etch mode (EP, OSP)	8 1 1 0 0	8 1 1 0 0

Table 3.

Descriptive statistics of the microleakage scores in groups.

Site of microleakage	Mode	Min	Max	Mean±SD	*P*
Enamel-filling interface	Total-etch mode (OSP)	0	2	0.4±0.7	>0.05
	Selective-etch mode (EP, OSP)	0	2	0.3±0.7	
Dentin-filling interface	Total-etch mode (OSP)	0	4	1.5±1.5	<0.05
	Selective-etch mode (EP, OSP)	0	2	0.3±0.7	

Analysis of the phase composition of the dentin surface revealed a weak peak at 2θ=2.40º, likely indicating hydroxyapatite crystal destruction after mechanical processing (Figure 8). Application of EP to the dentin surface resulted in the appearance of three peaks at 2θ=2.42°, 4.29°, and 6.32°, suggesting the formation of 10-MDP–Ca salts. Sequential application of EP and OSP onto the dentin surface also caused changes in both the number of peaks (2θ = 2.54º and 4.31º) and their slight shift toward higher angles.

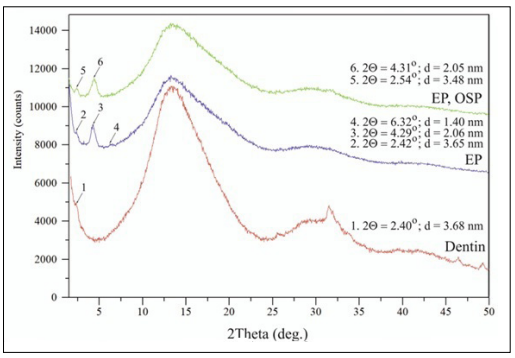

Fig. 8. *TF-XRD patterns of samples under study.*

Discussion

Minimal invasiveness and maximum biocompatibility remain priority principles for developing new materials and techniques for the treatment and restoration of teeth.[11] Thus, Buonocore's discovery was revolutionary in adhesive dentistry, shifting the field from macroretention to microretention of dental restorations.[12] Later, the development and introduction of acidic monomers capable of forming acid-base-resistant ionic bonds with dental hydroxyapatite enabled the transition from micro retention to nano retention.[9,13,14] Despite their high chemical reactivity, these compounds have high biocompatibility and low cytotoxicity, in contrast to the monomers that make up total-etch adhesive systems.[15]

Fifth-generation adhesive systems are complex mixtures that combine multiple monomers and other components. Their effectiveness depends on their ability to penetrate the surfaces of tooth enamel and dentin, which requires preliminary acid etching.[16]

Given the absence of active monomers in their composition, the main objective of this pilot study was to improve the adhesive potential of OSP by replacing the acid etching of dentin with the application of an experimental 10-MDP primer on its surface.

It should be noted that the SBS test protocol included certain features. Specifically, two consecutive tests were performed on each tooth sample after the application of the adhesive resin, allowing assessment of the bond strength of the composite material across different areas of the dentin surface and calculation of the difference between the SBS values.

The study results showed that applying experimental 10-MDP monomer (pH=2.4) prior to adhesive resin may be of practical value. Despite the lack of difference in the strength of adhesion to dentin between the groups, the SBS values of the experimental group samples were the most similar, which, to some extent, was indicative of the uniformity of the formed hybrid layer.

An analysis of SEM images of the filling-to-dentin interface of the tooth made it possible to establish fundamental differences in the quality of the hybrid layer of samples of Groups 1and 2, and to explain the reason for the significant difference in the bond strength between the average values of the first and second sequential tests in Group 1 samples.

The chemical structure of 10-MDP includes a phosphate group and a long carbon chain (hydrophobic), allowing it to interact with both the hydrophilic mineral phase of tooth structure and the hydrophobic monomers of dental adhesives. Due to its amphiphilic nature, 10-MDP can act as a surfactant, reducing surface tension and promoting wetting and the penetration of the hydrophobic adhesive resin into the tooth structure. This improved wetting can promote the formation of a strong and durable bond.[12,17]

Results of the microleakage test may strongly support the presence of stable adhesion between the resin composite and tooth dentin when an experimental 10-MDP primer is applied prior to the test, even after simulating the aging of the adhesive bond by conducting 5000 thermocycles.

Analysis of the phase composition of the dentin surface in samples from different groups revealed the presence of several

crystalline phases, with slight shifts in peak positions toward higher angles. For example, on the surfaces of samples from the control group, a peak was detected only at 2θ=2.40°, attributed to air-abrasive treatment of the dentin surface with an erythritol-based powder. However, no data in the available literature indicated the possibility of similar changes caused by air abrasion.

The appearance of additional crystalline phases (peaks #3 and #4) on the dentin surface of Group 1 samples in the range of 2θ=4.29º and 6.32º, as well as a slight increase in the angle of the first reflex (peak #2) to 2θ=2.42º, indicated the formation of 10-MDP–Ca salts. The position of these peaks corresponded to the literature data.[10,14]

Sequential application of EP and OSP on the dentin surface decreased the number of peaks (2θ = 2.54º and 4.31º) and increased the angles (peaks #5 and #6). Considering the small interplanar distance of peak #4 (2θ = 6.32º, d = 1.4 nm), the complete disappearance of this crystalline phase in Group 2 samples was attributed either to its dissolution or to its overlap with components of the OSP adhesive resin.

Thus, based on the data obtained, it was concluded that replacing traditional acid etching of dentin with the application of a 10-MDP-containing EP may constitute a new adhesive technique in clinical practice, facilitating reliable and predictable adhesion of composite materials to dentin when using fifth-generation adhesive systems with a selective acid etching approach. Also, the presence of 10-MDP–Ca salt peak at diffraction angle of 2θ=2.54º was probably the most significant for tooth dentin adhesion, as it represented the strong signal in XRD analysis, corresponding to the longest d-spacing (3.48 nm) of the nanolayered structure and underpinned the possibility of selective etch technique for adhesive system of fifth generation, but only in the case of 10-MDP primer application.

Ethical Statement

The study was approved by the Ethics Committee of the Institute of Medicine RUDN (Protocol Number: 29, dated 06.20.2024). Written informed consent was obtained from all participants prior to the processing of their teeth.

Competing Interests

The authors declare that they have no competing interests.

References

1. Perdigão J, Araujo E, Ramos RQ, Gomes G, Pizzolotto L. Adhesive dentistry: Current concepts and clinical considerations. J Esthet Restor Dent. 2021 Jan;33(1):51-68. doi: 10.1111/jerd.12692.
2. Sofan E, Sofan A, Palaia G, Tenore G, Romeo U, Migliau G. Classification review of dental adhesive systems: from the IV generation to the universal type. Ann Stomatol (Roma). 2017 Jul 3;8(1):1-17. doi: 10.11138/ads/2017.8.1.001.
3. Kumar S, Kumar PS, Vidhya S, Mahalaxmi S, Purushothaman PV. Influence of varying dry air temperatures on postoperative sensitivity, penetration depth, and push-out bond strength of an ethanol/water-based adhesive: An in vivo double-blind clinical trial and in vitro analysis. J Conserv Dent. 2023 Jan-Feb;26(1):88-93. doi: 10.4103/jcd.jcd_454_22.
4. Pheerarangsikul N, Wayakanon P, Wayakanon K. Effects of Various Functional Monomers on Adhesion Between Immediate Dentin Sealing and Resin Cement. Oper Dent. 2022 Sep 1;47(5):562-573. doi: 10.2341/21-057-L.
5. Melkumyan TV, Kakhkharova DJ, Dadamova AD, Kamilov NKh, Siddikova SSh, Rakhmatullaeva ShI, et al. Comparative analysis of in vitro Performance of Total-Etch and Self-Etch Adhesives. International Journal of Biomedicine. 2016; 6(4):283-286. 10.21103/Article6(4)_OA7
6. Giannini M, Makishi P, Ayres AP, Vermelho PM, Fronza BM, Nikaido T, Tagami J. Self-etch adhesive systems: a literature review. Braz Dent J. 2015 Jan-Feb;26(1):3-10. doi: 10.1590/0103-6440201302442.
7. Wang R, Shi Y, Li T, Pan Y, Cui Y, Xia W. Adhesive interfacial characteristics and the related bonding performance of four self-etching adhesives with different functional monomers applied to dentin. J Dent. 2017 Jul; 62:72-80. doi: 10.1016/j.jdent.2017.05.010.
8. Yoshida Y, Nagakane K, Fukuda R, Nakayama Y, Okazaki M, Shintani H, et al. Comparative study on adhesive performance of functional monomers. J Dent Res. 2004 Jun;83(6):454-8. doi: 10.1177/154405910408300604.
9. Yoshida Y, Yoshihara K, Hayakawa S, Nagaoka N, Okihara T, Matsumoto T, et al. HEMA inhibits interfacial nano-layering of the functional monomer MDP. J Dent Res. 2012 Nov;91(11):1060-5. doi: 10.1177/0022034512460396.
10. Zhou L, Wang Y, Yang H, Guo J, Tay FR, Huang C. Effect of chemical interaction on the bonding strengths of self-etching adhesives to deproteinised dentine. J Dent. 2015 Aug;43(8):973-80. doi: 10.1016/j.jdent.2015.05.010.
11. Yoshihara K, Nagaoka N, Nakamura A, Hara T, Yoshida Y, Van Meerbeek B. Nano-Layering Adds Strength to the Adhesive Interface. J Dent Res. 2021 May;100(5):515-521. doi: 10.1177/0022034520979133.
12. Carrilho E, Cardoso M, Marques Ferreira M, Marto CM, Paula A, Coelho AS. 10-MDP Based Dental Adhesives: Adhesive Interface Characterization and Adhesive Stability-A Systematic Review. Materials (Basel). 2019 Mar 7;12(5):790. doi: 10.3390/ma12050790.
13. Tian F, Zhou L, Zhang Z, Niu L, Zhang L, Chen C, et al. Paucity of Nanolayering in Resin-Dentin Interfaces of MDP-based Adhesives. J Dent Res. 2016 Apr; 95(4):380-7. doi: 10.1177/0022034515623741.
14. Ahmed MH, Esteban DA, Attik N, Awad MM. Nanomechanical interlocking mechanism of 10-MDP nanolayering. Sci Rep. 2025 Aug 5;15(1):28548. doi: 10.1038/s41598-025-14181-y.
15. Khabadze Z, Abdulkerimova S, Lokhonina A, Generalova Yu, Eremina I, Borlakova M, et al. Investigation of Cytotoxicity of Dental Light-Curing Composite Materials. Journal of International Dental and Medical Research. 2023; 16(4):1489-1493.
16. Hiraishi N, Tochio N, Kigawa T, Otsuki M, Tagami J. Monomer-collagen interactions studied by saturation transfer difference NMR. J Dent Res. 2013 Mar;92(3):284-8. doi: 10.1177/0022034512474310.
17. Yoshihara K, Nagaoka N, Yoshida Y, Van Meerbeek B, Hayakawa S. Atomic level observation and structural analysis of phosphoric-acid ester interaction at dentin. Acta Biomater. 2019 Oct 1;97:544-556. doi: 10.1016/j.actbio.2019.08.029.

***Corresponding author:** *Prof. Timur V. Melkumyan, PhD, ScD. Tashkent State Dental Institute Tashkent, Uzbekistan. Peoples' Friendship University of Russia (RUDN University), Moscow, Russia. E-mail: t.dadamov@gmail.com*

International Journal of Biomedicine 16(1) (2026) 107-110
http://dx.doi.org/10.21103/Article16(1)_CR1

CASE REPORT

INTERNATIONAL JOURNAL OF BIOMEDICINE

Comparative Surgical Strategies for Esophageal Injuries Following Penetrating Thoracoabdominal Gunshot Wounds: Two Case Reports and Literature Review

Valmira Abilaliaj[1*], Dritan Cela[1], Aldo Shpuza[2]

[1]*Department of Surgery, University Trauma Hospital, Tirana, Albania*
[2]*Department of Hospital Infection Prevention, University Trauma Hospital, Tirana, Albania*

Abstract

Background: Esophageal injuries following penetrating thoracoabdominal gunshot wounds are rare (<1% of trauma admissions) and carry substantial morbidity if diagnosis and treatment are delayed. We describe two patients with similar injury patterns who were managed with different surgical strategies and summarize the recent literature to contextualize decision-making.
Case Presentations: Case 1 involved a 28-year-old male with thoracoabdominal gunshot trauma, right hemopneumothorax, and distal esophageal leak. Following initial abdominal repair of the diaphragm and esophagus with jejunostomy, a persistent esophageal fistula was detected on postoperative day 5. Endoscopic stent placement achieved complete resolution within 4 weeks. Follow-up at 1, 3, and 6 months revealed normal swallowing with no late fistula.
Case 2 concerned an 11-year-old male with hemodynamic instability after a trans-thoracic gunshot wound causing bilateral diaphragmatic, gastric, and hepatic injuries. A right thoracotomy with primary esophageal repair was performed. Recovery was uneventful. At 3 and 6 months, oral intake was well tolerated with no fistula or stricture.
These cases emphasize tailoring the surgical approach to hemodynamic status and imaging findings. A stepwise strategy with delayed thoracic intervention and endoscopic stenting can limit initial invasiveness in stable patients, whereas immediate thoracotomy is lifesaving in unstable cases. Contemporary series support early diagnosis, selective use of endoscopy/stenting, and structured nutritional support to reduce leak risk and mortality.
Conclusion: Individualized timing and modality of surgical intervention, combined with multidisciplinary coordination, are pivotal to optimizing outcomes in penetrating esophageal trauma.(**International Journal of Biomedicine. 2026;16(1):107-110.**)

Keywords: penetrating trauma • thoracoabdominal gunshot wound • thoracotomy • endoscopic stent

For citation: Abilaliaj V, Cela D, Shpuza A. Comparative Surgical Strategies for Esophageal Injuries Following Penetrating Thoracoabdominal Gunshot Wounds: Two Case Reports and Literature Review. International Journal of Biomedicine. 2026;16(1):107-110. doi:10.21103/Article16(1)_CR1

Introduction

Penetrating esophageal trauma is uncommon, accounting for less than 1% of all trauma admissions, but it carries a high risk of morbidity and mortality due to delayed recognition, mediastinitis, and sepsis.[1] Early diagnosis remains challenging because clinical manifestations are often subtle and masked by concomitant thoracoabdominal injuries.[2] Optimal surgical management remains debated and largely depends on hemodynamic stability, extent of contamination, and associated organ injuries.[3] Immediate thoracotomy and primary repair are recommended in unstable patients or when contamination is severe, while staged or minimally invasive approaches—including endoscopic stenting and delayed repair—may be suitable for stable patients.[1,4] We report two cases of penetrating thoracoabdominal gunshot wounds involving the esophagus, managed with different surgical strategies according to physiological status: a stepwise approach versus immediate thoracotomy. Their comparison is followed by a brief review of the current literature to contextualize evolving surgical decision-making in this rare but life-threatening condition.[5]

The cases were retrospectively reviewed at the University Hospital of Trauma (Tirana, Albania), focusing on clinical presentation, imaging findings, surgical management, and postoperative outcomes. Diagnostic evaluation included

contrast-enhanced computed tomography (CT) and contrast swallow studies, performed according to institutional trauma protocols.

To provide clinical context and comparative interpretation, a brief review of relevant publications on penetrating esophageal injuries and their surgical management was conducted using PubMed. Priority was given to recent articles and reviews discussing the timing of intervention, the choice of surgical approach, and the role of endoscopic stenting. The aim was to situate the reported cases within the current evidence and highlight practical decision-making considerations.

Case Presentations

Case 1

A 28-year-old male sustained a thoracoabdominal gunshot wound. Initial imaging revealed a right hemopneumothorax, diaphragmatic laceration, and distal esophageal leakage. The patient underwent abdominal repair of the diaphragm and esophagus and a feeding jejunostomy. On postoperative day (POD) 5, clinical suspicion and imaging confirmed a persistent esophageal fistula (Grade 5). Endoscopic esophageal stenting was performed, with complete resolution within 4 weeks. Oral diet was progressively reinstated. Follow-up at 1, 3, and 6 months showed normal swallowing and no late fistula or stricture. Preoperative imaging is shown in Figure 1; postoperative imaging after endoscopic stent placement is shown in Figures 2 and 3.

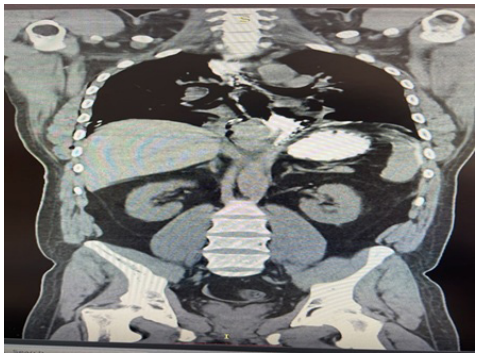

Fig. 1. *Preoperative CT scan showing right hemopneumothorax and distal esophageal leak.*

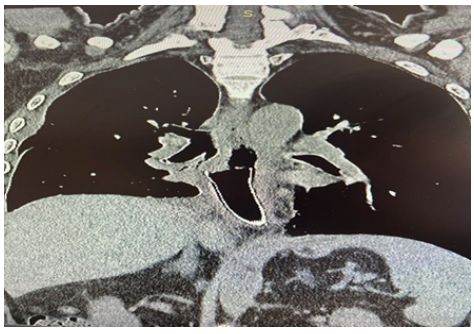

Fig. 2. *Postoperative CT scan after endoscopic stent placement demonstrating containment of the esophageal leak.*

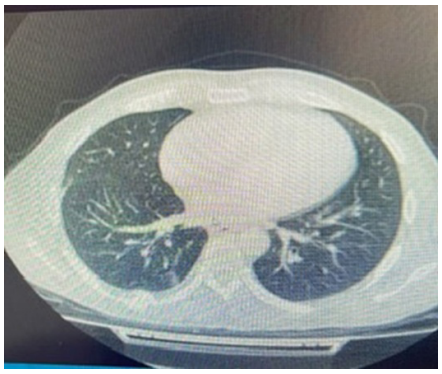

Fig. 3. *Six-month follow-up CT scan showing complete healing of the distal esophageal lesion with no evidence of leak or mediastinal collection. Lung fields are clear and symmetrically expanded.*

Case 2

An 11-year-old male presented hemodynamically unstable following a trans-thoracic gunshot wound with entry at the left anterior axillary line and exit at the right mid-axillary line. Emergency laparotomy identified bilateral diaphragmatic tears, gastric injury, and segment VII liver involvement. A contrast-enhanced CT scan subsequently demonstrated a lower esophageal leak. The patient underwent right thoracotomy with primary esophageal repair. Postoperative recovery was uneventful. At 3- and 6-month follow-up, oral feeding was well tolerated without dysphagia, fistula, or stricture. Preoperative imaging is shown in Figure 4; three-month postoperative imaging is shown in Figure 5.

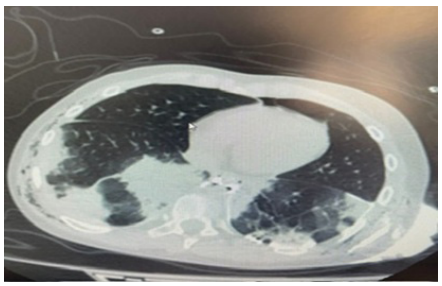

Fig. 4. *Preoperative CT scan demonstrating lower esophageal leak and associated thoracoabdominal injuries (diaphragm, stomach, and liver involvement).*

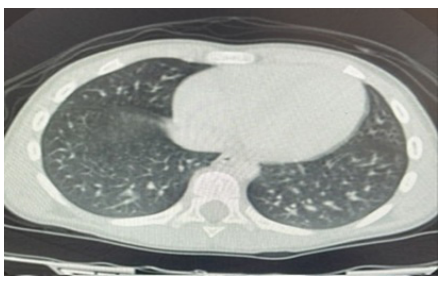

Fig. 5. *Three-month postoperative CT scan showing intact esophageal repair with normal mediastinal structures and no recurrence of leak.*

Discussion

These cases illustrate two complementary paradigms in managing penetrating esophageal injuries. In stable patients, staged management with early nutritional access, vigilant leak surveillance, and selective endoscopic stenting can obviate the need for immediate thoracotomy while achieving durable healing. In unstable patients or when contamination is extensive, prompt thoracic exploration and primary repair remain the standard. Key decision factors include hemodynamic status, injury location, contamination burden, associated injuries, and institutional expertise.

Endoscopic stenting has emerged as a valuable adjunct in managing postoperative leaks and selected traumatic perforations, serving as a bridge to recovery while protecting the repair and enabling enteral nutrition. A multidisciplinary approach—including trauma surgery, thoracic surgery, endoscopy, intensive care, radiology, and nutrition—optimizes timing and reduces complications. Reported predictors of adverse outcomes include delayed diagnosis (>24 hours), mediastinal contamination, and severe associated injuries. Early recognition, tailored repair or diversion, and structured follow-up are therefore essential. Representative images for both cases are shown in Figures 1–4.

Over the last decade, several multicenter and registry-based studies have refined the management of penetrating esophageal trauma. The AAST and EAST collaborative analyses [6,7] emphasize that early recognition within 24 hours remains the strongest predictor of survival. Contemporary reviews highlight the progressive role of endoscopic interventions, including stenting and vacuum-assisted closure, as adjuncts to surgical repair.[4]

Studies comparing immediate thoracotomy to staged or minimally invasive approaches show comparable mortality when the delay does not exceed 24 hours, and contamination is controlled.[8,9] Early nutritional support via jejunostomy and the selective endoscopic therapy have been associated with reduced mediastinitis and shorter hospital stay.

Literature increasingly emphasizes the role of coordinated care among trauma surgeons, thoracic surgeons, and endoscopists in individualizing treatment. The use of standardized postoperative imaging and nutritional follow-up, as illustrated in our two cases, aligns best with WSES recommendations.[5]

Our two cases exemplify opposite but equally valid management paths: a stable adult patient benefiting from minimally invasive stenting, and a hemodynamically unstable pediatric patient salvaged through immediate thoracotomy. Both strategies achieved leak control and functional recovery without stricture, consistent with the <10% leak rate reported in contemporary series when treatment is individualized.

Taken together, the synthesis of recent evidence supports a paradigm shift from a one-size-fits-all surgical model to physiology-driven decision-making. Early imaging, timely intervention, and the selective use of endoscopic stents have markedly improved survival and functional outcomes in penetrating esophageal trauma.

Penetrating esophageal injuries remain uncommon but clinically formidable because early signs can be subtle while the risk of mediastinitis and sepsis rises rapidly with delay. Extensive multiinstitutional experience emphasizes that timely diagnosis (ideally <24 hours), adequate source control, and restoration of alimentary continuity are the pillars of care.[6,10] Our two cases reinforce that the choice between immediate thoracic exploration and a staged approach should be individualized, primarily based on hemodynamic status, associated injuries, the anatomic location of the perforation, and contamination burden.

In unstable patients, prompt thoracic exposure with primary repair remains the standard because it achieves rapid control of contamination and bleeding and permits wide mediastinal debridement when needed.[6] By contrast, in physiologically stable patients without overwhelming contamination, a stepwise plan that prioritizes early nutritional access (e.g., feeding jejunostomy), vigilant leak surveillance, and delayed thoracic intervention can be both safe and organpreserving.[4] Observational series and contemporary reviews suggest that this selective strategy does not compromise outcomes when strict monitoring and early reintervention thresholds are observed.[4,7,8]

Therapeutic endoscopy with covered stent placement has emerged as an effective adjunct for postoperative leaks and certain contained traumatic perforations, reducing ongoing contamination, protecting the repair, and enabling enteral nutrition.[4,11,12] In Case 1, an esophageal fistula identified on POD 5 was successfully bridged with an endoscopic stent, with complete resolution after four weeks and excellent mediumterm function. Systematic appraisals indicate that stent therapy is most effective when instituted early, in the absence of uncontrolled sepsis, and when accompanied by drainage and antibiotic therapy; careful followup is essential to detect migration or stricture.[4]

Clinical suspicion must remain high in thoracoabdominal gunshot wounds that traverse the mediastinum. Crosssectional imaging with contrast, selective contrast swallow, and early endoscopy are complementary modalities; institutional protocols that integrate these tests shorten timetodiagnosis and improve outcomes.[5,10,13] The World Society of Emergency Surgery (WSES) guidelines support tailored diagnostic algorithms and emphasize damagecontrol principles in unstable patients.[5]

Across historical and contemporary cohorts, predictors of morbidity and mortality include delayed presentation (>24 hours), extensive mediastinal contamination, cervical vs. thoracic location differences, and severe associated injuries.[6,7,9,10] Registry analyses underscore that noniatrogenic esophageal trauma frequently coexists with major thoracoabdominal injuries, making coordinated, multidisciplinary management pivotal.[7,9] Our cases align with these observations: the unstable pediatric patient benefited from immediate thoracotomy and primary repair, whereas the stable adult patient achieved healing with a staged, minimally disruptive pathway. Implications for practice. These experiences support a pragmatic algorithm: (i) resuscitate and triage by physiology; (ii) obtain early crosssectional imaging ± endoscopy; (iii) choose immediate thoracic repair when unstable or when contamination is diffuse; (iv) consider staged management

with nutritional access and selective stenting when stable and contamination is limited; and (v) ensure structured followup to detect late complications such as leak, stricture, or dysphagia.[4-7,9] Within such a framework, individualized timing and modality of intervention, together with early nutrition and close surveillance, optimize functional recovery while minimizing reoperation and longterm morbidity.

Conclusion

Tailored surgical strategies based on physiological status and imaging are central to successful outcomes in penetrating esophageal trauma. Staged management with endoscopic stenting can be effective in stable patients, while immediate thoracotomy is indispensable in unstable scenarios. Multidisciplinary coordination and early nutritional planning are crucial to minimize leaks, infections, and long-term morbidity.

Conflicts of Interest

The authors declare that they have no competing interests.

References

1. Mubang RN, Sigmon DF, Stawicki SP. Esophageal Trauma. 2023 Jul 25. In: StatPearls [Internet]. Treasure Island (FL): StatPearls Publishing; 2025 Jan–. PMID: 29261892.
2. Petrone P, Kassimi K, Jiménez-Gómez M, Betancourt A, Axelrad A, Marini CP. Management of esophageal injuries secondary to trauma. Injury. 2017 Aug;48(8):1735-1742. doi: 10.1016/j.injury.2017.06.012. Epub 2017 Jun 19. PMID: 28648409.
3. Petrone P, Kassimi K, Jiménez-Gómez M, Betancourt A, Axelrad A, Marini CP. Management of esophageal injuries secondary to trauma. Injury. 2017 Aug;48(8):1735-1742. doi: 10.1016/j.injury.2017.06.012. Epub 2017 Jun 19. PMID: 28648409.
4. Sudarshan M, Cassivi SD. Management of traumatic esophageal injuries. J Thorac Dis. 2019 Feb;11(Suppl 2):S172-S176. doi: 10.21037/jtd.2018.10.86. PMID: 30906582; PMCID: PMC6389559.
5. Chirica M, Kelly MD, Siboni S, Aiolfi A, Riva CG, Asti E, et al. Esophageal emergencies: WSES guidelines. World J Emerg Surg. 2019 May 31;14:26. doi: 10.1186/s13017-019-0245-2. PMID: 31164915; PMCID: PMC6544956.
6. Asensio JA, Chahwan S, Forno W, MacKersie R, Wall M, Lake J, et al.; American Association for the Surgery of Trauma. Penetrating esophageal injuries: multicenter study of the American Association for the Surgery of Trauma. J Trauma. 2001 Feb;50(2):289-96. doi: 10.1097/00005373-200102000-00015. PMID: 11242294.
7. Raff LA, Schinnerer EA, Maine RG, Jansen J, Noorbakhsh MR, Spigel Z, et al.. Contemporary management of traumatic cervical and thoracic esophageal perforation: The results of an Eastern Association for the Surgery of Trauma multi-institutional study. J Trauma Acute Care Surg. 2020 Oct;89(4):691-697. doi: 10.1097/TA.0000000000002841. PMID: 32590561.
8. Bhatia P, Fortin D, Inculet RI, Malthaner RA. Current concepts in the management of esophageal perforations: a twenty-seven year Canadian experience. Ann Thorac Surg. 2011 Jul;92(1):209-15. doi: 10.1016/j.athoracsur.2011.03.131. PMID: 21718846.
9. Aiolfi A, Inaba K, Recinos G, Khor D, Benjamin ER, Lam L, Strumwasser A, Asti E, Bonavina L, Demetriades D. Non-iatrogenic esophageal injury: a retrospective analysis from the National Trauma Data Bank. World J Emerg Surg. 2017 Apr 27;12:19. doi: 10.1186/s13017-017-0131-8. PMID: 28465715; PMCID: PMC5408440.
10. Søreide JA, Viste A. Esophageal perforation: diagnostic work-up and clinical decision-making in the first 24 hours. Scand J Trauma Resusc Emerg Med. 2011 Oct 30;19:66. doi: 10.1186/1757-7241-19-66. PMID: 22035338; PMCID: PMC3219576.
11. Herrera A, Freeman RK. The Evolution and Current Utility of Esophageal Stent Placement for the Treatment of Acute Esophageal Perforation. Thorac Surg Clin. 2016 Aug;26(3):305-14. doi: 10.1016/j.thorsurg.2016.04.012. PMID: 27427525.
12. Papaefthymiou A, Gkolfakis P, Basiliya K, Ramai D, Tziatzios G, Sehgal V, Telese A, Norton B, Aslam N, Johnson G, Haidry R. Success rates of fixation techniques on prevention of esophageal stent migration: a systematic review and meta-analysis. Endoscopy. 2024 Jan;56(1):22-30. doi: 10.1055/a-2147-8294. Epub 2023 Aug 3. PMID: 37536365.
13. Makhani M, Midani D, Goldberg A, Friedenberg FK. Pathogenesis and outcomes of traumatic injuries of the esophagus. Dis Esophagus. 2014 Sep-Oct;27(7):630-6. doi: 10.1111/dote.12132. Epub 2013 Aug 29. PMID: 24033532; PMCID: PMC3938994.

***Corresponding author**: Valmira Abilaliaj, MD. E-mail: valmiraabili@gmail.com / valmira.abilaliaj@sut.gov.al*

International Journal of Biomedicine 16(1) (2026) 111-115
http://dx.doi.org/10.21103/Article16(1)_CR2

CASE REPORT

INTERNATIONAL JOURNAL OF BIOMEDICINE

Hidden Behind the Headache: A Rare Case Report of Childhood Nasopharyngeal Cancer

Danu Yudistira[1*], Sagung Rai Indrasari[2], Camelia Herdini[2], Nurul Annisa Shafira Maheswari[1]

[1]Faculty of Medicine, Public Health, and Nursing, Gadjah Mada University, Yogyakarta, Indonesia
[2]Department of Otorhinolaryngology–Head and Neck Surgery, Dr. Sardjito General Hospital, Yogyakarta, Indonesia

Abstract

Nasopharyngeal carcinoma is a rare malignancy in children, representing less than one percent of pediatric cancers, with incidence varying across regions. A fourteen-year-old boy presented with one month of right nasal obstruction, ear fullness, hearing loss, and progressive headache. Physical examination revealed a 20×20 mm mass at the level II of the neck. Anterior rhinoscopy revealed mucosal discharge and a friable mass occupying the right nasal cavity. The left nasal cavity showed inferior turbinate hypertrophy, livid mucosa, and mucous secretion, with a mass appearance suggestive of contralateral compression. Contrast-enhanced MSCT angiography of the head and neck revealed a bilateral solid nasopharyngeal mass (3.75×3.71×4.27 cm) with post-contrast enhancement, extending into the sphenoid sinus and associated with destruction of the right sphenoid and temporal bones. Because early symptoms are nonspecific, the diagnosis of nasopharyngeal carcinoma in children is often delayed. Early recognition and evaluation are essential to reduce morbidity and improve clinical outcomes.(**International Journal of Biomedicine. 2026;16(1):111-115.**)

Keywords: nasopharyngeal carcinoma • childhood • symptoms • epidemiology

For citation: Yudistira D, Indrasari SR, Herdini C, Maheswari NAS. Hidden Behind the Headache: A Rare Case Report of Childhood Nasopharyngeal Cancer. International Journal of Biomedicine. 2026;16(1):111-115. doi:10.21103/Article16(1)_CR2

Introduction

Nasopharyngeal carcinoma (NPC) is a malignant epithelial neoplasm of the nasopharyngeal mucosa and represents a distinct clinical entity within head and neck oncology.[1-3] In the pediatric population, NPC is rare, accounting for less than 1% of all pediatric malignancies, and is particularly uncommon before the age of 10, with incidence rising during adolescence.[4,5] Reported rates are approximately 0.5 per million in those aged 10–14 years and 1.1 per million in adolescents aged 15–17 years, with a first incidence peak between 10 and 20 years and a median diagnostic age of 12–15 years.[3,6-10] In contrast, NPC in the general population is most commonly diagnosed in adults aged 40–60 years old.[3,8,9,11,12] Globally, incidence varies substantially, reaching as high as 40 per 100,000 annually in endemic regions such as southern China, Southeast Asia, Alaska, and the Mediterranean Basin, but remaining below 1 per 100,000 in most industrialized countries.[4,13,14] SEER data also show higher incidence among African American children, adolescents, and young adults compared with Caucasian individuals, underscoring the combined influence of genetic susceptibility and environmental exposures in NPC pathogenesis.[15] Nasopharyngeal carcinoma originates in deep head and neck structures, and symptoms often appear only after substantial local invasion, contributing to diagnostic delay.[3] In children and adolescents, more than 90 percent present with invasive disease, and over 80 percent are diagnosed at stage III or IV, higher proportions than in adults, although distant metastasis is less frequent.[5,7,16,17] Despite advanced presentation, outcomes in younger patients have improved significantly with combined radiotherapy and chemotherapy, yielding five-year survival rates above 80 percent and an overall better prognosis compared with adults.[18] These diagnostic challenges underscore the need for

***Corresponding author:** Danu Yudistira, MD. E-mail: dhanoetht@gmail.com*

early recognition and timely evaluation, which are essential for optimizing treatment outcomes.

Case Presentation

A 14-year-old male presented with a one-month history of progressive right-sided nasal congestion, accompanied by ipsilateral ear fullness, conductive hearing impairment, and increasingly severe headaches. He denied epistaxis, diplopia, recent trauma, allergic symptoms, or abnormal bleeding tendencies. His past medical history was notable only for a tonsillectomy at age 5. He was a non-smoker, although his father was an active smoker. His dietary history revealed frequent consumption of grilled foods, while intake of instant foods, packaged beverages, and salted fish was infrequent.

Initially, the patient was ordered an EEG examination due to a suspicion of epilepsy. Coincidentally, upon physical examination, a 20×20 mm mass was detected at level II of the neck (Figure 1). Oropharyngeal examination showed small tonsils (T1/T1) without hyperemia or granulation. Anterior rhinoscopy revealed mucosal discharge and a friable mass occupying the right nasal cavity. The left nasal cavity showed inferior turbinate hypertrophy, livid mucosa, and mucous secretion, with a mass appearance suggestive of contralateral compression (Figure 2). Otoscopic findings were normal bilaterally.

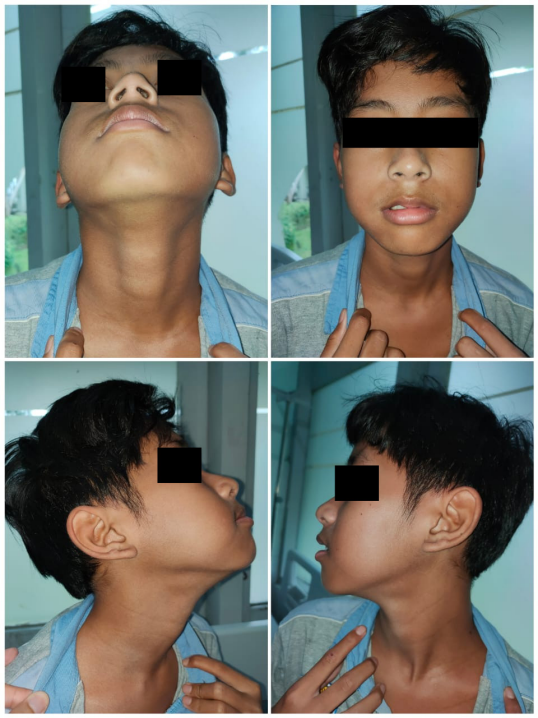

Figure 1. *Physical examination: A mass at the level II of the neck.*

Laboratory investigations demonstrated mild thrombocytosis (platelets 554 ×10³/µL) and a mildly prolonged APTT (42.4 seconds), with all other hematological, renal, hepatic, electrolyte, and viral serologic parameters within normal limits. Contrast-enhanced MSCT revealed a bilateral solid nasopharyngeal mass (3.75×3.71×4.27 cm) with post-contrast enhancement, extending into the sphenoid sinus and associated with destruction of the right sphenoid and temporal bones (Figure 3). Intracranial extension into the extra-axial prepontine space was noted, with vascular supply arising from the right ascending pharyngeal artery (branch of the internal maxillary artery). Bilateral ethmoiditis was also identified. No arterial thrombosis, stenosis, or aneurysm was observed. A prior contrast-enhanced head MSCT had demonstrated a similar malignant nasopharyngeal mass (3.56×2.80×3.80 cm) with intracranial extension, right mastoiditis, cerebral edema, and a metastatic-appearing nodule in the right level IIB cervical region. Chest radiography showed unremarkable cardiopulmonary findings. A bilateral nasopharynx mass biopsy revealed non-keratinizing squamous cell carcinoma (NK-NPC), undifferentiated subtype.

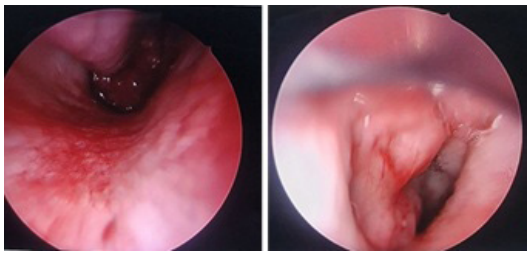

Figure 2. *Anterior rhinoscopy.*

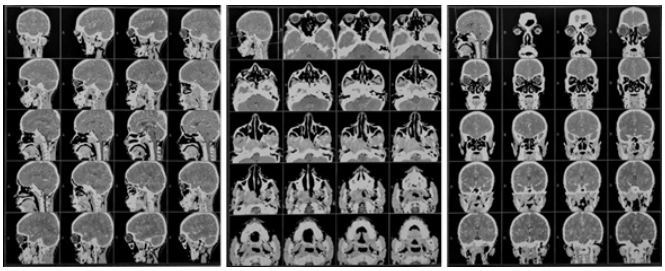

Figure 3. *Contrast-enhanced MSCT angiography of the head and neck.*

Discussion

Childhood nasopharyngeal carcinoma (NPC) is frequently diagnosed late, as its rarity, nonspecific early complaints, and anatomically deep location often keep it silent for a long time.[4,13] Initially, children with NPC present with a neck mass (60–90%), typically appearing as unilateral or bilateral, large, painless, non-inflammatory cervical lymphadenopathy.[5,14] Beyond this, additional nasal, auditory, and neurological symptoms may arise depending on the extent of primary tumor involvement. Nasal manifestations (obstruction, epistaxis, or mucous discharge) and auditory manifestations (otalgia, serous otitis media, and hearing impairment) are observed in 30-70% and 20–45% cases, respectively.[3-5] Compared with adolescents, nasal congestion was more frequently reported in younger children (36.8% vs. 9.4%), whereas ear-related symptoms were less common in this age group (15.8% vs. 53.1%). These

findings suggest that nasopharyngeal evaluation should be prioritized at initial presentation in younger children, whereas in adolescents, early assessment for auditory involvement is particularly warranted.[5] Less frequently, skull base invasion may result in cranial nerve palsies (5–22%), headaches (11–32%), and ocular symptoms (26%).[3,5,19,20] Other symptoms, such as trismus, taste disturbances, or dysphagia, are rarely described in pediatric NPC.[4] Nonspecific clinical manifestations, particularly in the absence of cervical lymphadenopathy, which is the most frequent presenting sign, may result in missed or delayed diagnosis.

In the present case, the patient presented with a one-month history of progressive right-sided nasal congestion, ear fullness, conductive hearing impairment, and worsening headaches. A 20×20 mm mass was found on examination, although the parents had not noticed or reported any neck swelling. Early symptoms of nasopharyngeal carcinoma are often misinterpreted as benign upper respiratory tract infections, underscoring the need for heightened clinical vigilance and thorough assessment of persistent or atypical symptoms in pediatric patients.

Accurate staging of pediatric NPC requires appropriate imaging and comprehensive clinical evaluation. The initial assessment should include a full physical examination of the cervical and supraclavicular lymph nodes and a thorough neurological evaluation, complemented by a contrast-enhanced MRI or CT scan of the head, neck, and supraclavicular regions.[14] MRI is generally superior to CT for evaluating the primary tumor and involved cervical and retropharyngeal lymph nodes in both adult and pediatric NPC, while CT may be useful when skull base invasion is uncertain.[21-25] In addition, chest and abdominal CT scans with iodine contrast should be performed to evaluate for distant metastases.[14] FDG PET/CT provides excellent detection of nodal and distant metastases.[26] When PET/CT is unavailable, combined CT and technetium bone scintigraphy may be used as an alternative.[27]

Staging of NPC requires precise assessment of locoregional tumor extension, skull base involvement, and distant metastases. Current staging practice follows the 8th edition of the American Joint Committee on Cancer (AJCC) Staging System, which provides standardized criteria for tumor (T), nodal (N), and metastatic (M) classifications to guide prognosis and treatment planning.[28] Nodal staging is based on clinical and radiologic findings. Lymph nodes are considered involved if the short-axis diameter exceeds 10 mm, demonstrates central necrosis or extracapsular spread on MRI/CT, or shows pathological uptake on FDG-PET.[3]

Cytological examination of enlarged nodes can aid diagnosis in ambiguous cases.[14] Histological confirmation is essential once clinical and radiological findings suggest NPC; this is preferably obtained via endoscopic exploration of the primary tumor, or alternatively, a large cervical lymph node may be biopsied. Nasopharyngeal endoscopy allows detailed evaluation of tumor location, extension, and potential complications such as bleeding. Pretreatment evaluation should include standard laboratory tests (hematological, hepatic, and renal function), oral and dental assessment, audiometry, DPD testing before 5-fluorouracil therapy, fertility preservation, serum and plasma EBV DNA evaluation, and molecular analyses.[14] Nearly all pediatric undifferentiated NPC cases show evidence of EBV infection in the primary tumor. High plasma EBV DNA levels have been identified as a negative prognostic factor in adults, and several pediatric studies have demonstrated similar trends.[3] Early-stage tumors may be subtle on endoscopy; therefore, MRI, PET/CT, and, when indicated, fine-needle aspiration of cervical nodes are commonly used. In children, diagnosis is most frequently established via biopsy of neck masses.[15,29]

According to the 4th edition of the WHO classification, NPC subtypes include keratinizing squamous cell carcinoma (KSCC, type I), non-keratinizing carcinoma (differentiated, type II; and undifferentiated, type III), and basaloid squamous cell carcinoma. KSCC, characterized by conventional squamous differentiation, intercellular bridges, and keratinization, is rare in children. Non-keratinizing undifferentiated carcinoma, the most common subtype in pediatric and young adult patients, is characterized by large tumor cells with prominent nuclei, scant cytoplasm, and high mitotic activity. KSCC accounts for less than 5% of NPCs, while non-keratinizing and anaplastic subtypes represent over 90% and are predominantly associated with Epstein-Barr virus (EBV) infection.[5,15,30-33] KSCC's relative radioresistance may contribute to poorer prognosis.[5]

This case underscores the importance of heightened clinical suspicion for NPC in children presenting with persistent unilateral nasal or otologic symptoms. Early distinction from common upper respiratory conditions is crucial. Failure to identify clinical warning signs, such as unilateral progressive obstruction, cranial nerve involvement, recurrent headaches, or epistaxis, may lead to a delayed diagnosis and significant consequences for prognosis and overall quality of life.

Conclusion

Pediatric nasopharyngeal carcinoma is rare yet frequently diagnosed at an advanced stage due to its deep location and initially nonspecific symptoms. This case highlights the need for heightened clinical suspicion when children present with persistent unilateral nasal or otologic complaints, particularly when accompanied by headaches or cranial nerve symptoms. Early recognition and timely diagnostic evaluation are essential, as prompt multimodal treatment can achieve favorable outcomes despite the typically advanced presentation.

Acknowledgment

We thank the patient's parents for permitting the authors to report their child's case.

Source of Funding

The authors received no specific grant from any funding agency in the public, commercial, or not-for-profit sectors

Competing Interests

The authors declare that they have no conflicts of interest.

References

1. Chang ET, Adami HO. The enigmatic epidemiology of nasopharyngeal carcinoma. Cancer Epidemiol Biomarkers Prev. 2006 Oct;15(10):1765-77. doi: 10.1158/1055-9965.EPI-06-0353. PMID: 17035381.
2. de Martel C, Ferlay J, Franceschi S, Vignat J, Bray F, Forman D, Plummer M. Global burden of cancers attributable to infections in 2008: a review and synthetic analysis. Lancet Oncol. 2012 Jun;13(6):607-15. doi: 10.1016/S1470-2045(12)70137-7. Epub 2012 May 9. PMID: 22575588.
3. Ben-Ami T. Nasopharyngeal Carcinoma in Children, Current Treatment Approach. J Pediatr Hematol Oncol. 2024 Apr 1;46(3):117-124. doi: 10.1097/MPH.0000000000002848. Epub 2024 Mar 5. PMID: 38447121; PMCID: PMC10956687.
4. Claude L, Jouglar E, Duverge L, Orbach D. Update in pediatric nasopharyngeal undifferentiated carcinoma. Br J Radiol. 2019 Oct;92(1102):20190107. doi: 10.1259/bjr.20190107. Epub 2019 Jul 31. PMID: 31322911; PMCID: PMC6774591.
5. Gong T, Liu Y, Jie H, Liang M, Wu W, Lu J. Retrospective analysis of clinical features and prognosis of nasopharyngeal carcinoma in children and adolescents. Front Pediatr. 2022 Sep 16;10:939435. doi: 10.3389/fped.2022.939435. PMID: 36186630; PMCID: PMC9523006.
6. Person L, Lacour B, Faure L, Guissou S, Poulalhon C, Orbach D, Goujon S, Berger C, Clavel J, Desandes E. Childhood head and neck cancer in France: Incidence, survival and trends from 2000 to 2015. Int J Pediatr Otorhinolaryngol. 2021 Nov;150:110858. doi: 10.1016/j.ijporl.2021.110858. Epub 2021 Aug 3. PMID: 34388659.
7. Casanova M, Bisogno G, Gandola L, Cecchetto G, Di Cataldo A, Basso E, Indolfi P, D'Angelo P, Favini F, Collini P, Potepan P, Ferrari A; Rare Tumors in Pediatric Age Group. A prospective protocol for nasopharyngeal carcinoma in children and adolescents: the Italian Rare Tumors in Pediatric Age (TREP) project. Cancer. 2012 May 15;118(10):2718-25. doi: 10.1002/cncr.26528. Epub 2011 Sep 14. PMID: 21918965.
8. Lei S, Chen L, Ji P, Li K, Li Q, Huang C, Wang G, Ma J, Guo R, Tang L. Global burdens of nasopharyngeal carcinoma in children and young adults and predictions to 2040. Oral Oncol. 2024 Aug;155:106891. doi: 10.1016/j.oraloncology.2024.106891. Epub 2024 Jun 14. PMID: 38878356.
9. Chang ET, Ye W, Zeng YX, Adami HO. The Evolving Epidemiology of Nasopharyngeal Carcinoma. Cancer Epidemiol Biomarkers Prev. 2021 Jun;30(6):1035-1047. doi: 10.1158/1055-9965.EPI-20-1702. Epub 2021 Apr 13. PMID: 33849968.
10. Pastore G, De Salvo GL, Bisogno G, Dama E, Inserra A, Cecchetto G, Ferrari A; TREP Group; CSD of Epidemiology Biostatistics, AIEOP. Evaluating access to pediatric cancer care centers of children and adolescents with rare tumors in Italy: the TREP project. Pediatr Blood Cancer. 2009 Aug;53(2):152-5. doi: 10.1002/pbc.22049. PMID: 19353626.
11. Bray F, Haugen M, Moger TA, Tretli S, Aalen OO, Grotmol T. Age-incidence curves of nasopharyngeal carcinoma worldwide: bimodality in low-risk populations and aetiologic implications. Cancer Epidemiol Biomarkers Prev. 2008 Sep;17(9):2356-65. doi: 10.1158/1055-9965.EPI-08-0461. PMID: 18768504.
12. Guo X, Cui J, Yuan X, Gao Z, Yu G, Wu H, Kou C. Long-term trends of nasopharyngeal carcinoma mortality in China from 2006 to 2020 by region and sex: an age-period-cohort analysis. BMC Public Health. 2023 Oct 20;23(1):2057. doi: 10.1186/s12889-023-16892-1. PMID: 37864181; PMCID: PMC10588046.
13. Dourthe ME, Bolle S, Temam S, Jouin A, Claude L, Reguerre Y, Defachelles AS, Orbach D, Fresneau B. Childhood Nasopharyngeal Carcinoma: State-of-the-Art, and Questions for the Future. J Pediatr Hematol Oncol. 2018 Mar;40(2):85-92. doi: 10.1097/MPH.0000000000001054. PMID: 29300240.
14. European Reference Network. Consensus Recommendations for Nasopharyngeal carcinoma in children and adolescents. Available from: https://siope.eu/media/documents/escp-nasopharyngeal-carcinoma-in-children-and-adolescents.pdf
15. Chen YP, Chan ATC, Le QT, Blanchard P, Sun Y, Ma J. Nasopharyngeal carcinoma. Lancet. 2019 Jul 6;394(10192):64-80. doi: 10.1016/S0140-6736(19)30956-0. Epub 2019 Jun 6. PMID: 31178151.
16. Cheuk DK, Billups CA, Martin MG, Roland CR, Ribeiro RC, Krasin MJ, Rodriguez-Galindo C. Prognostic factors and long-term outcomes of childhood nasopharyngeal carcinoma. Cancer. 2011 Jan 1;117(1):197-206. doi: 10.1002/cncr.25376. Epub 2010 Aug 24. PMID: 20737561; PMCID: PMC2994981.
17. Richards MK, Dahl JP, Gow K, Goldin AB, Doski J, Goldfarb M, Nuchtern J, Langer M, Beierle EA, Vasudevan S, Hawkins DS, Parikh SR. Factors Associated With Mortality in Pediatric vs Adult Nasopharyngeal Carcinoma. JAMA Otolaryngol Head Neck Surg. 2016 Mar;142(3):217-22. doi: 10.1001/jamaoto.2015.3217. PMID: 26769566.
18. Sahai P, Mohanti BK, Sharma A, Thakar A, Bhasker S, Kakkar A, Sharma MC, Upadhyay AD. Clinical outcome and morbidity in pediatric patients with nasopharyngeal cancer treated with chemoradiotherapy. Pediatr Blood Cancer. 2017 Feb;64(2):259-266. doi: 10.1002/pbc.26240. Epub 2016 Sep 29. PMID: 27681956.
19. Ayan I, Kaytan E, Ayan N. Childhood nasopharyngeal carcinoma: from biology to treatment. Lancet Oncol. 2003 Jan;4(1):13-21. doi: 10.1016/s1470-2045(03)00956-2. PMID: 12517535.
20. Qiu WZ, Peng XS, Xia HQ, Huang PY, Guo X, Cao KJ. A retrospective study comparing the outcomes and toxicities of intensity-modulated radiotherapy versus two-dimensional conventional radiotherapy for the treatment of children and adolescent nasopharyngeal carcinoma. J Cancer Res Clin Oncol. 2017 Aug;143(8):1563-1572. doi: 10.1007/s00432-017-2401-y. Epub 2017 Mar 25. PMID: 28342002; PMCID: PMC5504129.
21. Mohandas A, Marcus C, Kang H, Truong MT, Subramaniam RM. FDG PET/CT in the management of nasopharyngeal carcinoma. AJR Am J Roentgenol. 2014 Aug;203(2):W146-57. doi: 10.2214/AJR.13.12420. PMID: 25055290.
22. King AD, Vlantis AC, Bhatia KS, Zee BC, Woo JK, Tse GM, Chan AT, Ahuja AT. Primary nasopharyngeal carcinoma: diagnostic accuracy of MR imaging versus that of endoscopy

and endoscopic biopsy. Radiology. 2011 Feb;258(2):531-7. doi: 10.1148/radiol.10101241. Epub 2010 Dec 3. PMID: 21131580.
23. King AD, Teo P, Lam WW, Leung SF, Metreweli C. Paranasopharyngeal space involvement in nasopharyngeal cancer: detection by CT and MRI. Clin Oncol (R Coll Radiol). 2000;12(6):397-402. doi: 10.1053/clon.2000.9199. PMID: 11202093.
24. Cheuk DK, Sabin ND, Hossain M, Wozniak A, Naik M, Rodriguez-Galindo C, Krasin MJ, Shulkin BL. PET/CT for staging and follow-up of pediatric nasopharyngeal carcinoma. Eur J Nucl Med Mol Imaging. 2012 Jul;39(7):1097-106. doi: 10.1007/s00259-012-2091-2. Epub 2012 Apr 25. PMID: 22532252; PMCID: PMC3531235.
25. Zhang SX, Han PH, Zhang GQ, Wang RH, Ge YB, Ren ZG, Li JS, Fu WH. Comparison of SPECT/CT, MRI and CT in diagnosis of skull base bone invasion in nasopharyngeal carcinoma. Biomed Mater Eng. 2014;24(1):1117-24. doi: 10.3233/BME-130911. PMID: 24212004.
26. Shen G, Zhang W, Jia Z, Li J, Wang Q, Deng H. Meta-analysis of diagnostic value of 18F-FDG PET or PET/CT for detecting lymph node and distant metastases in patients with nasopharyngeal carcinoma. Br J Radiol. 2014 Dec;87(1044):20140296. doi: 10.1259/bjr.20140296. Epub 2014 Oct 28. PMID: 25348201; PMCID: PMC4243207.
27. Chua ML, Ong SC, Wee JT, Ng DC, Gao F, Tan TW, Fong KW, Chua ET, Khoo JB, Low JS. Comparison of 4 modalities for distant metastasis staging in endemic nasopharyngeal carcinoma. Head Neck. 2009 Mar;31(3):346-54. doi: 10.1002/hed.20974. PMID: 18972431.
28. Amin MB, Greene FL, Edge SB, Compton CC, Gershenwald JE, Brookland RK, Meyer L, Gress DM, Byrd DR, Winchester DP. The Eighth Edition AJCC Cancer Staging Manual: Continuing to build a bridge from a population-based to a more "personalized" approach to cancer staging. CA Cancer J Clin. 2017 Mar;67(2):93-99. doi: 10.3322/caac.21388. Epub 2017 Jan 17. PMID: 28094848.
29. King AD, Woo JKS, Ai QY, Chan JSM, Lam WKJ, Tse IOL, Bhatia KS, Zee BCY, Hui EP, Ma BBY, Chiu RWK, van Hasselt AC, Chan ATC, Lo YMD, Chan KCA. Complementary roles of MRI and endoscopic examination in the early detection of nasopharyngeal carcinoma. Ann Oncol. 2019 Jun 1;30(6):977-982. doi: 10.1093/annonc/mdz106. PMID: 30912815.
30. Ogun GO, Olusanya AA, Akinmoladun VI, Adeyemo AA, Ogunkeyede SA, Daniel A, Awosusi BL, Fatunla EO, Fasunla AJ, Onakoya PA, Adeosun AA, Nwaorgu OG. Nasopharyngeal carcinoma in Ibadan, Nigeria: a clinicopathologic study. Pan Afr Med J. 2020 Jun 9;36:82. doi: 10.11604/pamj.2020.36.82.19657. PMID: 32774641; PMCID: PMC7392876.
31. Liu W, Tang Y, Gao L, Huang X, Luo J, Zhang S, Wang K, Qu Y, Xiao J, Xu G, Yi J. Nasopharyngeal carcinoma in children and adolescents - a single institution experience of 158 patients. Radiat Oncol. 2014 Dec 5;9:274. doi: 10.1186/s13014-014-0274-7. PMID: 25477058; PMCID: PMC4264314.
32. Young LS, Dawson CW. Epstein-Barr virus and nasopharyngeal carcinoma. Chin J Cancer. 2014 Dec;33(12):581-90. doi: 10.5732/cjc.014.10197. Epub 2014 Nov 21. PMID: 25418193; PMCID: PMC4308653.
33. Pathmanathan R, Prasad U, Chandrika G, Sadler R, Flynn K, Raab-Traub N. Undifferentiated, nonkeratinizing, and squamous cell carcinoma of the nasopharynx. Variants of Epstein-Barr virus-infected neoplasia. Am J Pathol. 1995 Jun;146(6):1355-67. PMID: 7778675; PMCID: PMC1870892.

International Journal of Biomedicine 16(1) (2026) 116-119
http://dx.doi.org/10.21103/Article16(1)_CR3

CASE REPORT

INTERNATIONAL JOURNAL OF BIOMEDICINE

Clinical Features, Diagnosis, and Surgical Management of Multiple Magnetic Foreign Bodies of the Gastrointestinal Tract in Children (Based on a Clinical Case)

J. A. Djurayev[1,2*], A. A. Ismatov[3], D. R. Asadullayev[2], Sh. Z. Nizamxodjayev[2], M. A. G'aniyev[1], R. N. Ismailova[2], P. K. Sultanov[4,3]

[1]*Republican Scientific Center of Emergency Medical Care, Tashkent, Uzbekistan*
[2]*Kimyo International University in Tashkent, Tashkent, Uzbekistan*
[3]*Republic Specialized Scientific-Practical Medical Center of Nephrology and Kidney Transplantation, Tashkent, Uzbekistan*
[4]*Tashkent State Medical University, Tashkent, Uzbekistan*

Abstract

Magnetic foreign bodies of the gastrointestinal tract (GIT) in children represent a rare but hazardous type of foreign body, capable of causing severe complications such as multiple perforations and inter-intestinal fistulas. In recent years, their incidence has increased due to the widespread use of magnetic toys and construction sets. Diagnosis is particularly challenging, as parents are not always aware of the ingestion, and the clinical presentation may mimic other acute surgical conditions. The article presents a clinical case of a 1.5-year-old boy who ingested 5 magnetic beads, complicated by fistula formation and perforation, as well as an analysis of data from the Republican Scientific Center of Emergency Medical Care (RSCEMC), in the Department of Pediatric Emergency Surgery for the period 2014–2019, describing the features of diagnosis, treatment strategies, and outcomes. (**International Journal of Biomedicine. 2026;16(1):116-119.**)

Keywords: gastrointestinal tract • foreign body • magnetic bead • children

For citation: Djurayev JA, Ismatov AA, Asadullayev DR, Nizamxodjayev ShZ, G'aniyev MA, Ismailova RN, Sultanov PK. Clinical Features, Diagnosis and Surgical Management of Multiple Magnetic Foreign Bodies of the Gastrointestinal Tract in Children (Based on a Clinical Case). International Journal of Biomedicine. 2026;16(1):116-119. doi:10.21103/Article16(1)_CR3

Introduction

Foreign bodies of the gastrointestinal tract (GIT) in children are one of the most common problems in emergency pediatric surgery. According to the American Association of Poison Control Centers, approximately 75% of the 116,000 registered cases of foreign body ingestion occur in children under 5 years of age.[1] Most objects (coins, buttons, small toys) pass through the gastrointestinal tract on their own. However, batteries and magnets pose a particular threat. Unlike other foreign bodies, magnets can attract each other through the intestinal wall, leading to localized ischemia, necrosis, fistula formation, and perforations.[2,3] According to the Republican Scientific Center of Emergency Medical Care (RSCEMC), in the Department of Pediatric Emergency Surgery, during the period 2014–2019, an increase in the number of children with magnetic foreign bodies was noted, reaching 3% of all cases of foreign bodies, while more than 51.8% of them required surgical intervention.[4]

This study aimed to examine the clinical manifestations, diagnostic approaches, and surgical outcomes of children with multiple magnetic foreign bodies in the gastrointestinal tract, using the clinical case and RSCEMC data.

Case Presentation

A 1.5-year-old female patient was admitted to the Department of Pediatric Emergency Surgery with complaints of abdominal pain, repeated vomiting, anxiety, and general

***Corresponding author**: Dr. Jur'atbek A. Djurayev, PhD. E-mail: juratbek07djurayev@gmail.com*

weakness. According to the mother, the child had been ill for about 10 days. The illness began with restlessness and crying when the abdomen was palpated, then progressed to nausea and repeated vomiting. Initially, the patient was treated at an infectious disease hospital, where infusion therapy was administered without improvement. An abdominal X-ray revealed multiple metallic shadows, and the child was transferred to a specialized pediatric emergency surgery center.

Clinical Findings and Investigations

The child's general condition is moderate, approaching serious. The child is lethargic. Body temperature is 36.7°C. The abdomen is soft, diffusely painful upon palpation, without symptoms of peritoneal irritation. Stool has not passed for two days.

Plain abdominal radiography revealed fluid levels in the small bowel loops and five rounded metallic shadows consistent with magnetic foreign bodies (Figure 1). Ultrasound examination revealed moderate dilation of the small intestinal loops, thickening of their walls, weakening of peristalsis and the presence of a small amount of free fluid. (Figure 2). In complete blood count tests over time showed minor fluctuations in hemoglobin (118→100 g/L), moderate leukocytosis up to 9.2×10⁹/L, without a shift in the leukocyte formula.

Biochemical parameters were within the age-appropriate range, with the exception of a transient increase in glucose (15.5 mmol/L) and urea (16.3 mmol/L) upon admission, which returned to normal levels after fluid therapy. Urinalysis revealed no abnormalities.

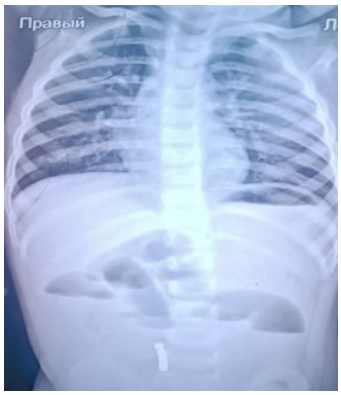

Fig 1. *Plain radiography of the abdominal organs.*

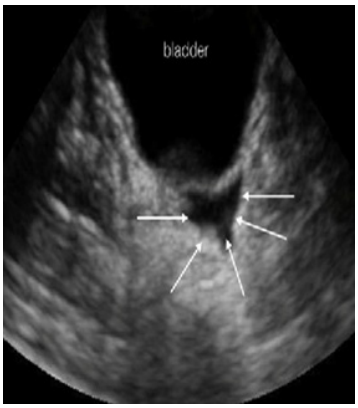

Fig 2. *Ultrasound of the abdominal organs.*

Surgical Treatment and Postoperative Course

Taking into account the clinical signs of intestinal obstruction, imaging data, and the high risk of perforation, a decision was made to perform emergency surgery. A mid-lower laparotomy was performed. Examination revealed dilated small bowel loops and serous effusion in the abdominal cavity. At a distance of approximately 30 cm from the ligament of Treitz, adhesions were found between loops of the small intestine, which arose as a result of the attraction of several magnetic foreign bodies located in different loops of the small intestine. Also, at this level of the proximal loop of the small intestine, there is a microperforation of the small intestine, which was sutured with a double-row suture. At a level of 40 cm from the Treitz ligament, two longitudinal perforations were detected, due to which a resection of a section of the small intestine approximately 10 cm long was performed with the formation of a side-to-side ileoileal anastomosis. Five magnetic foreign bodies were removed from the distal small intestine through a separate enterotomy. The abdominal cavity was debrided and drained (Figures 3-6).

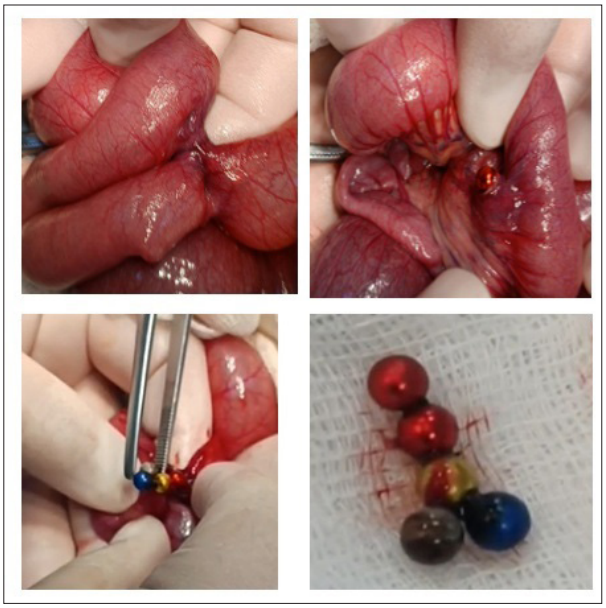

Fig. *3,4,5,6. Intraoperative picture.*

The postoperative course was uneventful. The patient received antibiotics and intravenous fluids, and nutrition gradually recovered. Bowel movements returned on the fourth postoperative day. The drains were removed 5–7 days after surgery. The postoperative wound healed by primary intention.

Discussion

Magnetic foreign bodies constitute a small proportion of all foreign bodies in the gastrointestinal tract in children, but they are characterized by the most severe course and the highest frequency of complications.[2,5] Late presentation, due to the lack of a reliable anamnesis and non-specific symptoms, significantly increases the risk of perforations and interintestinal fistulas.[3,6] According to several authors, more

than 40% of patients with multiple magnets require surgical treatment,[4,7] which is consistent with the presented clinical observation.

Between 2014 and 2019 alone, 1,046 children with gastrointestinal foreign bodies sought treatment at the RSCEMC. Patients ranged in age from 1 month to 18 years (mean age of 4.28±0.11 years). Depending on the time of treatment, the following were distinguished: urgent (<2 hours from symptom onset), emergency (2–24 hours), and late (>24 hours). According to the Russian Scientific Center for Emergency Medicine, only 25% of children with magnetic objects were admitted within the first day after swallowing, while the majority (75%) were admitted later than 24 hours (Figure 7). These results are comparable with the data of Singh et al.,[5] where late presentation for magnetic foreign bodies was observed in 68% of patients. Similar results are reported by Kim et al.,[6] indicating that it is the delay in treatment that is directly related to the high incidence of perforations.

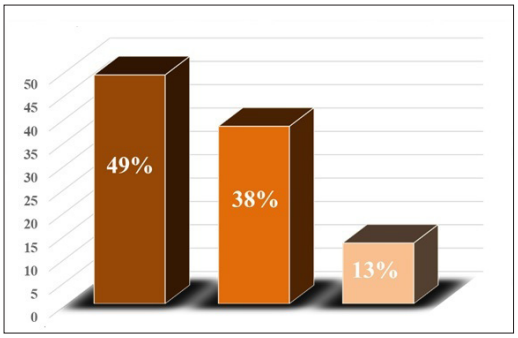

Fig. 7. *Time of admission: (a))urgence, (b) emergency, (c) late*

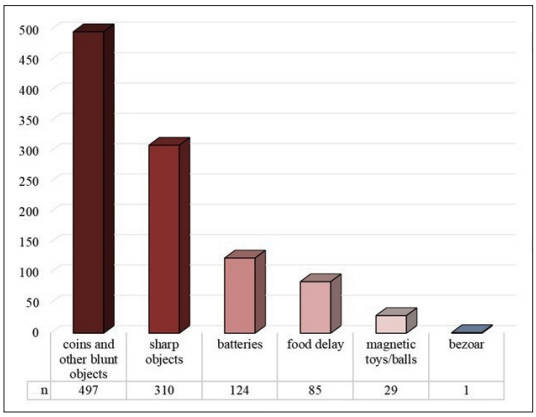

Fig. 8. *Frequency of gastrointestinal foreign bodies in children (according to the RSCEMC).*

Among all foreign bodies in children, blunt objects predominated - 497 (47%), sharp objects were found in 310 (30%), batteries - 124 (12%), magnets - 29 (3%), phytobezoar-1 (0.1%). Of these, magnetic objects were diagnosed in 3% of cases. Magnets were the most common cause of complications requiring open surgery (Figure 8).

Clinical manifestations at admission in children with magnetic foreign bodies of the gastrointestinal tract (n=29) were characterized by dysphagia, detected in 11 patients (38%), predominantly when the magnets were localized in the esophagus; vomiting in 9 children (31%), more often when foreign bodies were retained in the stomach or in the presence of early signs of intestinal obstruction; nausea in 8 patients (28%), frequently combined with vomiting and reflecting irritation of the mucosal lining; hypersalivation in 7 children (24%), mainly associated with difficulty in the passage of food through the esophagus (Figure 9).

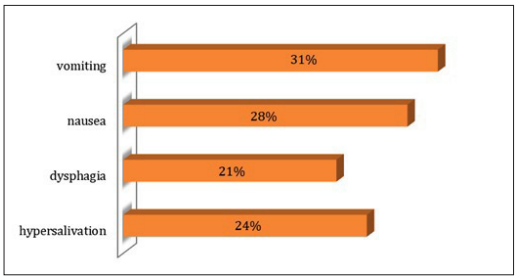

Fig. 9. *Clinical symptoms.*

These symptoms reflect both the mechanical impact of magnets and developing complications (swelling, inflammation, disruption of food passage). These data are consistent with the results of the study by Brown et al.,[3] in which most patients with magnets had predominant symptoms of swallowing disorders and vomiting, and pronounced signs of peritoneal irritation appeared only when complications developed. It is important to note that the initial symptoms often mimicked infectious diseases, which in some cases led to children being erroneously referred to infectious disease hospitals.

These patients underwent standard diagnostic methods: plain radiography of the chest and abdominal organs, radiocontrast examinations of the gastrointestinal tract, ultrasound, and multispiral computed tomography. When necessary, EGDS and colonoscopy were performed. Plain abdominal and chest radiography remains the gold standard for diagnosis, allowing the detection and quantification of metallic objects. However, the key difficulty is recognizing magnets, as they can form a single conglomerate and be mistaken for a single object. In our practice, the presence of free fluid on ultrasound and an increase in CRP to>100 mg/L were important predictors of a complicated course. According to Abbas et al.,[7] the combination of radiography and ultrasound increases the accuracy of diagnosing complications to 85%.

In total, endoscopic treatment was performed in 711 children (68%), of which endoscopic retraction was performed in 96.2% of cases, endoscopic fragmentation in 1.8%, and push-through in 2%. Our data are confirmed by Litovitz et al.,[1] where endoscopy was effective mainly with single magnets in the stomach (Table 1).

In our series, 51.8% of patients with magnetic foreign bodies required open surgery, in some cases with bowel resection. The relatively low rates of surgical intervention for coins and other blunt objects (less than 5%) highlight the exceptional danger posed by magnets. In a similar study

by Butterworth et al.,[2] surgical tactics were used in 43% of patients with magnets, which is generally comparable to our results.

Table 1.

Treatment methods for foreign bodies in the gastrointestinal tract in children (n = 1046).

Type of treatment	Magnetic foreign bodies n (%)	Other foreign bodies n (%)	n (%)
Endoscopic treatment	6 (20.7%)	705 (69.3%)	711 (68.0%)
Dynamic observation	5 (17.2%)	288 (28.3%)	293 (28.0%)
Laparoscopic surgery (with video assistance)	3 (10.3%)	12 (1.18%)	15 (1.43%)
Open surgical treatment	15 (51.7%)	12 (1.18%)	27 (2.58%)
Total	29 (100%)	1017 (100%)	1046 (100%)

In the general group of foreign bodies, open surgeries were performed in 27 children (2.58%), with the largest proportion of surgical interventions observed in patients with magnetic foreign bodies – more than half of them required laparotomy. At the same time, in cases of coins and other blunt objects, surgical treatment was required in less than 5% of cases.

Thus, our data and literature reviews demonstrate that magnetic foreign bodies constitute a distinct category with an extremely unfavorable prognosis when presented late. Early diagnosis and vigilance by primary care physicians can significantly reduce the risk of severe complications and the need for extensive surgical interventions.

Conclusions

Magnetic foreign bodies in the gastrointestinal tract in children account for a small proportion of all cases (about 3%), but are characterized by a high frequency of complications, making them the most dangerous category of foreign bodies.

Most patients present late (more than 24 hours after ingestion), due to unreliable anamnesis and the non-specific clinical picture.

Clinical manifestations most often include dysphagia, vomiting, nausea, and hypersalivation, but in some cases, the symptoms mimic acute infectious diseases, which complicate early diagnosis.

Endoscopic removal of magnets is possible only in isolated cases with early presentation and localization in the upper gastrointestinal tract. In most cases, late detection requires laparotomy and resection of the affected intestinal segments.

Timely X-ray diagnostics and surgeon vigilance can reduce the risk of serious complications.

Active preventative work with parents is necessary: informing them about the risks of magnetic toys and the need for immediate medical attention if swallowing is suspected.

Competing Interests

The authors declare that they have no conflicts of interest.

References

1. Litovitz T, Whitaker N, Clark L, White NC, Marsolek M. Emerging battery-ingestion hazard: clinical implications. Pediatrics. 2010 Jun;125(6):1168-77. doi: 10.1542/peds.2009-3037. Epub 2010 May 24. PMID: 20498173.
2. Butterworth J, Feltis B. Toy magnet ingestion in children: revising the algorithm. J Pediatr Surg. 2007 Dec;42(12):e3-5. doi: 10.1016/j.jpedsurg.2007.09.001. PMID: 18082689.
3. Strickland M, Rosenfield D, Fecteau A. Magnetic foreign body injuries: a large pediatric hospital experience. J Pediatr. 2014 Aug;165(2):332-5. doi: 10.1016/j.jpeds.2014.04.002. Epub 2014 May 16. PMID: 24836391.
4. Djurayev JA, Ismatov AA, Ismailova RN, Nizamxodjayev ShZ, G'aniyev MA, Sultanov PK. Clinical Features, Diagnostic Methods, and Treatment Approaches for Meckel's Diverticulum in Children and Adolescents: Experience of One Center. International Journal of Biomedicine. 2025;15(4):679-684. doi:10.21103/Article15(4)_OA5
5. Singh SJ, McGuirt WF. Multiple magnet ingestion: a growing hazard. World J Surg. 2019;43:2012-2018.
6. Kim JH, Lee JS, Kim MJ. Gastrointestinal complications caused by multiple magnet ingestion. Pediatr Surg Int. 2020;36:1071-1077.
7. Abbas MI, OlivaHemker M, Choi J. Utility of imaging in pediatric foreign body ingestion. Clin Pediatr. 2021;60(3):150–156.

International Journal of Biomedicine 16(1) (2026) 120-120
http://dx.doi.org/10.21103/Article16(1)_CRR

CORRIGENDUM

INTERNATIONAL JOURNAL OF BIOMEDICINE

[Corrigendum] Age- and Gender-Specific Dyslipidemia in Omani Young Adults: Metabolic Links to Cardiovascular Risk

Gulam Saidunnisa Begum[1], Salima Al Maqbali[2], Elham Said Ahmed Al Risi[2], Mariah N. Hafiz[3], Mohammed M. Jawad[3], Awadh Elkareem Abass[3], Shefaa A. Hejazy[4], Anshoo Agarwal[5], Nida Suhail[3]

[1]Department of Biochemistry, National University of Science and Technology, College of Medicine and Health Sciences, Sohar Campus, Oman
[2]Department of Pathology and Blood Bank, Sohar Hospital, Ministry of Health, Sohar, Oman
[3]Department of Medical Laboratory Technology, Faculty of Applied Medical Sciences, Northern Border University, Arar, Saudi Arabia
[4]Diagnostic Hematology, Clinical Laboratory Sciences, College of Applied Medical Sciences, Umm Al Qura University, Makkah, Saudi Arabia
[5]Pathology Department, Faculty of Medicine, Northern Border University, Arar, Saudi Arabia

Abstract

Corrigendum for 'Age- and Gender-Specific Dyslipidemia in Omani Young Adults: Metabolic Links to Cardiovascular Risk' by Begum GS, Agarwal A, Suhail N, Hafiz MN, Jawad MM, Abass AE, Hejazy SA. International Journal of Biomedicine 2025;15(4):668-673. doi:10.21103/Article15(4)_OA3.

Following the publication of this article, the authors have realized that errors were made with the description of the listed authors and affiliations. Therefore, the author's names and affiliations, in this paper, should have appeared as follows:
Gulam Saidunnisa Begum[1], Salima Al Maqbali[2], Elham Said Ahmed Al Risi[3], Mariah N. Hafiz[4], Mohammed M. Jawad[4], Awadh Elkareem Abass[4], Shefaa A. Hejazy[5], Anshoo Agarwal[6], Nida Suhail[4]

[1]Department of Biochemistry, National University of Science and Technology, College of Medicine and Health Sciences, Sohar Campus, Oman
[2]Department of Pathology and Blood Bank, Sohar Hospital, Ministry of Health, Sohar, Oman
[3]Sohar Hospital, Ministry of Health, Oman
[4]Department of Medical Laboratory Technology, Faculty of Applied Medical Sciences, Northern Border University, Arar, Saudi Arabia
[5]Diagnostic Hematology, Clinical Laboratory Sciences, College of Applied Medical Sciences, Umm Al Qura University, Makkah, Saudi Arabia
[6]Pathology Department, Faculty of Medicine, Northern Border University, Arar, Saudi Arabia

The authors apologize for any inconvenience caused.

For citation: Begum GS, Al Maqbali S, Al Risi ESA, Hafiz MN, Jawad MM, Abass AE, Hejazy SA, Agarwal A, Suhail N. [Corrigendum] Age- and Gender-Specific Dyslipidemia in Omani Young Adults: Metabolic Links to Cardiovascular Risk. International Journal of Biomedicine. 2026;16(1):120. doi:10.21103/Article16(1)_CRR

IJBM

INTERNATIONAL JOURNAL OF BIOMEDICINE

Instructions for Authors

International Journal of Biomedicine (IJBM) publishes peer-reviewed articles on the topics of basic, applied, and translational research on biology and medicine. International Journal of Biomedicine welcomes submissions of the following types of paper: Original articles, Reviews, Perspectives, Viewpoints, and Case Reports.

All research studies involving animals must have been conducted following animal welfare guidelines such as *the National Institutes of Health (NIH) Guide for the Care and Use of Laboratory Animals*, or equivalent documents. Studies involving human subjects or tissues must adhere to the *Declaration of Helsinki and Title 45, US Code of Federal Regulations, Part 46, Protection of Human Subjects*, and must have received approval of the appropriate institutional committee charged with oversight of human studies. Informed consent must be obtained.

Pre-submissions

Authors are welcome to send an abstract or draft manuscript to obtain a view from the Editor about the suitability of their paper. Our Editors will do a quick review of your paper and advise if they believe it is appropriate for submission to our journal. It will not be a full review of your manuscript.

Manuscript Submission

Manuscript submissions should conform to the guidelines set forth in the Recommendations for the Conduct, Reporting, Editing and Publication of Scholarly Work in Medical Journals (ICMJE Recommendations), available from www.ICMJE.org.

Original works will be accepted with the understanding that they are contributed solely to the Journal, are not under review by another publication, and have not previously been published except in abstract form.

All manuscripts must be submitted through the International Journal of Biomedicine`s online submission system (www.ijbm.org/submission.php). Manuscripts must be typed, double-spaced using a 14-point font, including references, figure legends, and tables. Leave 1-inch margins on all sides. Assemble the manuscript in this order: Title Page, Abstract, Key Words, Text (Introduction, Methods, Results, and Discussion), Acknowledgments, Sources of Funding, Disclosures, References, Tables, Figures, and Figure Legends. References, figures, and tables should be cited in numerical order according to first mention in the text.

The preferred order for uploading files is as follows: Cover letter, Full Manuscript PDF (PDF containing all parts of the manuscript including references, legends, figures and tables), Manuscript Text File (MS Word), Figures (each figure and its corresponding legend should be presented together), and Tables. Files should be labeled with appropriate and descriptive file names (e.g., SmithText.doc, Fig1.eps, Table3.doc). Text, Tables, and Figures should be uploaded as separate files. (Multiple figure files can be compressed into a Zip file and uploaded in one step; the system will then unpack the files and prompt the naming of each figure. See www.WinZip.com for a free trial.)

Authors who are unable to provide an electronic version or have other circumstances that prevent online submission must contact the Editorial Office prior to submission to discuss alternate options (editor@ijbm.org).

Cover Letter

The cover letter should be saved as a separate file for upload. In it, the authors should (1) state that the manuscript, or parts of it, have not been and will not be submitted elsewhere for publication; (2) state that all authors have read and approved the manuscript; and (3) disclose any financial or other relations that could lead to a conflict of interest. If a potential conflict exists, its nature should be stated for each author. When there is a stated potential conflict of interest a footnote will be added indicating the author's equity interest in or other affiliation with the identified commercial firms.

The corresponding author should be specified in the cover letter. All editorial communications will be sent to this author. A short paragraph telling the editors why the authors think their paper merits publication priority may be included in the cover letter.

Types of articles

Original articles

Original articles present the results of original research. These manuscripts should present well-rounded studies reporting innovative advances that further knowledge about a topic of importance to the fields of biology or medicine. These can be submitted as either a full-length article (no more than 6,000 words, 4 figures, 4 tables) or a Short Communication (no more than 2,500 words, 2 figures, 2 tables). An original

article may be Randomized Control Trial, Controlled Clinical Trial, Experiment, Survey, and Case-control or Cohort study.

Case Reports

Case reports describe an unusual disease presentation, a new treatment, a new diagnostic method, or a difficult diagnosis. The author must make it clear what the case adds to the field of medicine and include an up-to-date review of all previous cases in the field. These articles should be no more than 5,000 words with no more than 6 figures and 3 tables. Case Reports should consist of the following headings: Abstract (no more than 100 words), Introduction, Case Presentation (clinical presentation, observations, test results, and accompanying figures), Discussion, and Conclusions.

Reviews

Reviews analyze the current state of understanding on a particular subject of research in biology or medicine, the limitations of current knowledge, future directions to be pursued in research, and the overall importance of the topic. Reviews could be non-systematic (narrative) or systematic. Reviews can be submitted as a Mini-Review (no more than 2,500 words, 3 figures, and 1 table) or a long review (no more than 6,000 words, 6 figures, and 3 tables). Reviews should contain four sections: Abstract, Introduction, Topics (with headings and subheadings, and Conclusions and Outlook.

Perspectives

Perspectives are brief, evidenced-based and formally structured essays covering a wide variety of timely topics of relevance to biomedicine. Perspective articles are limited to 2,500 words and usually include ≤10 references, one figure or table. Perspectives contain four sections: Abstract, Introduction, Topics (with headings and subheadings), Conclusions and Outlook.

Viewpoints

Viewpoint articles include academic papers, which address any important topic in biomedicine from a personal perspective than standard academic writing. Maximum length is 1,200 words, ≤70 references, and 1 small table or figure.

Manuscript Preparation

Title Page

The first page of the manuscript (title page) should include (1) a full title of the article, (2) a short title of less than 60 characters with spaces, (3) the authors' names, academic degrees, and affiliations, (4) the total word count of the manuscript (including Abstract, Text, References, Tables, Figure Legends), (5) the number of figures and tables, and (6) the name, email address, and complete address of corresponding author.

Disclaimers. An example of a disclaimer is an author's statement that the views expressed in the submitted article are his or her own and not an official position of the institution or funder.

Abstract

The article should include a brief abstract of no more than 200 words. Limit use of acronyms and abbreviations. Define at first use with acronym or abbreviation in parentheses. The abstract should be structured with the following headings: Background, Methods and Results, and Conclusions. The Background section should describe the rationale for the study. Methods and Results should briefly describe the methods and present the significant results. Conclusions should succinctly state the interpretation of the data. Authors should supply a list of up to four key words not appearing in the title, which will be used for indexing. The key words should be listed immediately after the Abstract. Use terms from the Medical Subject Headings (MeSH) list of Index Medicus when possible.

Main text in the IMRaD format

Introduction should describe the purpose of the study and its relation to previous work in the field; it should not include an extensive literature review.

Methods should be concise but sufficiently detailed to permit repetition by other investigators. Previously published methods and modifications should be cited by reference. A subsection on statistics should be included in the Methods section.

Results should present positive and relevant negative findings of the study, supported when necessary by reference to Tables and Figures.

Discussion should interpret the results of the study, with emphasis on their relation to the original hypotheses and to previous studies. The importance of the study and its limitations should also be discussed.

The IMRaD format does not include a separate Conclusion section. The conclusion is built into the Discussion. More information on the structure and content of these sections can be found in the Recommendations for the Conduct, Reporting, Editing and Publication of Scholarly Work in Medical Journals (ICMJE Recommendations), available from www.ICMJE.org.

Acknowledgments, Sources of Funding, and Disclosures

Acknowledgments : All contributors who do not meet the criteria for authorship should be listed in an acknowledgments section. Examples of those who might be acknowledged include a person who provided purely technical help, writing assistance, or a department chairperson who provided only general support. Authors should declare whether they had assistance with study design, data collection, data analysis, or manuscript preparation. If such assistance was available, the authors should disclose the identity of the individuals who provided this assistance and the entity that supported it in the published article.

Sources of Funding: All sources of financial support for the study should be cited on the title page, including federal or state agencies, nonprofit organizations, and pharmaceutical or other commercial sources.

Disclosure and conflicts of interest: All authors must disclose any financial or other relations that could lead to a conflict of interest. If a potential conflict exists, its nature should be stated for each author. All sources of financial support for the study should be cited, including federal or state agencies, nonprofit organizations, and pharmaceutical or other commercial sources. Please use ICMJE Form for Disclosure of Potential Conflicts of Interest (http://www.icmje.org/conflicts-of-interest/).

References

References should follow the standards summarized in the NLM's International Committee of Medical Journal Editors (ICMJE) Recommendations for the Conduct,

Reporting, Editing and Publication of Scholarly Work in Medical Journals: Sample References webpage (www.nlm.nih.gov/bsd/uniform_requirements.html) and detailed in the NLM's Citing Medicine, available from www.ncbi.nlm.nih.gov/books/NBK7256/. MEDLINE abbreviations for journal titles (www.ncbi.nlm.nih.gov/nlmcatalog/journals) should be used.

References should be presented in the Vancouver style. The first six authors should be listed in each reference citation (if there are more than six authors, "et al" should be used following the sixth). Periods are not used in authors' initials or journal abbreviations. Examples of journal reference style:

Journal Article: Serruys PW, Ormiston J, van Geuns RJ, de Bruyne B, Dudek D, Christiansen E, et al. A Polylactide Bioresorbable Scaffold Eluting Everolimus for Treatment of Coronary Stenosis: 5-Year Follow-Up. J Am Coll Cardiol. 2016;67(7):766-76. doi: 10.1016/j.jacc.2015.11.060.

Book: Murray PR, Rosenthal KS, Kobayashi GS, Pfaller MA. Medical Microbiology. 4th ed. St. Louis: Mosby; 2002.

Chapter in Edited Book: Meltzer PS, Kallioniemi A, Trent JM. Chromosome alterations in human solid tumors. In: Vogelstein B, Kinzler KW, editors. The Genetic Basis of Human Cancer. New York: McGraw-Hill; 2002:93–113.

References should be numbered consecutively in the order in which they are first mentioned in the text. Identify references in text, tables, and legends by Arabic numerals in parentheses and listed at the end of the article in citation order.

Tables

Tables should be comprehensible without reference to the text and should not be repetitive of descriptions in the text. Every table should consist of two or more columns; tables with only one column will be treated as lists and incorporated into the text. All tables must be cited in the text and numbered in order of appearance. Tables should include a short title. Place explanatory matter in footnotes, not in the heading. Explain all nonstandard abbreviations in footnotes, and use symbols to explain information if needed. Each table submitted should be double-spaced, each on its own page. Each table should be saved as its own file as a Word Document. Explanatory matter and source notations for borrowed tables should be placed in the table footnote.

Figures and Legends

All illustrations (line drawings and photographs) are classified as figures. All figures should be cited in the text and numbered in order of appearance. Figures should be provided in .tiff, .jpeg or .eps formats. Color images must be at least 300 dpi. Gray scale images should be at least 300 dpi. Line art (black and white or color) and combinations of gray scale images and line art should be at least 1,000 dpi. The optimal size of lettering is 12 points. Symbols should be of a similar size. Figures should be sized to fit within the column (86 mm) or the full text width (180 mm). Line figures must be sharp, black and white graphs or diagrams, drawn professionally or with a computer graphics package. Legends should be supplied for each figure and should be brief and not repetitive of the text. Any source notation for borrowed figures should appear at the end of the legend. Figures should be uploaded as individual files.

Units of Measurement

Measurements of length, height, weight, and volume should be reported in metric units (meter, kilogram, or liter) or their decimal multiples. Temperatures should be in degrees Celsius. Blood pressures should be in millimeters of mercury. All measurements must be given in SI or SI-derived units. Drug concentrations may be reported in either SI or mass units, but the alternative should be provided in parentheses where appropriate.

Style and Language

The journal accepts manuscripts written in English. Spelling should be US English only. The language of the manuscript must meet the requirements of academic publishing. Reviewers may advise rejection of a manuscript compromised by grammatical errors. Non-native speakers of English may choose to use a copyediting service.

Abbreviations and Symbols

Use only standard abbreviations; use of nonstandard abbreviations can be confusing to readers. Avoid abbreviations in the title of the manuscript. The spelled-out abbreviation followed by the abbreviation in parenthesis should be used on first mention unless the abbreviation is a standard unit of measurement.

Drugs should be referred to by their generic names. If proprietary drugs have been used in the study, refer to these by their generic name, mentioning the proprietary name, and the name and location of the manufacturer, in parentheses.

Permissions

To use tables or figures borrowed from another source, permission must be obtained from the copyright holder, usually the publisher. Authors are responsible for applying for permission for both print and electronic rights for all borrowed materials and are responsible for paying any fees related to the applications of these permissions. This is necessary even if you are an author of the borrowed material. It is essential to begin the process of obtaining permission early, as a delay may require removing the copyrighted material from the article. The source of a borrowed table should be noted in a footnote and of a borrowed figure in the legend. It is essential to use the exact wording required by the copyright holder. A copy of the letter granting permission, identified by table or figure number, should be sent along with the manuscript. A permission request form is provided for the authors use in requesting permission from copyright holders.

Page Proofs

Page proofs are sent from the Publisher electronically and must be returned within 72 hours to avoid delay of publication. Generally, peer review is completed within 4-5 weeks.

It is important to note that when citing an article from IJBM, the correct citation format is **International Journal of Biomedicine.**

IJBM

INTERNATIONAL JOURNAL OF BIOMEDICINE

International Journal of Biomedicine (IJBM) is an open access journal. IJBM publishes peer-reviewed articles on aspects of basic, applied, and translational research in biology and medicine. The main purpose of IJBM is to establish a scientific platform for targeted promotion of new scientific ideas and biomedical technologies focused on the applied aspects of biomedicine.

The journal publishes articles on:

Internal Medicine
Cardiology
Pulmonology
Endocrinology
Neurology
Hepatology
Gastroenterology
Nephrology
Ophthalmology
Otorhinolaryngology
Radiology
Surgery
Obstetrics and Gynecology
Pediatrics
Dermatology and STD
Clinical Immunology
Oncology
Genomics and Proteomics
Population Genetics
Epidemiology and Population Health
Reproductive Health
Adolescent Health
Cell Biology
Experimental Biology
Biotechnology
Dentistry
Infectious Diseases
Sports Medicine

Authors are invited to submit:

Original articles
Review articles
Case reports
Perspectives
Viewpoints